CHARACTERISATION OF THE ROLE OF *SOX4* IN MOUSE EMBRYONIC DEVELOPMENT

CHRISTINE-MARGARET MULFORD

THESIS PRESENTED FOR THE DEGREE OF DOCTOR OF PHILOSOPHY
THE INSTITUTE FOR STEM CELL RESEARCH
AND THE CENTRE FOR CARDIOVASCULAR SCIENCE
UNIVERSITY OF EDINBURGH
2009

For my parents and my husband…..
who have always been so dedicated to me.

"All science, even the divine science, is a sublime detective story. Only it is not set to detect why a man is dead; but the darker secret of why he is alive."

GK Chesterton, *The Thing. CW. III 191.*

I declare that the work presented in this thesis is my own, unless otherwise stated.

Christine-Margaret Mulford.

FUNDING

This PhD would not have been possible without the financial support of the Wellcome Trust Cardiovascular Research Initiative. For the incredible opportunity to participate in this programme, I wish to thank Professor John Mullins and those who supported my application.

ACKNOWLEDGEMENTS

First and foremost, thanks so much to my supervisor, Val Wilson, for taking me on as a student with this project. I am extremely grateful for being able to receive your guidance over the past five years – THANK YOU!

Thank you to past and present members of Val's lab, especially to Ron who is both a gentleman and a scientist, and whom I will miss working with very much.

Thank you to Josh - your questioning of my results has made me a better photographer, I mean, scientist (honestly… thank you!). Thanks also to members of the Brickman lab and the Thursday morning meeting folk – for advice on which direction(s) this project should take; and for always being available to answer questions, no matter how daft or poorly thought through!

Special thanks to the Andy and Carol, and those who work in the animal unit, without you this project would not have been possible. Also, thank you to the support and technical staff in the ISCR, in tissue culture, and the transgenic group. I appreciate your help during my time in the building.

Lesley and Alistair, thank you for your advice during this project. Additionally, I am highly appreciative to Ruth and our collaborators at Harwell for the initial characterisation of the *Sox4* mouse line and for allowing me to take it on as a project. Especially, thank you Ruth for your advice in the stages of writing.

My post-viva thanks: So I took a while to do my corrections. Quite a while! And there are people I need to thank for stages of this process. As I had already started my Post-doc at the MRC HGU, my boss, Ian Jackson, was supportive enough to say "do the corrections here" rather than travelling back and forth to the ISCR on the other side of town. I am very grateful and want to express my thanks to Ian for the time I've been permitted to take to make this thesis what it is now – as you said, it is good training for the future. Thanks also to my colleagues for your patience and support during the hair-pulling months of extra wholemount and section *in situ* hybridisation and imaging (and the re-writing). Many thanks to Dr. Simon Bamforth, who was kind enough to take time over the past 6 months (including once on his holiday) to examine my H&E sections and help with phenotype analysis. Special thanks to Pleasie for your advice on the section *in situ* protocol, optimisation and imaging, and to Margaret for arranging the additional embryos. Thank you to Laura and Sally for providing extra *in situ* probes. Many thanks to Paul for training me (and further helping me) to use the microscopes here at the HGU. Thanks also to Craig for your help with use of Illustrator, for helping me re-create (re-creating for me) some of the introduction figures, and also for help with printing. I am also very grateful to my two reviewers, for describing what was needed such that this could be

a better work, both up to scratch for the degree, and something I could be proud of (and, sometime, publish something from!).

To my friends, especially my PhD comrades in the ISCR, for being quick to help and willing to give advice – thank you. In particular: Katrin and Hamood and Lorna thank you for all your support, well and beyond the call of duty!

To my family in Australia, thanks for your support over the past six years. Especially thank you to my parents for encouraging me to question, and to follow my path as a scientist; for never giving me the opportunity to doubt that I could do this; and for being so supportive, since I decided to choose a project on the other side of the planet.

Nigel…what can I say. You are my rock. I love you. Thank you.

ABSTRACT

The molecular complexity of cardiogenesis is revealed by the high incidence of heart phenotypes resulting from mutation to any of a vast number of genes across multiple pathways. Many proteins, in pathways critical for correct embryonic patterning, are thus also identified as playing a role in aspects of heart development. A developmental role for Sox4 has been shown in mouse cardiogenesis, as apparent by the phenotype of two published alleles. Both null and conditional null mutant alleles exhibit septation defects, oedema, and lethality by E14.5. However, the causative step in development, where a loss of functional Sox4 marks the beginning of the defect, has not been described; nor has it been uncovered whether mutation to *Sox4* results in dysregulation of other aspects of embryonic patterning.

This thesis documents the homozygous embryonic phenotype of two mouse lines, both harbouring an ENU-induced point mutation to the HMG-box of *Sox4*. In addition to the *Sox4* mutation, the first mouse line examined also contains the well-characterised *satin* (*sa*) coat mutation to the *Foxq1* gene, a mutation closely linked to *Sox4* on chromosome 13. This mutation had been used as a phenotypic recessive marker in the ENU mutagenesis screen from which the *Sox4* allele was isolated.

Phenotypic analysis of the $Sox4^{ENU/ENU}$ $Foxq1^{sa/sa}$ phenotype reveals that the primary cardiac defect of *Sox4* arises as early as E9.5. As the *satin* allele has been well characterised and does not result in cardiac dysmorphology, the cardiac phenotype observed can thus be attributed to the *Sox4* point mutation. At this developmental stage, mutant embryos can be grouped into three phenotypic classes, which vary in severity. A phenotype is evident at early stages of development in the most severely affected embryos, such that only a proportion of homozygotes can be examined for the later cardiac phenotype. At E12.5-E13.5, the cardiac phenotype of embryos resembles that of the published *Sox4* null allele. However, our analysis goes further to uncover abnormalities in the development of the atrial septum and atrioventricular structures. To expand on the understanding of this phenotype, a general analysis was conducted using key molecular markers, selected to reveal consequences of the phenotype.

Following description of the phenotype a comprehensive analysis of the expression of *Sox4* was carried out by wholemount and section *in situ* hybridisation. Since the mutant phenotype arises between gastrulation (for the most severe mutants) and E9.5 (for the mildest of mutants), *Sox4* expression was examined from pre-gastrulation stages to E12.5 in wholemount, and E9.5 to E12.5 by section *in situ* to cardiac regions. The most significant expression of relevance to cardiogenesis is the identification of *Sox4* transcripts in several domains. Early in development, expression is observed in the mesoderm lateral to the cardiac crescent, a region known to contribute to the posterior components of the heart tube, and the endoderm adjacent to the cardiac crescent and subsequent heart tube. Section analysis of the cardiac region of E9.5 embryos revealed the onset of specific expression of *Sox4* in the endocardium of the outflow tract and atrioventricular canal, with expression also identified in the emerging cushion mesenchyme. Endocardial and mesenchymal expression in the AVC and OFT continue at stages E10.5, E11.5 and E12.5. The spatiotemporal expression pattern of *Foxq1* is also shown, and exhibits a degree of overlap with *Sox4* in the endoderm and in anterior structures.

Through an extensive breeding programme, it was possible to segregate the mutant *Sox4* allele from *satin.* Phenotypic abnormalities evident in compound homozygotes but not in *Sox4* homoygotes are convincing evidence of a genetic interaction between *Sox4* and *Foxq1*, although the precise nature of this remains unknown.

The work carried out in this candidature provides novel evidence of the embryonic expression and function of Sox4. It has been possible to identify the origin of the cardiac defect caused by mutation to *Sox4* as well as reveal additional aspects of an early phenotype resulting from loss of function of *Sox4.* Thus, this study provides a significant contribution to understanding the function of this gene.

LIST OF COMMON ABBREVIATIONS

0B	zero bud (a stage of 7.5dpc)
AER	apical ectodermal ridge
AHF	Anterior heart field, also secondary (SHF)
ANF	atrial natriuretic factor
A/P	anterior-posterior
APS	aortico-pulmonary septum
AS	Atrial septum
ASD	atrial septal defect
AV	atrioventricular
AVC	atrioventricular canal
AVE	anterior visceral endoderm
AVS	atrioventricular septum
AVV	atrioventricular valves
BCIP	5-bromo-4-chloro-3-indolyl phosphate p-toluidine
βgal	β–galactosidase
BMP	bone morphophogenic protein
bp	base pair
BSA	bovine serum albumin
°C	degrees centigrade
cDNA	complementary DNA
CHD	congenital heart defect

cm	centimetre
CNS	central nervous system
CO_2	carbon dioxide
DEPC	diethyl pyrocarbonate
dH_2O	distilled (or reverse osmosis) water
DIG-11-dUTP	digozigenin-11-uridine-5'trisphosphate
DMP	dorsal mesenchymal projection, also vestibular spine; spina vestibuli.
DNA	deoxyribonucleic acid
DNase	deoxyribonuclease
dNTP	2'-deoxyribonucleotide 5'-triphosphate
DORV	double outflow right ventricle
D/V	dorsal-ventral
dpc	days post coitum (staging of mouse development)
E	embryonic day (staging of mouse development)
EB	early bud (a stage of 7.5dpc)
E. coli	Escherichia coli
EDTA	ethylenediaminetetraacetic acid
EMT	epithelial to mesenchymal transition
ES	embryonic stem
EtBr	ethidium bromide
EtOH	ethanol
EHF	early head fold
FCS	foetal calf serum

FGF	fibroblast growth factor
FHF	first heart field
Fox	Forkhead box
g (mass)	grams
GFP	green fluorescent protein
GMEM	Glasgow Minimum Essential Medium
HEPES	4-(2-hydroxyethyl)-1-piperazineethanesulfonic acid
HH	Hamburger and Hamilton (staging of chick development)
hrs	hours
ICM	inner cell mass
IFT	inflow tract
kb	kilobase (pairs)
kDa	kilo Dalton
l	litre
LA	left atrium
LB	late bud (a stage of 7.5dpc)
LB media	Luria-Bertani media
LIF	leukaemia inhibitor factor
LPM	lateral plate mesoderm
L/R	left right
LOH	loss of heterozygosity
LV	left ventricle
mA	milliampere

μ	micro
m	milli
m	metre
M	molar
M91	Mouse line derived from ENU mutagenesis screen which carries a *Sox4* mutation on mixed C3H/HeH and 101/HeH backgrounds
min	minutes
MRI	Magnetic resonance imaging
mRNA	messenger RNA
n	nano
NaOAc	Sodium acetate
NaCl	Sodium chloride
NBT	Nitro-Blue Tetrazolium Chloride
NC	Neural crest
NP-40	noniodet P-40
NTP	nucleotide triphosphate
OD	optical density
OFT	outflow tract
OP	Ostium primum; foramen primum; primary atrial foramen.
OPT	Optical projection tomography
ORF	open reading frame
PAS	primary atrial septum; septum primum
PBS	phosphate buffered saline

PCR	polymerase chain reaction
PE	pharyngeal endoderm
PS	primitive streak
RA	right atrium
RNA	ribonucleic acid
RNase	ribonuclease
rpm	revolutions per minute
RT	room temperature
RV	right atrium
SDS	sodium dodecyl sulphate
SE	surface ectoderm
sec	seconds
SHF	second heart field, also anterior (AHF)
Shh	sonic hedgehog
Sox	Sry-like HMG box
SSC	sodium chloride/sodium citrate buffer
Taq	*Thermus aquaticus*
TAE	tris acetate EDTA buffer
TBE	tris borate EDTA buffer
Tbx	T-box
Tcf	T cell factor-4
TGF	transforming growth factor
U	units

V/V	volume : volume
V	volts
VSD	ventricular septal defect
W	watts
W/V	weight : volume

TABLE OF CONTENTS

LIST OF FIGURES

LIST OF TABLES

CHAPTER 1: INTRODUCTION

This thesis presents findings from a study of the embryological and molecular basis of a mutation in *Sox4*. The precise role of Sox4 is not well-understood. However, *Sox4* expression appears to be required for appropriate heart development and, in adult tissue, significant for the progression of cancer. This introduction will first outline what is known about Sox4 function. Second, relevant aspects of mouse embryonic development and heart development are described, since the heart is the primary organ affected in the mouse line characterised in this project. Third, the genetic strategy used to generate the mouse line, which harbours an ENU-induced mutation in *Sox4*, is discussed.

1.1 Sox4

1.1.1 The Sox family of proteins and the group C member, Sox4.

The Sox (SRY-like HMG box) family of proteins function in a wide range of developmental and physiological processes. Sox proteins are conserved from invertebrates to mammals, with approximately 35 proteins spanning 11 phylogenetic groups (Bowles *et. al.* 2000). The family was first defined by homology with the HMG DNA binding domain of the testis-determining factor, SRY (Gubbay *et. al.* 1990). Structurally, the HMG domain comprises three alpha helices orientated into an L-shape (Figure1.1a), which binds the minor groove of DNA and regulates gene transcription (Bewley *et. al.* 1998; Wegner 1999). The L-shape structure of the HMG domain is maintained by a hydrophobic core of protein residues, which are highly conserved within the Sox family. Binding of the HMG domain to DNA results in a 70-85° bend and an unwinding of the DNA helix, in addition to widening of the minor groove (Ferrari *et. al.* 1992) (reviewed in (Wegner 1999)). The majority of Sox proteins appear to bind DNA as monomers, with a few identified exceptions: Members of phylogenetic group D (Sox5, Sox6) homodimerise *via* a leucine zipper motif, only identified in members of this group (Lefebvre *et. al.* 1998); SOX9 and Sox10 (within group E) have both been found to dimerise in a DNA-dependent manner (Peirano *et. al.* 2000). Furthermore, SOX9 dimerises to activate gene expression in chondrogenesis, while it acts as a monomer to activate expression of genes involved in sex determination (Bernard *et. al.* 2003).

Mouse Sox4 (RP23-262C6.1, AA682046 and Sox-4) and its orthologs in human (SOX4), rat (Sox4_predicted), *Xenopus* (sox4), chick (SOX4) and zebrafish (sox4a) are members of the group C division of Sox genes. In group C, Sox4 is phylogenetically related to Sox11 (mouse, human, rat, chick, *Xenopus* and zebrafish), Sox 12 (mouse), SOX12 (formerly SOX22) (human), Sox 24 (rainbow trout), and the invertebrate Sox C proteins (*C.elegans* and *D.melanogaster*). The *Sox4* locus resides on mouse chromosome 13 band A3-A5 (Critcher *et. al.* 1998) and the short arm of chromosome 6, 6p22.3 (Critcher *et. al.* 1998), in human.

A

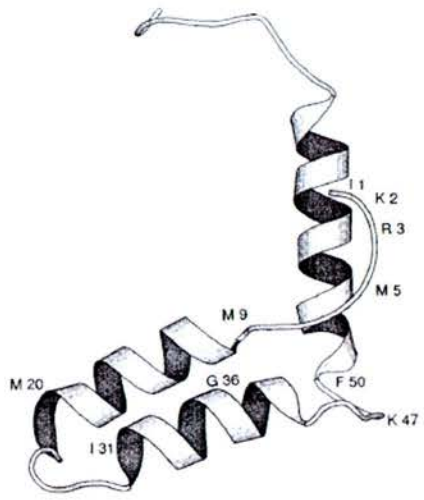

B

Figure 1.1: Domains of the Sox4 protein. (A) The L-shaped HMG box of Sox4 comprises three alpha helices; (B) The Sox4 protein harbours an HMG box DNA binding domain at the N terminus and a trans-activation domain at the C terminus. Additional motifs include a glycine-rich repeat (GRR) and a stretch of serine repeats (SRR) at the C terminus. Figure adapted from: (A) Van Houte *et.al.* 1995 and (B) Goldsworthy *et.al.* 2008.

Structurally, the HMG domain is located close to the N terminus (van de Wetering *et. al.* 1993). The Sox4 HMG domain is known to bind a strict DNA motif of 10 base pairs. Additional motifs include the nuclear localisation signal (NLS) (Rehberg *et. al.* 2002), glycine-rich repeats and the C-terminus serine-rich repeats which act as the transactivation domain (Goldsworthy *et. al.* 2008; van de Wetering *et. al.* 1993)(Figure1.1b).

The transactivation potential of Sox4 has been characterised with assays based on an early finding that Sox4 was capable of binding a T cell-specific enhancer of the *CD3ε* gene (van de Wetering *et. al.* 1993). Reporter-gene assays revealed that Sox4 activated transcription, and the transactivation domain was subsequently identified by fusion to the GAL4 DNA binding domain (van de Wetering *et. al.* 1993). More recently, a comparison of the transactivation ability of Group C Sox proteins has been conducted, using the same sequence from the *CD3ε* enhancer mediating reporter gene activation (Hoser *et. al.* 2008). Whilst all three Sox C proteins recognise this sequence, it was found that Sox11 exhibits the strongest transactivation potential, followed by Sox4, with Sox12 demonstrating a weak ability to activate transcription (Hoser *et. al.* 2008).

1.1.2 Expression of *Sox4* in model species, and its overlap with *Sox11.*

The expression of *Sox4* has been analysed in a range of tissues and animal models. In adult mouse tissue, *Sox4* expression has been shown in specific organs by *in situ* hybridisation and northern blotting. In the hair follicle, expression of *Sox4* is observed in the hair germ epithelial cells, located at the base of the hair follicle (Kobielak *et. al.* 2007). Adult tissues which express *Sox4* include: thymus, femur, heart, pancreas, liver, kidney, spleen, mammary gland, skeletal muscle, pituitary gland, skin, CNS (regions of the brain and spinal cord), eye, digestive tract, lung and gonads[1].

Since Sox4 and Sox11 recognise a conserved DNA sequence, and they also demonstrate functional overlap, it is possible that during development, co-expression

[1] http://www.informatics.jax.org/

of *Sox11* with *Sox4* might functionally compensate for ablation of Sox4 in mutant lines.

The expression of both *Sox4* and *Sox11* is detected in the developing mouse pancreas. At E12.5 and E14.5 *Sox4* and *Sox11* positive cells are broadly expressed in the epithelium. By E18.5 these two transcripts overlap in endocrine cells of the islets of Langerhans (Lioubinski *et. al.* 2003).

Furthermore, the expression of *Sox4* has been described in mouse central nervous system (CNS) development by wholemount *in situ* hybridisation at E8.5 and E10.5. Detailed analysis has been conducted on sections of the neural tube between E10.5 and E16.5, and on anterior forebrain sections between E11.5 and P7 (detailed in (Cheung *et. al.* 2000)). In the brain and spinal cord, the expression of *Sox4* predominantly overlaps with *Sox11*. Analysis by Cheung *et.al.* additionally revealed expression of *Sox4* in wholemount at E10.5 in the limb bud, dorsal root ganglia (DRG), and pharyngeal arches – expression domains which were present in chick at the equivalent stage (Maschhoff *et. al.* 2003).

During heart development, in both mouse and chick, the first reported expression of *Sox4* is at embryonic day (E)11.5 in mouse and HH18 (approximately equivalent to E10.5) in chick. *Sox4* expression is reported in the developing cushions of the atrioventricular canal (AVC) and the outflow tract (OFT) (Hoser *et. al.* 2008; Maschhoff *et. al.* 2003; Schilham *et. al.* 1996). The expression of *Sox11* does not overlap with *Sox4* in the heart. This has been shown by wholemount *in situ* hybridisation analysis to *Sox11* in mouse (Hargrave *et. al.* 1997; Kuhlbrodt *et. al.* 1998) and *sox11A* and *sox11B* in zebrafish (Rimini *et. al.* 1999). Additionally, the developmental expression of a β-galactosidase marker introduced into the *Sox11* locus reveals only weak cardiac expression from E14.5 at the arterial pole (Sock *et. al.* 2004) - subsequently confirmed by quantitative PCR, demonstrating extremely low expression of *Sox11* in the heart at E14.5, E16.5 and E18.5 developmental stages (Hoser *et. al.* 2008).

Although these studies have identified a wide range of tissues that express *Sox4*, its expression at cellular resolution in many sites is unclear, as is the subcellular localisation of the protein, particularly during embryonic development.

1.1.3 Known functions of Sox4.

The current understanding of the mechanism (or possible mechanisms) of action of Sox4 stems from analysis in multiple disciplines. A null allele was created in mouse and examined, to a limited degree, until embryonic death at E14.5. Expression of Sox4 in the immune system gave rise to an interest in the role of Sox4 during development of cells involved in immunological responses, B and T cells. Additionally, there is increasing evidence that *Sox4* is strongly upregulated in numerous types of cancer, and cancer cell lines. Thus considerable research is focused on increasing the understanding of the role of Sox4, its target genes, and its molecular function. The role of Sox4 in these systems is summarised below. The evidence for a role in heart development will follow in the next section (section 1.1.4).

Development and maintenance of biological systems

Sox4 is necessary for development of certain cells within the immune system. *Sox4* null embryos demonstrate inability of B cells to mature beyond the pro-B cell stage (Schilham *et. al.* 1996). Sox4 is activated through IL5-mediated signalling (Geijsen *et. al.* 2001). This activation requires binding of Sox4 to syntenin, which associates with the intracellular domain of the IL-5α receptor. Signalling through the IL-5α receptor is important for regulating B cell differentiation (Moon *et. al.* 2001). Furthermore, explanted cultures of the foetal thymic organ from null embryos indicated a deficiency in the ability to produce CD4 and CD8 positive T cells (Schilham *et. al.* 1997).

In the pancreas, embryos homozygous for the null mutation in *Sox4* demonstrate normal pancreatic bud formation and differentiation to E12.5. Explant culturing for eight days from E11.5, to examine differentiation beyond the cardiac lethality, showed that loss of *Sox4* does not prevent differentiation of endocrine cells, but

homozygous mutant pancreas fails to form normal islet structure (Wilson *et. al.* 2005). The molecular requirement for Sox4 in this process has not been described.

The role of Sox4 in CNS development has been explored (Cheung *et. al.* 2000). In a comparison of gene expression (*Sox2, Sox11, Mash1, Ngn1* and *Ngn2*) was carried out on forebrain and spinal cord sections from two E12 *Sox4* null embryos, little difference was observed between the expression of these genes. Hence, this group concluded that there was sufficient homology between *Sox4* and *Sox11* expression domains such that Sox11 could compensate for an absence of Sox4 at this developmental stage in the CNS.

Also in the CNS, control of the levels of *Sox4* is required for oligodendrocyte development (Potzner *et. al.* 2007). *Sox4* is expressed highly in oligodendrocyte precursor cells. However, overexpression of *Sox4* in oligodendrocyte precursor cells interfered with the ability of these cells to undergo terminal differentiation. A similar role of Sox4 is observed in glial cells suggesting that Sox4 counteracts differentiation (Hoser *et. al.* 2007).

Other roles of Sox4 have been described outside of the embryonic period. Physiologically, its expression is modulated by hormones in the mammary glands and uterus (Hunt *et. al.* 1999) and *in vitro* studies reveal that Sox4 functions to promote apoptosis *via* Caspase-1, following induction of the cellular cascade by PGA2 and delta12-PGJ2 (Ahn *et. al.* 1999; Ahn *et. al.* 2002).

It is evident from current work that Sox4 plays a dynamic role during development of a number of organ systems.

Tumorigenesis

The most well-described activity of SOX4 is within the field of cancer genetics. Indeed most SOX proteins have been implicated in tumorigenesis (Dong *et. al.* 2004). Research implicates SOX4 involvement in a diverse variety of carcinomas. *SOX4* expression is upregulated in: breast cancer cell lines (Graham *et. al.* 1999); small cell lung carcinoma (Friedman *et. al.* 2004); myeloid tumours (Boyd *et. al.* 2006; Tonks *et. al.* 2007); adenoid cystic carcinoma of the salivary gland (Frierson *et. al.* 2002); prostate cancer (Liu *et. al.* 2006); and colon cancer (McCracken *et. al.*

1997). Additionally, SOX4 has been identified as a marker between desmoplastic medulloblastoma (in which *SOX4* expression is low) and the more aggressive classical medulloblastoma, which exhibits a high level of both *SOX4* and *SOX11* (Lee *et. al.* 2002).

Blocking *SOX4* expression in a prostate cancer cell line (LNCaP) and breast cancer cell lines (MCF-7 and BT-474), by siRNA, induces apoptosis (Liu *et. al.* 2006). Expression of *SOX9* appeared to be up- or down- regulated in parallel to levels of *SOX4*, suggesting that regulation of *SOX9* may be, in part, by the action of SOX4. In addition, Liu *et.al.* revealed that expression levels of *BCL10*, *CSF1* and *NcoA4/ARA70* fluctuated in parallel to altered levels of *SOX4*. Moreover, it was identified that SOX4 could bind to the promoters of both TLE1 and PUMA/BBC3. However the implications of this binding action for the development of prostate cancer has not been described.

In tumourigenesis, SOX4 has been suggested as a regulator of metastasis, since inhibitory RNAs which bind SOX4 transcripts are expressed in normal breast epithelial cells. Expression of microRNA is lost in tumour cells undergoing metastasis (Liao *et. al.* 2008; Tavazoie *et. al.* 2008). Additionally, knockdown of *SOX4* transcript *in vitro* is capable of reducing proliferation of colon carcinoma cells (SW480), while overexpression enhances cells proliferation (Sinner *et. al.* 2007). This effect is thought to occur *via* an interaction of SOX4 with β-catenin, thereby regulating canonical-Wnt target genes, including *CyclinD1*.

Thus, it appears that Sox4 plays extensive roles in developmental, physiological and pathological processes. None of these roles are fully understood.

1.1.4 The role of Sox4 in cardiogenesis – Information from the study of a *Sox4* targeted null allele and a conditional *Sox4* allele.

A targeted null mutant allele of *Sox4* has been described (Schilham *et. al.* 1996). The phenotype was described as being a severe heart phenotype, with inadequate septation and valve development. Additionally mutants demonstrated an inability of B cells to differentiate. The *Sox4* null mutant was then further investigated with embryos staged between E12–14, in which the heart phenotype was described as

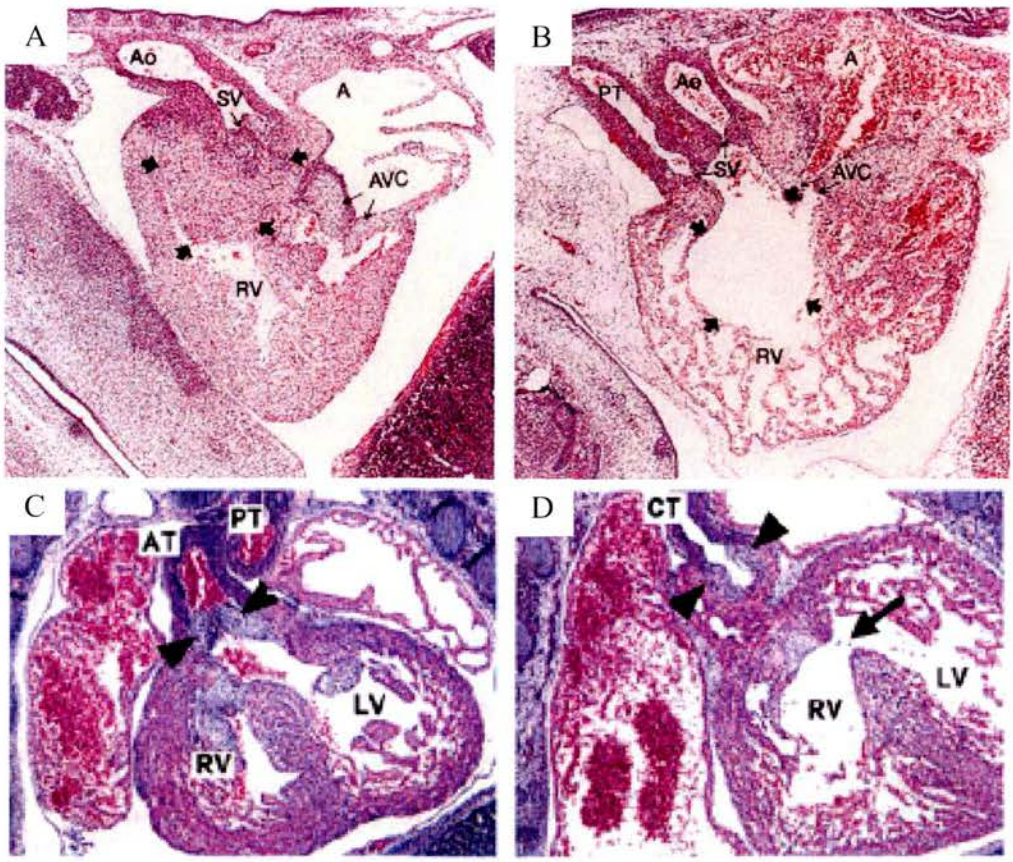

Figure 1.2: Null alleles of *Sox4* demonstrate a cardiac phenotype at E13.5-14. Schilham *et.al*. described the E14 *Sox4* null cardiac phenotype (sagittal sections, wild-type A; mutant B). (A) The wild-type heart demonstrates normal septation of the outflow tract and ventricles (thick black arrows). Additionally, atrioventricular valves are normal. (B) In contrast, *Sox4* null mutant hearts demonstrate a failure of septation (thick black arrows) and additionally common arterial trunk from the right ventricle. Penzo-Mendez *et.al*. described the *Sox4* conditional null phenotype, inactivated throughout the embryo (frontal sections, wild-type C, mutant D). (C) The wild-type heart demonstrates normal septation and semilunar valve formation (black arrowheads). (D) Mutant hearts demonstrate ventricular septal defects (black arrow) and semilunar valve hypoplasia (black arrowheads) and common arterial trunk. Abbreviations: A, atrium; Ao, Aorta; AT, aortic trunk; AVC, atrioventricular canal; CT, common arterial trunk; LV, left ventricle; PT, pulmonary trunk; RV, right ventricle; SV, semilunar valves. Images A and B from Schilham *et.al.* 1996; Images C and D from Penzo-Mendez *et.al.* 2007.

highly variable ranging from severe valve and septation defects to a mild septation defect of the right ventricle (Figure 1.2a and b). Left-right abnormalities were not described. The cardiac phenotype was considered to be a consequence of a lack of expression in the endocardial-derived cushions of the AVC and OFT, at E12.5. Interestingly, it was reported that no macroscopic phenotype was observed prior to E13.5. Embryos were only examined from E12-14.5. Yet a gap in this work can be seen when examining the percentages of homozygous mutants obtained in their genetic crosses (Ya *et. al.* 1998b). Ya *et.al.* reported that 18-20% of embryos in their study were homozygous for the *Sox4* null mutation. In order to satisfy the Mendelian ratio, this implies that the mutation must result in variable lethality from an earlier stage of development, which was not addressed in their paper.

In 2007, over ten years after the targeted null allele was described, a report of a conditional null allele was published (Penzo-Mendez *et. al.* 2007). When inactivated in all tissues, the phenotype of embryos was reported to be the same as that previously proposed for the null allele (Figure 1.2c and d). Given that *Sox4* demonstrates multiple expression domains throughout embryogenesis, the conditional allele will be highly useful to examine the function of Sox4 in other systems, without embryos succumbing to cardiac insufficiency.

1.1.5 Overlap of the *Sox11* null phenotype with the *Sox4* null phenotype.

As already described, Sox4 and Sox11 are phylogenetically related, and thus there may be functional overlap in their common expression domains (described in section 1.1.2).

Little is known about the function of Sox11 in developmental pathways. Limited expression domains have been described and overlap considerably with those published for *Sox4* (section 1.1.2), particularly in the developing nervous system. Sox11 has been proposed to be involved in epithelial-to-mesenchymal transition (EMT), given that its expression domains predominantly include regions of EMT during development (Hargrave *et. al.* 1997). Cardiac aspects of the *Sox11* null phenotype also overlap with that described for the *Sox4* mutant (Sock *et. al.* 2004). Hearts of *Sox11* null embryos exhibit ventricular septal defects, double outflow tract

from the right ventricle and inadequate OFT septation. Interestingly, *Sox11* null mice survive gestation and die shortly after birth, presumably from aberrant heart function. It has been suggested by Sock *et.al.* that Sox4 and Sox11 may be partially functionally redundant (Sock *et. al.* 2004), but clearly in cardiogenesis this is limited – especially since expression of *Sox11* in the heart is not detected until E14.5. How this reconciles with the phenotype in *Sox11* mutant embryos has not been described. Additionally it has been proposed that Sox4 may regulate *Sox11* in heart development (Sock *et. al.* 2004). This is one possible explanation for the increased severity, and thus earlier lethality, in the *Sox4* null. The third mouse Group C Sox gene, *Sox12*, does not demonstrate a phenotype when inactivated and it has been proposed that the presence of functional Sox4 and/or Sox11 render Sox12 redundant (Hoser *et. al.* 2008).

1.1.6 Summary

In summary, Sox4 has been demonstrated to be involved in multiple pathways in both embryonic development and adult physiology. The dramatic change in expression observed in tumorigenesis suggests that it may play a role in proliferation (as supported by analysis in cell lines) or in repressing terminal differentiation (a concept supported by the requirement of oligodendrocytes and glial cells of the CNS to downregulate *Sox4* expression in order to reach full maturity). Alternatively, in some tumours SOX4 is required for metastasis, thus may be required for EMT. Additionally, Sox11 has been proposed to be involved in EMT. There is considerable overlap in the published expression domains and null phenotypes between *Sox4* and *Sox11* suggesting that they may, to a certain degree, be functionally redundant, with the exception of heart development prior to E14.5, as only *Sox4* is expressed in this organ at these stages. Nevertheless, the convincing evidence of Sox4 being essential for appropriate cardiogenesis warrants further investigation to determine the embryonic origin of this phenotype. Determining the requirement for Sox4 in one developmental system (cardiogenesis) may indirectly contribute to the understanding of its action, and thus be useful for deciphering its activity in other processes.

1.2 EARLY MOUSE DEVELOPMENT

The blastocyst is a symmetrical polar structure which implants into the uterine wall at 4.5 days *post coitum* (dpc). It comprises trophectoderm cells to enclose the cells of the inner cell mass (ICM) and the blastocoel cavity lined by primitive endoderm (PE). The trophectoderm forms extraembryonic tissue while only the ICM contributes to embryonic tissue. The ICM can be harvested, *in vitro*, to enable derivation of embryonic stem (ES) cells. *In vivo,* the ICM expands into the blastocoel cavity to form a sheet of single-layer epithelial cells - the embryonic ectoderm, also called "epiblast". The primitive endoderm overlying the embryonic ectoderm expands with the ICM into the blastocoel cavity as a monolayer termed the visceral endoderm. In parallel, primitive endoderm adjoining trophoblast cells forms parietal endoderm. Together, trophectoderm and parietal endoderm are termed Reichert's membrane (this and following paragraph describing morphogenic changes and embryonic anatomy are more extensively described in (Kaufman 1992; Lu *et. al.* 2001)) (Figure 1.3)).

In mouse at 6dpc, a cluster of distal visceral endodermal cells move anteriorly within the visceral endoderm to form anterior visceral endoderm (AVE) (Figure 1.3). Around 6.5dpc posterior cells of the proximal embryonic ectoderm, at a point opposite the AVE, undergo a transformation to convert from epithelia to cells of a mesenchymal nature in the process of gastrulation. The region where this transition takes place is called the primitive streak, and the mesenchymal cells emerging are mesoderm. Mesoderm expands and migrates in three directions: proximally to become extraembryonic mesoderm of the allantois; bi-laterally around the embryonic ectoderm to form the mesodermal wings, contributing to the heart and head mesenchyme; and mesoderm which exits anteriorly from the primitive streak contributes to axial mesoderm. In addition to the formation of mesoderm, embryonic endoderm (also referred to as definitive endoderm), surface ectoderm and neural ectoderm are also created from the embryonic ectoderm. Definitive endoderm (so called to distinguish it from the visceral endoderm and parietal endoderm which are both extra-embryonic lineages) is formed by cells which exit the streak at the most anterior region and displace the adjacent layer of visceral endoderm (Lawson *et. al.*

1987) (reviewed in (Tam *et. al.* 1992)). The boundaries of this endoderm are continuous with the extraembryonic visceral endodermal layer. Embryonic ectoderm adjacent to the AVE is responsive to inductive signals to become neural ectoderm of the future head, while along the axis ectoderm contributes to the node and is retained adjacent to the primitive streak developing into posterior neural tissue as axial elongation proceeds. Once neural tube closure is complete, surface ectoderm covers the whole amniotic surface of the embryo.

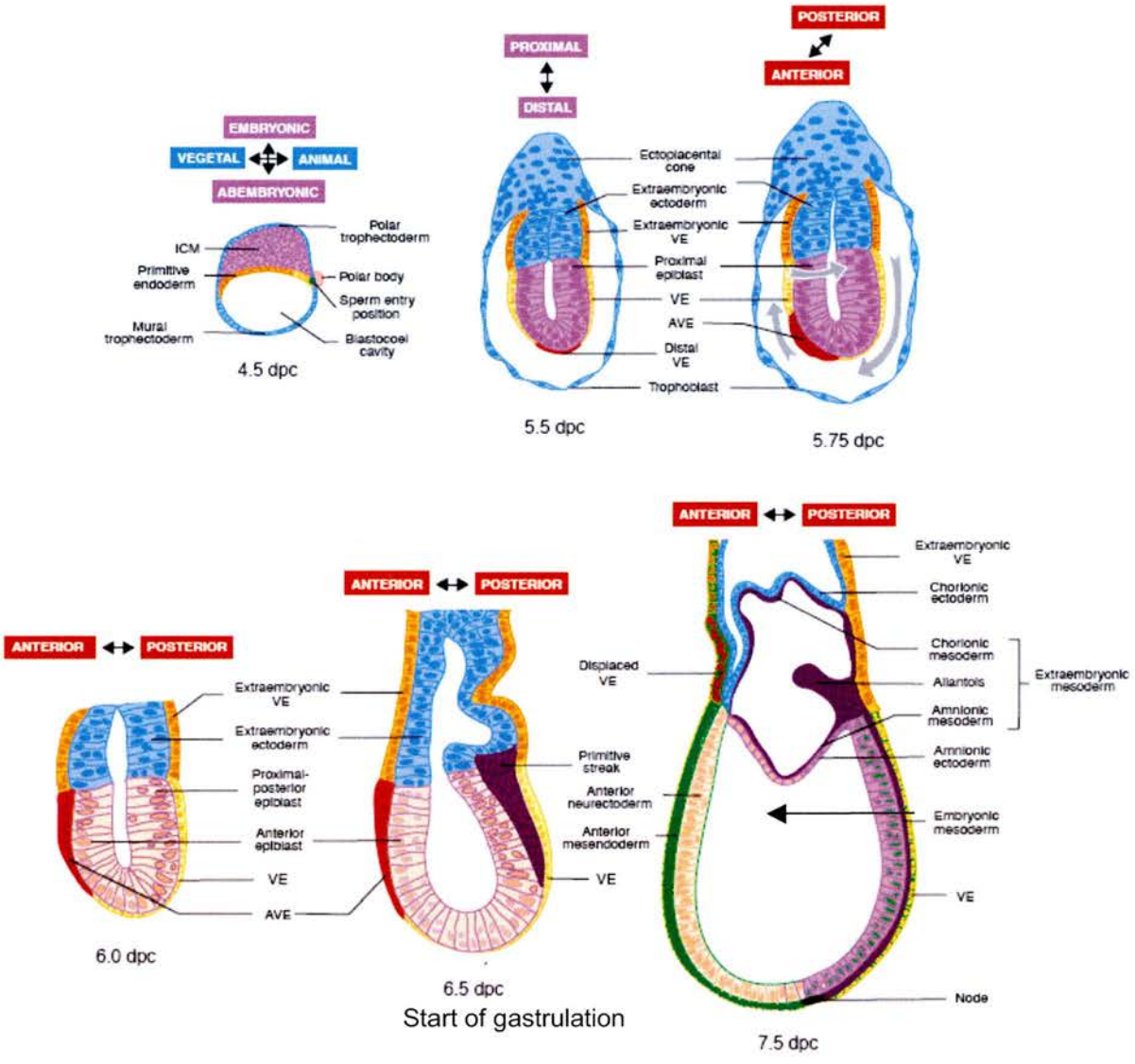

Figure 1.3: Early mouse embryonic development. The inner cell mass (ICM; purple at 4.5dpc) develops into the epiblast, surrounded by extraembryonic endoderm (5.5dpc and 5.75dpc) (VE; visceral endoderm). Anterior movement of the anterior visceral endoderm (AVE) occurs about 6.0dpc. Mesoderm is produced upon the start of gastrulation at 6.5dpc at the primitive streak (purple). By 7.5dpc the cardiogenic mesoderm has migrated away from the primitve streak, laterally around the embryo (direction is indicated by arrow). Adapted from Lu *et.al.* 2002.

1.3 FORMATION OF THE MOUSE HEART

The heart is one of the first organs to develop and become fully functional in vertebrate embryogenesis. It is a complex organ, whose formation requires not only the coordinated interaction of cells to form the different structural tissues, but also organisation to give rise to left-right asymmetry of the chambers, the valves, and also the vessels. The valves and vessels deliver blood to the heart and expel it into the vascular system.

At the physical level, formation of the heart is one of the well-defined processes of embryogenesis. Much of the knowledge of this process comes from the study of model organisms. At the molecular level, many factors are known to contribute to cardiogenesis. In contrast to our understanding of the morphological changes, the network of molecular interactions is far from being completely characterised. Selected aspects of cardiogenesis are described here, together with some description of molecular regulation, as a reference for that which is discussed elsewhere in the thesis.

1.3.1 Early heart development: cardiac progenitor cells; heart tube formation and looping; and early chamber specification.

Early heart development

Cardiac progenitors migrate within the mesodermal wings, transiting laterally from the streak to the anterior side of the embryo. At the early-headfold stage, the bi-lateral mesoderm meets and forms the cardiac crescent. The lateral mesoderm separates into two layers (Linask 1992) – the somatopleuric (or somatic) and the splanchnopleuric (or splanchnic) mesoderm separated by the intra-embryonic coelom, which is precursor to the pericardial cavity (Figure 1.4a). Splanchnic mesodermal cells in the anterior, or 'leading edge', of the lateral mesoderm are cardiogenic, as they contain precursors to both myocardial and endocardial cells (Manasek 1968). The mesoderm at the crescent is in close proximity to the sheet of definitive endoderm (foregut) (Parameswaran *et. al.* 1995). Endocardial precursor cells delaminate into the space between the endoderm and splanchnic mesoderm (Viragh *et. al.* 1989) preceding formation of the heart tube. Within both this

mesoderm and adjacent endoderm there is a specific region of *Nkx2.5* expression (Lints *et. al.* 1993). Expression of *Nkx2.5* continues throughout early cardiogenesis since it plays critical roles in regulation of gene expression leading to the four-chambered heart.

Structure and formation of the heart tube

The heart tube is a structure comprised of bi-lateral endocardial tubes surrounded by a layer of myocardial cells which adjoin the intra-embryonic coelomic cavity (DeRuiter *et. al.* 1992) (Figure 1.4b). The endocardial tubes fuse to form the internal endothelial layer of the central tube. Blood is pumped anteriorly in a unidirectional fashion, from the venous pole to the arterial pole. The surrounding myocardial layer contributes to myocardium. The extracellular matrix develops between the endocardium and myocardium, and is termed cardiac jelly (discussed in (Manasek 1975)). Structurally, from the venous pole of the heart tube, the inflow tract (IFT) comprises the left and right sinus venosus regions connected *via* a common atrial chamber to the ventricular chamber and from there to the bulbus cordis and finally the outflow tract (OFT) which is segmented into the conus arteriosus (proximal OFT) and truncus arteriosus (distal OFT) connected to the aortic sac (Stalsberg *et. al.* 1969). The aortic sac connects with the vessels of the arch arteries (within branchial arches connected to the OFT). The heart tube is connected by the dorsal mesocardium to the body wall.

The myocardium of the heart is patterned from two fields of cells whose lineage separates very early during cardiogenesis from one original precursor population (Meilhac *et. al.* 2004; Meilhac *et. al.* 2003) (Reviewed in (Buckingham *et. al.* 2005; Dunwoodie 2007)) (Figure 1.5c). Clonal analysis has shown that the first heart field (FHF) comprises myocardial cells of the cardiac crescent and subsequent heart tube. Mesoderm of the second (also termed secondary or anterior) heart field (SHF) is located adjacent to the involuting foregut endoderm from the crescent stage until heart looping (Figure 1.5a, b). Initially, SHF mesoderm develops into the dorsal mesocardium, adjoining the heart tube to the body wall. Subsequently, dorsal mesocardial cells of the SHF integrate into the heart tube at both the venous and atrial poles. SHF cells contribute with FHF cells to the atria and atrioventricular

canal. Also, cells of the SHF form the OFT and right ventricle (RV), where they predominante over the FHF contribution. The left ventricle (LV) is entirely populated by FHF cells (Meilhac *et. al.* 2004; Meilhac *et. al.* 2003) (Figure 1.5d, e).

Initial rightward looping of the linear heart tube occurs from E8.0 and is accompanied by expansion ('balloon-like' growth) of the prospective heart chambers (reviewed in (Christoffels *et. al.* 2004a)) (Figure 1.4c). This looping leads to the arrangement of what will become the four chambers of the mature heart (Figure 1.4d). Looping is required for appropriate juxtaposition of the presumptive chambers. It is additionally required for the establishment of inner and outer curvature. Along the inner curvature, cushion development is necessary for septation, while the outer curvature is the site of trabeculation. It is the differences in gene expression in the SHF and the FHF, along both the rostral-caudal and dorso-ventral axes that gives rise to the variations between ventricles, atria and intermediate regions, as well as the left and right side of the heart.

Molecular identity of the primary and secondary heart fields

Clonal analysis has contributed to understanding the movement and contribution of two distinct populations of cells within the heart. However, because of the integration of SHF into most FHF regions, few genes are characterised as being "FHF markers". Determining whether a gene is important for the FHF is possible by examining mutants for a left-ventricular phenotype: *Hand1* (*Heart and neural crest derivatives expressed transcript 1*) is expressed in left ventricular myocardium and mutants demonstrate defects of the left ventricle (McFadden *et. al.* 2005); *Tbx5* (*T-box5*) is expressed strongly at the cardiac crescent and later in the atria and left ventricle, while mouse mutants for *Tbx5* present with left ventricular hypoplasia (Bruneau *et. al.* 1999; Bruneau *et. al.* 2001).

An understanding of the contribution of SHF cells to the OFT has come from analysis of the *Fgf10-lacZ* reporter mouse line (Kelly *et. al.* 2001). Furthermore, the dynamic contribution of SHF cells to the heart tube is dependent upon the differential expression of several genes, as shown by the phenotype upon gene inactivation. Some of these are listed here:

- Hearts of *Isl1* (*Islet-1*) mutant embryos lack the OFT, right ventricle and much of the atria (Cai *et. al.* 2003). *Isl1* has been proposed to be a key regulator of proliferation and migration of the SHF.

- An immediate downstream target of Isl1 (*via* interaction with Gata4; (Dodou *et. al.* 2004)) is *Mef2c (Myocyte enhancer factor 2c)*. The *Mef2c* mutant cardiac phenotype includes an absence of the right ventricle and underdeveloped OFT and atria (Lin, Q *et. al.* 1997). The primitive singular ventricular chamber of *Mef2c* mutants demonstrates a significant reduction in cell proliferation (Vong *et. al.* 2006).

- Both *Hand2* and *Foxh1* mutants demonstrate right-ventricular hypoplasia (Srivastava *et. al.* 1997; von Both *et. al.* 2004).

- Nkx2.5 has also been found to regulate proliferation of cells that form the SHF (Prall *et. al.* 2007). *Nkx2.5* mutant hearts appear to form a primitive heart tube with myocardium and endocardium (Lyons *et. al.* 1995). The defect was evident at E8.25-8.5 when looping morphogenesis was unable to occur, and embryos lacked expression of the ventricular marker *Mlc2v* (*Myosin light chain 2v* also *myosin, light polypeptide 2, regulatory, cardiac, slow*; *Myl2*). Nkx2.5 is critical for suppression of genes which (1) promote the maintenance of cardiac progenitor cells; and (2) negatively regulate SHF proliferation. Thus the *Nkx2.5* null phenotype appears to be a consequence of an inability of progenitor cells to proliferate and mature into SHF cells (Prall *et. al.* 2007).

In summary, the developing heart tube is formed from two distinct populations of cardiac cells arising from originally common progenitors. Work in this field has contributed greatly to the understanding of the cellular movements within the developing heart. However, the genetic regulation of cells within this process is far from being clearly understood.

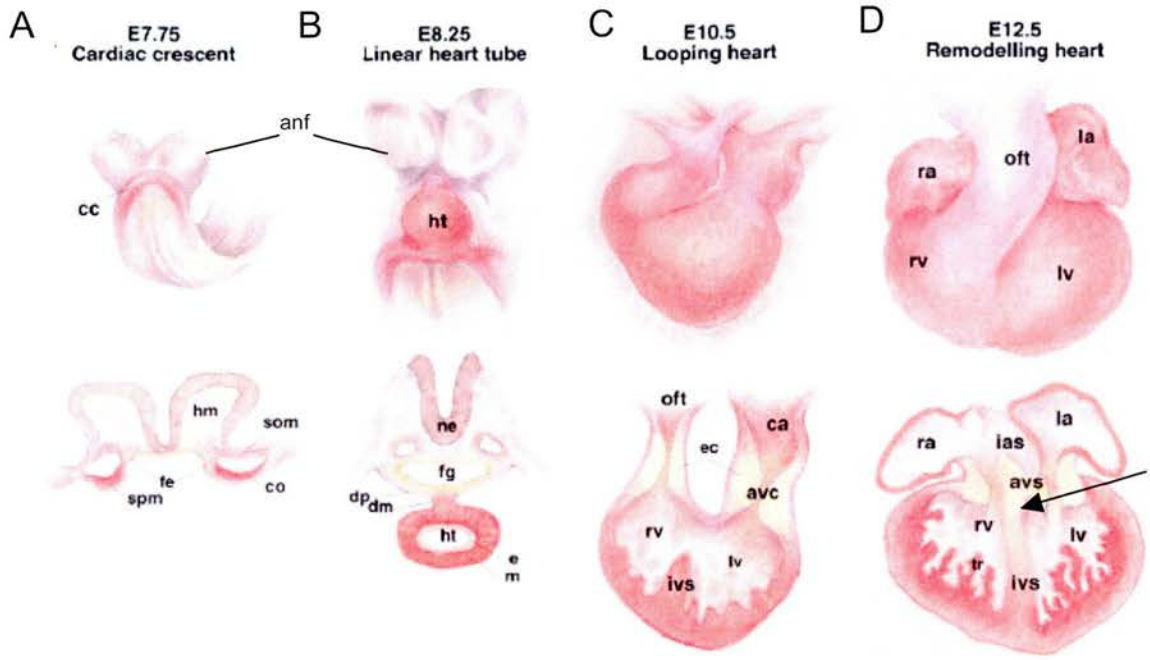

Figure 1.4: Mouse cardiac development from the cardiac crescent to the four-chambered heart. (A) Lateral mesoderm meets on the anterior side of the endoderm and forms the cardiac crescent at about E7.75. A section through this region reveals the two mesodermal layers of somatic and splanchnic mesoderm separated by the intra-embryonic ceolom, and adjacent to the foregut endoderm. The cardiac crescent develops into the heart tube (B) which is comprised of endocardial and myocardial layers, attached to the body wall by the dorsal mesocardium. (C) As the heart tube loops the endocardial cushions develop and the interventricular septum begins to form as do trabeculae from the outer myocardium of the ventricles. (D) By E12.5, the four-chambers of the heart are evident and septation, as well as valve formation has occurred. Arrow indicates the fusion of the muscular septum to the membranous region of the atrioventricular septum. Abbreviations: anf, anterior neural folds; avc, atrioventricular canal; avs, atrioventricular septum; ca, common atrium; cc, cardiac crescent; dm, dorsal mesocardium; dp, dorsal pericardium; e, endocardium; ec, endocardial cushions; fe, foregut endoderm; fg, foregut; hm, head mesenchyme; ht, heart tube; ias, inter-atrial septum; ivs, interventricular septum; co, intra-embryonic coelom; la, left atrium; lv, left ventricle; m, myocarium; ne, neurectoderm; ra, right atrium; rv, right ventricle; OFT, outflow tract; som, somatic mesoderm; spm, splanchnic mesoderm; tr, trabeculae. Adapted from Stennard and Harvey, 2005.

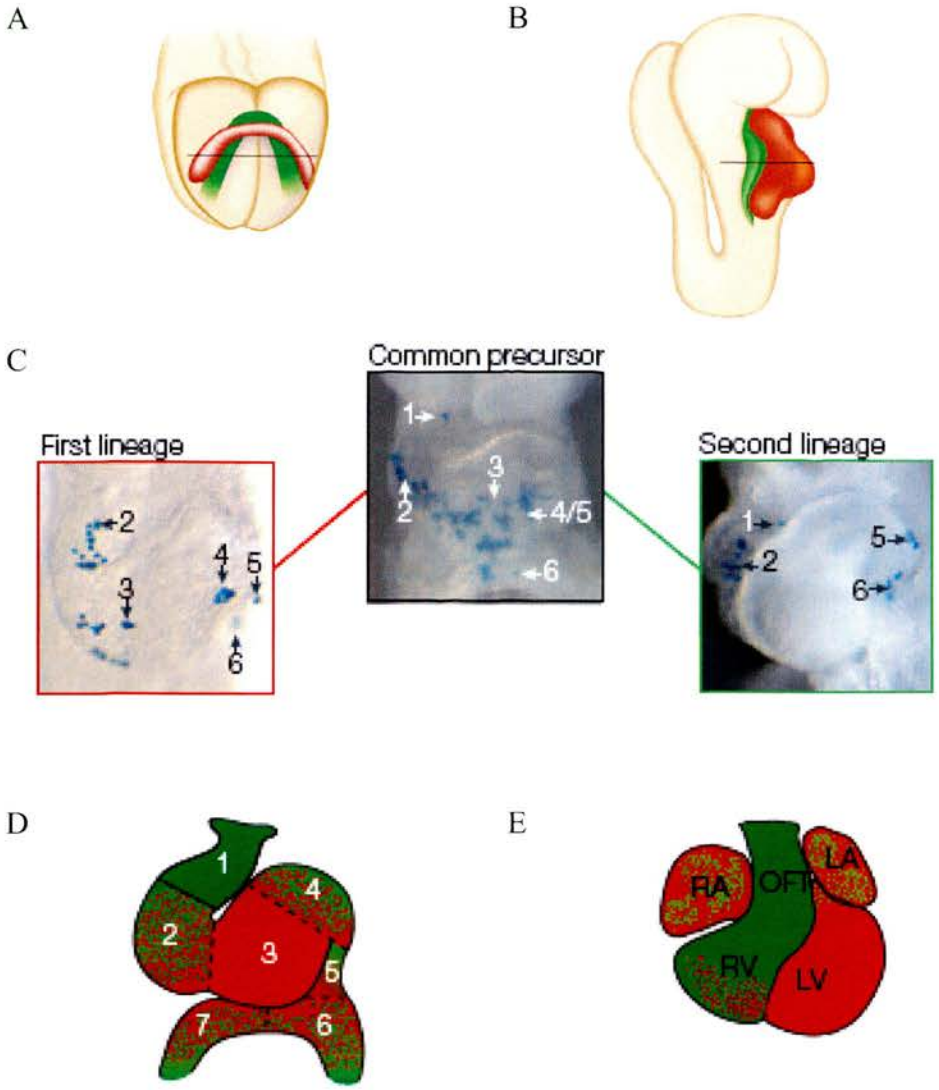

Figure 1.5: Contribution of the first and second heart fields to the developing heart. The heart is patterned from two fields of myocardial precursor cells which arise from an early common precursor. First heart field is marked as red. Second heart field is marked as green (A) Crescent-stage myocardium develops from the first heart field lineage, while the second heart field comprises adjacent mesoderm. By E8 (B), the heart tube has formed from the FHF lineage, while the SHF comprises adjacent dorsal mesenchyme. (C) Lineage analysis of lacZ positve cells (blue) in E9 hearts revealed that the first and second lineages arise from a common precursor. At E9 (D) and E10.5 (D) both first and second lineages contribute to the heart. First heart field comprises regions shown in red; Second heart field contributes to the regions shown in green. Abbreviations: 1, outflow region; 2, primitive right ventricle; 3, primitive left ventricle; 4/5, atrioventricular region; 6/7, primitive atrium; LA, left atrium; LV, left ventricle; OFT, outflow tract; RA, right atrium; RV, right ventricle. Adapted from (A-B) Dunwoodie, 2007; and (C-E) Buckingham *et.al.*, 2005.

1.3.2 Ventricular chamber formation: Trabeculation and formation of the ventricles

Specification of the expanding and looping heart tube requires differential gene expression. This must occur within both chamber and non-chamber myocardial regions, such that each region acquires a distinct physiological function. Chamber myocardium expands along the outer curvature, while non-chamber myocardium undergoes a different series of morphological changes (discussed below, section 1.3.3). Upon looping, some genes, which are widely expressed in the linear heart tube, become more regionalised in their domains. For example, *Gata6* and *Hand2* are both expressed throughout the heart tube. Yet by E9, *Gata6* expression becomes restricted to the AVC and OFT, while expression of *Hand2* becomes largely restricted to the OFT and future right ventricle (Davis *et. al.* 2001; Thomas *et. al.* 1998). In contrast, *Hand1* expression is restricted in the heart tube. By E9, the domains of *Hand1* expression subsequently develop into *Hand1* expressing regions of the OFT and outer curvature of the left ventricle (Biben *et. al.* 1997; Thomas *et. al.* 1998).

Chamber formation requires the initiation of a myocardium-specific programme of gene expression, to promote differentiation, or to permit contractility. Some of these genes include: *Gap junction protein, alpha 1 (Gja1; Connexin43; Cx43), Gap junction protein, alpha 5 (Gja5; Connexin40; Cx40), Small muscle protein, X-linked (Smpx; Chisel; Csl), Iroquois related homeobox 5 (Irx5)* and *Natriuretic peptide precursor type A (Nppa;* previously *Atrial Natriuretic Factor, ANF)*. Expression of *Cx40* and *Cx43* is timed with the appearance of rhythmic contractions in the heart tube, with expression becoming restricted to working myocardium (Delorme *et. al.* 1997). The connexin proteins form gap junction channels between cardiomyocytes to facilitate cardiac electrical conduction (Jalife *et. al.* 1999). *Chisel* is a marker of chamber myocardium while *Irx5* marks chamber-specific endocardium (Christoffels *et. al.* 2000; Palmer *et. al.* 2001). Expression of *Nppa* marks the transition from primary myocardium to mature myocardium (Houweling *et. al.* 2005; Zeller *et. al.* 1987). Within chamber myocardium, *Nppa* expression is directed by the cooperative action of Nkx2.5 and Tbx5 on the *Nppa* promoter (Hiroi *et. al.* 2001). In contrast,

expression of *Nppa* in non-chamber myocardium, such as in the atrioventricular canal and OFT, is restricted by Tbx2 or Tbx3, which bind the *Nppa* promoter with Nkx2.5 (Habets *et. al.* 2002). Tbx2 also represses expression of *Cx40 and Cx43. Tbx2* is expressed in myocardium of non-chamber regions (Christoffels *et. al.* 2004b). The function of Tbx2 is not just to restrict regions of non-chamber myocardium from differentiating into chamber myocardium. It is thought that an additional function of Tbx2 is to restrict proliferation in these domains, since Tbx2 has been shown to repress *Nmyc1* expression directly (Cai *et. al.* 2005). *Nmyc1* (also *v-myc myelocytomatosis viral related oncogene, neuroblastoma derived; Mycn*) null embryos demonstrate severe cardiac hypoplasia, indicating that Nmyc1 is required for early myocardial proliferation (Davis, A *et. al.* 1993; Davis, A C *et. al.* 1993). Expression of *Tbx2* is tightly regulated by its repressor, Tbx20 (Cai *et. al.* 2005; Singh *et. al.* 2005; Stennard *et. al.* 2005), which is expressed throughout the heart from the early crescent stage (Kraus *et. al.* 2001b). Clearly, some factors are required for both chamber formation and intermediate regions, although their role is dependent upon local gene expression.

Trabeculae are an essential morphological feature of ventricular chamber myocardium (reviewed in (Wagner *et. al.* 2007)). Development of the trabeculated myocardium commences on the 10^{th} day of gestation (Figure 1.6). Specified cells of the outer curvature myocardium form projections of cardiomyocytes into the lumens of the ventricular chambers (Icardo *et. al.* 1987). Trabeculation requires the endocardium to establish contact points with the myocardium. The myocardium then proliferates and some myocardial cells emerge as extensions into the ECM, towards the endocardium (Icardo *et. al.* 1987) (Figure 1.7). Signalling during trabeculation has been described to some extent, exploring the molecular cross-talk between the endocardium and myocardium, *via* the ECM. Some of these processes are discussed here. Most notably, Neuregulin 1 (Nrg1) is essential for trabeculation (Kramer *et. al.* 1996). Neuregulin 1 (Nrg1) is an epidermal growth factor signalling molecule expressed by cells of the endocardium in the early heart tube, while its receptors ErbB2 and ErbB4 are presented on the surface of the myocardium (Lemmens *et. al.* 2006). Loss of signalling through the ErbB2/ ErbB4 dimer results in defective

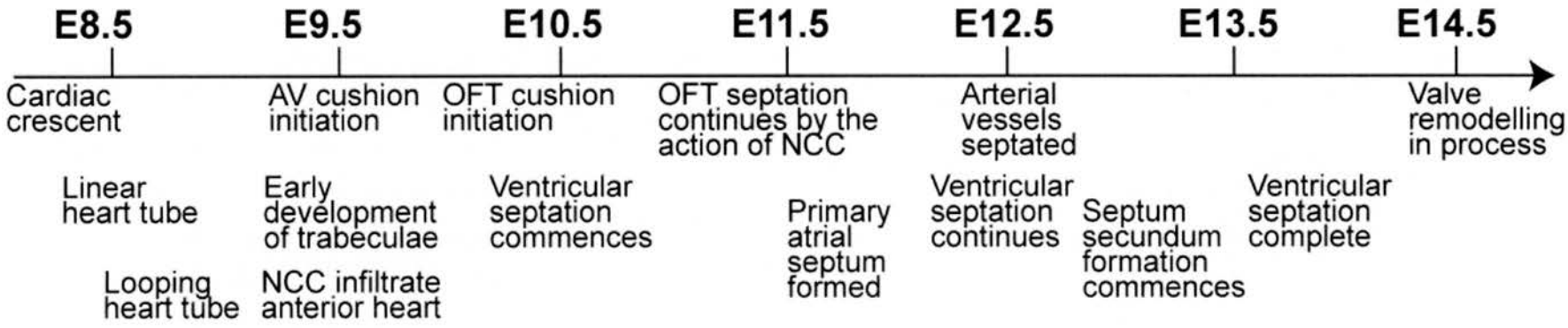

Figure 1.6 : Timeline for key events in the formation of the mouse heart. The temporal sequence of events in the morphological development of the mouse heart commences with the visible formation of the cardiac crescent and continues through to the formation of the four chambered, septated heart. Adapted from Henderson *et. al.* 2009; Webb *et. al.* 1998.

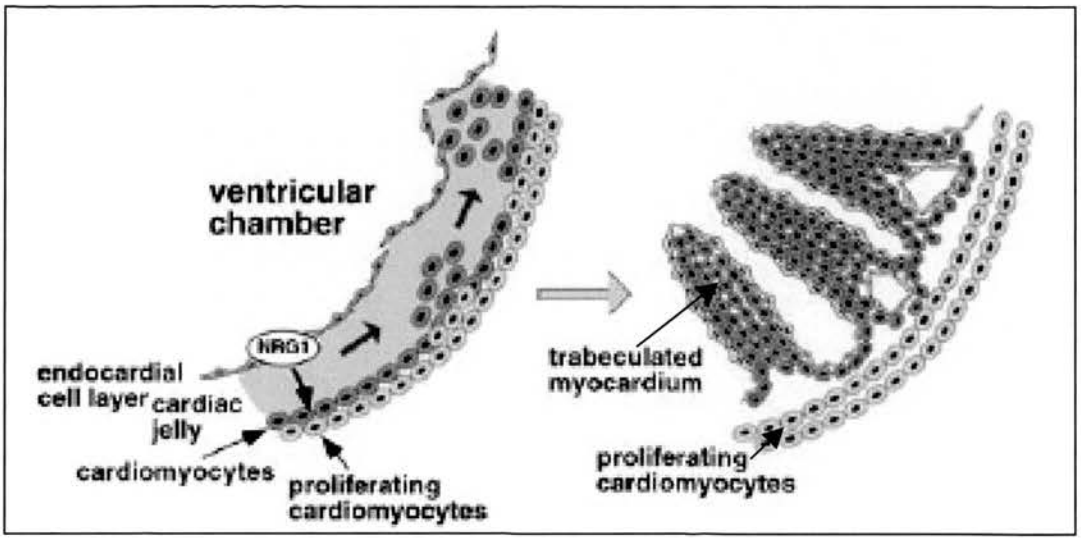

Figure 1.7: Formation of the trabeculated myocardium. Cells of the endocardium and myocardium send and receive morphogenetic cues to produce trabeculae. Myocardium is induced to proliferate and form projections into the extracellular matrix (cardiac jelly) towards the endocardium. Expression of *Neuregulin 1 (NRG1)* from the endocardium is a key factor in this process. Adapted from Wagner *et.al.*, 2007.

trabeculation and a lethal cardiac phenotype (also reviewed in (Garratt *et. al.* 2003)). Additionally, Bmp10 (Bone morphogenic protein 10) has been shown to be a necessary factor in the process of trabeculation. Ablation of *Bmp10* results in severe hypoplasia (Chen, H *et. al.* 2004). Examination of the phenotype of *Bmp10* mutant hearts revealed that Bmp10 has dual activities within cardiac development. Its first function is to maintain cardiac gene expression, since expression of *Nkx2.5* and *Mef2c* are drastically reduced in *Bmp10* null hearts at E9.5. The second function of Bmp10 is either to prevent the premature activation, or antagonise the activity of the cell cycle regulator p57kip2 at E13.5. Through this, Bmp10 represses premature terminal differentiation and promotes proliferation of cardiomyocytes (Chen, H *et. al.* 2004). Thus, aspects of some signalling pathways are known to be necessary for trabeculation, yet the complete network of communication, which results in the formation of two distinct myocardial layers – compact myocardium and trabecular myocardium – requires considerable investigation.

1.3.3 Development of the endocardial cushions of the AVC and OFT and subsequent valve and septum formation

Endocardial cushion formation

Endocardial cushions develop from E9.5 between the common atria and ventricle (atrioventricular) and from E10 within the outflow tract (Figure 1.6). They are precursors to the valves of the heart as well as the mesenchymal-derived septum. Thus, in this way, cushion mesenchyme contributes to septation of the heart into the four-chambered pump, ensuring that blood flows in one direction (Figure 1.8). Formation of the cushions relies on early signalling, from the looping heart tube stage onwards, between the endocardium and adjacent non-chamber myocardium, across the ECM. This signalling results in an epithelial-to-mesenchymal transition (EMT) and the production of mesenchyme within the ECM (Markwald *et. al.* 1977) (Figure 1.9a). The process of EMT requires initial induction of the endocardial cells to delaminate. In order for this to occur, endocardial expression of the cell adhesion molecule VE-cadherin, must be downregulated. VE-cadherin is negatively regulated by Tgfβ and BMP signalling from the myocardium (Boyer *et. al.* 1999; Nakajima *et. al.* 2000; Romano *et. al.* 2000; Timmerman *et. al.* 2004) (Figure 1.9b). After

induction, endocardial cells migrate into the ECM (delamination), acquire cell-matrix connections and adopt a mesenchymal character. In the ECM, mesenchymal cells proliferate, mature and undergo terminal differentiation into cells of either the mature valves or membranous septum.

Genes expressed in the cushions, but not in other regions of the heart, may play a role in endocardial cushion formation. Additionally, by examining embryonic expression domains, the expression of a gene may be shown to coincide with other regions of EMT in the embryo. Several key molecular aspects have been characterised as being required for this process (reviewed extensively in: (Mercado-Pimentel *et. al.* 2007; Schroeder *et. al.* 2003; Srivastava *et. al.* 2000; Wagner *et. al.* 2007)). As examples, Notch signalling and Vegf signalling are both necessary for EMT in the heart.

Levels of Notch signalling, *via* Delta4, contributes to the process of EMT, by reducing cellular adhesion between endocardial cells programmed to delaminate (Grego-Bessa *et. al.* 2007; Timmerman *et. al.* 2004). Ablation of Notch target genes *Hey1* and *HeyL* produces a cardiac phenotype consistent with impaired EMT (Fischer *et. al.* 2007). Endocardial cells with mutations in Notch pathway factors (*Hey1/L. Hey2, Notch1*) are able to delaminate but are unable to transform into mesenchymal cells. Loss of Hey1/L function results in a reduced expression of *matrix metalloproteinase-2* (*Mmp2*). Mmp2 is normally responsible, in part, for degrading the ECM as the mesenchyme proliferates and occupies the region (Song *et. al.* 2000). Thus Notch signalling functions at two stages of EMT – delamination and ECM reconstitution.

Additionally, Vegf signalling play an important role in both initiating and ending the process of EMT (Dor, Y *et. al.* 2001; Dor, Y *et. al.* 2003) (Figure 1.9c). In the local region of the developing cushion, low Vegf signalling is required for delamination of endocardium. Levels of Vegf signalling are strictly regulated by *NFATc1* expression in the endocardium (Chang *et. al.* 2004). Initially, at E9 NFAT signalling is required for repression of myocardial Vegf. A second wave of NFAT signalling later occurs in the endocardium at E11 to facilitate the construction of valves.

The mesenchymal atrioventricular cushions (AVC) are separated spatially into the inferior (IC) and superior (SC) cushions. Proliferation of the mesenchyme within the endocardial cushions results in expansion of the cushions. This is tightly regulated by NFATc which coordinates the switch from mesenchyme proliferation to valve formation in specific regions of the atrioventricular cushions (Chang *et. al.* 2004). The endocardial-derived mesenchyme of the AVC assists in the formation of the atrial septum, as well a contributing to the ventricular septum, atrioventricular septation, mitral and tricuspid valves, and to septation of the outflow tract by juxtaposition of AVC mesenchyme with the outflow tract cushions. The process of septation within the heart, beyond the initial cushion formation, is complex. It requires dynamic tissue rearrangements to correctly align the heart chambers. The understanding of anatomy and tissue movement resulting in formation of the septal structures has come from detailed serial sectioning and histology across specific stages of gestation from the 10^{th} day of gestation (E9.5). These processes will be detailed in the following sub-sections.

Valve formation

Unidirectional valves develop between the atria and ventricles on either side of the heart, as well as between the ventricles and the arterial vessels. This is essential for maintaining the flow of blood within the heart. The functionality of valves relies on the development of the valve leaflets, as well as the fibrous structure through which the leaflets remain attached to the heart and the supporting tendinous cords and papillary muscles. The leaflet mesenchyme differentiates into fibrous connective tissue at both the ventricular inlet and outlet (Lamers *et. al.* 1995).

In the atrioventricular channels, the mitral (also, bicuspid) valve forms on the left side of the heart and the tricuspid valve forms on the right. The mitral valve develops with two leaflets (the mural and aortic leaflets) while the tricuspid valve develops three leaflets (the cranial and caudal mural leaflets, and the septal leaflet). In the OFT, the aortic and pulmonary semi-lunar valves form between the ventricles and the arterial vessels (aorta and pulmonary artery).

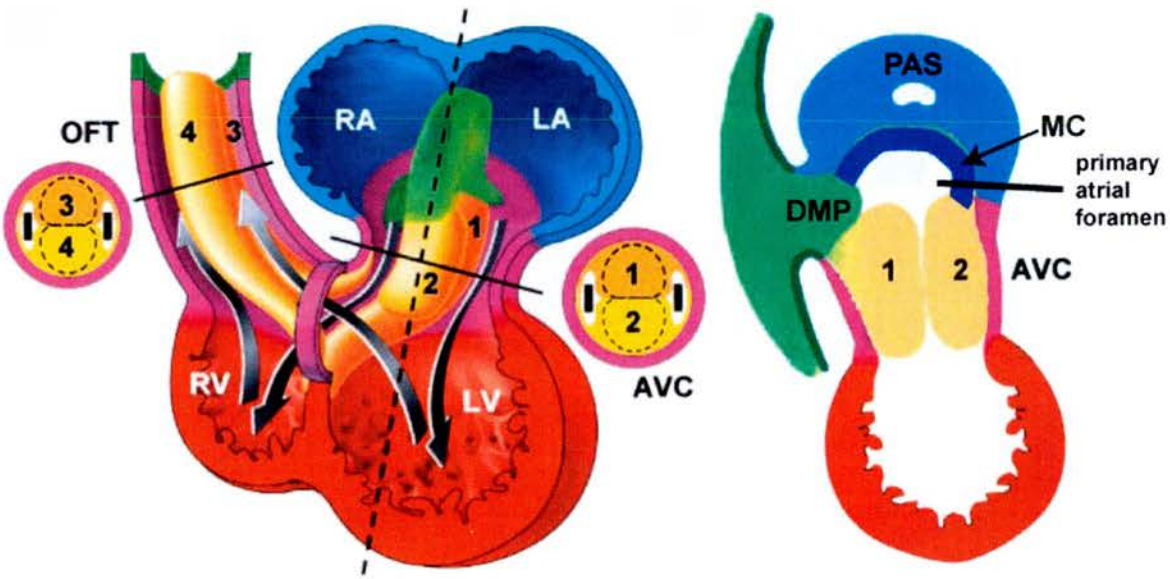

Figure 1.8: Formation of the cushions and septal structures in the developing heart. Diagram representing a section through the developing four-chambered heart, just before septation. Endocardial cushion mesenchyme (yellow/orange) contributes to the atrioventricular canal (numbers 1 and 2; image cross section as indicated by solid black line on right) and the outflow tract (numbers 3 and 4; image cross section as indicated by solid black line on left). The mesenchyme also contributes to atrioventricular septation. Section through the plane marked by a dashed line reveals the positioning of the atrioventricular cushions with respect to the dorsal mesenchymal projection (DMP) and the mesenchymal cap (MC) of the primary atrial septum (PAS). The mesenchmal components fuse with the cushion mesenchyme to close the primary atrial foramen. Abbreviations; AVC, atrioventricular canal; DMP, dorsal mesenchymal projection; LA, left atrium; LV, left ventricle; MC, mesenchymal cap; PAS, primary atrial septum; OFT, outflow tract; RA, right atrium; RV, right ventricle. Image adapted from Lamers *et.al.*, 2002.

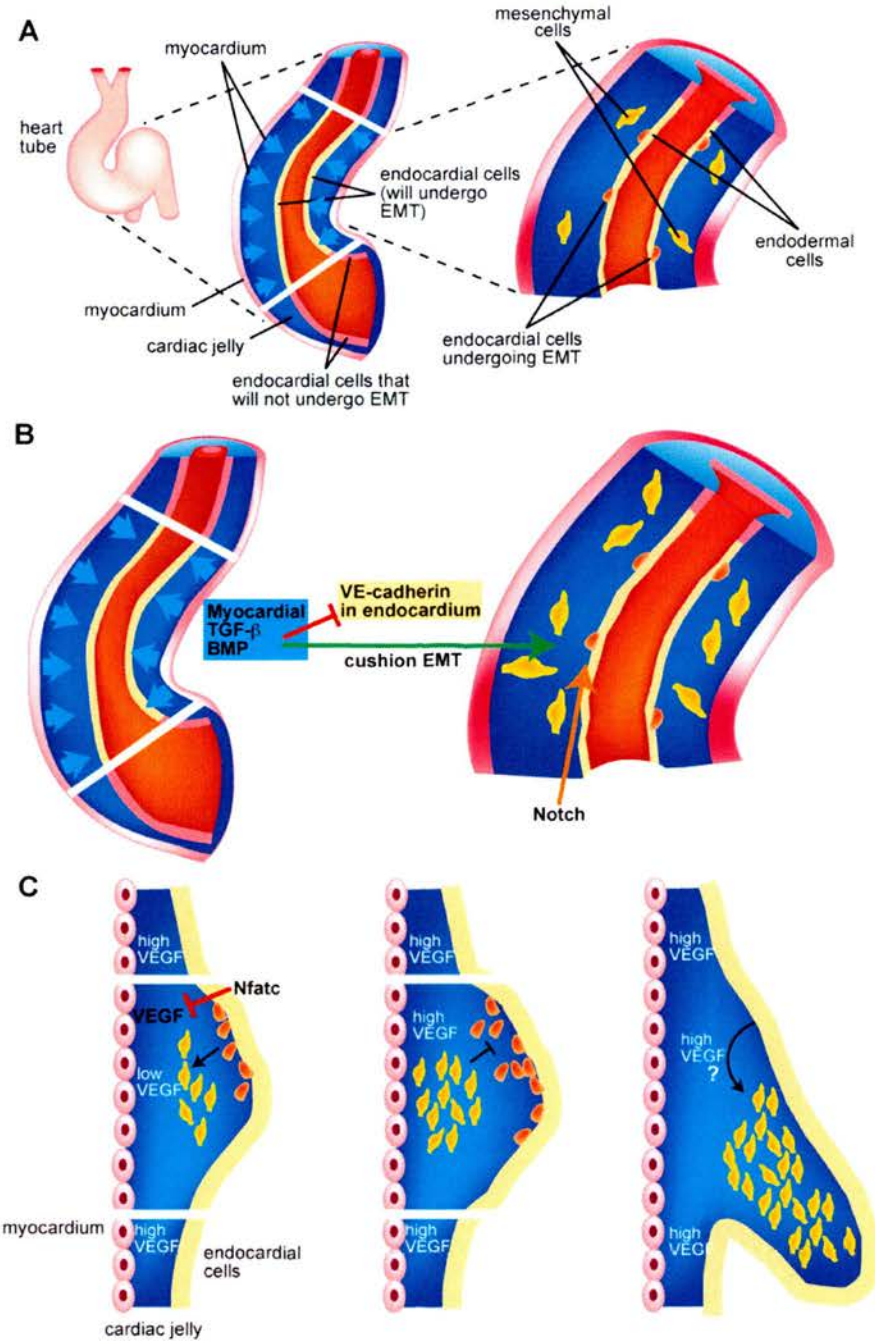

Figure 1.9: Formation of the endocardial cushions and their contribution to the developing heart. (A) Within the atrioventricular canal and outflow tract, regions of endocardium are programmed to undergo an epithelial-to-mesenchymal transition and delaminate into the extracellular matrix (cardiac jelly). (B) Several signalling pathways have been identified as playing key roles in this process. BMP and TGF-β signalling from the myocardium act on the endocardium to repress expression of VE-cadherin and promote EMT. Additionally, Notch signalling in the endocardium and nascent mesenchymal cells is required (described further in the text). (C) The process of cushion and valve formation is reliant upon a local decrease in the levels of VEGF, as a result of Nfatc signalling from the endocardium. Outer regions of cushion still retain high levels of VEGF expression. Once sufficient mesenchymal cells have been produced, central VEGF levels are elevated and the process of EMT ceases. The mesenchyme then develops into the valves of the outflow tract, atrioventricular canal and contributes to atrioventricular septation. Adapted from (A, B) Kirby, 2006; and (B) Wagner *et.al.*, 2007

Lineage analysis has revealed that the mature developed valves are predominantly derived from endocardially-derived mesenchyme, with no contribution from epicardial-derived cells or cardiac neural crest (de Lange *et. al.* 2004; Lincoln *et. al.* 2004), although whether or not cardiac neural crest contribute to the valves appears dependent upon genetic background (Hildreth *et. al.* 2008; Nakamura *et. al.* 2006). A small proportion of myocardial cells contribute in a transitory manner to the mural valves, but are subsequently replaced by endocardially-derived cells (de Lange *et. al.* 2004). One of the key signalling pathways required by the endocardium, involved in valve development and maturation, is that of NFATc/calcineurin (Chang *et. al.* 2004). Blocking NFAT signalling at E11 in mouse resulted in valvular defects including a failure of the atrioventricular valves to elongate and a failure of OFT valve morphogenesis from the endocardial cushions (Chang *et. al.* 2004).

The leaflets develop in different ways (de Lange *et. al.* 2004; Lincoln *et. al.* 2004). The aortic and septal leaflets of the mitral and tricuspid valves develop from atrioventricular cushion mesenchyme, by proliferation up to E11.5, and are continuous with the mesenchyme of the atrioventricular septum. The septal leaflet develops with a connection to the interventricular myocardium until late gestation, while the aortic leaflet develops without connections to the myocardium. In contrast, the mural leaflets of both the mitral and tricuspid valves develop *via* a protrusion of atrioventricular myocardium on the left at E9.5 and the right E10.5. The protrusion extends into the ventricular lumen, and from E11.5 endocardial-derived mesenchyme proliferates on the myocardial scaffold to develop into the fibrous mural leaflets (de Lange *et. al.* 2004). Within the OFT, at the end of the 11th day of gestation, the endocardial cushions fuse and develop into mesenchymal swellings of the future valves of the aorta and the pulmonary trunk (Webb *et. al.* 1998a). Valve development in the OFT will be further discussed in the context of cardiac neural crest.

Atrial septation

Leading up to atrial septation, the common atrium is the source of entry into the heart. The venous entry is initially composed anatomically of the left and right sinus horns. As cardiogenesis continues, by E11 the pulmonary vein develops through the mesocardium and enters left of the midline of the atrial chamber (Anderson *et. al.* 2006; Webb *et. al.* 1998b). The once bilateral sinus horns rotate for systemic circulation to enter the heart from the right side of the mouse heart at the left and right superior caval veins, separated at this stage by a fold in the right arterial wall termed the sinus septum. Also by E11, the sinoatrial valves (left and right venous valves) have developed to mark the boundary of the left and right sinus venosus and the right atrium (Webb *et. al.* 1998a).

The muscular primary atrial septum (also, septum primum, PAS) develops at the midline of the common atrium, from the atrial wall, and grows towards the endocardial cushions (Anderson *et. al.* 1999) (Figure 1.10a). Molecular markers, such as *Pitx2*, have indicated that in mouse cardiogenesis the primary atrial septum arises from cells of the left atrium (Campione *et. al.* 2001; Franco *et. al.* 2000). The primary atrial septum is surrounded by a cap of endocardially-derived mesenchyme.

Mesenchyme from the dorsal mesocardium (the dorsal mesenchymal projection, DMP, also vestibular spine or spina vestibuli) migrates into the atria between the left and right pulmonary ridges at E10.5 (Anderson *et. al.* 1999; Mommersteeg *et. al.* 2006; Webb *et. al.* 1998a). This is a second contribution to the atrial septum and this mesenchyme is of SHF origin and expresses *Isl1* (Mommersteeg *et. al.* 2006; Snarr *et. al.* 2007). As the DMP develops towards the endocardial cushions, contributing to the closure of the PAS, mesenchyme differentiates into atrial myocardium, as shown by expression of *Mlc2a*, but retains a non-myocardial mesenchymal cap, establishing continuity with the mesenchymal cap of the primary atrial septum – although of different origin (Mommersteeg *et. al.* 2006).

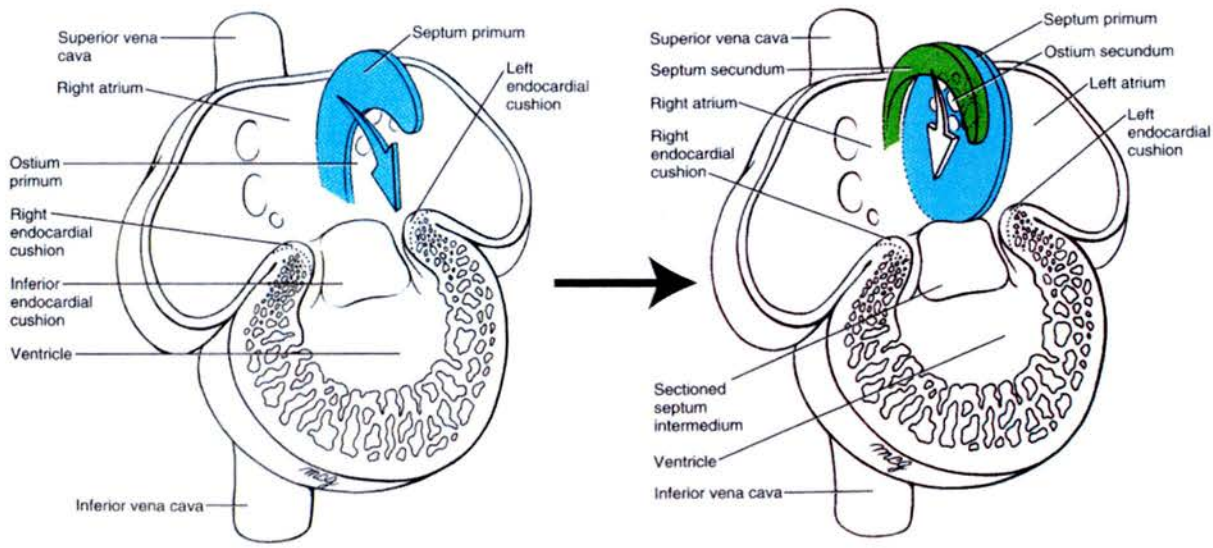

Figure 1.10: Formation of the primary atrial septum. (A) Initially, the septum primum (blue) develops from myocardium of the atrial chamber, with a cap of endocardial-derived mesenchyme. It fuses with mesenchyme of the atrioventricular cushions and dorsal mesenchymal projection to form the primary septum and close the ostium primum. Small ruptures develop in the septum primum, forming the ostium secundum as connections between the two atria. (B) The septum secundum (green) forms as infoldings from the myocardium adjacent to the primary septum. Human development, adapted from Larsen *et.al.* 2001.

The connecting channel which remains between the left and right atrium at the AVC, encircled by the developing primary atrial septum, is termed the primary atrial foramen (also, foramen primum or ostium primum). As the primary atrial septum grows to close up the primary atrial foramen, fenestrations appear in the anterior region of the septum, thus forming the secondary foramen (also, foramen secundum or ostium secundum) (Anderson *et. al.* 1999; Webb *et. al.* 1998a). Closure of the primary atrial foramen occurs on the 12th day of gestation when the mesenchymal cap from the atrial septum and the mesenchyme from the dorsal mesocardium fuse with the atrioventricular cushions (Mommersteeg *et. al.* 2006; Webb *et. al.* 1998a) (Figure 1.6). Less well described is the, closure of the secondary foramen, which commences during the 13th day of gestation by in-foldings (also, septum secundum) of the adjacent atrial myocardium (Anderson *et. al.* 1999) (Figure 1.10b).

Ventricular septation and the atrioventricular septum.

By the E11, there is a further contribution to ventricular chamber morphogenesis - the construction of the muscular interventricular septum. Development of the muscular ventricular septum commences about E10.5 from the myocardium on the apical side of the heart in a region between the two ballooning ventricular chambers. It is composed of myocardium and extends towards the mesenchyme of the atrioventricular cushion and outflow tract. The interventricular foramen, a connecting space between the left and right ventricles, remains open until septation is complete at the end of embryonic day 13 (Webb *et. al.* 1998a).

The anterior-most portion of the interventricular septum (IVS) is of mesenchymal origin (Strauss *et. al.* 1987; Wenink *et. al.* 1982). As the septum is remodelled, the interventricular foramen is closed off in two parts: The primary (ventral) interventricular junction remains open as a ring of mesenchyme, for further remodelling events (described below), while the secondary (dorsal) region is closed by mesenchymal contributions from the atrioventricular cushions (Lamers *et. al.* 1992; Strauss *et. al.* 1987; Wenink *et. al.* 1982).

The atrioventricular septum (AVS) initially forms as a central mesenchymal mass (also termed septum intermedium). It is comprised predominantly of the developing

SC and IC atrioventricular cushions (Webb *et. al.* 1998a). Development of the AVS involves remodelling of the inner curvature of the heart to result in separation of the right and left sides of the heart. At about E10.5-E11, the atrioventricular canal expands rightward, followed by expansion leftward, to enable three events to occur: (1) Since the AVC is connected to the ring of mesenchyme of the primary interventricular junction, rightward pulling enables positioning of the right atrium over the right ventricle. This movement also results in alignment of the muscular ventricular septum with the developed atrial septum (Webb *et. al.* 1998a) (Figure 1.11); (2) Rightward movement of the AVC enables juxtaposition with the developing sub-aortic cushions of the OFT to bring the sub-aortic region of the OFT in connection with the left ventricle; and (3) the final result of this movement is a sealing off of the interventricular connection (Henderson *et. al.* 2009; Lamers *et. al.* 1992; Webb *et. al.* 1998a).

To summarise, the connection of the interventricular septum with the mesenchyme of the atrioventricular cushion is essential for septation of the right and left ventricles. Moreover, this mesenchyme is continuous with the cushions of the OFT such that the ventricles also makes the appropriate arterial connections.

Septation of the outflow tract

It has been shown by lineage tracing that the myocardium of the OFT undergoes a counterclockwise rotation between the stages of E9.5 and E12.5 – in preparation for septation and positioning of the future aorta and pulmonary trunk (Bajolle *et. al.* 2006). Septation of the OFT is necessary for the developing arterial circulation and commences in the 11th day of gestation (Webb *et. al.* 1998a) (Figure 1.12). It is at this stage that the outflow ridges meet and fuse. Cushions of the distal OFT, together with cells of cardiac neural crest origin, contribute to septation of the intrapericardial segments of the aorta and pulmonary trunk (Kirby, M. L. *et. al.* 1995) (reviewed in (Anderson *et. al.* 2003; Webb *et. al.* 2003)). By E12, the ridge mesenchyme, largely of neural crest origin, contributes to a septal structure within the OFT dividing the aortic and pulmonary outlets (Jiang *et. al.* 2000; Webb *et. al.* 1998a) (Figure 1.6). It is within each of the outlets of the proximal OFT, that the mesenchyme of the cushions develops into the leaflets of the semi-lunar valves.

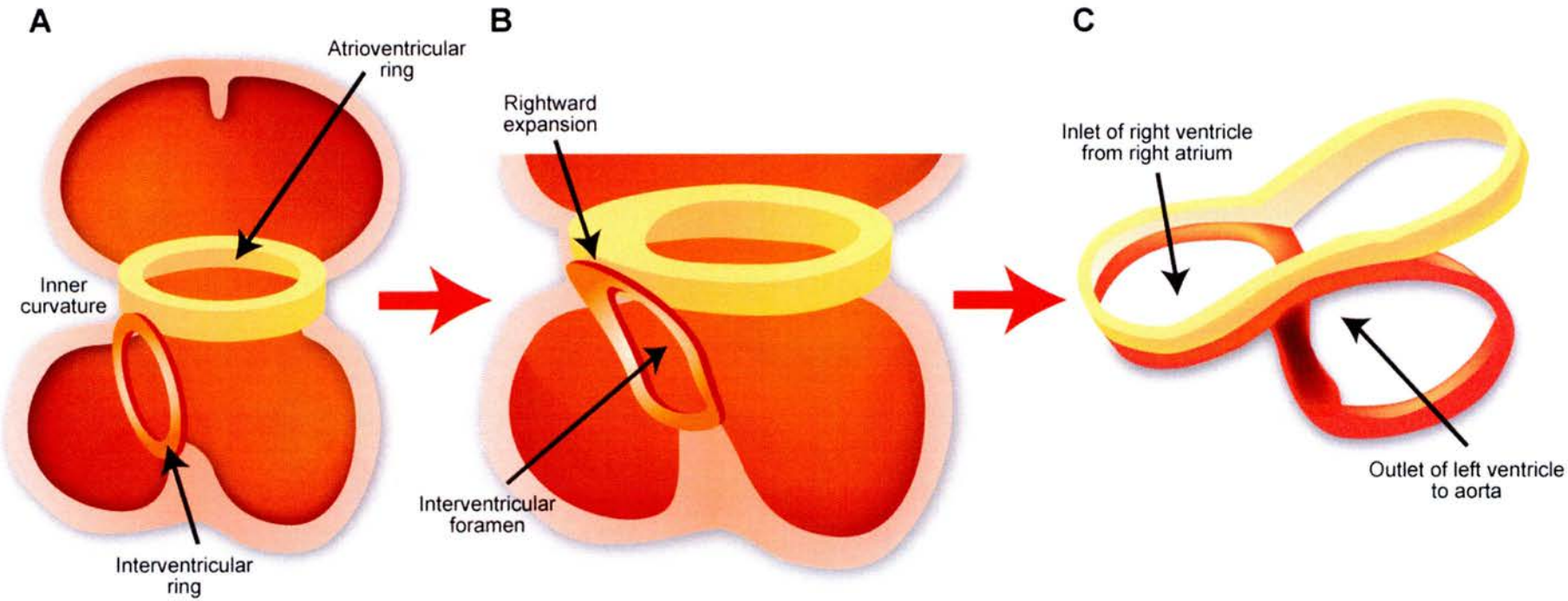

Figure 1.11: Expansion of the atrioventricular canal. (A) Initially the mesenchyme of the atrioventricular canal connects with mesenchyme of the ventricular septum, which surrounds the interventricular foramen. Initial rightward expansion of the atrioventricular canal (in B) followed by leftward expansion, results in (C) the positioning of the right atrium over the right ventricle and the left atrium over the left ventricle, and also moves the sub-aortic region of the OFT into connection with the left ventricle. Adapted from Henderson *et. al.*, 2009 and Lamers *et. al.* 1992.

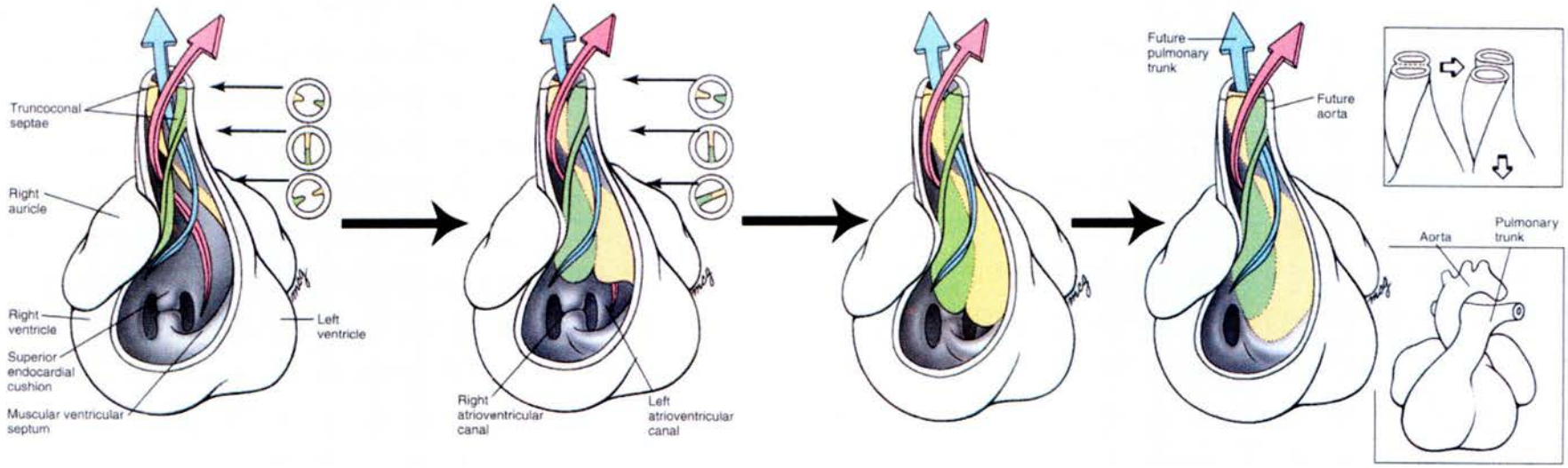

Figure 1.12: Septation of the outflow tract. The outflow tract (OFT) cushions (green and yellow) expand towards each other involving cardiac-derived cells and NCC. The OFT undergoes a rotation such that the cushions spiral prior to fusion, placing the subaortic region (pink arrow) in connection with the left ventricle and the pulmonary trunk (blue arrow) in connection with the right ventricle. As the cushions expand, they also connect with the developing atrioventricular cushions and ventricular septum. Image is Human development, adapted from Larsen *et.al.* 2001.

The proximal aspect of the outflow cushions is continuous with the mesenchyme that contributes to atrioventricular septation and results in the connection of the aorta to the left ventricle. The mesenchymal septal structure undergoes a process of myocardialisation through an influx of cardiac myocytes from the wall of the OFT, and connects to the mesenchyme at the tip of the ventricular septum (Lamers *et. al.* 1992; McBride *et. al.* 1981; van den Hoff *et. al.* 1999). Furthermore, the SHF contributes myocardium and smooth muscle to the remodelling of the OFT (Waldo *et. al.* 2005b).

In addition, remodelling of the OFT is intimately linked to the presence and infiltration of cells of extra-cardiac origin – the cardiac neural crest cells.

Contribution of cardiac neural crest to the developing outflow tract

Neural crest cells delaminate from the dorsal neural tube along the axis of the embryo. It is known that the migration of NC cells results in their contribution to an extensive range of tissues (Le Douarin 1982). Cardiac neural crest cells (NCC) exist as a subpopulation of neural crest cells and originate from rhombomeres 6-8 (Fukiishi *et. al.* 1992). In mouse, NCC delaminate during the 8th embryonic day (Lo *et. al.* 1997). NCC subsequently traverse the 2nd, 3rd, 4th and 6th pharyngeal arch arteries to contribute both to aortic arch artery remodelling and (*via* the 3rd, 4th and 6th pharyngeal arch arteries) to the heart (Jiang *et. al.* 2000; Kirby, M. L. 1990; Kirby, M. L. *et. al.* 1995; Lo *et. al.* 1997)(Figure 1.13).

Cardiac neural crest cells contribute to several facets of outflow tract remodelling and indeed are essential for the morphogenesis of pulmonary and aortic arteries. In *Wnt1-Cre/R26R* embryos, β-galactosidase positive labelled cells (marking NCC) are first observed in the aortic sac and adjacent to the endocardium in the distal OFT (truncus arteriosus) at E9.5 (Jiang *et. al.* 2000) (Figure 1.6). By E10.5, again in *Wnt1-Cre/R26R* embryos, but also in embryos with *Pax3-Cre/R26R* or *Cx43-LacZ*, NCC are found to constitute the majority of the distal OFT cushions, and a proportion of the proximal OFT cushions (also, conotruncal region) where they contribute with endocardial-derived mesenchyme (Epstein *et. al.* 2000; Jiang *et. al.* 2000; Lo *et. al.* 1997).

Appropriate outflow tract septation occurs as consequence of the correct timing of the development of the outflow cushions, OFT rotation and the infiltration of NCC. Septation occurs concurrently within both the proximal and distal OFT. In the proximal OFT the conotruncal septum develops during the 11th day of gestation. This septum develops from both the conotruncal cushions of cardiac origin and the extra-cardiac NCC (Jiang *et. al.* 2000). The NCC form a sub-endocardial layer within the cushions as the cushions fuse (Jiang *et. al.* 2000). Following formation of the septum, the contribution of NCC to the vessel walls is minimal (Jiang *et. al.* 2000). At E10.5 in the distal OFT, NCC begin to form the transitory spiral (aorticopulmonary) septal (APS) structure which results in division of the aortic sac, such that the exiting arterial vessels are divided by E12.5 (Epstein *et. al.* 2000; Jiang *et. al.* 2000). The mesenchymal outlet septum is subjected to myocardialisation, with cells being replaced by cardiomyocytes (van den Hoff *et. al.* 1999). Also by E12.5, NCC surrounding the arch arteries, together with the APS led to vessel remodelling, and dorsal aorta regression such that the pulmonary trunk now connects with the left 6th arch artery, while the aorta connects on the left to the 4th and on the right to the 3rd arch arteries (Jiang *et. al.* 2000).

A third contribution of NCC to cardiogenesis is their presence in the developing semi-lunar valves. In E12.5 *Wnt1-Cre/R26R* embryos, labelled cells are evident in the developing valve leaflets (Jiang *et. al.* 2000; Nakamura *et. al.* 2006). Their presence is transitory, since it has been identified that in the mature crescent-shaped cusps of the valves, contribution by cells of NCC origin is minimal (de Lange *et. al.* 2004; Jiang *et. al.* 2000).

Significant understanding of the roles of NCC in the remodelling of the mouse OFT has come from studies of NCC deficient *Splotch (Sp)* mutants, in particular the Sp^{2H} allele. *Splotch* mutants harbour mutations in the *Pax3* transcription factor (Chalepakis *et. al.* 1993). In the developing heart, the majority of Sp^{2H} homozygotes present with defective interventricular septation as well as a single outflow vessel (persistent truncus arterious; PTA) in which both the pulmonary tract and aorta ascend from the right ventricle (double outlet right ventricle, DORV) (Conway *et. al.* 1997). It has been identified through lineage tracing (*Pax3-cre/R26R* embryos) that

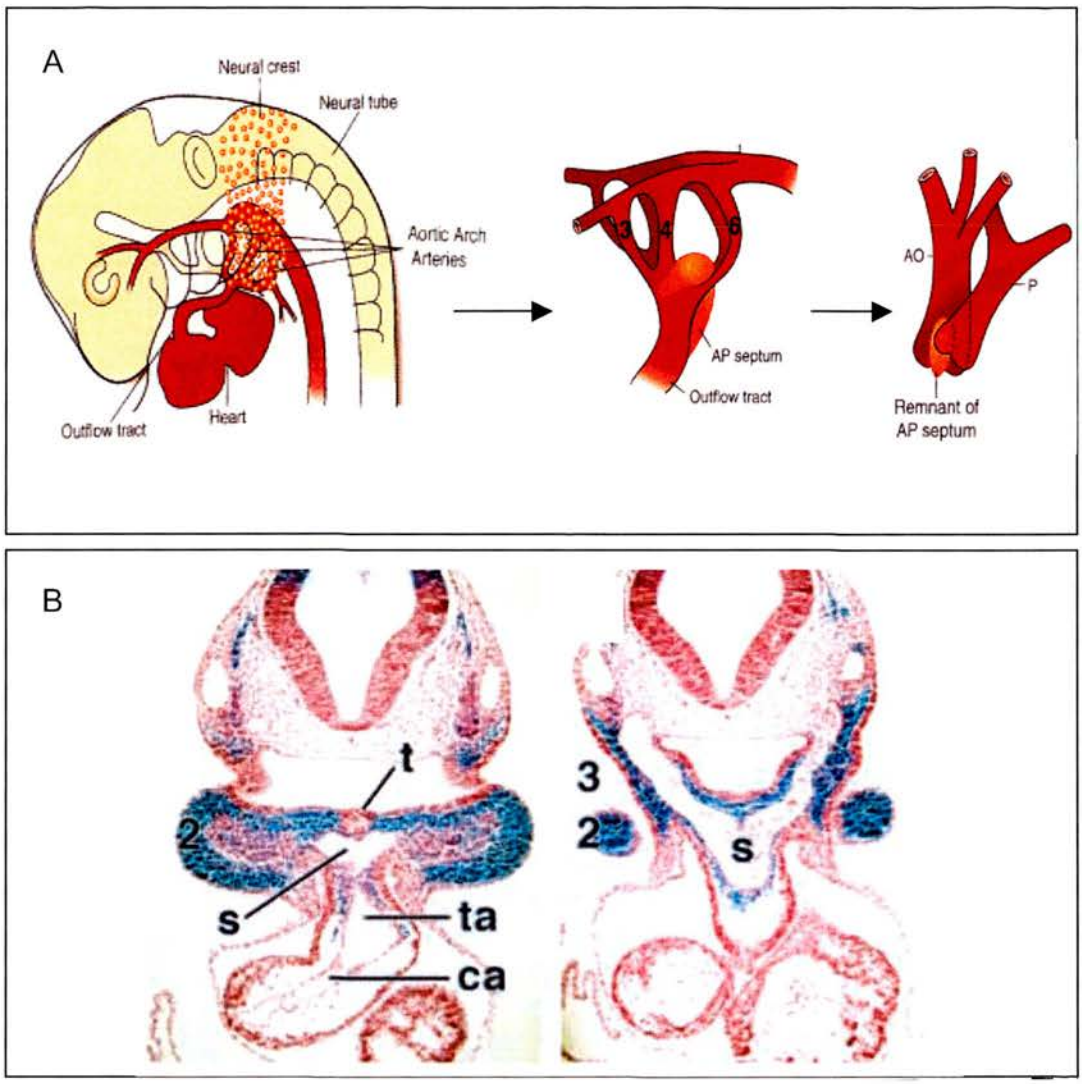

Figure 1.13: The contribution of cardiac neural crest cells to the outflow tract. (A) Cardiac neural crest cells migrate from the dorsal neural tube, through the 3rd, 4th and 6th pharyngeal arch arteries into the anterior heart. Within the outflow tract, neural crest cells contribute transiently to the aortico-pulmonary septum (AP), before being replaced by myocardium. Abbreviations: AO, aorta; AP, aortico-pulmonary septum; P, pulmonary tract. (B) Contribution of labelled NCC (blue) to the distal ouflow tract of the heart, arch arteries and pharyngeal mesenchyme at E9.5. Abbreviations - ca, conus arteriosus; s, aortic sac; t thyroid diverticulum; ta truncus arteriosus; numbers mark pharyngeal arches. (A) Adapted from Maschoff *et.al.*, 2000 ;(B) Image directly from Jiang *et.al.* 2000.

Pax3-expressing progenitors are fated to migrate into the heart as NCC (Epstein *et. al.* 2000). The abundance of NCC in the OFT is reduced in *Splotch* mutants and the distribution of the available NCC is abnormal (Epstein *et. al.* 2000).

The proximity of NCC migrating into the heart, through pharyngeal mesenchyme, as well as within the developing OFT, to cells of the SHF is suggestive of signalling between the two cell populations. Studies in chick have shown that a lack of NCC results in a failure of SHF myocardium to contribute to remodelling of the arterial pole (Waldo *et. al.* 2005a). In addition, the signalling molecule Sonic hedgehog (Shh) is secreted from the pharyngeal endoderm and acts independently on each of these lineages, but reveals that they are regulated by similar signalling pathways (Goddeeris *et. al.* 2007). Furthermore, in Sp^{2H} homozygotes, a deficiency of NCC disrupts the distribution of SHF within the outflow and pharyngeal regions (Bradshaw *et. al.* 2009). Thus the function of NCC in the OFT is entwined with that of SHF cells, and both must be considered when examining defects of the outflow region of the developing heart.

1.3.4 The requirement for endoderm in heart development

The formation of the cardiac crescent is partly due to the responsiveness of cardiogenic cells to the inductive signals of the adjacent endoderm (Jacobson *et. al.* 1988) (Reviewed in (Lough *et. al.* 2000)). Studies in chick have revealed that the expression of *Myocardin* in the mesoderm is dependent upon the presence of the adjacent endoderm (Warkman *et. al.* 2008). Myocardin is a co-factor for Serum Response Factor (SRF) - an early marker of cardiogenesis which, together with Nkx2.5 directs expression of the contractile protein α-cardiac actin (Chen, C Y *et. al.* 1996; Wang *et. al.* 2002). In mouse, expression of *Gata4* in the endoderm is essential for cardiogenesis. *Gata4* null embryos are unable to form the heart tube, even though in these embryos myocardial specification can occur, as observed by the presence of contractile cardiomyocytes (Kuo *et. al.* 1997). It was subsequently shown that by enabling expression of *Gata4* in the endoderm the cardiac phenotype could be abrogated (Narita *et. al.* 1997). *In vitro*, endoderm is not essential for the generation of cardiogenic mesoderm, as shown by cardiac gene expression analysis

(Gannon *et. al.* 1995). Likewise it is not required for terminal differentiation of cardiomyocytes prior to formation of the heart. Thus, the requirement for endoderm in cardiomyocyte differentiation appears to be for a short time-window between initiation of cardiac gene expression and the onset of contraction.

Molecular signalling from the endoderm also plays a significant role in the development of the second heart field during the stages of outflow tract cushion formation and septation. As two examples of factors that act as remote signalling molecules, *Shh* and *Fgf8* are expressed from the pharyngeal endoderm (PE) (Crossley *et. al.* 1995; Echelard *et. al.* 1993). Both of these signalling factors have been shown to play important and complex roles in cardiogenesis. Segregation of these functions has come from conditional inactivation using selected *cre recombinase*-drivers, which are expressed in domains overlapping the PE. The action of Shh and Fgf8 on the second heart field, particularly in the formation of the OFT is discussed here.

Shh

Germline loss of *Shh* expression results in extensive embryonic defects including abnormal development of the RV, ventricular septum and OFT, as well as atrial and atrioventricular septation defects in the heart (Chiang *et. al.* 1996; Washington Smoak *et. al.* 2005). It is known that loss of *Shh* expression from the PE causes the *Shh* null cardiac defects since aspects of this phenotype can be recapitulated upon conditional inactivation of *Shh* in the endoderm using an *Nkx2.5-cre* driver, whose expression overlaps with that of *Shh* only in the endoderm (Goddeeris *et. al.* 2007). This finding prompted further study of the cells that respond to Shh signalling, and the mechanism of Shh action in the heart.

The *Ptch1-LacZ* reporter was used to examine the effect of loss of *Shh* in the endoderm on the cardiac cells which respond to Shh signalling, since *Ptch1* is also a Shh target gene. The SHF-derived DMP was found to be affected by ablation of endodermal *Shh* (Goddeeris *et. al.* 2008). The DMP contributes to atrial and AV septation (Washington Smoak *et. al.* 2005). Knowing that the Shh responsive cells were predominantly of SHF origin, SHF responsiveness to Shh was ablated by

conditional inactivation of *Smoothened* (*Smo*), the membrane-bound transducer of Shh signalling, under the *Mef2C-AHF-Cre* (Goddeeris *et. al.* 2008; Verzi *et. al.* 2005):

It was found that in the absence of Shh signalling, the dorsal mesocardium did not generate its projection into the atria. Analysis of the migratory potential of dorsal mesocardium in culture identified that the proportion of migratory cells could be significantly reduced by treatment with the drug cyclopamine, which inhibits Shh signalling (Goddeeris *et. al.* 2008). This provides a mechanism by which Shh signalling in the SHF can result in septal defects resulting from inhibited migration of the DM into the heart.

Given that the OFT is composed mostly of SHF-derived cells, it can be hypothesised that Shh expression is required for second heart field specification and/or maturation. Conditional inactivation of *Smo* revealed that responsiveness to Shh signalling is necessary in the SHF and NCC (through conditional inactivation of *Smo* with the *Wnt1*-cre) of the OFT for septation (Goddeeris *et. al.* 2007). The most recent refinement of this understanding of how Shh signalling may be acting in the SHF has come from studies in chick (Dyer *et. al.* 2009). Again through use of the Shh inhibitor cyclopamine, blocking Shh signalling resulted in reduced proliferation of SHF within the OFT in regions normally responsive to Shh (as indicated by expression of the Shh target gene *Ptc2*) (Dyer *et. al.* 2009).

Fgf8

Correct expression of *Fgf8* is also crucial for cardiogenesis and the second heart field. *Fgf8* is expressed in multiple domains through which it may act on the developing heart (Crossley *et. al.* 1995). Expression relevant for cardiogenesis commences in the mesoderm at the cardiac crescent and subsequently the pharyngeal endoderm and ectoderm. As constitutive targeted inactivation of *Fgf8* results in arrest of development at gastrulation (Sun *et. al.* 1999), thus the understanding of particular roles of *Fgf8* in cardiogenesis comes from studies of conditional inactivation and hypomorphs. A series of hypomorphic mutant embryos were examined for the cardiac phenotype and it was shown that the cardiac defects were

variable but included failed OFT septation [persistent truncus arteriosus (PTA)], atrial septal defects (ASD), ventricular septal defects (VSD) and, in a small proportion, valve defects (Abu-Issa *et. al.* 2002). The finding that the OFT was predominantly affected in *Fgf8* mutant embryos suggested that one of the roles of Fgf8 is to act on the SHF. Comprehensive studies have since been conducted to explore the requirement of *Fgf8* expression on the heart, including conditional inactivation of the PE expression domain of *Fgf8* (Park, E J *et. al.* 2006).

Isl1-cre was used to conditionally remove *Fgf8* expression from the pharyngeal endoderm, however *Isl1-cre* is also expressed in the SHF (Park, E J *et. al.* 2006). Since *Fgf8* is initially expressed in early SHF mesoderm, the phenotype of *Fgf8* inactivated under the *Mef2C–AHF-cre* was examined. Only embryos in which *Fgf8* was inactivated by *Isl1-cre* demonstrated defective OFT septation. Thus *Fgf8* expression in the PE is required by cells within the OFT for septation (Park, E J *et. al.* 2006). Whether this requirement for endodermally-derived *Fgf8* is specifically depended on by SHF cells or NCC (or both) has not yet been described.

1.3.5 The septum transversum mesenchyme and the development of epicardium

The septum transversum mesenchyme (STM) contributes to the development of several organs during embryogenesis, including the heart and liver. Expression analysis of *Cited2* revealed a domain of expression in the anterior-most embryonic mesoderm which, in progressive stages, moves posteriorly to the base of the developing heart, adjacent to the invaginating foregut endoderm (Dunwoodie *et. al.* 1998). In its final location, this domain of *Cited2* expression correlates to the tissue known as the STM. Hence it is thought that this is the origin of the STM. The pro-epicardium (also pro-epicardial organ, PEO) originates as mesothelial projections from the STM. By embryonic day 9 cells have begun to migrate over the adjacent surface of the developing atrium and ventricle, reaching the anterior cardiac structures by E11 (Komiyama *et. al.* 1987).

Of relevance to heart development, several genes are known to be involved in the transformation of the STM into the PEO and the subsequent cellular migration. Functional Gata4 is essential for the formation of the PEO, since conditional ablation

of *Gata4* specifically in the embryonic region (by tetraploid aggregation) results in a complete absence of the PEO and epicardium (Watt *et. al.* 2004). The PEO cells migrate over the heart *via* essential molecular interactions involving VCAM-1 (Kwee *et. al.* 1995) and α4-integrin (Sengbusch *et. al.* 2002) thus forming the epicardium ((Viragh *et. al.* 1989); and reviewed in (Manner *et. al.* 2001)). The earliest cardiac phenotype examined in mouse, as a consequence of a complete absence of the epicardium, has been studied in embryos deficient for *Gata4* (Watt *et. al.* 2004). At E9.5, the myocardium of the presumptive ventricular region is thinner with fewer developing trabeculae in *Gata4*$^{-/-}$ hearts compared with control hearts. Additionally, *Gata4*$^{-/-}$ hearts are unable to undergo adequate looping (Watt *et. al.* 2004). A later myocardial phenotype has been demonstrated in chick whereby inhibition of the PEO outgrowth leads to a decrease in cardiomyocyte proliferation, and thereby leading to a thinner compact myocardium (Pennisi *et. al.* 2003). This was accompanied by an increase in myocardial cell death (Pennisi *et. al.* 2003). This phenotype in chick develops into defects of the OFT and septum of the chambers (Gittenberger-de Groot *et. al.* 2000).

The epicardium overlies the myocardium as an epithelial sheet. From this stage, they contribute to cardiogenesis in a number of ways. The PEO and subsequent epicardium express both Wt1 (Moore *et. al.* 1999) and Tbx18 (Kraus *et. al.* 2001a). Much of the understanding of the roles of epicardium in cardiogenesis has involved utilising this expression. *Wt1* knockout mice exhibit cardiac defects including thin ventricular myocardium (Moore *et. al.* 1999). In these mice the epicardium is present but malformed. The E10.5 stage epicardium has been shown to be a source of retinoic acid and fibroblast growth factor (FGF) signalling (Fgf9, Fgf16 and Fgf20) which regulate myocardial proliferation (Lavine *et. al.* 2005; Stuckmann *et. al.* 2003).

Lineage tracing epicardial cells using the *Tbx18-cre/R26R* and *Tbx18-nLacZ* reporter transgenes has revealed the contribution of epicardial cells to cells of the cardiomyocyte lineage (Cai *et. al.* 2008). As early as E9.75, cells which expressed *Tbx18* have migrated into the heart. By E10.5 cells of the epicardial lineage have entered the heart and differentiated into cardiomyocytes evident in the developing

ventricular septum and scattered within the walls of the ventricles and atria (Cai *et. al.* 2008). The contribution of *Wt1*-expressing epicardial cells to the cardiomyocyte lineage is also evident at E15.5 within the heart (Zhou, B *et. al.* 2008).

A second wave of entry of epicardial cells into the heart occurs from E12.5 to contribute to the smooth muscle cells of the coronary vessels through to adult stages (Cai *et. al.* 2008). Furthermore, an additional population of endothelial cells which also originate in the PEO as the early epicardium play a key role in endothelial development of the coronary vasculature (Lie-Venema *et. al.* 2005).

The molecular and cellular mechanisms for the formation of the epicardium and its contribution to the heart are still poorly understood. Thus any genetic deficiencies, which yield phenotypes similar to those known for epicardial defects, may contribute to understanding this process.

1.4 AN ENU MUTAGENESIS PHENOTYPE-DRIVEN SCREEN IDENTIFIES RECESSIVE MUTATIONS ON MOUSE CHROMOSOME 13.

1.4.1 Introduction to ENU mouse mutagenesis

Mouse mutagenesis is a powerful tool for modelling human diseases. One approach is to isolate models that exhibit a particular phenotype using a so-called phenotype-driven mutagenesis screen. The power of this unbiased approach and its ability to dissect complex biological systems has been amply demonstrated in a variety of organisms including zebrafish and the mouse (Baraban *et. al.* 2007) (Cordes 2005; Hrabe de Angelis *et. al.* 2000; Rathkolb *et. al.* 2000). The success of this approach is critically dependent on the availability of a highly efficient mutagen. This is important because the rate of mutagenesis determines how many novel mutations will be examined for a given number of animals. For example, if a mutagen introduces 30 mutations per animal then examining 50 animals surveys 150 new mutations. In the mouse the chemical N-ethyl-N-nitrosourea (ENU) is well-established as an efficient mutagen suitable for phenotype-driven screens (Barbaric *et. al.* 2007; Justice *et. al.* 1999; Russell *et. al.* 1979). Through transfer of an ethyl group to a DNA base, ENU causes mispairing or base substitution during DNA replication. ENU predominantly affects A/T base pairing in GC-rich regions. The concentration of mutagen has been optimised (Russell *et. al.* 1982; Weber *et. al.* 2000) and although the exact mutation frequency achieved will vary between experiments the average frequency of mutations in mouse experiments is $1x10^{-3}$ per locus (Hitotsumachi *et. al.* 1985). In practice, if we assume that the mouse genome contains 30,000 genes this translates to a rate of 30 new mutations per animal surveyed in a phenotype-driven screen.

An additional advantage of ENU is that because it induces point mutations it can lead to the creation of loss-of-function or gain-of-function mutations. Allelic series can be created for a gene of interest. A point mutation could affect coding sequence, a splice site, or a critical base within the promoter or enhancer of a gene. In this way, ENU can alter protein levels and /or function. Using this approach it is possible to

garner novel information about gene regulation and function that may otherwise not be determined by a targeted null mutation.

1.4.2 A region-specific phenotype-driven mutagenesis screen to create mouse models of human 6p deletion syndromes.

A phenotype-driven screen was conducted to create mouse models with a recessive mutation in genes in a region of chromosome 13 (Bogani *et. al.* 2005). The region of interest on chromosome 13 correlates to human chromosome 6p and thus mutants identified could potentially be examined as animal models for, and represent, 6p deletion syndromes. Deletions of chromosome 6p are rare, yet the phenotype is multifaceted and is characterised broadly by heart and kidney defects and craniofacial abnormalities (Davies *et. al.* 1996; DeScipio 2007; Suzuki *et. al.* 2006), indicating that the region contains genes required for correct embryonic development. By creating mouse models with aspects of the abnormalities of 6p deletion syndrome, it is possible to determine the developmental origin of the phenotype. This not only generates models which can be used to investigate the function of individual genes but also allows an investigation of possible gene interactions, which may underlie aspects of contiguous gene deletion syndromes.

Two mouse lines were essential for this mutagenesis screen (Figure 1.14). Firstly, the *Del(13)Svea36H* mouse line, which harbours a chromosomal deletion of 12.7 Mb across the region of interest on mouse chromosome 13 (Arkell *et. al.* 2001; Mallon *et. al.* 2004). This region is syntenic to the deleted region of human 6p. Secondly, the $Foxq1^{sa/sa}$ mouse line contains *satin* allele - a recessive visible marker for coat appearance (Hong *et. al.* 2001; Major 1955)(described below, section 1.4.4 and associated Figure 1.16). *Foxq1* falls within the limits of the *Del(13)Svea36H* chromosomal deletion. Thus it is possible, using a standard two-generation deletion breeding protocol, to uncover recessive mutations that lie within the deleted region (Brown *et. al.* 1996).

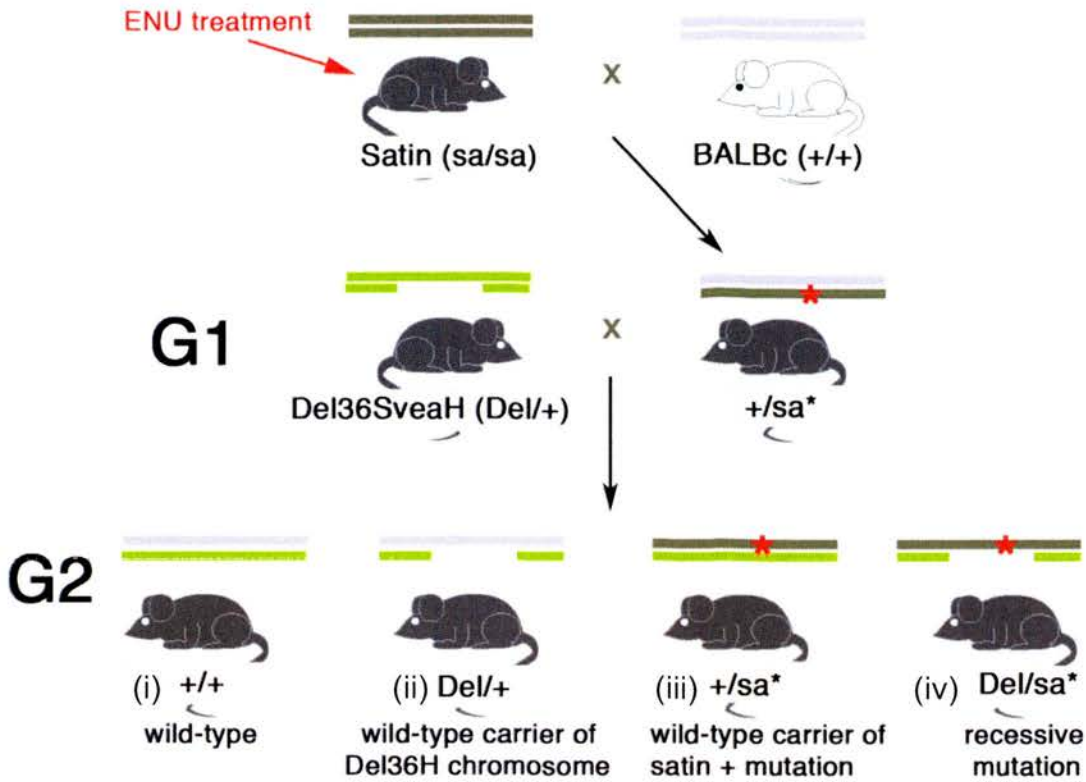

Figure 1.14: Genetic crosses conducted in the recessive ENU mutagenesis screen. Satin mice were mutagenised with ENU, and crossed to BALBc wild-type mice. G1 progeny, harbouring novel mutations (red asterisk) were crossed to mice harbouring the *Del36SveaH* chromosomal deletion. *Del36SveaH* mice are hemizygous for a region of chromosome 13, as a result of the chromosomal deletion. Thus crossing *Del36SveaH* mice to the G1 progeny, results in mice hemizygous for satin and the surrounding loci (iv). G2 progeny were either (i) wild-type, (ii) wild-type carriers of the deletion, (iii) wild-type carriers of the satin allele and a novel ENU mutation (red asterisk) or (iv) harbouring a novel recessive mutation linked to satin. Abbreviations: Del, deletion chromosome; sa, satin allele. Adapted from Willoughby, 2006.

To perform the genetic screen, *Foxq1*$^{sa/sa}$ males were treated with ENU and then crossed to BALB/cOlaHSD females (Figure 1.14). Thirty male offspring (G1) from each ENU treated male were paired with females carrying the *Del(13)Svea36H* chromosome. The *Del(13)Svea36H* mouse line was utilised such that, in some offspring, the region of interest would be hemizygous, while the remainder of the genome is heterozygous. Thus, only a mutation which falls within the limits of the hemizygous region would result in a recessive phenotype. Nearly two thousand G1 crosses were completed (n=1730). To identify embryonic lethal mutations, offspring from the G1 cross (G2) were scored for the appearance of the *satin* phenotype. Strains in which less than or equal to one progeny amongst 25 exhibited the satin coat were presumed to harbour a newly-induced recessive lethal mutation located within the *Del(13)Svea36H* region and were subjected to further breeding and inheritance testing (Bogani *et. al.* 2005). Overall 13 lines were found to carry a heritable mutation and phenotype linked to the satin locus.

1.4.3 Identification of an ENU mutation in *Sox4*.

Recombination mapping in one of the lines, termed "M91", indicated that the causative mutation resided within 0.8cM either side of the *satin* allele. *Sox4* was considered a strong candidate gene, since the recessive lethal phenotype of line M91 phenocopied that published for the targeted allele of *Sox4* (Schilham *et. al.* 1996). Sequence analysis of *Sox4* confirmed that a point mutation had been introduced into the *Sox4* sequence. The mutation was identified as a T to C transition at nucleotide 896[2], which results in an amino acid change from a serine to proline at position 70 (Ser70Pro) (Figure 1.15a). Ser70 is a residue in the middle of the first alpha-helix of the HMG box of the Sox4 protein. Homozygous mutant embryos of this allele recapitulate the *Sox4* null phenotype at E14.5 (section 1.1.4), and shows septal defects (VSD) and double outlet right ventricle (DORV) (Bogani *et. al.* 2005) (Figure 1.15b).

[2] RefSeq accession number NM_009238

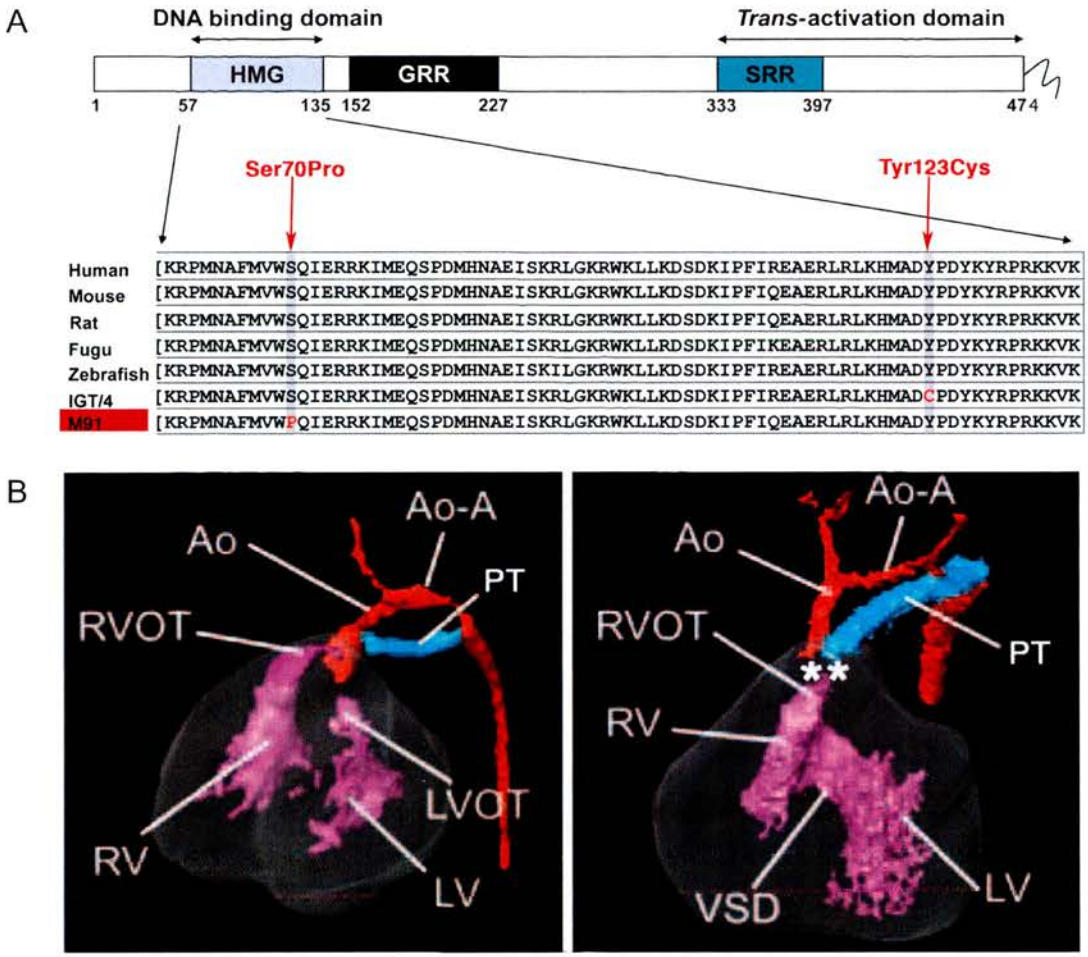

Figure 1.15: ENU-induced mutations to *Sox4*. (A) The ENU-induced serine-70-proline mutation falls within the HMG domain of Sox4 (Red letter; Line MUD91). An additional mutation was identified to cause a tyrosine to cysteine substitution (Red letter; Line IGT/4). There is conservation of these residues between mouse and other species (human, rat, fugu, zebrafish). (B) The serine-70-proline mutation results in cardiac defects at E14.5. 3D reconstruction from magnetic resonance imaging of the heart of a wild-type embryo (left), demonstrates normal septation and outflow from the ventricles. Homozygous mutant embryo (right) demonstrates a ventricular septal defect (VSD) and double outlet right ventricle (asterisk). Abbreviations: Ao, aorta; Ao-A, aortic arch; GRR, glycine rich repeat; HMG, HMG box domain of Sox4; LV, left ventricle; LVOT, left ventricular outflow tract; PT, pulmonary trunk; RV, right ventricle; RVOT, right ventricular outflow tract; SRR, serine rich repeat; VSD, ventricular septal defect. Adapted from Goldsworthy *et.al.*, 2008 and Bogani *et.al.*, 2005.

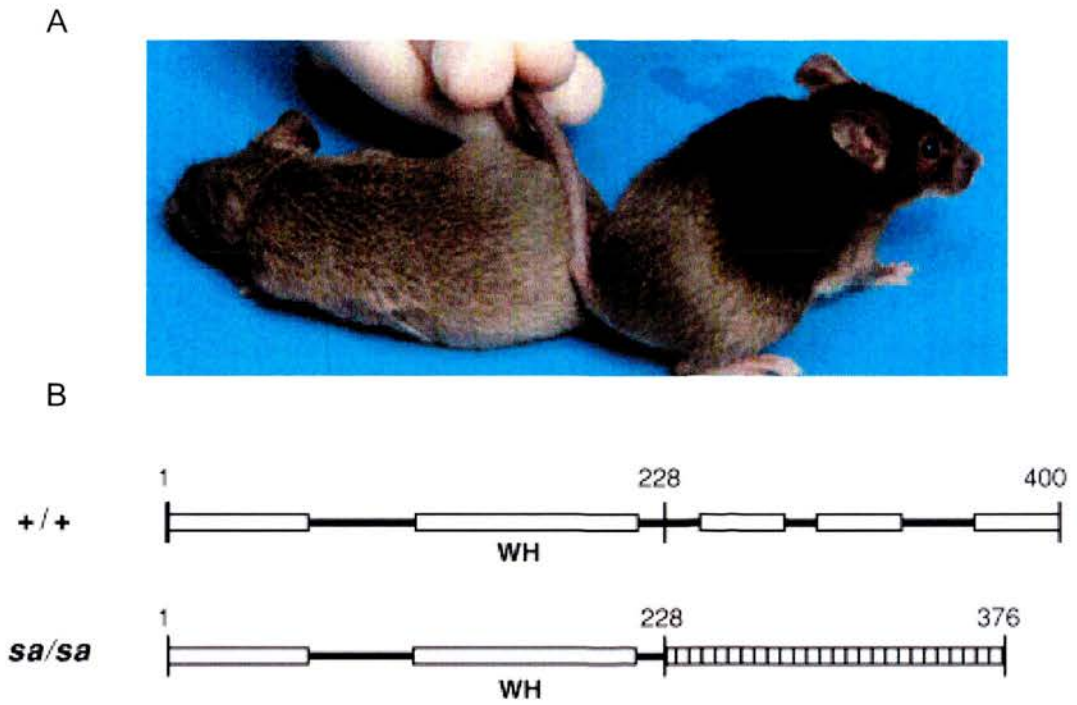

Figure 1.16: Diagram indicating the domains of Foxq1 and the consequence of the *satin* deletion. (A) *Satin* mice (right), exhibit a glossy coat compared with wild-type littermates (left). (B) Foxq1 demonstrates a winged-helix (WH) DNA binding domain and other regions of conserved sequence. In *satin* mutants (*sa/sa*) a frameshift occurs from residue 228, as a consequence of a 67bp intergenic deletion. Adapted from Hong *et.al.*, 2001.

As in any mutagenesis experiment it is possible that a second, unidentified mutation is responsible for the observed phenotype. Three lines of evidence argue against this. Firstly, since the identification of the M91 strain the line has been maintained by continuous outcross to non-mutagenised animals followed by selection of the *Sox4* mutation, this will have the effect of removing the mutagenised genome other than in the area immediately surrounding *Sox4*. A second mutation would need to be linked extremely tightly to *Sox4* to persist within the *Sox4* mutant animals studied within this thesis. Secondly, if we assume an average mutagenesis frequency (1×10^{-3}) (Hitotsumachi *et. al.* 1985) and a Poisson distribution (Keays *et. al.* 2006), the likelihood of the *Del(13)Svea36H* segment containing two mutations is extremely low (3.8×10^{-9})(Bogani *et. al.* 2005). Thirdly, the availability of additional alleles of *Sox4* allows us to conclude the allele isolated in the screen at *Del(13)Svea36H* phenocopies the spectrum of defects seen in the targeted allele of *Sox4* (Penzo-Mendez *et. al.* 2007; Schilham *et. al.* 1996; Ya *et. al.* 1998b), as well as in a second ENU-induced allele of *Sox4*, termed "IGT/4" (Goldsworthy *et. al.* 2008)(Figure 1.15a). Moreover, complementation tests between the two ENU-induced alleles demonstrate that these both result from mutations in *Sox4* (Bogani *et. al.* 2005; Goldsworthy *et. al.* 2008). These three lines of evidence demonstrate that a second, unidentified mutation causing the phenotypes observed in the M91 strain is extremely unlikely.

1.4.4 Foxq1

Foxq1 (Forkead box, subclass q, member 1; formerly Hepatocyte nuclear factor-3 homologue 1 or Hfh1) is a member of the family of Forkhead box (Fox) transcriptional regulators, defined by the presence of the "winged helix" or "forkhead box" domain, which is responsible for recognising specific DNA target sites (Clevidence *et. al.* 1994; Clevidence *et. al.* 1993). Little is known about the function of this protein, beyond its DNA binding ability.

Three mutant alleles of *Foxq1* have been created. Previous annotation of the phenotype caused by mutant alleles of *Foxq1* revealed a disorder in the development of hair follicles – giving rise to the satin phenotype (Figure 1.16a). The first

identified allele (the allele used for the mutagenesis screen, section 1.4.2) (*Foxq1*^{sa}) harbours a radiation-induced intragenic 67 base-pair deletion of nucleotides 686 to 752 and two additional base substitutions at positions 766 and 767[3] (Hong *et. al.* 2001; Major 1955). The deletion is predicted to alter the protein sequence by causing a novel translocated frame of 148 amino acids after the winged-helix domain (Figure 1.16b). A second allele of *Foxq1* (*Foxq1*$^{sa\text{-}e1}$) was generated by ENU mutagenesis, which induced a T to G transversion at nucleotide 383 (not shown). This point mutation results in the replacement of an isoleucine residue by a serine residue in the winged-helix domain (Hong *et. al.* 2001). The *Foxq1* null allele was created and the phenotype examined (Goering *et. al.* 2008). In addition to the satin phenotype, it was found that Foxq1 is involved in gastric physiology and in gastric acid secretion in the adult. *Foxq1* null adults are otherwise normal.

Little is known about the role of Foxq1 in embryonic development, since phenotypes are not described. Only on a specific hybrid genetic background (129/Sv x C57Bl/6J) does the *Foxq1* null reveal an embryonic lethality, which is not fully penetrant (Goering *et. al.* 2008). In homozygous crosses of this specific genotype, approximately 50% of embryos demonstrate abnormal forebrain development at E10.5 and death at E12.5. Of these crosses, the remaining homozygotes are viable. The cause of embryonic lethality remains unknown as extraembryonic tissues, as well as the heart and liver, develop normally. Thus the role of Foxq1 in development remains poorly understood.

1.4.5 Purpose for examining the recessive phenotype of *Sox4*$^{ENU/ENU}$ *Foxq1*$^{sa/sa}$ embryos.

In human, *SOX4* and *FOXQ1* are sometimes deleted in cases of 6p deletion syndrome, making either locus hemizygous. Terminal deletions of 6p have been found to include the *FOXQ1* locus, while interstitial deletions of 6p have been shown to delete the *SOX4* locus (Davies *et. al.* 1996). Mutations in *SOX4* have not been described for human disease. However, because of its chromosomal location, and overlap in expression domains with *SOX11* in other systems, SOX4 has been recently proposed as a candidate for human nonsyndromic cleft lip and palate

[3] GenBank accession number AF154426. Numbers are from the translation initiation site.

(Juriloff *et. al.* 2008). The *Sox4*^{ENU} *Foxq1*^{sa} mouse line provides a new means to study the compound phenotype resulting from disruption to the function of both genes. Additionally, given the absence of evidence for a role of *Foxq1* in heart development (with any of the mutant alleles), it is possible to consider a cardiac phenotype as solely the consequence of the ENU mutation in *Sox4.*

1.5 AIMS OF THIS THESIS.

Little is known about the developmental requirement for Sox4. It has been shown in earlier sections of this chapter, that interest in Sox4 is increasing in other biological systems such as cancer. The ENU mutant allele discussed in the previous section provides a novel system in which to explore the developmental requirement for Sox4 further and may thereby contribute to the important body of work deciphering the biological function of Sox4. The fundamental concern of this thesis is to contribute to the understanding of Sox4 in mouse embryonic development, with a particular focus on its role in cardiogenesis. This is specifically detailed in the following aims:

1. **To analyse aspects of the cardiac phenotype present in *Sox4*^{ENU} *Foxq1*^{sa} mutant embryos.** Here, the aim was to determine exactly when the mutant phenotype arises during development and at what point is the mutation lethal; how this phenotype is presented specifically in cardiac tissue at specific stages of development; and, upon analysis of cardiac tissue, can the phenotype be related to the expression domains explored in **Aim 2** below. Studies of the cardiac phenotype of the mutant line are reported in **Chapter 3.** Also to contribute to this aim, although extending beyond research examining the cardiac phenotype, **Appendix 1** records the derivation of mouse embryonic stem cells from *Sox4*$^{ENU/ENU}$ *Foxq1*$^{sa/sa}$ homozygous mutant blastocysts, and an examination of mutant ES cell contribution in chimæric mice.

2. **To characterise the expression of *Sox4* and *Foxq1* during mouse embryogenesis by *in situ* hybridisation.** The phenotype of the line harbouring these mutant alleles is the basis for an examination of the expression patterns of both *Sox4* and *Foxq1*. To achieve this fully with *Sox4* and establish the underlying developmental expression, domains must be explored by *in situ* hybridisation of both whole and sectioned embryos. This work is presented in **Chapter 4** as a comprehensive account of the spatiotemporal expression domains of *Sox4* and *Foxq1* during mouse embryogenesis, which extends published accounts of *Sox4* and *Foxq1*

expression by including more developmental stages and greater detail than that published to date.

3. To examine molecular marker expression in *Sox4*^{ENU} *Foxq1*^{sa} compound mutants. Building on **aim 1**, the phenotype presented Chapter 3 was further explored using key molecular markers of heart development. This data is reported **Chapter 5**.

4. Commence analysis of the phenotype of *Sox4*$^{ENU/ENU}$ embryos wild type for *Foxq1* combining methods of analysis used in Aims (1) and (3). Following an extensive breeding programme, it was possible to segregate the *satin* allele from the *Sox4*^{ENU} mutation. **Chapter 6** describes the homozygous phenotype and mRNA *in situ* expression of selected molecular markers in embryos mutant solely for the *Sox4* ENU allele.

The final chapter of this thesis (**Chapter 7**) provides a summary of the key results made in this project and a discussion of future directions made possible by the discoveries presented in the body of the thesis.

CHAPTER 2: MATERIALS AND METHODS

2.1 MATERIALS

2.1.1 Components of buffers and solutions.

General solutions and buffers

Standard solutions were made as described in Sambrook *et.al.* (Sambrook *et. al.* 1989). Chemicals were of analytical grade and predominantly were supplied by Sigma or Invitrogen. Restriction enzymes were purchased from either New England Biolabs or Roche. Solutions of alcohols and Xylene were purchased from Fisher Scientific.

For general laboratory use, solutions were prepared using milli-Q water and sterilised were appropriate. Solutions for use in RNA applications were prepared using DEPC-treated milli-Q water and autoclaved, with the exceptions of PBS, EDTA and SSC, which were DEPC-treated directly and autoclaved.

Embryo dissection – solutions and buffers

Embryos were dissected either in 10% FCS - FCS diluted to 10% in PBS, filter sterilised through a 0.2μ filter (Millipore, Billerica, MA, USA); or in M2 (Invitrogen).

In situ hybridisation – solutions and buffers

Hybridisation solution: Hybridisation solution was pre-prepared and frozen at -20 °C. The solution comprised 50% ultrapure formamide, 5x SSC pH 4.5, 0.1% Triton X-100, 0.5% CHAPS, 5mM EDTA and made to volume with DEPC-treated water. Prior to probe addition, 50μg/ml yeast tRNA and 100μg/ml heparin were added to the solution.

PBT: PBS with 0.1% Tween.

PBTx: PBS with 0.1% Triton X-100.

PFA: 4% paraformaldehyde in PBS.

0.1M TEA: 6.67ml of 7.49M Triethanolamine, make to 450ml with DEPC-treated dH_2O, pH to 7.8-8 and adjust volume to 500mL. Store at 4 °C.

TBTX: 50mM TrisCl (pH 7.5), 150mM NaCl, 0.1% Triton X-100.

TBST: TBS with 0.1%Tween

NTMT: 100mM NaCl, 100mM Tris.Cl (pH 9.5) 50mM $MgCl_2$ 0.1% Tween-20.

RNA extractions

Extraction kits was used for all RNA extractions:

- miniRNA extraction (Qiagen).
- microRNA extraction (Qiagen).

Plasmid DNA extraction

Extraction kits were used for all plasmid DNA extractions:

- miniprep extraction (Qiagen).
- maxiprep extraction (Qiagen).

PCR clean-up

Two kits were utilised for the purification of PCR products depending upon what the product would next be used for. Alternatively, for most products to be sequenced, PEG precipitation was carried out (section 2.3.8).

- DNA Clean and Concentrator (Zymo Research, Orange, CA, USA): if the product was to be subsequently subcloned, or sequenced.
- Gel DNA recovery kit (Zymo Research): if the product was to be subcloned, or was not the sole amplicon of the PCR.

Tissue culture – solutions and medium

Solutions were prepared depending upon the cell line to be cultivated:

General ES cell Culture Medium

Serum medium

Solutions were prepared and sterilised, or supplied ready-made by the Institute for Stem Cell Research (ISCR) tissue culture staff. General ES cell culture medium comprised Glasgow Minimal Essential Medium (GMEM, Sigma) supplemented with 10% foetal calf serum (Biosera, Ringmer, East Sussex, UK), 0.1% (0.1mM) MEM Non-Essential Amino Acids Solution (Invitrogen), 2mM L-glutamine (Invitrogen), 1mM sodium pyruvate (Invitrogen), 0.1mM 2-mercaptoethanol and 100U/ml LIF.

Serum-free medium

Serum-free ES cell culture solution was made and supplied by Stem Cell Sciences UK Ltd. (Cambridge, England, UK).

Freezing Medium

Cells were frozen in 5-10% DMSO in culture medium with 10% serum.

2.1.2 Equipment

Unless otherwise specified, thermocycling was performed in either:

PCR: Gene Amp PCR system 9700 (Applied Biosystems Inc. Foster City, CA, USA).

qPCR and Light-cycler genotyping PCR: Light cycler 480 (Roche).

2.1.3 Oligonucleotides.

Oligonucleotides were constructed by MWG-Biotech (Eurofins MWG Operon, Ebersberg, Germany). Primers used for results shown in this thesis are listed in Table 2.1.

Table 2.1: List of oligonucleotide sequences and their target gene, for results presented in this thesis.

Target locus	Forward sequence	Reverse sequence
Satin (genotyping)	GAGATCAACGAGTACCTCATGGG	CGAAGGAGCTGGAGAACTTG
Sox4 (genotyping)	GAGCACTTCAGCGGTGA	GGAGATCTCGGCGTTGT
Sox4 light cycler amplicon	GGGACAGCTCGGACTCG	GGAGATCTCGGCGTTGT
Sox4 light cycler a/d	acceptor: CTGCGACCACACACTAAAGC	donor: GCTCCATGATCTTGCGCCGCTCG
Wnt11	CTGCATGAAGAATGAGAAGGTG	ACTGCCGTTGGAAGTCTTGT
Fzd7	TGCAATGTTCTTCAGTTTCTCAG	GTAATCTGTCCTCCCGACAATG
TgfB2	TGGAGTTCAGACACTCAACACA	AAGCTTCGGGATTTATGGTGT
TBP	GGGGAGCTGTGATGTGAAGT	CCAGGAAATAATTCTGGCTCA

occurred during the night. Pregnant females were sacrificed by cervical dislocation and embryos dissected. Embryo dissections were conducted in either M2 medium, DEPC-PBS supplemented with 10% foetal calf serum, and filter sterilised, or DEPC-PBS. Embryos were staged by the emerging pattern of extraembryonic ectoderm or the allantois (for 7.5dpc) (Downs *et. al.* 1993) while later stages were staged by somite number or the presence of developmental landmarks (limb development, eye pigmentation etc).

2.2.4 Microdissection

To facilitate comparative gene expression between regions of the heart, microdissection was carried out. Glass pipettes were pulled above a Bunsen flame and used to slice tissue, in dissection medium, under a microscope.

2.3 Molecular Biology Protocols

2.3.1 Primer design

Primers for standard PCR and for the generation of *in situ* hybridisation probes were designed using the online programme Primer3 (v0.3.0; Whitehead Institute for Biomedical Research). Primers for quantitative PCR were designed online using software of the Universal Probe Library Assay Design Center (Roche Applied Science, Roche).

2.3.2 Cloning of DNA, Bacterial Cell Transformation and Culture

Probes designed were amplified by PCR from either cDNA from tissue known to express the gene of interest, or from the appropriate I.M.A.G.E. clone. The appropriate band was extracted (if it were not the sole band from the PCR) and ligated into either pTOPO (Invitrogen) or pGEM-Teasy (Promega Corporation, Madison, WI, USA) vectors, according to company instructions.

Plasmids, obtained from other laboratories, were resuspended from filter paper in 50μl TE or dH_2O. Samples were quantitated and an appropriate amount was transformed into bacterial cells.

In all instances, competent TOP10 cells (Invitrogen) were transformed with ligation products, or other plasmid constructs, by the heat shock method according to the manufacturers instructions. Cells were spread on warmed LB-agar plates, containing the appropriate antibiotic (Ampicillin or Kanamycin) dependent on the plasmid transformed. Plates were incubated at 37°C to facilitate bacterial growth for a minimum of 16-18hrs.

To obtain DNA, on average 10 colonies were picked and used to inoculate 3ml LB broth containing the appropriate antibiotic. Once at the appropriate density, bacterial broths containing plasmids which required further screening (say, for *in situ* probe generation where knowledge of insert orientation was required) were used to streak a section of an LB-agar/antibiotic plate and the remainder subjected to mini-preparation according to the manufacturers instructions. Plasmid DNA was screened for insert orientation by a test restriction digest. Appropriate clones could then be

grown in larger cultures for maxi-preparation (according to the manufacturers instructions).

Cultures growing bacteria containing plasmids which did not require screening (say, plasmids which were obtained from other laboratories or pre-existed in the laboratory of this candidature) were used to inoculate a larger culture of growth medium for maxi-preparation the following day.

For each plasmid bacterial cells were archived by freezing in 10% glycerol. Glycerol stocks were stored at -80°C. If it was required to re-grow the bacteria from glycerol stocks, a sterile pipette tip was used to stab the frozen cell-solution (without thawing the glycerol stock), and inoculated in warmed growth media for culture.

2.3.3 Preparation of Nucleic Acids

Plasmid preparation

Bacterial culture growth volume was dependant upon the amount of plasmid required. Minipreps or maxipreps were performed by use of kits according to the manufactures instructions (Qiagen).

Genomic DNA preparation for genotyping - from adult mice

Ear tissue samples were digested for 2 hours at 55°C in 400μl TE SDS and Proteinase K. DNA was extracted by chloroform/salt treatment and precipitated, then washed, in ethanol. DNA was resuspended in an appropriate volume of TE.

Genomic DNA preparation for genotyping - from embryos

A small amount of embryo-derived tissue (usually the ectoplacental cone or a portion of the yolk sac, or amnion) was digested directly in PCR buffer lacking magnesium , but supplemented with Proteinase K. Samples were incubated at 55°C for 2 hours before proteinase K inactivation at 70°C for 10 minutes. Normally, 0.5μl of digested tissue was used in a 20µl PCR, although occasionally it was necessary to dilute the sample further.

2.3.4 Quantitation of Nucleic Acid

All spectrophotometric quantitation of nucleic acid was performed using a NanoDrop ND-1000 (NanoDrop technologies/ ThermoScientific Wilmington, DE, USA).

2.3.5 Polymerase Chain Reaction (PCR)

In general, DNA was amplified by PCR in a 20μl volume containing 1.5mM $MgCl_2$ (Qiagen), 1x PCR buffer (Qiagen), 0.2mM dNTP (Qiagen), 1mM of each primer 1unit of Taq DNA polymerase (Qiagen, unless otherwise stated).

Satin Genotyping

The *satin* allele harbours a 67bp intergenic deletion (Figure 2.1a). Using PCR primers that flank the deletion embryos/ mice containing the mutant allele can be genotyped (Bogani *et. al.* 2005; Willoughby 2006). This produces bands of 388bp for the wild type and 321bp product for the *satin* allele. It was necessary to perform a touch-down PCR for this amplicon. Conditions for this are as follows. 95°C 1 min, followed by 19 cycles of: 95°C for 10 sec, 65°C 30 sec (-0.5°C per cycle), 72°C for 20 sec. This was followed by 14 cycles of: 95°C for 10 sec, 55°C for 20 sec; 72°C for 20 sec. A final extension of 10 min was performed at 72°C. To enhance amplification, the PCR required addition of 1M betaine (Sigma).

Sox4 PCR for Sequence Analysis

The ENU induced point mutation can be amplified for sequence analysis using the following PCR conditions (Bogani *et.al.* 2005; Willoughby 2006). 95°C 10 min, followed by 13 cycles of: 95°C for 30 sec, 59°C 60 sec (-0.5°C per cycle), 72°C for 60 sec. This was followed by 32 cycles of: 95°C for 30 sec, 52°C for 60 sec; 72°C for 60 sec. A final extension of 5 min was performed at 72°C. In addition, standard PCR conditions were optimised with 10% DMSO. It was necessary to use Amplitaq gold (Applied Biosystems) as the polymerase (Figure 2.1b, c).

2.3.6 Genotyping the *Sox4*^{ENU} allele using the Roche Light Cycler 480.

ENU usually induces point mutations into the genome. The *Sox4*^{ENU} allele harbours a point mutation making it impossible to genotype by PCR alone. The majority of genotyping throughout this project relied upon detecting the *Foxq1*^{satin} intergenic

deletion – a 67bp difference which could be resolved by PCR across the locus. At each generation a select number of mice from backcross litters and embryos from intercross litters were additionally genotyped for the *Sox4 ENU* allele by sequence analysis. Part-way through the breeding programme, it was decided that genotyping should be carried out for both loci. To facilitate this, it was necessary to design a strategy for use of the *Roche* light cycler and the 'genotyping master' programme and reagents (Figure 2.2). Amplification across the mutation produces a product of 220bp. PCR reactions were prepared according to the manufacturers instructions (Roche Genotyping Master kit), although conditions were optimised with the addition of 1M betaine (Sigma).

2.3.7 Gel electrophoresis

In order to resolve the 67bp deletion of the *Satin* mutation, PCR products were run on an Invitrogen pre-cast E-Base system with a 2% gel. For other applications separation of DNA fragments generated by PCR or restriction digest, or RNA following extraction, was carried out by standard agarose gel electrophoresis. Gel concentration was typically 1-2% w/v agarose with 0.5μg/ml ethidium bromide in 1xTAE running buffer. Samples were diluted in 1x loading dye and run at 100V for an appropriate time. Bands were visualised on a UV transilluminator.

2.3.8 Purifying PCR products - PEG precipitation

An inexpensive and effective method of removing enzymes and nucleotides from a PCR for sequence analysis is precipitation by polyethylene glycol (PEG). This was used predominantly for products which required sequencing. PEG precipitation makes use of a 20% PEG, 2.5M NaCl solution (20g PEG 8000, 14.6g NaCl and dH_2O to 90 ml, shake; leave 20+ min at 37°C to allow the PEG to go into solution, then make up mixture to 100ml). In a 1.5ml eppendorf tube, combine each PCR solution and an equal volume of PEG/salt, then incubate for 15 minutes at 37°C. Centrifuge the solution at maximum speed for 15 minutes to pellet the precipitate then discard the solution. Wash the pellet with 125μl 80% EtOH, centrifuge at maximum speed for 2 minutes, after which discard the supernatant and re-wash,

before leaving the pellet to dry. Resuspend the DNA PCR pellet in dH_2O at a volume half of the original PCR solution.

2.3.9 Sequencing

Purified PCR products were submitted for automated sequence analysis by the University of Edinburgh's School of Biological Sciences Sequencing Service. For this, 8ng of DNA in 5μl was combined with 1μl of 3.2pmol uni-direction primer. Sequencing reactions were carried out according to the manufacturers specifications, using the ABI PRISM Big-dye terminator premix sequencing kit (Perkin-Elmer Waltham, MA, USA). Samples were subject to sequencing thermocycling then run on an ABI sequencer (Applied Biosystems).

2.3.10 Restriction enzyme digest

Restriction enzyme and buffers (NEB Inc. or Roche), were used to carry out restriction enzyme digests on plasmid DNA prior to the creation of *in situ* probes (Table 2.2) according to the manufacturer's instructions. Digests were incubated at 37°C or another temperature if specified. Incubations were carried out for 2 hours or overnight, and then electrophoresis was performed to verify complete digest.

2.3.11 RNA Extraction and Analysis

RNA Extraction and Quantitation

For the purpose of expression analysis RNA was extracted from tissue of interest. Two kits were utilised for this purpose. For general RNA extraction (ES cells or tissue with relatively large cell number), a miniRNA (Qiagen) kit was used. In cases of extraction from tissue of small sample size (for example, outflow tracts of the heart), a microRNA (Qiagen) kit was used. In both cases, the manufacturers instructions were followed.

Reverse Transcriptase - PCR

To enable determination of RNA expression, RNA was reverse transcribed. For this, the SuperScript III Reverse Transcriptase kit (Invitrogen) was used. Reactions were set up and procedure carried out according to the manufacturers instructions.

Quantitative PCR

To examine the gene expression in micro-dissected outflow tracts. The Roche Light-cycler PCR machine was used in conjunction with the Light cycler 480 Probes master kit solutions and probes (Roche). For the purpose of determining gene expression of *Wnt11*, *Fzd7* and *Tgfb2*, as well as the *Tbp* internal control, probe numbers 96, 20, 73 and 97 (respectively) were used. Primers (Table 2.1) were used at a concentration of 1μM; probes were used at a concentration of 0.1μM. Standard curves were created using wild type cDNA as template. Samples were prepared and run with reagents in conditions according to the manufacturers instruction.

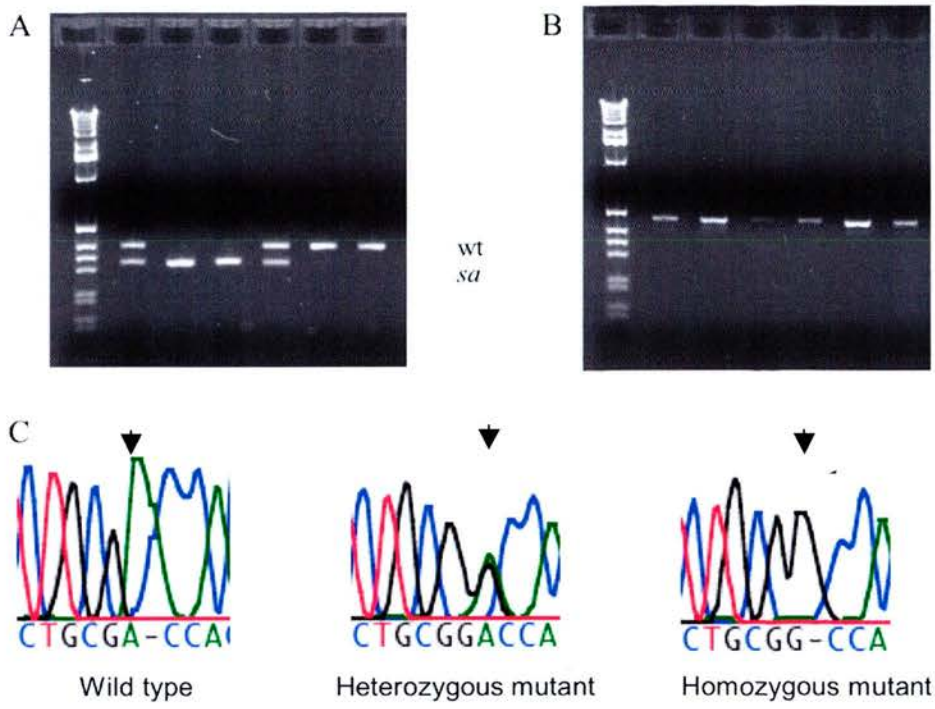

Figure 2.1: Genotyping assays for DNA from mice and embryos harbouring the *Foxq1 satin* deletion and the *Sox 4* ENU mutation.

(A) Image of a 2% agarose gel following electrophoresis of the *Foxq1* wild type and *satin* amplicons, demonstrating the 67bp intergenic deletion; (B) Image of an agarose gel following electrophoresis of the *Sox4* amplicon which, for genotyping required sequencing (C) Sequence traces of *Sox4* amplified from mice wild type, heterozygous and homozygous for the ENU locus (arrowhead indicates the base change, as described in the text of section 1.4.3).

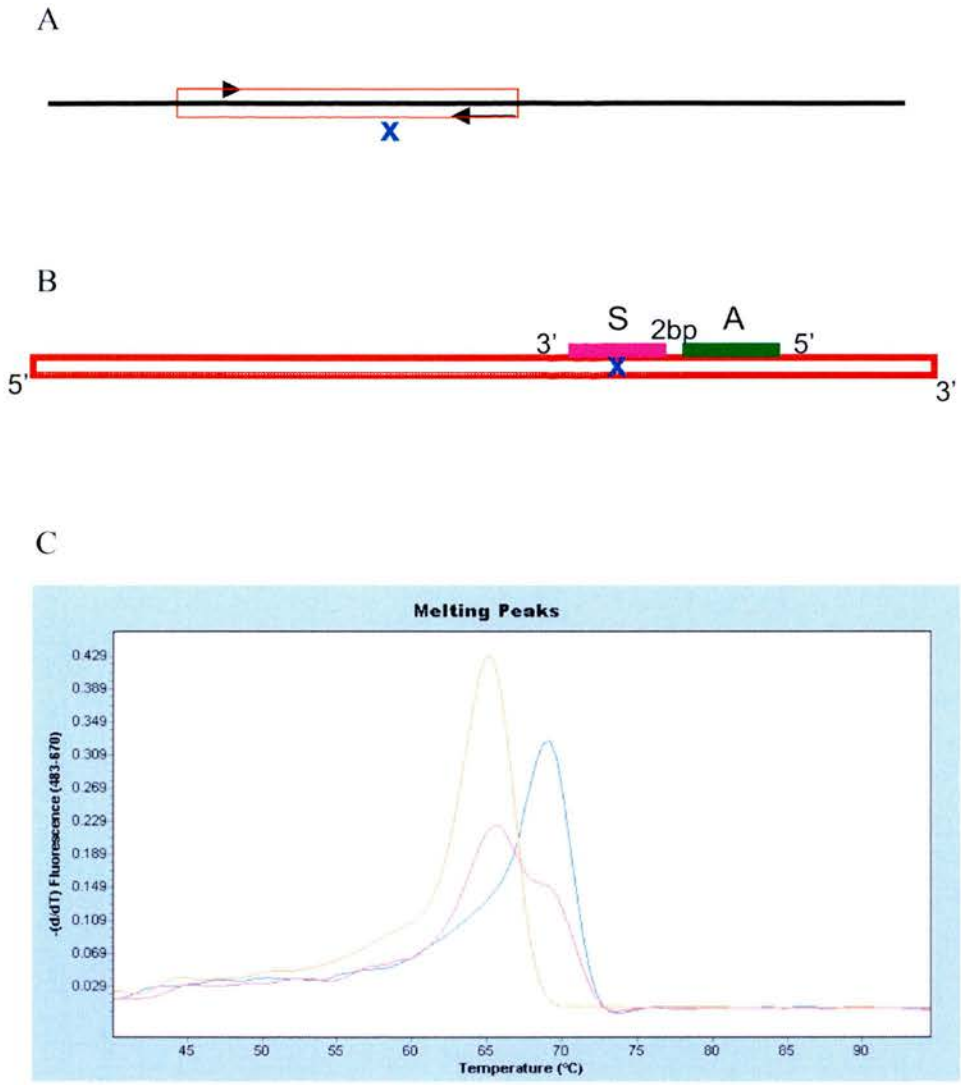

Figure 2.2: Method for use of the *Roche* Light Cycler 480 for mutation analysis of the *Sox4* allele.

(A) Amplification around the ENU point mutation produces a product of 220bp. PCR was optimized with 1M betaine and 0.5mM primers; (B) Following the PCR programme, products were subjected to a melt curve programme by denaturation at 95°C, then annealing at 60°C, 50°C and 40°C of the probes. The 22bp sensor probe [S] was 5' labelled with Cy5 and a 3' phosphatase, the 23bp anchor probe [A] was labelled at the 3' end with fluorescein. Annealed probes and amplicons were melted to 95°C with continuous acquisitions of fluorescence at 670nm; (C) Melting temperature of amplicons for the alleles of Sox4. The wild type allele melts at 66-67°C and the ENU mutant peak at 70-71°C. Wild type peak is yellow, heterozygous peaks are pink and homozygous peak is blue.

2.4 WHOLE MOUNT *IN SITU* HYBRIDISATION (WMISH)

2.4.1 *In situ* hybridisation probes.

Plasmids containing probe sequences for *in situ* hybridisation were sourced from various laboratories if not already existing in a laboratory at the ISCR (Table 2.2).

The expression profile of *Sox4* and *Foxq1* transcripts (Chapter 4) were detected using *in situ* hybridisation. Since *Sox4* expression was relatively widespread, alterations to the stringency of the post-hybridisation washes were made to examine which tissues demonstrate the highest gene expression.

Two probes were used to analyse *Sox4* expression. Initially, a probe comprising bases 516 to 2031 (coding sequence bases 662 to 1984, 146bp 5' UTR, 47bp 3'UTR) demonstrated a complex expression pattern, readily appearing in most tissues analysed. To determine whether this probe, which included the HMG box, specifically detected *Sox4* expression, a second probe was constructed to recognise 535bp of the 5' untranslated region (UTR) - bases 144 to 678. Primers spanning the region were designed using the online programme Primer3 (v0.4.0; Whitehead Institute for Biomedical Research). This second probe yielded the same expression pattern as the original *Sox4* probe and ruled out the possibility that the HMG homology resulted in detection of other Sox genes. To examine whether expression, detected by the probe, was due to non-specific binding, embryos were overstained with sense (control) and antisense Sox4 probes in parallel. Neither the full-length (Figure 2.3) nor the short 5'UTR sense probe (Figure 4.4a) produced a signal.

In order to document *Foxq1* expression for mouse embryogenesis, it was necessary to design and generate an *in situ* probe. Again the programme Primer3 was used to design primers flanking a 208bp sequence comprising bases 495-683 of the 5'UTR of *Foxq1* (NM_008239.4). The *Foxq1* sense probe did not produce a signal when treated in parallel to embryos hybridised to the anti-sense probe (Figure 4.12c).

The primers used to amplify the sequences for the *Foxq1* and *Sox4* (5'UTR) probes are shown in Table 2.2.

2.4.2 Probe generation directly from PCR

For generation of new antisense probes by PCR amplification, a T7 polymerase site (ATATATTAATACGACTCACTATAGG) was incorporated directly to the 5' end of the reverse complemented reverse primer. To generate the control sense probe, the T7 recognition sequence is placed on the forward primer. PCR products were gel checked, band extracted and then subcloned and sequenced for future use.

2.4.3 Preparation of plasmid for probe synthesis

Plasmid was linearised as described (section 2.3.10) and gel checked to ensure complete digestion. If digestion was incomplete, the digested band was gel extracted as described (section 2.3.8). Addition of 40 µl RNase-free 3M sodium acetate, DEPC water to the volume of 500 µl and an equal volume of phenol-chloroform-isoamylalcohol (ratio 25:24:1), enabled DNA purification. DNA was precipitated in ethanol, resuspended in 50µl and quantitated.

2.4.4 Digoxigenin (DIG) labeled RNA probe synthesis

In situ probes were generated using, predominantly, reagents from Roche. 1 µg plasmid was made to 12.5 µl, or 12.5 µl of purified PCR product, was combined with 2 µl 10x transcription buffer, 2 µl 10x DIG, 1.5 µl RNase inhibitor and 1 µl of the appropriate RNA polymerase. Reactions were incubated for 1hr at 37°C, an additional 1 µl of polymerase was added and then incubated for another hour. Probe RNA was DNAse treated with DNase (Promega) in the presence of 10x buffer, according to the manufacturers instructions. Usually, probe RNA was then purified as follows: Samples were diluted to 50µl with DEPC-treated milliQ water. 5µl of RNase-free 3M NaOAc was added, followed by 2.5x volume of RNase-free 100% ethanol. To precipitate, samples were incubated at -20°C for 30 minutes and then pelleted in a refrigerated microfuge for 10 minutes. Pellets were washed twice with RNase-free 70% ethanol to remove unincorporated nucleotides.

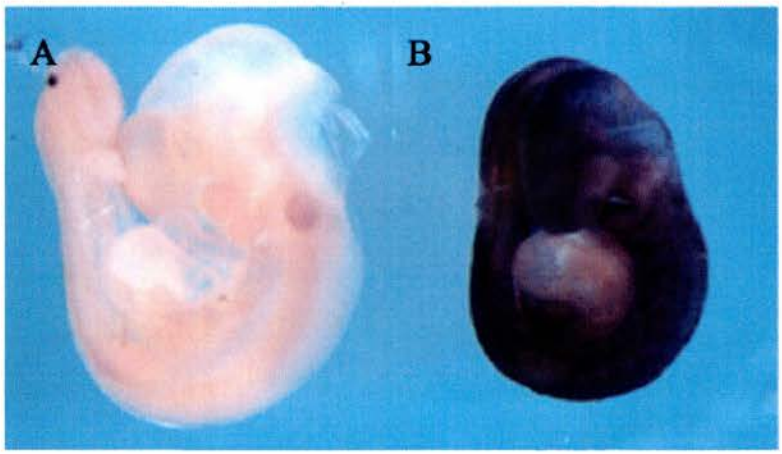

Figure 2.3: *In situ* hybridisation with sense transcripts of the full-length *Sox4* probe does not produce a signal.

(A) A wild-type 9.5dpc embryo subjected to in situ hybridisation with the sense probe of full-length Sox4. With the exception of the probe hybridisation, the embryo in (A) was treated in the same solutions throughout the procedure as that of the antisense full length probe in (B); (B) Overstained (24 hours) antisense probe.

Table 2.2: List of probes for *in situ* hybridization for results presented in this thesis.

Probe	Template	Restriction site	RNA Polymerase	Source
Sox4	plasmid	*Apa1*	SP6	Cadmann, M.
Hand1	plasmid	*Not1*	T7	Olson, E.
Hand2	plasmid	*EcoR1*	T7	Olson, E.
Nppa	plasmid	*EcoR1*	T3	Arkell, R.
Pitx2	plasmid	*Sac1*	T3	Ryan, A.
Shh	plasmid	*HindIII*	T3	McMahon, A.
Fgf8	plasmid	*HindIII*	T3	Martin, G.
Bmp2	plasmid	*XbaI*	T3	Hogan, B.
Nfatc1	plasmid	*Not1*	T3	Burn, S.
Probe	Template	Forward Primer	Reverse primer (T7 promoter sequence shown in red)	
Sox4 5'UTR	PCR product	ATTCATGCCGGTCTGTTGC	ATATATTAATACGACTCACTATAGGTTGGTCTGTTGTACCATGG(	
Foxq1	PCR product	GTAAGGACAGCACTGCACCA	ATATATTAATACGACTCACTATAGGGAGGTCGTAGGAAGCGAG	

2.4.5 Wholemount *in situ* hybridisation on mouse embryos

The wholemount *in situ* hybridisation protocol used successfully for the *in situ* results presented in this thesis was described extensively in (Christiansen *et. al.* 1995) and later published separately in (Hargrave *et. al.* 2006). It is based on the Wilkinson protocol (Wilkinson 1992). Embryo powder was not used.

Variation to the protocol for some Sox4 in situ hybridisation

In each of the documented *in situ* images, it is important to note that variation in the time of developing altered signal intensity. Additionally a modification in this protocol was made to increase the stringency of probe-transcript binding. To examine levels of *Sox4* expression the concentration of CHAPS in the hybridisation step and post-hybridisation washes was increased by a factor of 10.

2.4.6 Section *in situ* hybridisation on mouse embryos

Sections of embryonic tissue were prepared on slides as described (section 2.6.1). All steps were conducted in glass staining dishes unless otherwise stated, with slides moved on a metal rack. All equipment was baked overnight prior to use.

Preparation of slides for hybridisation

Slides were de-waxed in two 10min. changes of Xylene, and rehydrated through an Ethanol series to PBS. Tissue was treated for 20-35 min. (depending on age of embryo) in a solution of 10 ug/ml proteinase K in PBS at 37 °C. Slides were rinsed in PBS and immediately re-fixed in 4% PFA for 10min. Slides were rinsed thoroughly in PBS and then acetylated for 10 min. in a solution of 0.1M Triethanolamine/0.25% acetic anhydride. Slides were washed through several changes of PBS, then dehydrated through an ethanol series and dried for up to 1hr.

Probe hybridisation

Probes were denatured in hybridisation solution as for wholemount *in situ* hybridisation, then made to a volume of 200µl with pre-warmed hybridisation solution. An incubation chamber was prepared. This was a pipette tip box, humidified with a paper towel in the bottom chamber soaked in a formamide/SSC

solution to the same proportions as in the hybridisation buffer (but using less pure formamide and non-DEPC-treated SSC). Three slides were placed in each box, elevated above the paper towel. Probe solution was applied to each slide and a piece of parafilm cut to the dimensions of the slide, was placed over each slide. Slides were incubated from 55-65 °C overnight.

Post-hybridisation

Slides were washed in a decreasing concentration of SSC (5x, 2x, 0.2x) then washed several times in TBST. Slides were placed in a humidified (with TBST) incubation box for subsequent blocking and antibody steps. Tissue was blocked in 1x blocking reagent (Roche) for at least 1hr at room temperature. Anti-DIG antibody was applied at a concentration of 1/2000, diluted in TBST with 1x blocking reagent. Antibody incubation was performed for at least 2hrs at room temperature, but in most cases overnight at 4 °C. Slides were subsequently washed in several changes of TBST, with the last two changes also containing 2mM Levamisole. Slides were washed in NTMT with 2mM Levamisole, before being placed back in the incubation chamber.

Detection of signal and slide processing

Slides were incubated with BM purple (Roche) at room temperature during the day, then 4 °C overnight, until adequate signal had developed. Slides were washed in PBSTx (1mM EDTA), then dH_2O prior to dehydration in 70% and 100% Ethanol solutions. Slides were treated in Xylene and mounted with DePeX mounting media (BDH/ VWR international, LLC. West Chester, PA, USA).

2.5 DETECTION OF APOPTOSIS

Wholemount TUNEL was performed using the ApopTag *In Situ* Apoptosis detection kit (Chemicon/ Millipore, Billerica, MA, USA). Embryos were dissected as described (section 2.2) fixed in PFA and dehydrated in a MeOH/PBT series to 100% MeOH. If embryos were visible, the following steps were performed in 2ml snap-lock tubes with as much solution as possible. Embryos were permeabilised by rehydration to PBT and incubated in proteinaseK (at 10μg/ml) for an appropriate time. Embryos were washed in 2mg/ml glycine/PBT for 2 minutes and then subjected to further washes in PBT. Embryos were post-fixed in 4%PFA for 20

minutes at room temperature and then further washed in PBT five times. Embryos were further fixed in prechilled ethanol:acetic acid (mixed in a ratio of 2:1) on ice, for 10 minutes and then washed three times in PBT. For terminal transferase reaction, the procedure is as follows: Embryos were incubated for one hour at room temperature in equilibration buffer, then the solution was replaced with working strength TdT enzyme, with sufficient liquid to cover the embryos. Working strength TdT was prepared by a 2:1 ratio of reaction buffer and TdT enzyme with tritonX-100 to a final concentration of 0.3%. Embryos were incubated at 37°C overnight. The following morning the reaction was stopped by washing several times over 3 hours at 37°C in working strength stop/wash buffer (1:17 with distilled water) followed by a final wash thrice in PBT. Embryos were blocked in 2mg/ml BSA, 5% sheep serum in PBT for a minimum of one hour. Antibody solution was prepared as for wholemount ISH, (section 2.4) with 1/2000 anti-digoxygenin AP-conjugated Fab fragments (Roche) in PBT with 1% sheep serum and 2mg/ml BSA. Antibody solution replaced blocking solution and embryos were incubated for a minimum of two hours at room temperature or overnight at 4°C. Embryos were washed several times the following day with an overnight wash in PBT supplemented with 2mg/ml BSA. Detection of labelled tissue was by equilibrating the embryos in fresh NTMT and then incubating in NBT/BCIP (Roche) according to the manufacturers instructions. Stain was visible from 5 minutes and stopped shortly after depending on intensity, by washing in PBT. Embryos were fixed in 4%PFA for 30 minutes, washed in PBT and photographed immediately.

2.6 HISTOLOGY

The majority of histology procedures for this project were carried out by Mr Ron Wilkie (ISCR Histology Department).

2.6.1 Wax embedding and microtome sectioning

Embryos or tissue regions were dehydrated through an ethanol series (70%, 80%, 90%, 95%, 100%) then cleared in 100% xylene. Using a plastic pipette, embryos were transferred to pre-prepared molten wax in glass embryo cups at 65°C. Depending on the size of the embryo, the wax was twice changed after an

appropriate time. Embryos were orientated under a microscope as the wax solidified. Wax blocks were mounted on microtome cassettes and sectioned at 7μm intervals. Sections were floated in a water bath at 37°C and collected onto gelatinised slides. Sections were dried overnight at 37°C prior to further staining. For cutting sections for use in section *in situ* hybridisation, embryos were dehydrated in ethanol solutions made with DEPC-treated dH_2O. Water bath water was DEPC-treated; slides were washed in DEPC-treated dH_2O prior to collecting sections. Collected sections were dried overnight in an oven at 42 °C and stored at room temperature prior to RNA *in situ* hybridisation (section 2.4.6).

2.6.2 Haematoxylin and Eosin staining

To characterise tissue morphology, embryos which had been wax-sectioned were subjected to staining with haematoxylin and eosin. Sections were de-waxed through two 5 minute xylene washes and rehydrated in 2 minutes each of a decreasing ethanol series (90%, 70%, 50%, 30%) and washed in running tap water for 2 minutes. For optimal colour staining, sections were stained in a haematoxylin solution for 2 minutes washed in tap water and stained in 0.5% eosin for 15 sec. Slides were transferred quickly to 70% EtOH and then to 100% EtOH. Slides were incubated in two consecutive xylene washes, each for 5 minutes, and then mounted using DPX and coverslipped.

2.6.3 Gelatin embedding and cryostat sectioning

Embryos demonstrating *in situ* stain were sectioned by a cryostat. Treated embryos were returned to a PBS solution, then placed into 7.5% sucrose/PBS for incubation at 4°C from 30 minutes to overnight depending upon embryo size. The solution was then changed to a 15% solution of sucrose/gelatin. Embryos were incubated in this solution at 37°C until the solution had fully penetrated the embryo and the embryo had sunk in the tube. Embryos were orientated and set in this solution, then frozen in liquid nitrogen. Sections were cut to 8μm thickness using a Leica CM1900 cryostat (Leica Microsystems, Wetzlar, Germany), mounted onto charged slides and coverslipped using an aqueous mounting solution.

2.7 CELL CULTURE

2.7.1 Derivation of mouse ES cells

ES cell derivation, under serum-free conditions was performed as published in (Nichols *et. al.* 2006), using serum-free medium (Stem Cell Sciences Inc.).

2.7.2 General Culture of mouse ES cells

Derived ES cells were plated on gelatinised plates or flasks and passaged when they reached confluency. For passaging, cells were rinsed in PBS (culture grade, Invitrogen), treated with 0.1% Trypsin and incubated at 37°C for a few minutes. Once detached from the flask, culture medium was added to the cells and the solution of cells was transferred into a tube for centrifugation. Cells were gently pelleted (3 min 300 rcf) and then re-suspended for plating into a pre-equilibrated gelatinised flask. Cells were maintained in culture at 37°C under 7% CO^2.

2.8 GENERATION OF CHIMÆRIC MICE

Derived ES cells were injected into C57BL/6J blastocysts and transferred into recipient psuedopregnant mice by the ISCR transgenic facility. Transgenic pups were born and assessed for ES cell contribution by coat colour.

Adult mouse tissue contribution by ES cells was determined as follows: Tissue was harvested from organs (see below) and DNA extracted (Section 2.3.3). Tissue was genotyped by PCR for the *satin* allele (Section 2.3.5). By reducing the PCR cycle number by 10 cycles, the PCR was able to be interpretated as semi-quantitative.

Tissue examined: gut, eye, tongue, brain, ovary, telencephalic lobes, thymus, lung, thyroid, diaphragm, tail, skin, skull, spleen, pancreas, kidney, liver, skeletal muscle, femur bone, bone marrow, atria, interventricular septum, ventricle.

2.9 MICROSCOPY

A Zeiss Stemi SV11 microscope (Carl Zeiss, Welwyn Garden City, UK) with bright field optics, fitted with Zeiss achromat objectives and a Coolsnap-*cf* camera (Photometrics Ltd, Tucson, AZ, USA), was used for some whole mount embryo imaging, photography of *in situ* cryo-sections and some photography of

Haematoxylin and eosin stained section (figures 3.9 and 3.10). Images were captured using Open lab software (Improvision/ PerkinElmer, Coventry, UK).

An Olympus IX51 (Olympus, Essex, UK), fitted with UplanFLN objectives and a QImaging camera (QImaging, Burnaby, BC, Canada) was used to image ES cells in culture. Images were captured using QCapture software (QImaging).

A Nikon AZ100 macroscope (Nikon UK Ltd, Kingston-on-Thames, UK) fitted with 0.5x, 1x, 2x, 4x and 5x objectives and a Qimaging Micropublisher 5 cooled colour camera (QImaging) was used to image some wholemount *in situ* staining of embryos and some section *in situ* staining by placing slides on an agarose-filled petridish, inverted on a white page for minimising background shadow. Image capture was performed using IPLab Spectrum (Scanalytics Corp, Fairfax, VA).

A Zeiss Axioplan II fluorescence microscope with Plan-neofluar or Plan Apochromat objectives (Carl Zeiss, Welwyn Garden City, UK) and a Qimaging Micropublisher 3.3mp cooled colour CCD camera (QImaging) was used to image most haematoxylin and eosin stained sections and section *in situ* slides. Images were captured using in-house scripts (MRC, HGU) written for IPLab Spectrum software.

2.10 Image Analysis

All images were processed in Adobe Photoshop CS3 (Adobe Systems Inc., San Jose, CA, USA). Scale-bars are demonstrated where necessary. Determining the size of scale bars was achieved by photographing a microscale rule and calibrating the OpenLab or IPLab software to interpret length in place of pixels.

CHAPTER 3: ANALYSIS OF THE *Sox4*^{ENU} *Foxq1*^{SA} PHENOTYPE.

3.1 INTRODUCTION

The Sox4 transcription factor has been shown to be critical for embryonic development, since the null mutation in *Sox4* causes lethality by E13. Embryonic death in homozygous nulls has been attributed to heart defects and oedema (section 1.1.4) (Penzo-Mendez *et. al.* 2007; Schilham *et. al.* 1996). A novel mutant allele of *Sox4* (termed M91 and hereafter referred to as this in the context of the work by Bogani *et.al.*, prior to the allele being used for this work) was identified from a phenotype driven recessive ENU mutagenesis screen (Bogani *et. al.* 2005). This allele carries a point mutation predicted to alter the protein sequence of the highly conserved HMG box domain of Sox4 (section 1.4.3). Given that ENU-induced mutations can produce alleles of different severity and function, this allele may enable further characterisation of Sox4, beyond that determined from the published null alleles.

Initial observations of the M91 embryonic phenotype were carried out during screening of the ENU line (Bogani *et. al.* 2005). The heterozygous mouse line carried mutations in *Sox4* and *Foxq1*, and was maintained on a mixed C3H/HeH and 101/HeH background. Crossing this line to mice heterozygous for the *Del(13)Svea36H* deletion produced embryos hemizygous for the *Sox4* and *Foxq1* mutant alleles. Crosses to yield homozygous embryos of this allele generated the same embryonic phenotype as the crosses to *Del(13)Svea36H*. An additional ENU mutation in *Sox4* was identified in a parallel mutagenesis screen (with non-*satin* males chemically mutagenised). Genetic crosses were carried out between heterozygotes of each *Sox4* allele (Dr. Ruth Arkell *pers.comm.*). Compound heterozygous mutant embryos from these crosses, revealed the same embryonic phenotype as that described for homozygotes for either ENU-induced *Sox4* mutant

allele (Bogani *et. al.* 2005; Goldsworthy *et. al.* 2008). This, and other lines of evidence discussed in Chapter 1 (section 1.4.3) indicate that mutation in *Sox4* is responsible for the cardiac phenotype observed.

At E14.5, M91 *Sox4* mutant embryos demonstrated significant overlap with the published null phenotype (Bogani *et. al.* 2005 compared with Schilham *et. al.* 1996 and Ya *et. al.* 1998b). The published phenotypic outcome of targeted germline inactivation of *Sox4* includes both OFT defects and VSD at E14 (Schilham *et. al.* 1996; Ya *et. al.* 1998b). The phenotype is described at E13.5 in the analysis of the conditional *Sox4* null allele (Penzo-Mendez *et. al.* 2007). This was observed at E14.5 in an M91 mutant by magnetic resonance imaging (MRI). The M91 mutant published by Bogani *et.al.* also shows an atrial septal defect in the primary atrial septum, a common atrioventricular junction and a dysplastic mitral valve at E14.5 (Bogani *et.al.* 2005), which have not been described from the histological analysis of nine E14 or eight E13 *Sox4* null embryos examined by Ya *et.al.* (Ya *et. al.* 1998b). Whether this additional atrial and atrioventricular phenotype is a fully penetrant phenotype in the M91 line is unclear. If the atrial and atrioventricular phenotypes are a consequence of the $Sox4^{ENU}$ allele, then this suggests an additional function of the ENU allele of *Sox4* not uncovered by complete gene inactivation. However it remains possible that differences in genetic background may modulate the phenotype of the *Sox4* null and $Sox4^{ENU}$ alleles. To determine whether this is the case would require a parallel study of these alleles on the same genetic background.

Formation of the heart commences at the late head-fold stage six days prior to the published *Sox4* phenotype. Earlier still, patterning of cardiac progenitors occurs during gastrulation. The cardiac phenotype of the conditional *Sox4* null allele was examined at E13.5 (Penzo-Mendez *et. al.* 2007). The *Sox4* null allele was examined at E12-E14 (4xED12, 8x ED13, 9xED14) (Ya *et. al.* 1998b). Schilham *et.al.* had previously reported that a macroscopic phenotype was not observed at E13, yet *Sox4* null embryos rapidly develop a macroscopic phenotype and are dead (or dying) by E14 (Schilham *et. al.* 1996). At E12-E14, it was observed that *Sox4* null mutant embryo constitute only 18-20% of embryos dissected, instead of the expected Mendelian ratio of 25% [Materials and Methods in (Ya *et. al.* 1998b)]. Bogani *et.al.*

show that the M91 mutation results in a final embryonic lethal time-point which is the same as that of the null (mutants dead or dying during E14) (Bogani *et.al.* 2005). At E15.5, in the same series of genetic crosses, all hemizygote mutant embryos (n=25) were dead (compared, with dead or dying during E14), and comprised 16% of embryos dissected at this stage (Dr Ruth Arkell *pers.comm.*). This finding, together with the percentage of mutant embryos in the data provided by Ya *et.al.* suggests that *Sox4* mutations result in lethality earlier than E14. These observations prompted the present study of earlier embryonic stages to examine the timing of lethality and whether an uncharacterised *Sox4* homozygous phenotype exists, forming the basis of this chapter of my thesis, with the aim: *To conduct detailed wholemount and histological section analysis of the cardiac defects present in* $Sox4^{ENU/ENU}$ $Foxq1^{sa/sa}$ *mutant embryos.*

Homozygotes have been examined from E7.5 to the starting point of the known lethality (E13.5). Since the ENU mutagenesis screen was carried out on mice that harboured the *satin* allele of *Foxq1*, this study also provides an opportunity to examine whether an extra-cardiac *Sox4* phenotype is modulated by the *satin* mutation in *Foxq1* (and equally, whether the *satin* phenotype is altered by the mutation in *Sox4,* as the *satin* phenotype is well characterised). Given that the null allele of *Foxq1* does not demonstrate cardiac dysmorphologies (Goering *et. al.* 2008), it is unlikely that the *satin* allele plays a role in cardiogenesis (section 1.4.4). This, and the genetic crosses described (section 1.4.3), implies that the abnormal cardiac phenotype in these embryos is a consequence of the mutation in *Sox4*.

3.2 RESULTS

To explore the phenotype of the *Sox4*^{ENU} allele, the M91 mouse line (as published in Bogani *et.al.*) was imported into the ISCR animal unit and backcrossed to C57Bl/6J. Subsequent generations of mice were intercrossed to characterise the homozygous phenotype on this background.

3.2.1 Homozygosity of the *Sox4*^{ENU} allele causes cardiac abnormalities in E12.5 and E13.5 embryos on a C57Bl/6J background.

One of the first points of investigation was to examine the phenotype of the *Sox4*$^{ENU/ENU}$ *Foxq1*$^{sa/sa}$ embryos. This intent was twofold: (1) to examine the E12.5 and E13.5 phenotype of the *Sox4* ENU mutation since published information was limited to E14.5 (Bogani *et. al.* 2005) and (2) to compare this with the cardiac phenotype of the *Sox4* null (Schilham *et. al.* 1996; Ya *et. al.* 1998b).

Upon dissection, mutant embryos could be visually distinguished from unaffected siblings. At E12.5 and E13.5 embryos showed oedema and haemorrhaging (E12.5 not shown; E13.5 Figure 3.1b, c), in contrast to the morphologically normal stage-matched control embryo (E12.5 not shown; E13.5 Figure 3.1a). This was verified by section analysis to reveal the severity of the oedema, both immediately below the body wall and around internal structures (E12.5 not shown; Figure 3.1e, f, compared to control, d). Haemorrhaging and oedema are indicative of a lowering of vascular integrity and increased pressure on vascular endothelial cells as a consequence of cardiac deficiency and inadequate movement of fluid. Oedema was identified as part of the phenotype of *Sox4* null homozygosity, thus this is the first visible overlap in phenotype of the *Sox4*^{ENU} allele with that of the null allele.

Embryos staged E12.5-13.5 and homozygous for both *Sox4* and *Foxq1* mutant alleles were examined by sectioning and staining with haematoxylin and eosin. Sections through cardiac tissue revealed that all mutant embryos examined at these two stages exhibit a number of abnormalities within the heart (Table 3.1). Outflow tract anomalies include early evidence for incomplete septation between the pulmonary trunk and aorta below but not above the developing endocardial ridges at E12.5. At E13.5, this phenotype is more notable with persistent truncus arteriosus (PTA) being

present at or below the developing semi-lunar valves. In the control E13.5 heart, the outflow septation is complete, while E13.5 mutants also demonstrate double outlet right ventricle (DORV). Sectioning through the interventricular septum in mutant embryos showed incomplete ventricular septum formation. Although the septum was not fully closed in the control hearts, in mutant hearts the interventricular foramen was more prominent. Mutants also showed abnormal atrioventricular valve (AVV) morphogenesis. In most embryos, evidence for valve development could be observed on both the left and right sides of the atrioventricular septal mesenchyme, in the regions which will develop into the mitral and tricuspid valves. In one of four E12.5 embryos and one of two E13.5 it could not be determined from the sections whether the heart had both right and left sided valve development (Table 3.1). Subsequent figures reveal aspects of the phenotypes in more detail.

Defective septation in mutant embryos was evident at or below the endocardial ridges at E12.5 and E13.5. At E12.5 development of the septum was not obvious in mutants (Figure 3.2f, j, compared with control b). The endocardial ridges developing in both the pulmonary trunk and aorta appeared smaller in mutants than wild type (Figure 3.2g, k, compared with control b and c). At E13.5 development of the semi-lunar valves from the endocardial ridges appeared delayed (and therefore are termed 'ridges', not 'valves') (Figure 3.3f, g, k, l compared with control a, b, c). Although it was not possible to conclude from these sections whether valve development would occur in a correct manner such that the development of the valve leaflets occurs normally with respect to both position and leaflet number.

At E12.5, the developing OFT cushions at the boundary with the right ventricle also appeared reduced in size, and furthermore did not appear to make contact across the lumen (bracket Figure 3.2h and l, compared with control d). Outflow tract defects were more prominent in embryos staged E13.5. At or below the appearance of the endocardial ridges, it was evident that septation had not proceeded. The lumen of the aorta was open to the pulmonary tract in both mutant embryos (Figure 3.3f, g, j, k, compared with control b, c). PTA was accompanied by DORV as the common trunk

Figure 3.1: *Sox4*$^{ENU/ENU}$ *Foxq1*$^{sa/sa}$ embryos demonstrate pericardial swelling, haemorrhaging and oedema at E13.5. Wholemount images and haematoxylin and eosin-stained transverse trunk sections of E13.5 control (A,D) and homozygous mutant (B,C,E,F) embryos. (A,D) Control embryo does not demonstrate pericardial effusion, haemorrhaging or oedema. Homozygous mutant embryos demonstrate both pericardial swelling (white arrowhead) and haemorrhaging (black arrowhead) in wholemount (B,C) and sections (E,F). Black arrow indicates oedema at the body wall; orange arrow marks swelling at inner regions. (B,C) Mutant embryos also demonstrate abnormal anterior development, also indicated by lack of eye pigmentation. Scale bar: A-C 360μm; D-F 296.7μm.

A
B
C
D
E
F

Table 3.1: Cardiac abnormalities in *Sox4*$^{ENU/ENU}$ *Foxq1*$^{sa/sa}$ embryos at E12.5 and E13.5.

Cardiac structure or cardiac abnormality:	E12.5		E13.5	
	Mutant	Evident in wildtype littermate?	Mutant	Evident in wildtype littermate?
Septation above endocardial ridges	5/5	Yes	2/2	Yes
Endocardial ridge formation	5/5	Yes	2/2	Yes
Septation below endocardial ridges	0/5	Yes	0/2	Yes
Double outlet right ventricle	5/5	Yes	2/2	No
Incomplete ventricular septation	5/5	Yes	2/2	Yes - middle of heart
Evidence of left and right AVV development	3/4	Yes	1/2	Yes
Incomplete atrial septation	4/4	Yes	2/2	Yes
Extra-cardiac defects:				
Oedema	5/5	No	2/2	No
Haemmorhaging	5/5	No	2/2	No

* in cases where only 4 embryos were examined, it was not possible to determine this region from the sections

Figure 3.2: Histological analysis of the outflow tract cardiac defects in *Sox4*$^{ENU/ENU}$ *Foxq1*$^{sa/sa}$ embryos at E12.5. Haematoxylin and eosin-stained sections of control and mutant embryos were examined for outflow tract morphology at E12.5. (A, B, C and D) Transverse sections through a control embryo reveal the normal morphology of the heart at this stage, while defects are observed in sections through two homozygous mutant hearts (E-H, I-L). In the most anterior region of the heart, at the level of and above the endocardial ridges of the pulmonary trunk (PT-R), the aorta (A) and pulmonary trunk are septated in the control (black arrowhead A) and mutants (black arrowhead E, I). At the level of the endocardial ridges of the aorta, the developing aorticopulmonary septum (black arrowhead) is not as prominent in the mutants (F, J) as in the control (B). Endocardial ridge development at this stage is evident in both the pulmonary trunk and the aorta (A-R), although mutant tissue (black arrow G, H, K, and L) is not as well developed as control heart ridges (black arrow, C and D). The OFT endocardial cushions appear smaller than wild type and do not appear to be approaching contact across the lumen (bracket marked by asterisk in H and L). In both mutant and control at this stage, both the aorta and pulmonary trunk exit the unseptated ventricular chambers (D, H, L). Abbreviations: A aorta; A-R endocardial ridges of the aorta; LA left atrium; LV left ventricle; PT pulmonary trunk; PT-R endocardial ridges of the pulmonary trunk RA right atrium; RV right ventricle. Dorsal-Ventral orientation is as shown in A. Scale bar: 200μm.

+/+
ENU/ENU
ENU/ENU
A
B
C
D
E
F
G
H
I
J
K
L
RA
LA
A
A-R
PT-R
V
P
RV
LV
*

Figure 3.3: Histological analysis of cardiac defects in the outflow tract of *Sox4*$^{ENU/ENU}$ *Foxq1*$^{sa/sa}$ embryos at E13.5. Haematoxylin and eosin-stained transverse sections of control and mutant embryos were examined for cardiac morphology at E13.5. (A, B, C and D) Transverse sections through a control embryo reveal the normal morphology of the heart at this stage, while abnormalities are observed in sections through two homozygous mutant hearts (E-H, I-L). Hearts are compared at similar planes of sectioning as indicated by the positioning of images into four columns. In the most anterior region of the heart, above the developing valves of the pulmonary trunk (PT-V), the aorta (A) and pulmonary trunk (PT) are septated in the control (black arrowhead in A) and mutants (black arrowhead in E and I). In the control heart, septation is also evident at the level of the pulmonary trunk valves (in B) and the valves of the aorta (A-V in C). Also in the control embryo, septation is complete such that the pulmonary trunk exits the right ventricle, while the aorta exits the left ventricle (arrow head, D). In the mutant embryos, at the level of the endocardial ridges (prior to development into semi-lunar valves) (PT-R and A-R) the septum is incomplete (black arrowhead E, J) and the pulmonary trunk is open to the aorta (F, G, J and K). In both mutants, this open lumen ascends from the right ventricle (Asterisk, H and L). Abbreviations as shown in figure 3.2 and additionally: A-V aorta semi-lunar valves LSVC left superior caval vein; PT-V pulmonary trunk semi-lunar valves; RSVC right superior caval vein; SVS systemic venous sinus. Dorsal-ventral orientation is as shown in A. Scale bar: 500μm.

A
B
C
D
E
F
G
H
I
J
K
L
RSCV
LSCV
PT
LA
RA
PT-V
AV
RV
A-R
+/+
ENU/ENU
ENU/ENU

ascended from the right ventricle (Figure 3.3h and l, compared with control d). These defects of the outflow tract further reflect aspects of the cardiac phenotype of the *Sox4* null allele (Ya *et. al.* 1998b).

At the anterior-most region of the outflow tract, at both E12.5 and E13.5 it was observed that the pulmonary trunk and aorta were septated above the endocardial ridges (E12.5 control and mutant embryos and E13.5 mutant embryos) and developing semi-lunar valves (E13.5 control embryos) of the pulmonary trunk in all hearts examined (E12.5, Figure 3.2a, e, i; and E13.5, Figure 3.3a, e, i).

Deviating from the phenotype described by Ya *et.al.* in their publication of the *Sox4* null allele, the $Sox4^{ENU}$ allele also demonstrates abnormal development of the atrioventricular septum mesenchyme and associated tricuspid and mitral valves. One of the more prominent defects was inadequate formation of the atrioventricular septum and developing atrioventricular valves (AVV) at E12.5 and E13.5. Development of these structures is disrupted with the mesenchyme of the developing valves appearing malformed at both E12.5 (Figure 3.4e-g and i-k, compared with control a-c) and E13.5 (Figure 3.5 d-f and g-i compared with control a-c). Whilst formation of both left and right atrioventricular valves is evident to a certain degree, in some sections it appears that there is a common atrioventricular valve between the right atrium or common atrium and both ventricles. This was particularly pronounced in the more severely affected E13.5 embryo in which atrial septation was considerably delayed (Figure 3.5e). It is possible that this phenotype is partially a consequence of the developmental delay observed in this mutant line. If the sections from one of the two E13.5 mutants (Figure 3.5g h and i) are compared with the control sections for E12.5 (Figure 3.4a, b and c) the development of the muscular ventricular septum appears to be a similar. The development of the tricuspid and mitral valves also appears more closely matched between the E13.5 mutant and the E12.5 control hearts.

Septation and valve formation in the OFT are disrupted in embryos with defective cardiac neural crest migration (Kirby, M. L. 1990; Nishibatake *et. al.* 1987). The published *Sox4* null phenotype was initially attributed to a neural crest deficiency

(Schilham *et. al.* 1996). However the *Sox4*$^{ENU/ENU}$ *Foxq1*$^{sa/sa}$ phenotype possibly extends beyond that attributable to NCC, since it was also observed that mutants demonstrated defects of atrioventricular septation and atrioventricular valve formation. Analysis of contribution of the NCC lineage to the AVV is ambiguous (section 1.3.3) and furthermore, the requirement for NCC in the development of these structures is unknown. Thus it is possible that Sox4 plays two roles in cardiac development – one in the region of NCC infiltration, to contribute to OFT septation and the second in the atrioventricular cushions, to contribute to their appropriate morphogenesis.

In *Sox4* mutants, atrial septation is inadequate for E12.5 and E13.5, although it is not clear from these sections whether septation is delayed and thus incomplete, or arrested. At both E12.5 (Figure 3.6) and E13.5 (Figure 3.7) variable septation of the atria is observed. At E12.5 in the control embryo, the ostium primum has closed by the merging of the mesenchymal cap with that of the atrioventricular septal cushion and the vestibular spine. At this stage the primary atrial septum has developed with the interatrial connection of the secondary interatrial foramen (also oval fossa/ ostium secundum) (Figure 3.6a, adjacent section in b). Mutant littermates demonstrate incomplete closure of the ostium primum with sections showing regions where the mesenchymal cap has not yet fused with the mesenchyme of the atrioventricular septum (Figure 3.6c and e). However, neighbouring sections show that the mesenchymal contribution to the atrial septum has developed such that the opening of the ostium primum is limited (Figure 3.6d and f). In one E13.5 mutant a less developed atrial septum was present with the ostium primum unclosed (figure 3.7c, adjacent section in d). In the second E13.5 mutant and littermate control, the primary septum had developed with the oval fossa/ ostium secundum connecting between atrial chambers (Figure 3.7 control a and mutant e). This is not abnormal for this stage as detailed histological analysis of wild type embryos by Webb *et.al.* has shown that the atrial connection is not closed by the infolding of the myocardium (as the secondary atrial septum) until late on the 13th day of gestation (Webb *et. al.* 1998). Furthermore, it is possible that a developmental delay may account for some of the variability between control and mutant embryos and this must be considered in

interpreting the results. The atrial septum of the mutant E13.5 embryo depicted (Figure 3.7e and f) resembles more closely the atrial septum of the E12.5 control embryo (Figure 3.6a and b), than the E13.5 control embryo (Figure 3.7a and b). The formation of the primary septum in two E12.5 mutants (Figure 3.6c and e), with the extension of the mesenchymal cap towards the atrioventricular mesenchyme across the ostium primum, resembles the phenotype of wild type atrial septation from E11.5 stage gestation (Webb *et. al.* 1998a).

Given that the control littermates demonstrate incomplete atrial septation, it is possible that the $Sox4^{ENU/ENU}$ $Foxq1^{sa/sa}$ mutants are simply delayed in this septation. This observation appears inconsistent with that published by Bogani *et.al.*, but our homozygotes were not examined at E14.5. It is possible that the atrial septal defect might be retained in $Sox4^{ENU/ENU}$ $Foxq1^{sa/sa}$ mutants until E14.5. It may also be possible that the embryos examined by Bogani *et.al.* were sufficiently delayed in cardiogenesis to be closer to E13.5. To determine this conclusively, it would be necessary to revisit the data produced by Bogani *et.al.* and examine in parallel mutant and control littermates at E14.5 and, to account for the possibility of developmental delay, at E15.5. At E15.5 the *Sox4* mutant embryos would be dead, although a degree of histological analysis may still be possible. If embryos were developmentally delayed by one embryonic day at E14.5 then dissecting at E15.5 would eliminate any possibility that atrial septation was simply incomplete. Nevertheless, this is still inconsistent with the work of Ya et.al. who examined embryos at E12-E14 and did not describe an atrial septal phenotype, although their focus lay with the outflow tract. It is possible that, in our mutants, although the mesenchymal cap on the primary atrial septum was present, this mesenchyme may not have been patterned correctly. This requires a knowledge of the expression of *Sox4* in and surrounding this cardiac structure. The mesenchyme is continuous with the mesenchyme of the atrioventricular septum. This is a region in which we also observed a defect (E12.5 Figure 3.4; E13.5 Figure 3.5). Thus it is likely that any possible defects in the atrial septum are linked to a defect within the mesenchyme.

Figure 3.4: Histological analysis of cardiac defects in the atrioventricular region of *Sox4*$^{ENU/ENU}$ *Foxq1*$^{sa/sa}$ embryos at E12.5. Haematoxylin and eosin-stained sections of embryos were examined for cardiac morphology. (A, B, C and D) Transverse sections through a control embryo reveal the normal morphology of the heart at this stage, while defects are observed in sections through two homozygous mutant hearts (E-H, I-L). (A) Control littermate heart showing incomplete ventricular septation at this stage, between the right (RV) and left (LV) ventricles (marked with an asterisk [*]). This incomplete septation is resolved towards the outer region of tissue (black arrowhead, D). Evidence of atrioventicular valve formation is seen on both right and left sides of the atrioventricular cushion mesenchyme (black arrows, A-C). The systemic venous sinus (SVS) is seen to enter the right atrium (RA) between the left and right venous valves. Due to the plane of sectioning, little of the left atrium (not labelled) is observed in these series. (E – H; and I – L) Two mutant hearts are compared with the similar plane of section through the control heart (as shown by the four columns of the figure). Mutant hearts demonstrate evidence for the process of valve formation on both the left and right sides of the atrioventicular cushion (arrow E-G and I-K), however valve development in the mutants is abnormal with spaces between the developing valves on both sides. (J) In this mutant heart, the developing atrial septum has not fused with the atrioventricular cushion mesenchyme (ASD, marked by oval). Abbreviations as shown in previous figures and additionally: ASD atrial septal defect; Dorsal-ventral orientation is as shown in A. Scale bar (shown in L): 200μm.

A
B
C
D
E
F
G
H
I
J
K
L
+/+
END/END
END/END
SVS
RA
RV
D
V
ASD

Figure 3.5: Histological analysis of cardiac defects in the atrioventricular region of *Sox4*$^{ENU/ENU}$ *Foxq1*$^{sa/sa}$ embryos at E13.5. Haematoxylin and eosin-stained sections of embryos were examined for cardiac morphology. (A, B and C) Transverse sections through a control embryo reveal the normal morphology of the heart at this stage, while defects are observed in sections through two homozygous mutant hearts (D-F, G-I). Control littermate heart showing a small degree of incomplete interventricular septation at this developmental stage (asterisk, in C). While in mutant hearts, a ventricular septal defect is more prominent in most sections through the heart (asterisk D, E, F, H and I). The control heart demonstrates the normal formation of the mitral (MV) and tricuspid (TV) valves, whilst in mutant hearts this development appears defective. Although it is possible to identify less developed regions of MV or TV valves in both mutant hearts. Through some sections, the developing atrial septum had not fused with the atrioventricular cushion mesenchyme (ASD, marked by oval in D), thus in this heart, the atrial chambers appear to connect with the ventricular chambers *via* a common atrioventricular valve (bracket, in E). Abbreviations as shown in previous figures and additionally: AS atrial septum; MV mitral valve; TV tricuspid valve. Dorsal-ventral orientation is as shown in A. Scale bar: 500μm.

A
B
C
D
E
F
G
H
I
+/+
ENU/ENU
ENU/ENU
RA
AS
LSCV
MV
RV
LV
TV
SVS
*

Figure 3.6: Histological analysis of the atrial septum in *Sox4*$^{ENU/ENU}$ *Foxq1*$^{sa/sa}$ embryos at E12.5. Haematoxylin and eosin-stained sections of E12.5 embryos were examined for atrial septum morphology. (A and B) Transverse sections through a control embryo reveal the normal morphology of the atrial septum at this stage. (A) The secondary interatrial foramen (arrow, in A) is visible between the segments of the primary atrial septum (PAS), although the opening is limited as shown by a continuous PAS in (B). In mutant hearts (C and E) the mesenchymal cap (MC) has not fused with the endocardial cushion mesenchyme which forms the developing atrioventricular septum (AV) and the ostium primum (OP) is still present (arrow, in C, E). In subsequent sections the mesenchyme has connected, revealing the limits of the OP. Abbreviations as shown in previous figures and additionally: AV atrioventricular septum; MC mesenchymal cap; PAS primary atrial septum. Scale bar: 100μm.

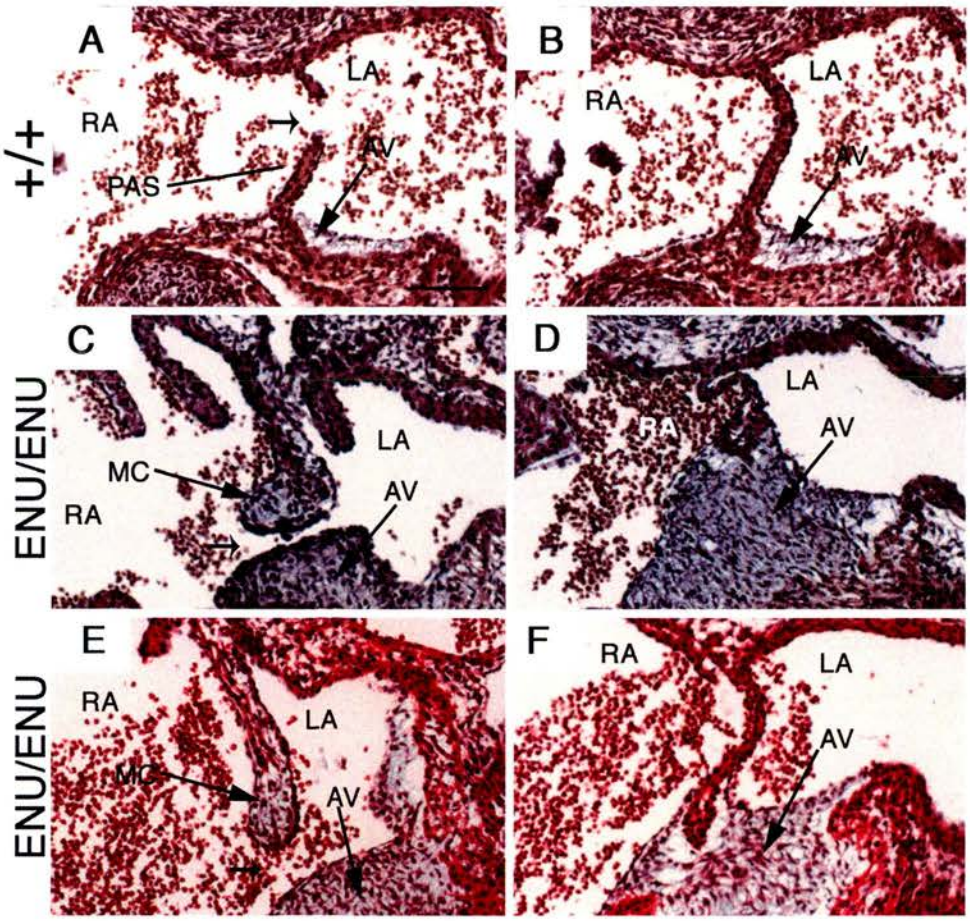
A
B
C
D
E
F
+/+
ENU/ENU
ENU/ENU
RA
LA
AV
PAS
MC

Figure 3.7: Histological analysis of the atrial septum in *Sox4*$^{ENU/ENU}$ *Foxq1*$^{sa/sa}$ embryos at E13.5. Haematoxylin and eosin-stained sections of E13.5 embryos were examined for atrial septum morphology. (A and B) Transverse sections through a control embryo reveal the normal morphology of the atrial septum at this stage. (A) The secondary interatrial foramen is visible between the segments of the primary atrial septum (arrowhead, A), although the opening is limited as shown by adjacent sections (B). In mutant hearts it is possible to see the OP in one heart (arrowhead C), while the other mutant demonstrates a visible secondary interatrial foramen (arrowhead, E). In both mutants, the openings of the septum are limited (oval, D and F). Abbreviations as shown in previous figures; Scale bar: 200μm.

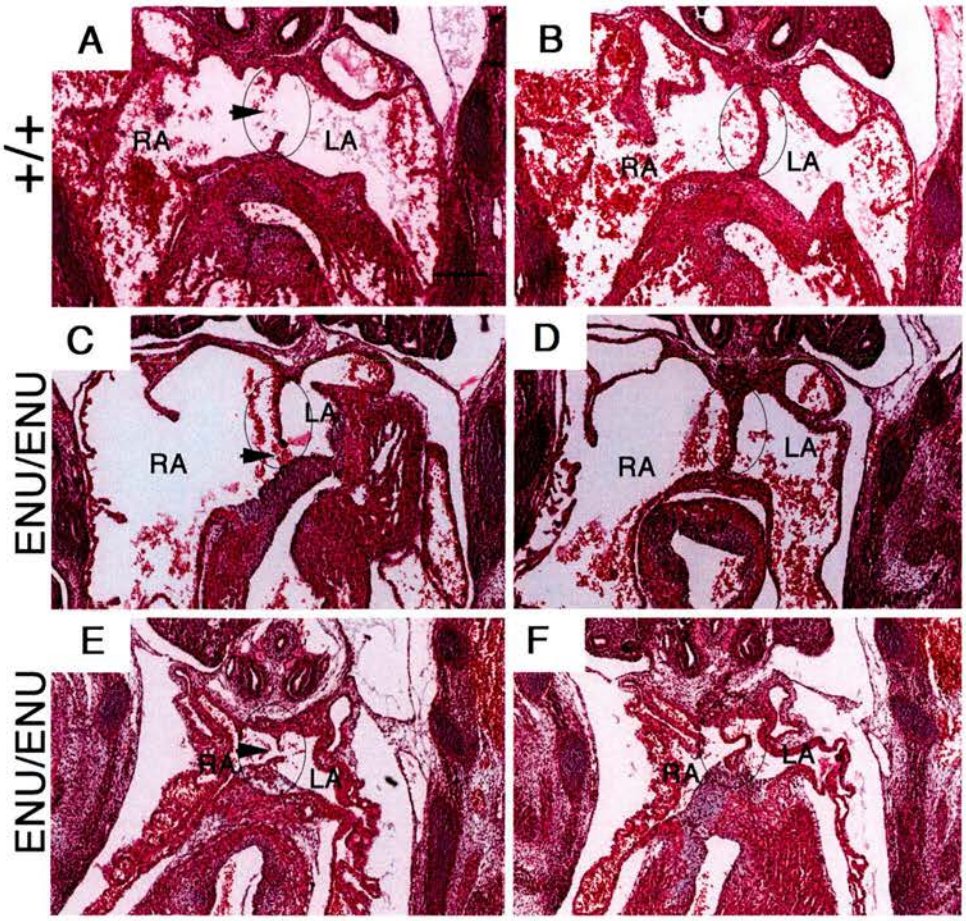
A
B
+/+
RA
LA
RA
LA
C
D
ENU/ENU
LA
RA
RA
LA
E
F
ENU/ENU
RA
LA
RA
LA

3.2.2 $Sox4^{ENU/ENU}Foxq1^{sa/sa}$ E9.5 embryos produce a variable phenotype, which appears independent of genetic background.

To examine the ontogeny of the cardiac phenotype, we examined embryos at earlier stages of development. The analysis presented here is representative of findings from backcrossing the M91 line to C57Bl/6J. During the course of this candidature, studies were performed on embryos after backcrossing to two different inbred strains – C57Bl/6J and also 129/Ola after two generations of crossing to C57Bl/6J from the M91 line. Embryos resulting from intercrosses of the alleles on a predominantly 129/Ola background did not demonstrate any consistent significant differences from the phenotype observed on the predominantly C57Bl/6J background. For this reason, only analysis on the C57Bl/6J background is presented here.

$Sox4^{ENU/ENU}$ $Foxq1^{sa/sa}$ embryos were examined from E7.5 to E13.5. After genotyping (Chapter 2; Figure 2.1 and 2.2), it became apparent that most homozygous embryos (n=45/50; 90%) could be visibly distinguished by E9.5. At this stage, these embryos demonstrated a variable phenotype in wholemount (Figure 3.8d to l, compared with control in a, b and c). The heart was swollen to varying degrees, and other organ systems also appeared to be affected. The phenotype of embryos at this stage could be grouped into three classes (Table 3.2):

Class-I

The least severe of the three classes, class-I mutants demonstrate a swollen heart, with inappropriate shape of the atria and ventricles (Figure 3.8d, e and f). Despite this distension, it is still possible to distinguish regions of the heart by the presence of the AV groove, VS groove and the narrowing and bending between the presumptive RV and OFT, as well as bending between the distal and proximal OFT. Despite being malformed, the class-I hearts still appear to undergo rightward looping with the future left ventricle and AV region left of the midline, while the presumptive right ventricle appeared correctly displaced to the right of the midline to varying degrees (section 1.3.1; Figure 1.4c). Some class-I mutants also demonstrate defects in the formation of the forebrain/ anterior-most neural tube. In these cases, it appears that the neural tissue is slightly truncated, or underdeveloped. Of the E9.5 embryos

examined, the class-I phenotype comprises 42% of homozygotes and 10.5% of any given intercross litter (Table 3.2).

This phenotype also appeared in 3% of heterozygotes (Table 3.2), although the number of embryos examined is too small to conclude whether this represents a haploinsufficient phenotype, or whether the phenotype in this 3% of all examined (n=90) heterozygotes is unrelated to the *Sox4*^{ENU} and *satin* alleles.

Class-II

In class-II mutants, the severe cardiac swelling of these embryos, did not permit the presumptive chambers and interconnecting regions to be distinguished in wholemount with certainty. In most embryos, the heart tube simply extended ventrally from the body and, possibly due to the distension, did not undergo adequate looping, although the looping which occurred appeared to be directionally rightward (Figure 3.8g, h and i). The remainder of the body was severely developmentally delayed and the forebrain/anterior defect was more pronounced. This phenotype class was observed in 28% of homozygote mutants (approximately 7% of an intercross litter) (Table 3.2).

Class-III

The most severe defects were apparent in class-III mutant embryos, comprising 20% of E9.5 *Sox4*$^{ENU/ENU}$ *Foxq1*$^{sa/sa}$ embryos (Figure 3.8j, k and l)(Table 3.2). Development of embryos with this phenotype was severely disrupted, to the degree that cardiomyogenic cells could only be identified as a mass of beating tissue. Whilst embryos did demonstrate anterior-posterior patterning and a degree of somitogenesis, class-III mutants revealed disruption to the remainder of body patterning. This suggests disturbance to key early patterning signals, and/or inappropriate differentiation. Clearly, in these embryos, abnormality must have its inception early in development to result in such a severe phenotype by E9.5. As results for the next chapter show that Sox4 is expressed in the embryonic ectoderm (section 4.2.1) prior to and during gastrulation, it is possible that this severe class-III

Table 3.2: Proportions of classes of *Sox4*$^{ENU/ENU}$ *Foxq1*$^{sa/sa}$ embryos at E9.5 on a C57Bl/6J background.

Class	Heart Phenotype	Forebrain Phenotype	Homozygotes (% of total homozygotes) {% of litter; expected 25%}	Heterozygotes (% of total heterozygotes)	Wildtype (% of total wildtype)
Indistinguishable from wildtype	None apparent	None apparent	5 (10) {2.5}	87 (97)	49 (100)
Class-I	Mild to moderate swelling, correct looping	None or mild defect	21 (42) {10.5}	3 (3)	0
Class-II	Severe swelling, inadequate looping	Severe anterior defect	14 (28) {7}	0	0
Class-III	No visible heart or forebrain and/or severe axial defects.		10 (20) {5}	0	0
Total number of embryos of each genotype			50	90	49
Total number of embryos examined			189		

Figure 3.8: The phenotype of *Sox4*$^{ENU/ENU}$ *Foxq1*$^{sa/sa}$ E9.5 embryos can be grouped into three classes. (A) Lateral view of a control E9.5 embryo. Magnified view of the left (B) and right (C) side of a control heart at E9.5. (D,E,F) Lateral view of class-I mutant embryos demonstrating swollen and inadequately looped hearts. Anterior development is also abnormal in these embryos. (G,H,I) Lateral view of class-II mutant embryos demonstrating a severely enlarged heart tube and severe anterior defects. (J,K,L) Lateral view of class-III embryos displaying severe developmental abnormalities. Abbreviations: AVC, atrioventricular canal; BC, bulbus cordis; LV, left ventricle; OFT, outflow tract. Scale bar: A,D,E,F,G,J 500μm; K, 380μm.

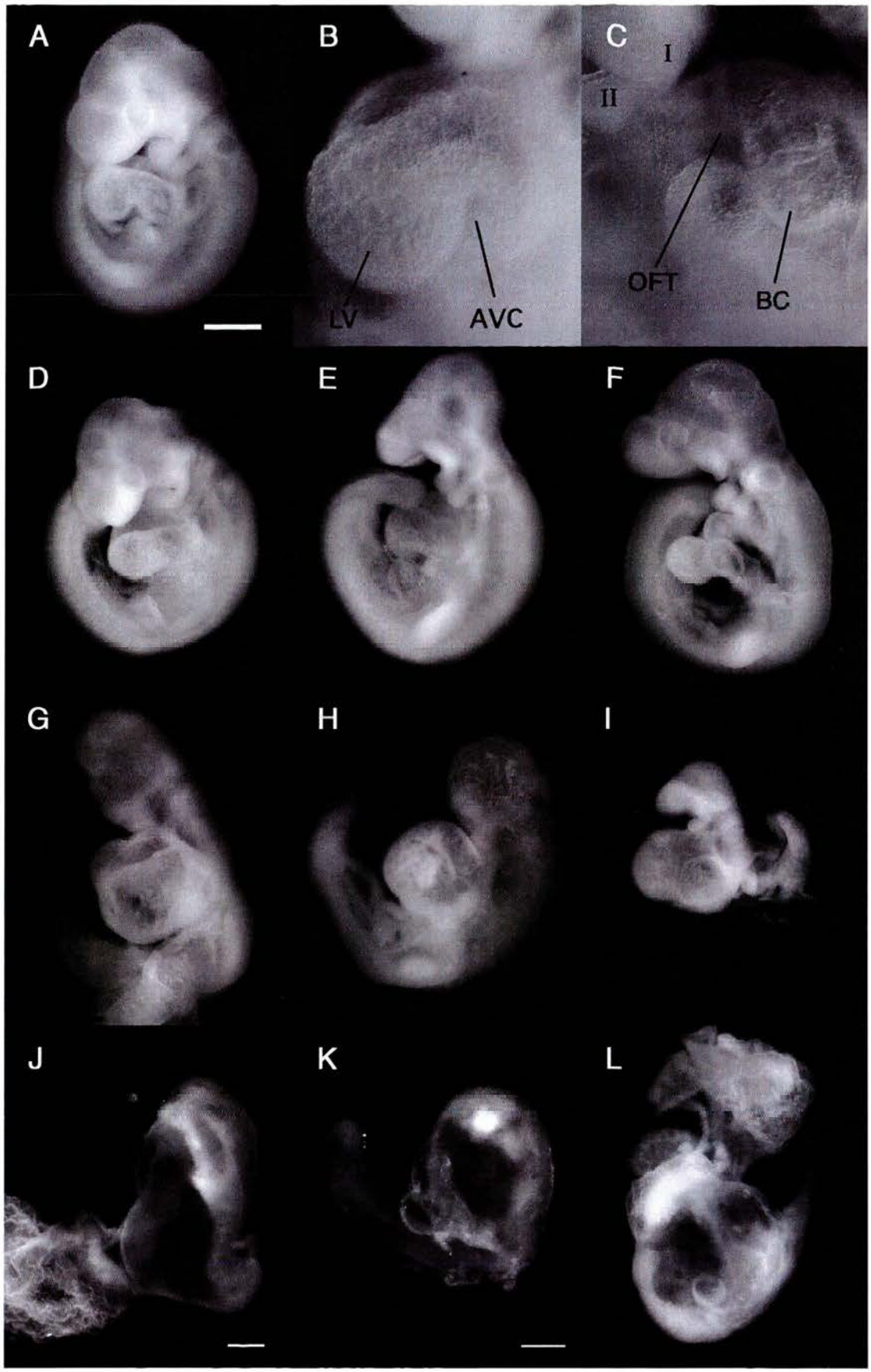
A
B
C
I
II
LV
AVC
OFT
BC
D
E
F
G
H
I
J
K
L

Table 3.3: Genotype of embryos from a *Sox4*$^{+/ENU}$ *Foxq1*$^{+/sa}$ intercross across selected stages of development on a C57Bl/6J background.

Stage	Total	Homozygous		Heterozygous		Wildtype		Chi-square value	probability df=2
		Observed	% litter	Observed	% litter	Observed	% litter		
7.5	54	14	26%	27	50%	13	24%	0.03704	p>0.9
8.5	65	15	23%	33	51%	17	26%	0.13846	p>0.9
9.5	189	50	26%	90	48%	49	26%	0.43915	p>0.9
10.5	131	36	27%	61	47%	34	26%	0.67939	0.9>p>0.5
11.5	31	6	19%	18	58%	8	26%	0.80645	0.9>p>0.5
12.5	17	5	29%	7	41%	5	29%	0.52941	p>0.9
13.5	43	6	14%	27	63%	10	23%	3.55814	0.5>p>0.1
pooled 11.5-13.5	91	17	19%	52	57%	23	25%	2.38462	0.5>p>0.1

Stage, embryonic stage of development; Number, observed number of embryos genotyped at the *Sox4* locus, subsequently grouped according to genotype. Findings are depicted as both the number of embryos for each stage and genotype, and the percentage for each genotype per stage. The ratio of geneotypes were tested for whether the data fits a 1:2:1 Mendelian ratio to evaluate whether non-Mendelian results are statistically significant.

phenotype arises at this stage. Class-III mutants comprise as little as about 5% of any litter (Table 3.2). Therefore it would require a very extensive breeding programme to generate sufficient embryos to study this early phenotype in detail with reproducibility. In this thesis, analysis presented is thus restricted to class-I and some less severe class-II mutants.

3.2.3 Examining the time of lethality for *Sox4*$^{ENU/ENU}$ *Foxq1*$^{sa/sa}$ embryos.

To establish when the *Sox4*$^{ENU/ENU}$ *Foxq1*$^{sa/sa}$ phenotype is lethal, the frequency of homozygosity was examined by pooling all genotyping results for litters. Initially embryos were all genotyped for the *satin* allele, with some samples randomly selected for sequencing at the *Sox4* locus. Embryos from fourth and fifth generation intercrosses were all genotyped at both loci, as it was in these generations that segregation of the two alleles was first observed. Since *Sox4*$^{ENU/ENU}$ *Foxq1*$^{sa/sa}$ embryos phenocopy published findings for *Sox4* null homozygotes, litters were only examined up to E13.5 – the known time point preceding the ultimate lethality of the null allele. No homozygous animals were born from heterozygous intercrosses (data not shown), indicating that the recessive lethal phenotype is fully penetrant on the backgrounds studied.

The frequency of homozygous mutant embryos does not deviate from the expected 25% prior to E11.5 (Table 3.3). The ratio of genotypes were tested for whether non-Mendelian segregation is statistically significant, by chi-squared analysis with two degrees of freedom. At E7.5 and E8.5 most mutant embryos appeared morphologically normal (data not shown). The first evidence of a cardiac phenotype arises about E9.5. Even at this stage, 10% of examined homozygotes did not demonstrate any dysmorphology (Table 3.2). It is presumed that this class would develop into the least severe of cardiac phenotypes by E13.5. At about E11.5, homozygotes comprise approximately 20% of the litter. This 5% decrease (from an expected 25%) is likely to represent loss and reabsorption of the class-III embryos. Very few embryos were examined at these later stages of gestation. However, it is still evident at E13.5 that embryos with the severest phenotype have died and are reabsorbed (with no embryo-derived tissue available to genotype). The proportion of

homozygotes in the litter drops to 14% (from the expected 25%) (Table 3.3), suggesting that the majority of class-II mutants are also reabsorbed by this stage. Homozygous embryos dissected at E12.5-13.5 all demonstrated a degree of craniofacial abnormality, from a mild reduction in eye pigmentation to severe anterior deformities.

These genetic ratios are consistent with that described for the *Sox4* null lethality, whereby 18-20% (n=21) of E12.5-E14.5 embryos were homozygous (Ya *et. al.* 1998b). If the E11.5-13.5 stages for the study presented in this chapter are pooled, homozygotes comprise 18.6% (n=17) (Table 3.3).

Given that the phenotype is variable, by keeping the frequency of lethality separate for stages, it thus appears that there are two peaks of lethality/reabsorption in homozygotes (Table 3.3). Although implantation sites may be present, there is a lack of definitive embryonic tissue for genotyping. The first peak is between E10.5-E11.5, when a loss of the 5% of abnormally developed class-III mutants is observed. A second wave of embryonic death occurs during the two days prior to E13.5, such that by E13.5, only the cardiac phenotype is apparent as a likely consequence of the *Sox4* mutation.

3.2.4 Embryos homozygous for the *Sox4*$^{ENU/ENU}$ *Foxq1*$^{sa/sa}$ mutations demonstrate an early cardiac phenotype at E9.5-E10.5.

To determine the developmental basis for the cardiac phenotype observed later in gestation, hearts of embryos were examined at E9.5-E10.5, about the stage that class-I mutants demonstrate a morphological abnormality.

Mutants exhibit trabeculation defects

Serial sections of E9.5 homozygote mutant hearts were analysed for ventricular abnormalities. In control embryos, myocardial cells which remain at the wall of the heart show a flattened morphology, which is suggestive of differentiated characteristics - forming contractile muscle. Myocardial cells which form trabeculae are morphologically distinct, being spherical with fewer cell-cell contacts and extending towards the endocardium which lines the ventricular lumen (Figure 3.9a).

Figure 3.9: *Sox4*$^{ENU/ENU}$ *Foxq1*$^{sa/sa}$ embryos exhibit variable trabeculation defects at E9.5. Haematoxylin and eosin-stained sections cut transverse through the ventricular chamber of the control embryo (A), class-I mutant (B,C) and class-II mutant (D) embryos, at the level indicated in wholemount. In all embryos it appears that the endocardium makes contact points with the myocardium (black arrowhead). (A) Control embryos demonstrate normal production of trabecular myocardium extending towards the endocardium (black arrows). (B) A less severe class-I mutant embryo demonstrates some formation of trabecular myocardium (black arrows), although not to the same degree as wild type. (C) A more severe class-I mutant embryo demonstrates inadequate formation of trabecular myocardium (black arrows). (D) The class-II mutant embryo does not appear to produce trabecular myocardium. Additionally, the distance between endocardium and myocardium is more pronounced (bracket). Scale bar: Wholemount images 380μm; Sections A – D 22 μm.

A
B
C
D

Figure 3.10: The pro-epicardium is still visible in *Sox4*$^{ENU/ENU}$ *Foxq1*$^{sa/sa}$ embryos at E9.5. Haematoxylin and eosin-stained sections examined at the level of the migrating pro-epicardium in a control littermate (A), class-I mutant (B,C) and class-II mutant (D) embryos at E9.5. All embryos demonstrate the presence of migratory pro-epicardial cells, as indicated (black arrowhead). Scale bar: Wholemount images 380μm; Sections A, 110μm; B, 110μm; C, 90μm; D, 90μm.

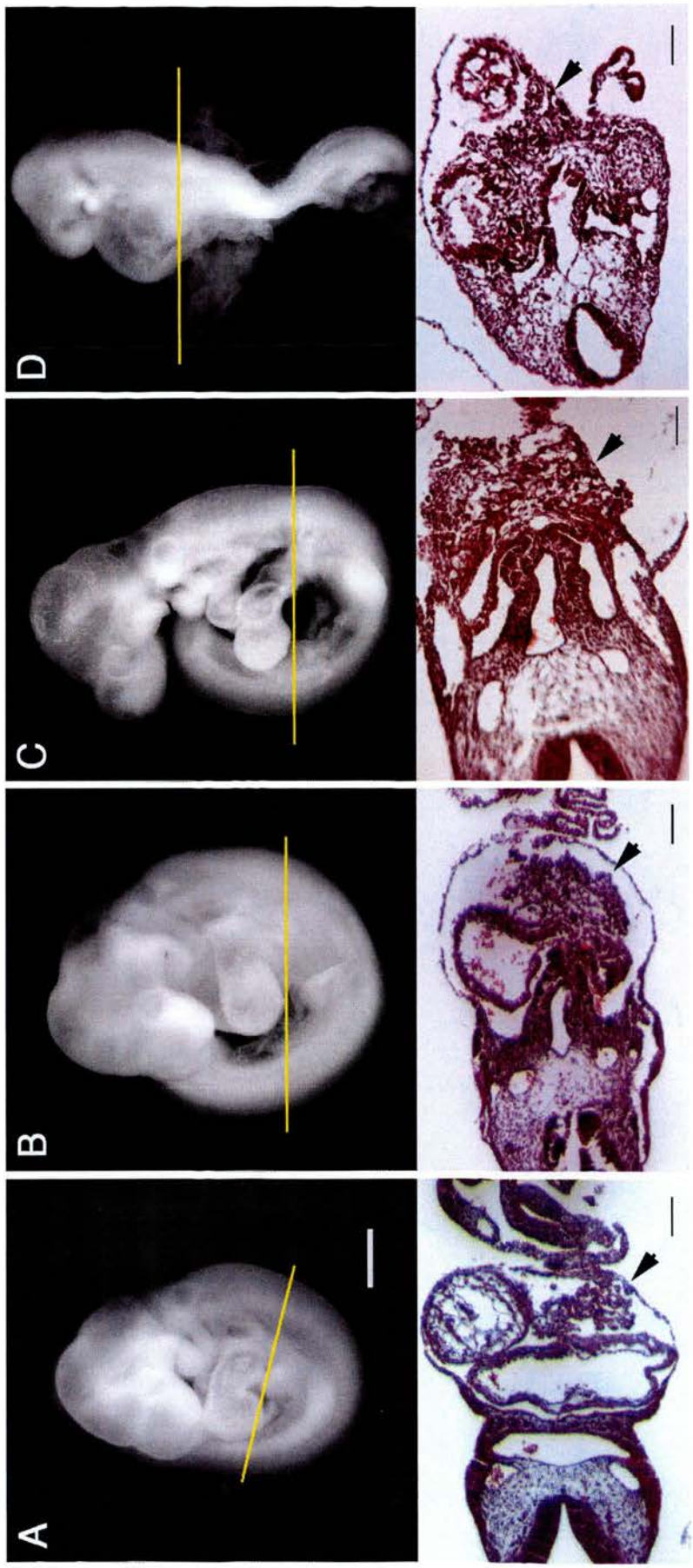
A
B
C
D

In contrast, mutant embryos revealed varying extents of poorly developing ventricular trabeculae (Figure 3.9b, c and d). Between mutant embryos of the class-I phenotype, differences were observed. Embryos of the milder class-I phenotype appeared able to form trabeculae, however the base of the trabeculae appears to lack cellularity. It appeared that the myocardium was inadequately populated, with insufficient cells able to undergo the transformation into trabeculae (Figure 3.9b). A more severe class-I mutant seemed unable to construct any trabeculae. Instead, cells retained the elongated morphology of the myocardial wall (Figure 3.9c). In this embryo, the cells of the wall of the myocardium also appeared sparse. The ventricular wall of embryos of the Class-II phenotype did not appear to undergo formation of trabeculae (Figure 3.9d). In mutants of this class, the myocardium was sparse and the space between endocardium and myocardium was more prominent.

The proepicardium is present in mutant embryos.

In the case of embryos null for *Gata4* (generated by tetrapoloid aggregation), defective formation of trabeculae at E9.5 is attributed to the absence of the proepicardium (also pro-epicardial organ; PEO; discussed chapter 1, section 1.3.5) (Watt *et. al.* 2004). However, as yet, there is no further molecular evidence for this link (such as factors secreted from the epicardium, acting on the early myocardium). To examine whether the PEO was present in *Sox4* mutant embryos, serial sections of class-I and class-II embryos were examined for the presence of the PEO (Figure 3.10). There was no notable difference in the appearance of the PEO in mutant embryos of the class-I (Figure 3.10b, c) and class-II phenotypes (Figure 3.10d, compared with control, a). Therefore, absence of the PEO cannot explain the phenotype observed in the developing trabeculae in E9.5 *Sox4* hearts. This does not exclude the possibility that cells of the epicardium are abnormal at later stages, since they go on to play a significant role at later stages in myocardial proliferation and maturation of compact myocardium (as discussed in section 1.3.5)

Section analysis of the AVC and OFT at E9.5.

In order to examine when the endocardial cushion defects first arise, E9.5 embryos were examined in transverse sections at the early stages of cushion formation. At

about E9.5, in the looped heart tube, cardiac EMT commences in the AVC with cells from the endocardium delaminating into the underlying extracellular matrix (ECM). Slightly later this process also occurs within the cushions of the outflow tract. Later, at E10.5, mesenchymal cells are more prominent in the AVC and also in the OFT. In both regions it is possible to visualise cells that have already delaminated from the endocardium and migrated into the ECM. It is also possible at these stages to visualise sub-endocardial cells in the distal OFT, which are likely to correspond to NCC infiltrating the anterior heart.

Atrioventricular canal

Class-I embryos dissected at E9.5 demonstrate cardiac swelling and inadequate looping of the heart (Figure 3.8). Sections through the heart of a control E9.5 embryo show the normal development of the AVC cushions for this stage (Figures 3.11a-c; 3.12a-c; 3.13a-c). In contrast, all mutant embryos reveal abnormal AVC development. Class-I embryos (n=4 presented in this figure) demonstrated a degree of cushion development, although morphology was abnormal compared with control (Figure 3.11d-f; Figure 3.11g-i; Figure 3.11j-l; Figure 3.11m-o, compared with control Figure 3.11a-c). In some sections, the developing mesenchyme (black arrows Figures 3.11) does not appear to populate the cushion, but rather clusters below the endocardium. This suggests a defect in the process of EMT, although this phenotype could also be a result of aberrant differentiation, proliferation or maintenance of mesenchyme in the cushion, rather than production *per se.* Furthermore, in some sections of the cushions, mesenchyme did not appear to be present (oval marked in Figure 3.11j and o). Although it is possible that this is a consequence of the developmental delay exhibited by the class-I embryos, and thus a delay may also be an explanation for the limited mesenchyme production in class-II embryos: AVC defects were more prominent in sections through class-II mutant embryos which showed limited (black arrows Figure 3.12d, e) or no mesenchyme production within the atrioventricular cushions (Figure 3.12f, g-i).

A developmentally delayed E10.5 embryo also demonstrates abnormal population of the cushions with mesenchyme (black arrows Figure 3.13). Here, the mutant embryo

(Figure 3.13d-f) is compared with sections through a control E9.5 embryo (Figure 3.13a-c) and also a control E10.5 littermate control (Figure 3.13g-h). This comparison shows that the low density of mesenchymal cells in the mutant cushions is more similar to that in the E9.5 control than the E10.5 littermate control. Note that the E9.5 embryo was sectioned transversely, while the two E10.5 staged embryos are sectioned to cut in plane with the main length of the OFT and thus are mid-way between transverse and frontal, but still allow a visual estimation of mesenchymal cell density.

Outflow tract

In wholemount, the OFT of *Sox4* mutant hearts appeared swollen at E9.5 (Figure 3.8, and data not shown). Sections through the OFT reveal the variability in this swelling between class-I mutants (Figure 3.14d-f; Figure 3.14g-i; Figure 3.14j-l; Figure 3.14m-o) compared with control (Figure 3.14a-c). Also evident in these sections is the early production of mesenchyme within the proximal OFT cushions. This commences by E10, later than the initiation of mesenchyme production in the AVC (discussed section 1.3.3). The wild type sections reveal the normal mesenchyme production for this developmental stage (black arrows, Figure 3.14a, b). In comparison, the process is either delayed or reduced for this stage in the mutant hearts, since fewer mesenchymal cells are observed upon examining serial sections through this region (black arrows, Figure 3.14e, h, j, k, m, n). Interestingly, sub-endocardial cells are present at the distal OFT, adjacent to the aortic sac. Although not quantified, it is evident in all mutant and control hearts that sub-endocardial cells are present within this region (red arrows, Figure 3.14). This region was examined at higher magnification in both control (red arrows, Figure 3.14c, lumen of OFT marked with red asterisk) and mutant (red arrows, Figure 3.14f, i, l, o, lumen of OFT marked with red asterisk). The migratory appearance of the sub-endocardial cells, together with the spatiotemporal positioning, suggests that they may be the infiltrating NCC, although marker analysis is necessary to determine this conclusively.

Also within the OFT, class-II mutant hearts did not appear to demonstrate mesenchyme production in the proximal cushions in any of the sections examined (Figure 3.15d,e and Figure 3.15g-i, compared with control Figure 3.15 a and b), while the developmentally delayed mutant E10.5 heart demonstrated limited production of mesenchyme in the OFT cushions (Figure 3.16d, compared with E10.5 control in h). To characterise the presence or absence of the mesenchyme accurately, further than what can be determined from haematoxylin and eosin stained sections, it would be necessary to analyse this region with mesenchymal markers. As with the AVC, it is possible that the lack of mesenchyme in this region of the OFT is a consequence of a developmental delay. The E9.5 control shown in these two figures was developmentally matched to the class-I mutant embryos. Given the substantial defects observed in class-II and the E10.5 mutant hearts, there is not a more appropriate control for this analysis. It would, in retrospect, for the purpose of uncovering the origin of the cardiac phenotype, be more useful for section analysis to be conducted on class-II embryos from E8.5-E9. To determine the extent of the phenotype at E10.5, it is necessary to examine more mutant embryos that are less developmentally delayed.

It is also evident from the class-II E9.5 and the E10.5 sections that there are sub-endocardial cells within the distal OFT. This is more prominent in the less severe class-II mutant heart (red arrows, Figure 3.15 d-e, magnified in f) than in the more severe class-II mutant heart (red arrow, Figure 3.15g), while the E10.5 embryo demonstrated a degree of population which resembled the E9.5 control (red arrows, Figure 3.16e and f, compared with Figure 3.16b and c) more closely than the E10.5 littermate (red arrows Figure 3.16g, h and i). As described for class-I mutant hearts, the distal OFT is the site of entry of NCC into the anterior heart. It is likely that these cells are the beginning of NCC infiltration, yet this can not be said with certainty as marker analysis has not been conducted on this population of cells.

Figure 3.11: *Sox4*$^{ENU/ENU}$ *Foxq1*$^{sa/sa}$ class-I embryos exhibit variable atrioventricular canal cushion defects at E9.5, as shown by histological analysis. Haematoxylin and eosin-stained sections through the developing cushions of the atrioventricular canal (between the common atrium marked A and common ventricle marked V) of a developmentally matched E9.5 control embryo (A, B, C) compared with four class-I mutant embryos (D,E,F; G,H,I; J,K,L; M,N,O). Hearts were examined through similar regions comparing the approximate posterior, middle and anterior regions of the canal (three columns of figure), as determined by examination of all sections through the heart. (A-C) The control embryo demonstrates the normal endocardial cushion swelling and mesenchyme production, with some mesenchyme cells evident (black arrows). However throughout this region in the four mutant embryos (D-F, G-I, J-L, M-O) abnormal cushion swelling and variable mesenchyme production (black arrows) is evident. In some sections through class-I mutant hearts, the developing cushions appeared devoid of mesenchymal cells (regions marked by oval in J and O). Abbreviations: A atrium; V ventricle; Scale bar: 100μm (shown in C).

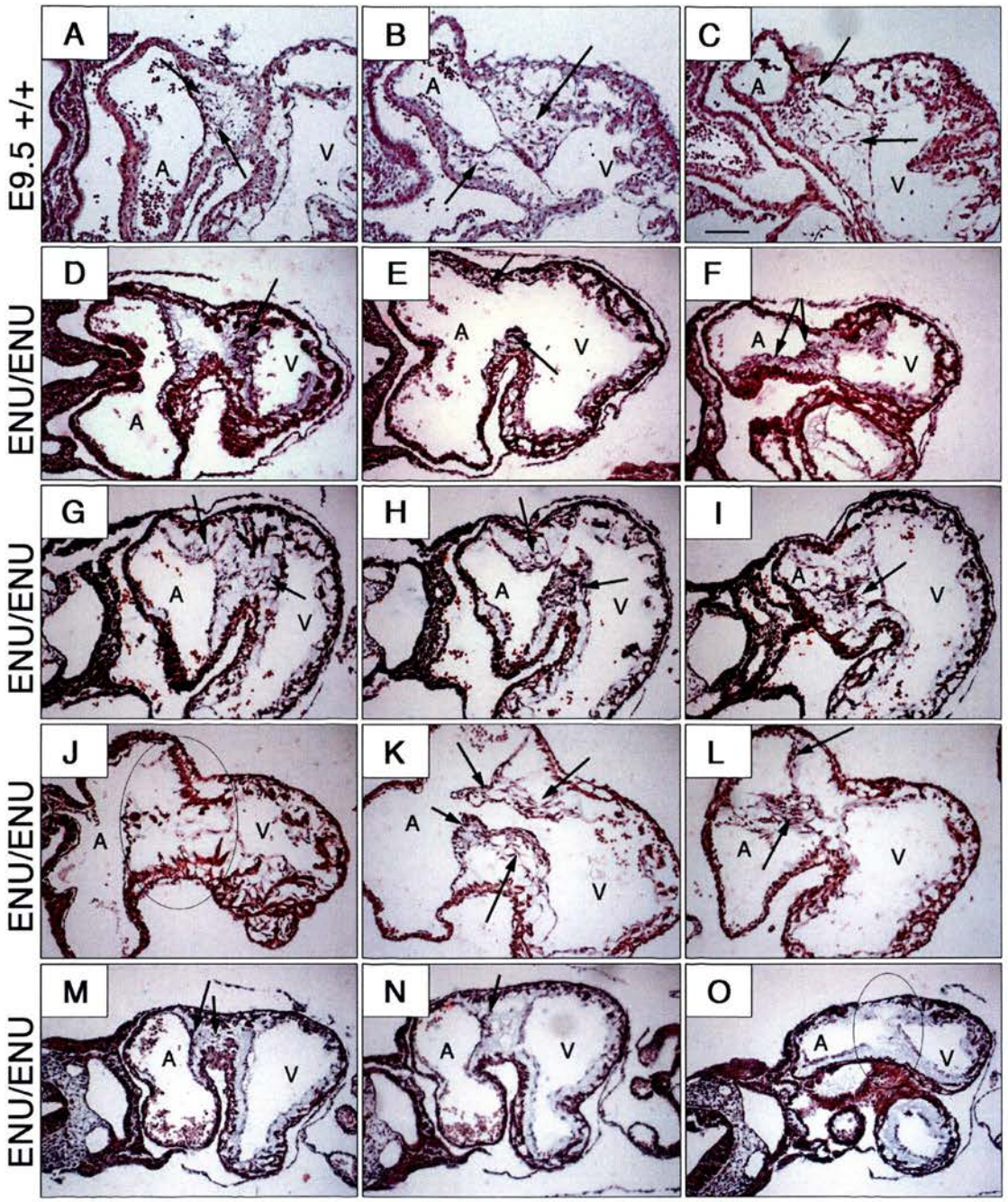
E9.5 +/+
ENU/ENU
ENU/ENU
ENU/ENU
ENU/ENU
A
B
C
D
E
F
G
H
I
J
K
L
M
N
O
A
V

Figure 3.12: *Sox4*$^{ENU/ENU}$ *Foxq1*$^{sa/sa}$ class-II embryos exhibit variable atrioventricular canal cushion defects at E9.5, as shown by histological analysis. Haematoxylin and eosin-stained sections through the developing cushions of the atrioventricular canal (between the common atrium marked A and common ventricle marked V) of an E9.5 control embryo (A, B, C) compared with two class-II mutant embryos (D,E,F; G,H,I). Hearts were examined through similar regions comparing the posterior, middle and anterior regions of the canal, as determined by examination of all sections through the heart. (A-C) The control embryo demonstrates the normal endocardial cushion swelling and mesenchyme production, with some mesenchyme cells evident (black arrows). However mutant embryos (D-I) demonstrate abnormal cushion swelling and variable mesenchyme production (D, E). In all hearts, regions of mesenchyme production are indicated by black arrows. The less severe mutant demonstrates some mesenchyme production through most sections (D,E). However, the more severe mutant (G-I) does not demonstrate production of mesenchyme in this region (marked by oval in F-I). Abbreviations as in previous figures; Scale bar: A-F (shown in C) 100μm; G-I 100μm.

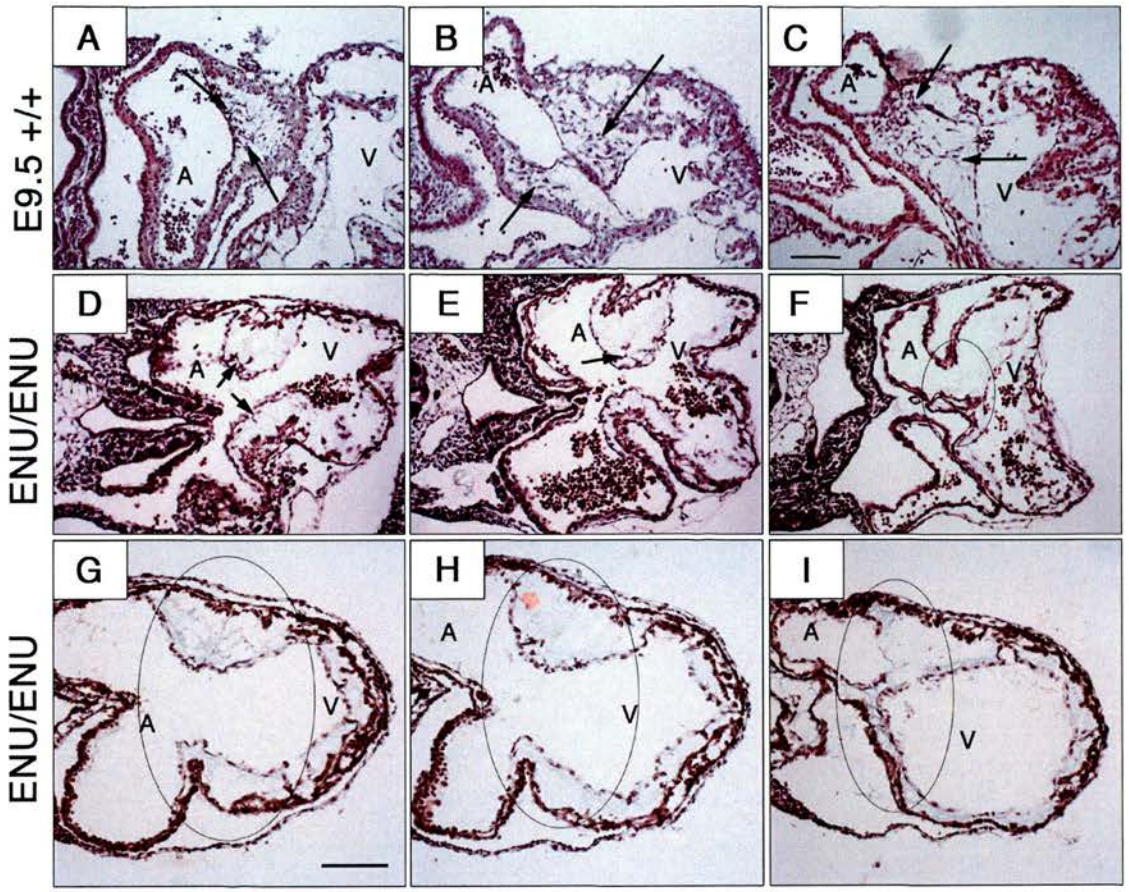
E9.5 +/+
ENU/ENU
ENU/ENU
A
B
C
D
E
F
G
H
I
A
V

Figure 3.13: A *Sox4*$^{ENU/ENU}$ *Foxq1*$^{sa/sa}$ E10.5 embryo exhibits atrioventricular canal cushion defects, as shown by histological analysis. Haematoxylin and eosin-stained sections through the developing cushions of the atrioventricular canal (between the common atrium marked A and common ventricle marked V) of an E9.5 control embryo (A, B, C; sectioned in the transverse plane) a developmentally delayed E10.5 mutant embryo (D,E,F; sectioned midway between transverse and frontal, in plane with the angle of the outflow tract) and a stage-matched E10.5 littermate control (G,H,I; sectioned midway between transverse and frontal, in plane with the angle of the outflow tract). Hearts were examined through similar regions comparing the posterior, middle and anterior regions of the canal, as determined by examination of all sections through the heart. (A-C) The E9.5 control embryo demonstrates the normal endocardial cushion swelling and mesenchyme production, with some mesenchyme cells evident (black arrows). However the mutant embryo (D-I) demonstrates abnormal cushion swelling and variable mesenchyme production. There appears to be a significant defect or delay in mesenchyme production of the one mutant compared with the E10.5 littermate control embryo (G-H). In all hearts, mesenchyme production is indicated by black arrows. In the mutant heart, the region of cushion adjacent to the ventricle appears devoid of mesenchyme (marked by oval in F). Abbreviations as in previous figures, but additionally: AS aortic sac; Scale bar: A,B,C (shown in C) 100μm; D,E,F 100μm; G,H,I 100μm.

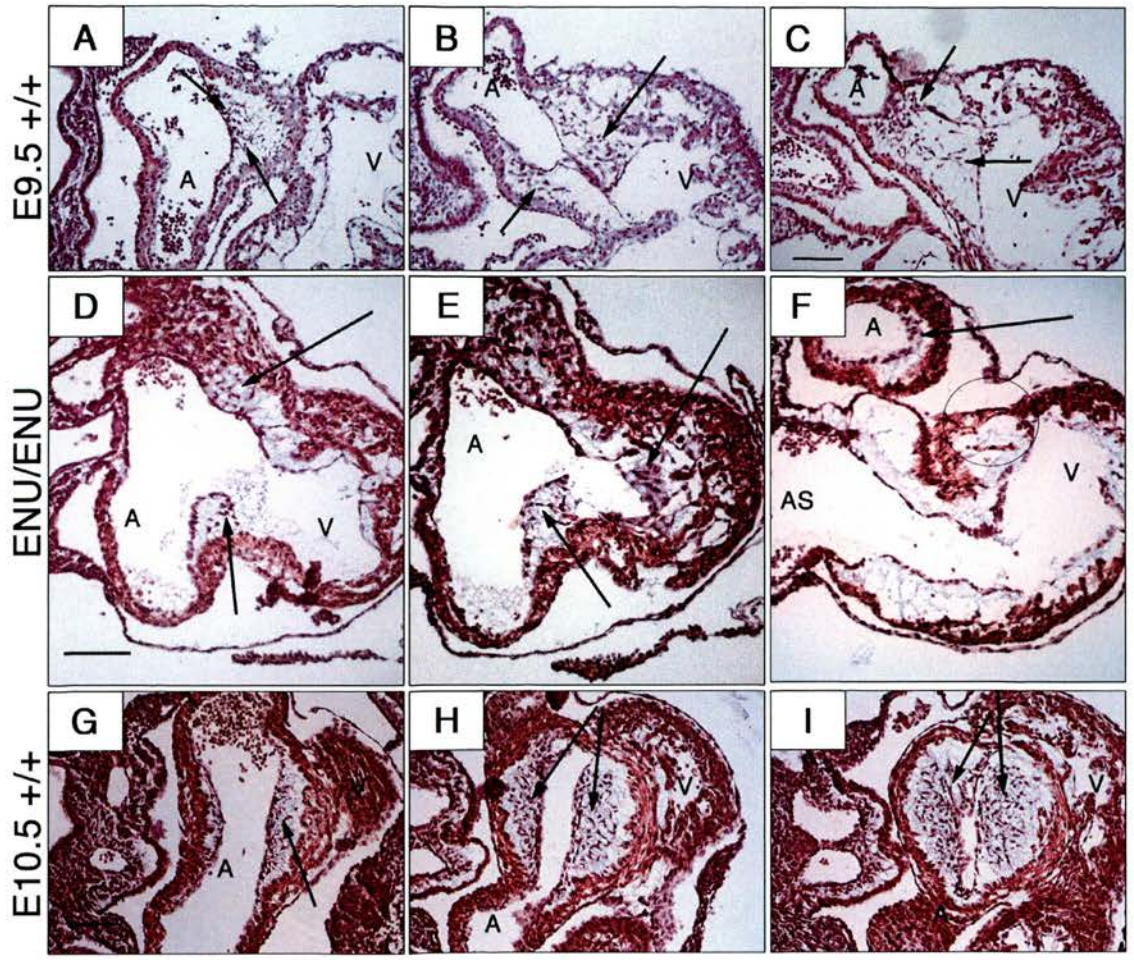
E9.5 +/+
ENU/ENU
E10.5 +/+
A
B
C
D
E
F
G
H
I
A
V
AS

Figure 3.14: *Sox4*$^{ENU/ENU}$ *Foxq1*$^{sa/sa}$ class-I embryos exhibit variable outflow tract development at E9.5, as shown by histological analysis. Haematoxylin and eosin-stained transverse sections through the developing outflow tract (OFT) of an E9.5 control embryo (A,B,C) compared with and developmentally matched to four class-I mutant embryos (D,E,F; G,H,I; J,K,L; M,N,O). Hearts were examined through similar OFT regions comparing two different levels (first and second columns of figure), as determined by examination of all sections through the heart. (A,B) The control embryo demonstrates the normal OFT cushion swelling and infiltration of sub-endocardial cells in the distal OFT, possibly corresponding to cardiac neural crest (red arrows A,B). Additionally, mesenchyme production is evident in the cushions of the proximal region of the OFT adjacent to the bulbus cordis (BC; black arrows A). (D-O) In the four mutant embryos swelling of the outflow tract and abnormal cushion development is evident, with little evidence for mesenchyme production in the proximal cushions in these sections. Class-I OFT demonstrate the presence of sub-endocardial cells within the distal OFT (red arrows D-O). Higher magnification (4x) of the distal OFT in control (C) and class-I mutant (F,I,L,O), reveals the presence of sub-endocardial cells adjacent to the lumen of the OFT (red asterisk). Abbreviations: AS aortic sac; BC bulbus cordis; FG foregut. Scale bar: A,B,D,E,G,H,J,K 100μm; M,N 150μm; C,F,I,L,O imaged at the same higher magnification.

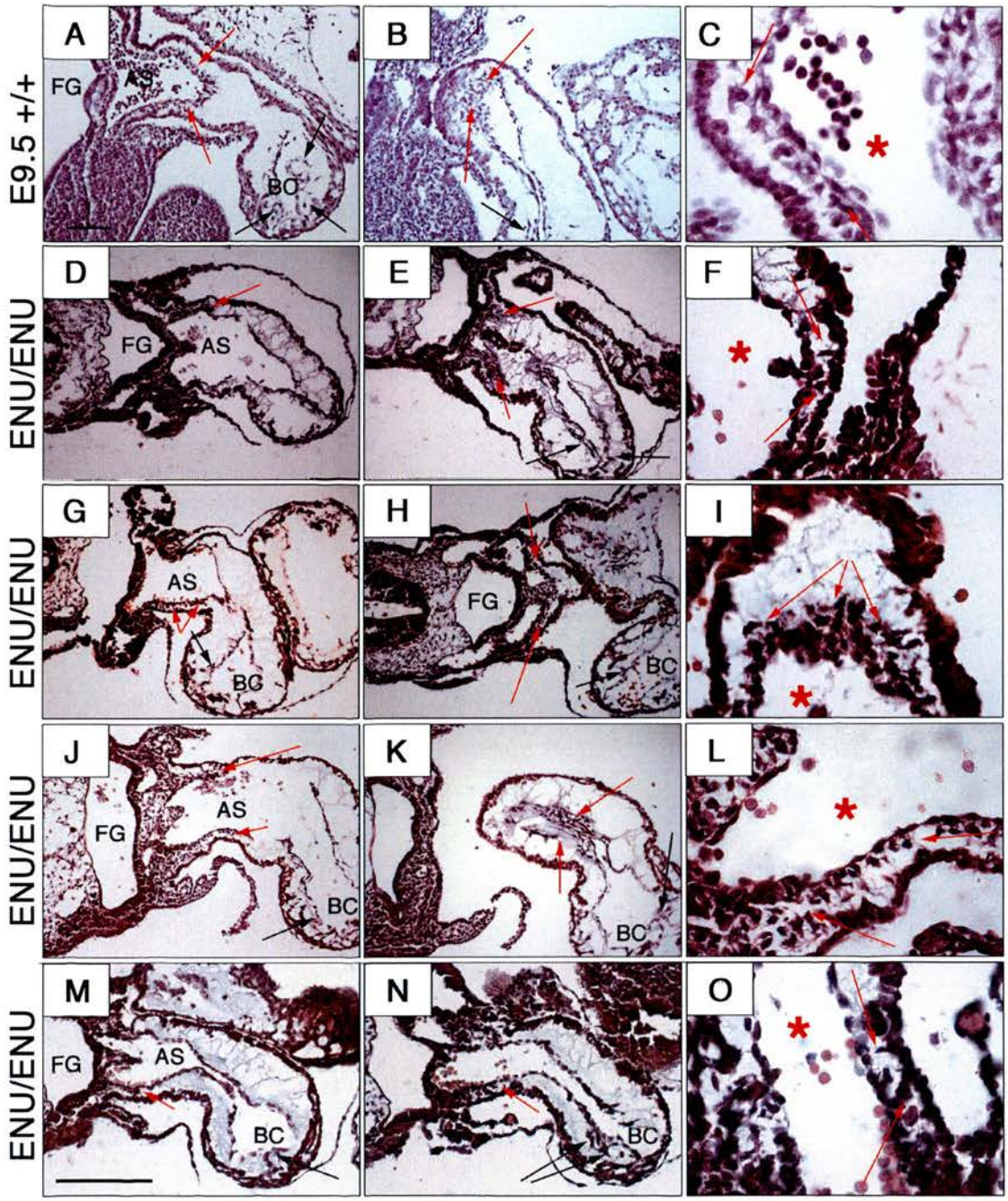
E9.5 +/+
ENU/ENU
ENU/ENU
ENU/ENU
ENU/ENU
A
B
C
D
E
F
G
H
I
J
K
L
M
N
O
FG
AS
BC

Figure 3.15: *Sox4*$^{ENU/ENU}$ *Foxq1*$^{sa/sa}$ class-II embryos exhibit variable outflow tract development at E9.5, as shown by histological analysis. Haematoxylin and eosin-stained transverse sections through the developing outflow tract (OFT) of an E9.5 control embryo (A,B,C) compared with two class-II mutant embryos (D,E,F; G,H,I). Hearts were examined through similar OFT regions comparing two different levels (first and second columns of figure), as determined by examination of all sections through the heart. (A,B) The control embryo demonstrates the normal OFT cushion swelling and infiltration of sub-endocardial cells in the distal OFT, possibly corresponding to cardiac neural crest (red arrows A,B). Additionally, mesenchyme development is evident in the cushions of the proximal region of the OFT (BC; black arrows A). (D-I) In two mutant embryos swelling of the outflow tract and abnormal cushion development is evident, with no evidence for mesenchyme production in the proximal cushions in these sections. One class-II OFT demonstrates the presence of sub-endocardial cells within the distal OFT (red arrows D,E). Higher magnification (4x) of the distal OFT in a control (C) and a class-II mutant (F), reveals the presence of sub-endocardial cells adjacent to the lumen of the OFT (red asterisk). (G,H,I) A second class-II mutant embryo does not demonstrate sub-endocardial cells in the distal OFT in these sections. Abbreviations as in previous figures; Scale bar: A,B,D,E 100μm; G,H,I 100μm; C,F same magnification.

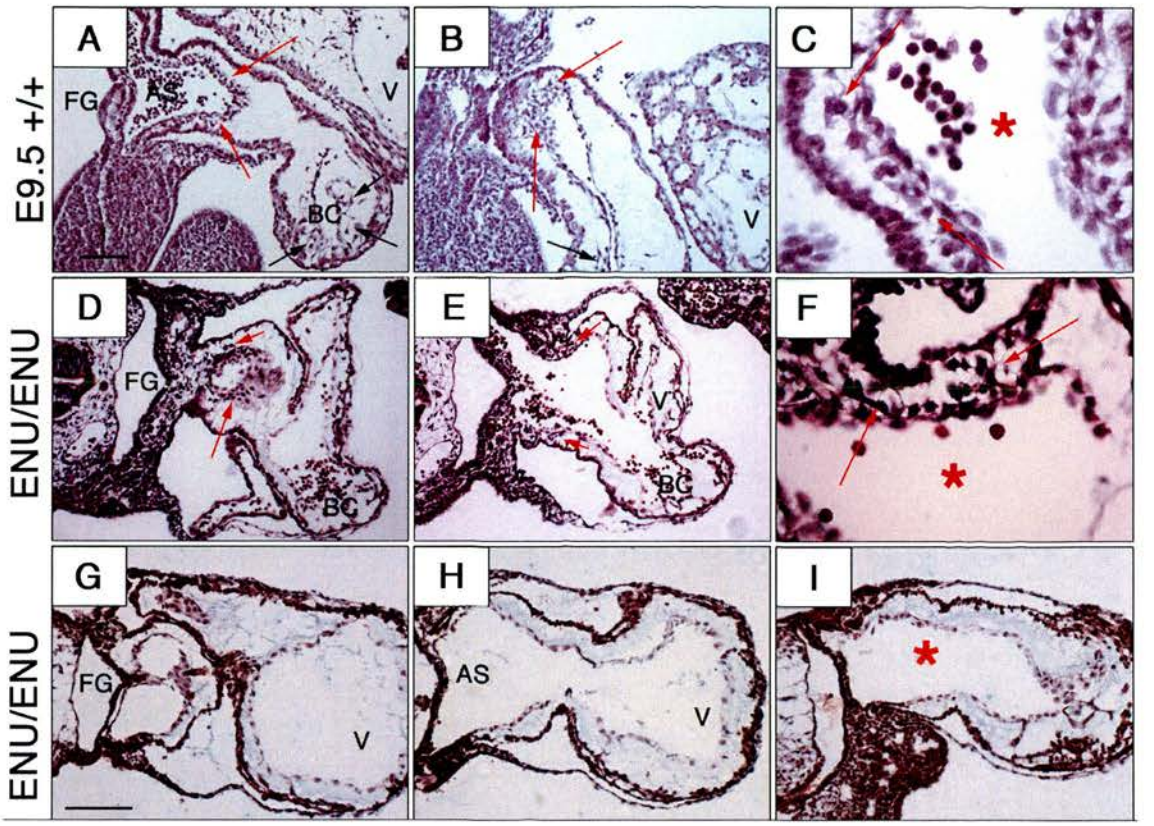
E9.5 +/+
ENU/ENU
ENU/ENU
A
B
C
D
E
F
G
H
I
FG
AS
V
BC
*

Figure 3.16: A *Sox4*$^{ENU/ENU}$ *Foxq1*$^{sa/sa}$ E10.5 embryo exhibits abnormal outflow tract development, as shown by histological analysis. Haematoxylin and eosin-stained transverse sections through the developing outflow tract (OFT) of an E9.5 control embryo (A,B,C; sectioned in the transverse plane) compared with equivalent sections of one E10.5 mutant embryo (D,E,F; sectioned midway between transverse and frontal, in plane with the angle of the outflow tract) and a stage-matched E10.5 littermate control (G,H,I; sectioned midway between transverse and frontal, in plane with the angle of the outflow tract). Hearts were examined through similar regions comparing two different levels of the OFT (first and second columns of figure), as determined by examination of all sections through the heart. (A,B) The control E9.5 embryo demonstrates the normal OFT cushion swelling, production of mesenchyme is evident in the proximal OFT cushions adjacent to the bulbus cordis (BC; black arrows A, B), and infiltration of sub-endocardial cells in the distal OFT, possibly corresponding to cardiac neural crest (red arrows A,B). (D-E) In one mutant E10.5 embryo swelling of the outflow tract and abnormal cushion development are evident, with limited mesenchyme production in the proximal cushions in these sections (black arrows, D). Additionally, sub-endocardial cells are present in the mutant distal OFT (red arrows, E). Development of the mutant heart appears to be delayed with compared with the E10.5 littermate control embryo (G-H), which demonstrates the normal presence, for this stage, of subendocardial cells (red arrows, G, H) and mesenchyme production in the proximal cushions (black arrow, H). Higher magnification (4x) of the distal OFT in control (E9.5, C; E10.5, I) and the E10.5 mutant (F), reveals the presence of sub-endocardial cells adjacent to the lumen of the OFT (red asterisk). Scale bar: A,B 100μm; D,E 100μm; G,H 100μm; C,F,I same magnification.

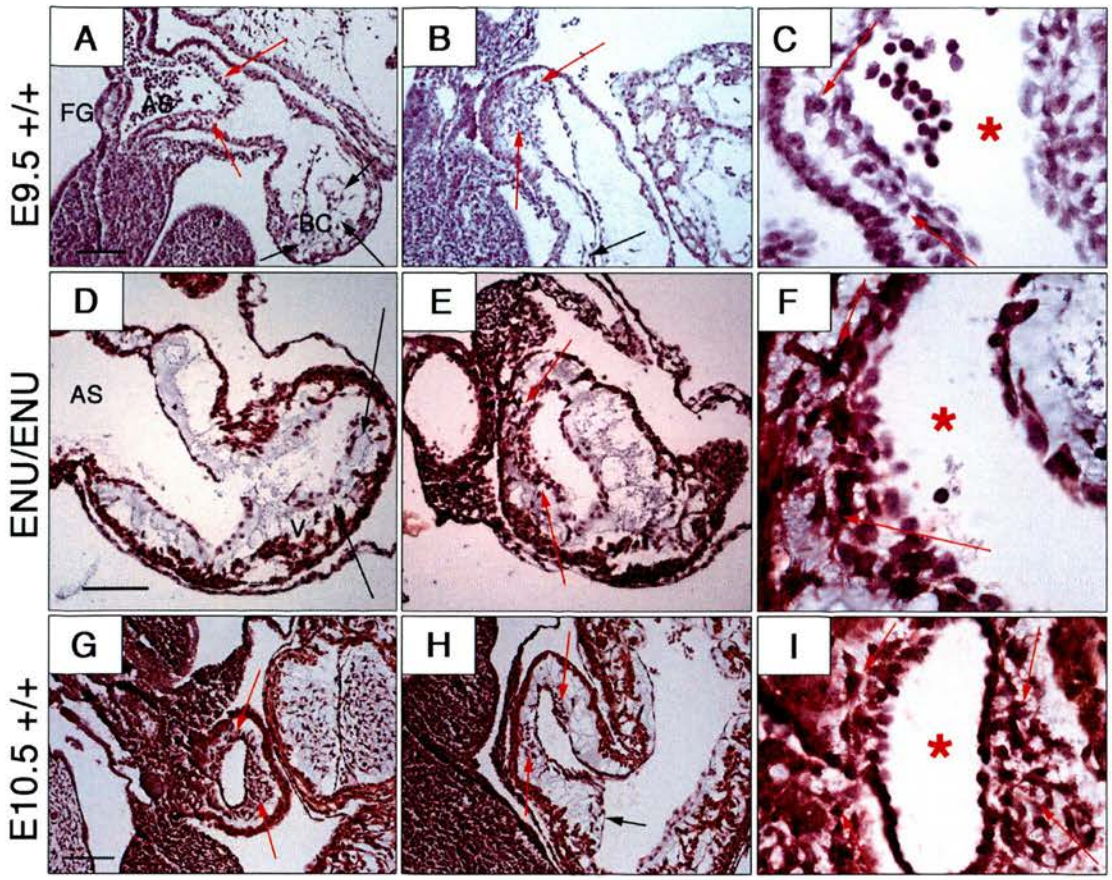
E9.5 +/+
ENU/ENU
E10.5 +/+
A
B
C
D
E
F
G
H
I
FG
AS
BC
V

3.2.5 E12.5 *Sox4*$^{ENU/ENU}$ *Foxq1*$^{sa/sa}$ embryos demonstrate craniofacial defects.

Anterior defects are characteristic of 6p deletion syndromes (section 1.4.2). An examination of embryos hemizygous for *satin*, arising from a *Foxq1*$^{sa/sa}$ *Del(13)Svea36H* cross, revealed abnormalities of forebrain development (Willoughby 2006), PhD Thesis. This phenotype overlaps with the E9.5 anterior phenotype observed in class-I and class-II *Sox4*$^{ENU/ENU}$ *Foxq1*$^{sa/sa}$ embryos, suggestive of a genetic interaction between the *Sox4* mutant allele and *satin*.

The wholemount E9.5 forebrain phenotype has been described according to classes-I and -II (Presented as classes in Figure 3.8). In addition, we examined the anterior phenotype in embryos dissected at E12.5-E13.5 (which were examined for the cardiac phenotype, Figures 3.1 in wholemount and, prior to sectioning, the embryos examined in Figures 3.2 – 3.7; numbers in Table 3.3). In this study, control embryos showed normal anterior development, with appropriate retinal pigmentation, nasal grooves and lower jaw (Figure 3.17a, d). It was found that, in addition to cardiac abnormalities, *Sox4*$^{ENU/ENU}$ *Foxq1*$^{sa/sa}$ E12.5-13.5 embryos demonstrated defective morphology of anterior structures. It is presumed that mutants with a less obvious phenotype would represent further development of E9.5 class-I embryos, while more severe phenotypes would represent class-II. At E12.5, less severe mutants (n=3/5) demonstrated a smaller lower jaw in proportion to the upper jaw and nasal process, although early vibrissae formation is evident (Figure 3.17b, e). Also in this class of mutants, eye pigmentation was markedly decreased or delayed relative to other hallmarks of developmental stage (eg. limb buds, somites). Some homozygotes (n=2/5) demonstrated a more severe phenotype exhibiting severe neural and anterior defects. In these embryos, the forebrain did not appear to have formed, the presumptive lower jaw was malformed and facial structures of the optic vesicle and nasal process were absent (Figure 3.17c, f). One embryo demonstrated severe exencephaly of the hindbrain (Figure 3.17c). As these more severe phenotypes were not described for any *Sox4* or *Foxq1* alleles, it is likely that these additional anterior phenotypes are a consequence of a genetic interaction between the two mutant alleles and thus a combined *Sox4; Foxq1* deficiency.

3.2.6 Placental appearance of E12.5 *Sox4*$^{ENU/ENU}$ *Foxq1*$^{sa/sa}$ embryos.

Placental insufficiency is a major cause of embryonic death after E9.5. The placenta may either show gross morphological abnormalities, or appear normal but in both cases, it is possible that its function for maternal-foetal interaction may be in some way compromised. Defects of the yolk sac can also result in embryonic lethality due to insufficient circulation. Whilst an extraembryonic defect may be intrinsic to the yolk sac, it also may be a consequence of cardiac defects and problems with blood flow.

During the process of dissection, some embryos could be identified as homozygotes prior to removal of the extraembryonic membranes and placenta. From E10.5, some homozygotes showed decreased blood flow through the yolk sac when compared with control yolk sacs. At E12.5, the visual difference of some mutant placentas was investigated by serial sectioning and tissue staining. The placental layers can be identified by histological analysis. The layers of labyrinth, spongiotrophoblast cells, trophoblast giant cells and maternal decidua were identified in all placentas examined. Sectioning through the placentas revealed morphological differences compared with the same region in the control. However by sectioning further into the mutant placentas, each of the four cell layers could be identified (Figure 3.18b, c and d, compared to control a). Whilst it is possible that there could be an extraembryonic phenotype caused by mutation in *Sox4* and *Foxq1*, this remains to be explored. Since a specific cardiac phenotype can be observed at E9.5, and this cardiac phenotype demonstrates overlap with that of mutation in other cardiac genes, it is more likely that the cardiac abnormalities originate from an embryonic requirement for *Sox4* expression, and that the placental malformation is secondary to, or independent of, this.

Figure 3.17: *Sox4*$^{ENU/ENU}$ *Foxq1*$^{sa/sa}$ embryos demonstrate a variable anterior phenotype at E12.5. (A,D) control embryos demonstrate normal anterior development (eye pigmentation; nasal structure is indicated by yellow bracket), pericardial swelling and haemorrhaging are not observed in control embryos. (B,C,E,F) mutant embryos all demonstrate pericardial swelling (white arrow head) and haemorrhaging (black arrowhead, B,C,E). Additionally, variable anterior defects are observed. Less severe mutants (B,E) demonstrate reduced pigmentation in the eye and a mild defect of the nasal structure (yellow bracket). Severe mutants (C,E) demonstrate abnormal nasal structure (red arrow) and a lack of a visible optic development. Embryo in (C) also demonstrates open hindbrain neural folds (grey arrow). Scale bar A- F: 360μm.

A
+/+
B
ENU/ENU
C
ENU/ENU
D
+/+
E
ENU/ENU
F
ENU/ENU

Figure 3.18: Some *Sox4*$^{ENU/ENU}$ *Foxq1*$^{sa/sa}$ embryos demonstrate a placental phenotype at E12.5. Haematoxylin and eosin-stained sections cut through the placenta of *Sox4*$^{ENU/ENU}$ *Foxq1*$^{sa/sa}$ embryos. (A) Control placenta demonstrates the formation of four layers comprising labrynth cells, spongiotrophoblast cells, giant trophoblast cells and maternal decidua. (B,C,D) *Sox4*$^{ENU/ENU}$ *Foxq1*$^{sa/sa}$ embryos demonstrate the ability to form all four layers of the placenta however layer proportion varies between embryos. Abbreviations: Lab, labyrinth; Sp, spongiotrophoblast; Gc, giant cells; Dec maternal decidua. All images same magnification.

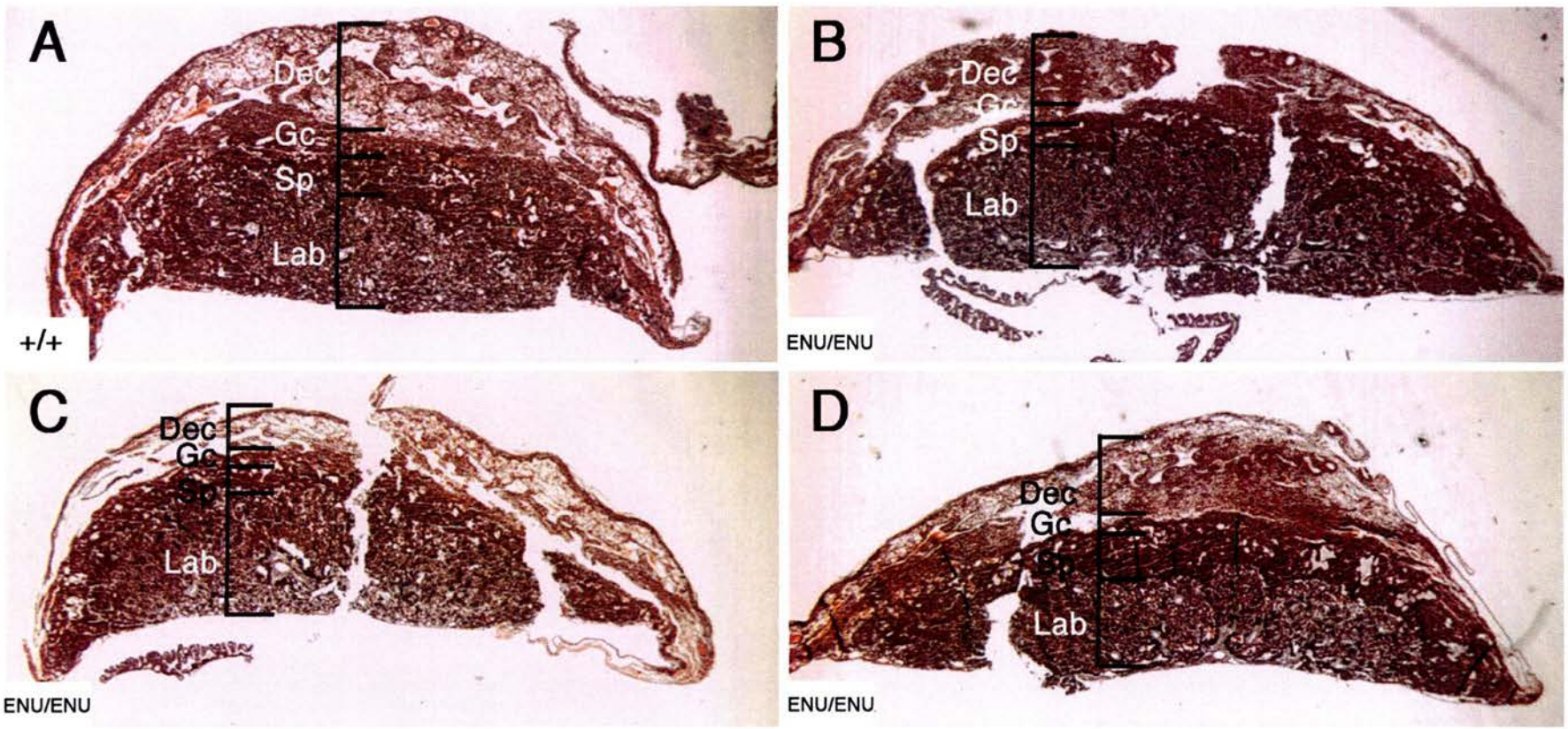
A
Dec
Gc
Sp
Lab
+/+
B
Dec
Sp
Lab
ENU/ENU
C
Dec
Gc
Sp
Lab
ENU/ENU
D
Dec
Gc
Sp
Lab
ENU/ENU

3.3 DISCUSSION

The results presented in this chapter demonstrate the phenotypic consequence of the *Sox4*^{ENU} and *Foxq1*^{sa} mutations. Since mutant alleles of *Foxq1* do not demonstrate a cardiac phenotype, the cardiac aspects of this study may be attributed to the mutation in *Sox4* and therefore this discussion of the cardiac phenotype relates exclusively to *Sox4*. A separate aspect of the *Sox4*$^{ENU/ENU}$ *Foxq1*$^{sa/sa}$ phenotype, aberrant forebrain development, reveals a possible genetic interaction between *Sox4* and *satin*. This finding will be discussed at the end of this section.

DETERMINING A ROLE FOR SOX4 IN CARDIOGENESIS

Since the publication of the *Sox4* null phenotype in late heart development (Schilham *et. al.* 1996; Ya *et. al.* 1998b), its role has received little attention, despite major advances in the understanding of heart development over the last 10 years, and the suggestion that an earlier defect is present in these mutants (Ya *et. al.* 1998b). This doctoral research has utilised a mutant allele of *Sox4* (*Sox4*^{ENU}) - which demonstrates cardiac dysmorphology and lethality that is similar to the phenotype of the null allele at E14.5 (Bogani *et. al.* 2005; Schilham *et. al.* 1996; Ya *et. al.* 1998b). Additionally, the *Sox4* mutation is recessive and genetic crosses suggest that it results in a loss of function. Therefore, it is likely that the *Sox4*^{ENU} mutation leads to loss of function of Sox4.

Our mutant allele presents with a phenotype earlier than that described for the null allele and shows a cardiac phenotype from the 10th embryonic day. Previous studies (Dr Ruth Arkell *pers.comm.*; Ya *et. al.* 1998b) showed that some homozygotes (approximately 5-7%) must be lost before E14.5, when the remainder of mutants die. Our examination of the *Sox4*$^{ENU/ENU}$ phenotype at stages leading up to E14.5 suggests that this loss occurred between E10.5 and E11.5, since up to E10.5, 26% of embryos from intercrosses are homozygous (115/439), and thereafter, only 19% (17/91) are recovered. Interestingly, the percentage of homozygous embryos lost prior to E11.5 corresponds well to the proportion of Class-III homozygotes dissected at E9.5 (5%; 20/189), while class-I and-II homozygotes together constitute around 17% of the litter (70/189). This strongly suggests that the published phenotype in E14.5 mutant

embryos must have origins in the defects, (most probably those in Class-I and –II mutant categories) observed from E9.5. In this chapter, therefore, the E9.5 phenotype has been studied in detail. Since published studies of this allele do not provide an account of the progression of heart defects (Bogani *et. al.* 2005), the phenotype at E12.5-E13.5 was also examined comprehensively. This discussion will first discuss the later-stage phenotype, in the context of what could further be examined. Then the mutant phenotype presented will be compared with those of other published mutants where known cardiac cell populations are affected, to arrive at a set of possible cell types and processes affected by disruption of Sox4. Approaches for further study of these possibilities will be discussed.

3.3.1 Discussion of the E12.5-E13.5 phenotype of the *Sox4*^{ENU} mutant.

This analysis is the first in which the *Sox4*^{ENU} allele has been examined during the stages of cardiac septation; thus providing the first detailed phenotypic characterisation of this mouse line, as a novel model for further characterising the molecular regulation of cardiogenesis. For the allele examined in this study, we have shown that the aspects of the outflow tract phenotype at E12.5 and E13.5 resemble the outflow tract phenotype described for the null allele (Ya *et. al.* 1998b), but in addition, we have identified atrioventricular cushion abnormalities which implicates Sox4 in a further role of atrioventricular valve formation, atrial septation and atrioventricular septation.

Histological analysis of embryos homozygous for the *Sox4*^{ENU} allele has revealed aspects of the *Sox4* mutant phenotype at E12.5 and E13.5, preceding the published E14.5 ultimate lethal phenotype. Outflow tract septation was inadequate at E12.5 and incomplete at E13.5, with mutants demonstrating PTA and DORV. This development appeared delayed, with septation of some mutant embryos at E13.5 resembling that of E12.5 control hearts. It was noted that the anterior regions of the pulmonary trunk and aorta had septated, suggesting that the aorticopulmonary septum and the distal ridges of the outflow tract had developed to a degree.

At E12.5 and E13.5, it was observed that mutants developed endocardial ridges and appeared to initiate formation of the semi-lunar valves of the OFT. However ridges

appeared smaller in the mutant hearts at both developmental stages - even accounting for a possible developmental delay. Further analysis is needed to examine the construction of the semi-lunar valves in the mutants, and whether they develop in the appropriate number and orientation. For this, it would be most useful to examine the anterior heart from the stages shown through to E14.5, both by sectioning and histology, as well as by either MRI or OPT to whole embryos. Since the null allele was examined by histology up to E14, Ya *et.al.* were able to describe the initial formation of the semi-lunar valves in their mutant. Such analysis could be conducted with the $Sox4^{ENU}$ allele, particularly since the semi-lunar valvular deficiency, resulting in an oscillatory movement of blood at the anterior pole, has been reported as the likely cause of lethality in all *Sox4* alleles at E14.5 (Bogani *et. al.* 2005; Penzo-Mendez *et. al.* 2007; Schilham *et. al.* 1996; Ya *et. al.* 1998a).

Furthermore, the progressive development of this phenotype should be examined. This analysis was conducted to an extent in this project, by histology on E9.5 embryos. Analysis would involve examining the quantitative contribution of cells to the developing valves from the cushion stages of development. In parallel to this, examination of the removal of cells, by apoptosis, would be further useful. Analysis with cell-type specific markers could be conducted to reveal whether the regions of myocardium, endocardium and mesenchyme are appropriately patterned for their developmental stage. Given the cardiac domains affected by the mutation and the phenotype observed, analysis of the contribution of the NCC and the SHF cells would be a logical next step.

This phenotype may have its origins earlier in development. At E9.5 whole embryos demonstrate severe swelling of the heart tube and inadequate cardiac looping, while section analysis has shown that there appears to be a defect in the process of trabeculation of the early ventricular chamber and a defect or delay in the production or maintenance of cushion mesenchyme within the developing atrioventricular cushions. Although this has so far only been examined at E9.5, it may subsequently lead to a variable phenotype being present in derivatives of this tissue – namely the AVS, and the mitral and tricuspid valves (sometimes appearing as a common atrioventricular valve), as well as the mesenchymal contribution to the

atrioventricular, atrial and ventricular septa. Since the process of EMT is a key factor involved in the production and initial patterning and maintenance of the cardiac mesenchyme, it is possible that *Sox4* plays a role at some level in cardiac EMT.

Thus, three potential developmental roles of Sox4 must be considered, namely (1) that it is required in regions of NCC infiltration into the heart; and/or (2) that it is required in some regions where SHF derivatives contribute to cardiogenesis; and/or (3) that it is required during the process of EMT, whether this be in the endocardial layer, the delaminating endocardium, or the mesenchyme from E9.5 and the start of cushion formation.

The mutant phenotype implies a requirement for Sox4 function in regions of NCC infiltration.

Defects at the arterial pole of the heart of *Sox4* mutants closely overlap with those in mouse models with defective cardiac neural crest cell (NCC) function -particularly with respect to the septation defects. It is evident from sections of $Sox4^{ENU/ENU}$ class-I and some class-II embryos at E9.5 that the subendocardial space of the OFT is in the process of being populated with what may be NCC (Chapter 1, section 1.3.3, Figure 1.13) – although marker analysis is essential to verify this. The density of subendocardial cells appears variable between embryos through visual analysis of serial sections, although this was not subjected to quantitative analysis in serial sections of a high number of developmentally matched embryos, it is possible that either this variation is a consequence of the developmental differences between control embryos and mutant classes, or it reflects a variably penetrant phenotype. Even a delay in the infiltration of NCC may result in an inappropriate molecular programme in cells of the OFT, and thus contribute to abnormal development – although the specific requirements for correct timing of infiltration have not been examined in models with OFT defects.

Certainly the number of infiltrating NCC is a contributing factor to the development of the anterior heart. This has been shown in detail by analysis of the Pax3 *Splotch* mutant alleles. In the Sp^{2H} allele, NCC fail to colonise the OFT adequately, resulting in PTA or DORV without a common arterial trunk (Bradshaw *et. al.* 2009; Conway

et. al. 1997; Epstein *et. al.* 2000). The lethality of the Sp^{2H} homozygotes about E13.5 from cardiac failure, thus makes it possible that the inadequate OFT septation in *Sox4* mutant embryos contributes to the embryonic lethality. In addition to the septal defects, Sp^{2H}/Sp^{2H} hearts further reveal shortening of the OFT (Bradshaw *et. al.* 2009), and this feature could be examined by histology in *Sox4* mutant hearts at E10.5. In chick, ablation of NCC has been shown to contribute to this conotruncal malformation by a reduction in cellular contribution (Yelbuz *et. al.* 2002). In particular, it is the SHF which exhibits defective contribution to the anterior heart in both NCC ablated chick embryos, and Sp^{2H}/Sp^{2H} embryos (Bradshaw *et. al.* 2009; Yelbuz *et. al.* 2002). To examine NCC contribution in $Sox4^{ENU/ENU}$ mutants would require crossing of the $Sox4^{ENU}$ line onto the *Wnt1-lacZ* line (Echelard *et. al.* 1994) or *Wnt1-cre* crossed to the *ROSA26-LacZ* reporter (*R26R*) line (Jiang *et. al.* 2000; Soriano 1999). Conducting these crosses onto the $Sox4^{ENU}$ background would enable examination of the infiltration of NCC into the anterior heart. When examined over a developmental time period, such analysis could be quantitative to determine whether a reduction in the infiltration of NCC correlates with the severity of the cardiac phenotype.

Analysis with a *Wnt1*-reporter may also enable examination of the possible contribution to other cardiac regions such as the AVC and primitive valves in the $Sox4^{ENU/ENU}$ mutant. The contribution of NCC in these domains appears to be dependent on genetic background (Hildreth *et. al.* 2008; Nakamura *et. al.* 2006). Interestingly, the study reported by Nakamura *et.al.* used mice which had been substantially backcrossed to a C57BL/6J background. A C57Bl/6J strain background was the predominant background used in this analysis of the $Sox4^{ENU}$ allele. Thus it is possible that the genetic modifiers on this strain background may contribute to infiltration of NCC into the AVC and valves and thereby exacerbate the *Sox4* phenotype of this ENU allele, from that observed in the study of the null allele.

Whilst NCC have been shown to contribute to the mesenchymal population of the developing OFT (Epstein *et. al.* 2000; Jiang *et. al.* 2000), as maturation of the valves proceeds, the NCC are replaced by cells of endocardial origin (discussed section 1.3.3; (de Lange *et. al.* 2004)). Analysis of this cellular replacement in *Sox4* mutant

embryos could be examined by using a *Tie2* reporter allele (*Tie2-cre/ R26R* (Kisanuki *et. al.* 2001; Soriano 1999)) on a *Sox4*-mutant background for cells of endocardial origin. Furthermore the *Wnt1-LacZ* reporter on the *Sox4* mutant background could be utilised in crosses to examine the distribution of NCC (as described, above). Although it would require an extensive breeding programme, ablation of *Sox4* from the endocardial lineage (by crossing *Tie2-cre* with the conditional $Sox4^{fl/fl}$ (Penzo-Mendez *et. al.* 2007)) would enable clarification as to whether the requirement of the OFT for Sox4 resides within endocardial-derived cells, where *Sox4* is known to be expressed (shown in subsequent chapters, Chapter 4). Examining the phenotype and distribution of NCC in the OFT of embryos in which *Sox4* expression had been removed from the endocardium, (possibly by involving a further genetic cross to the *Wnt1-LacZ* line (Echelard *et. al.* 1994), or by use of NCC antibodies), would assist in determining whether NCC require the adjacent endocardial layer to express *Sox4*.

Outwith the developing cardiac structure, remodelling of the aortic arch arteries and regression of the right dorsal aorta is also regulated by NCC. Whilst this was not examined thoroughly in the present study, it is possible that a NCC defect may be revealed if *Sox4* mutant embryos exhibit abnormal persistence of the right dorsal aorta, or abnormal regression of the 3^{rd}, 4^{th} and 6^{th} arch arteries, and is certainly an aspect of the mutant phenotype which should be examined.

To summarise, it is possible that the *Sox4* OFT septation defects are a consequence of dysregulation of NCC function. The comparison with the NCC deficient *Splotch* mutant has shown that a disruption to NCC function and septation in the anterior heart may be sufficient to result in the E14.5 lethality observed with *Sox4* mutant alleles. Nevertheless, it remains possible that the valvular deficiency may be derived from abnormalities in the endocardial-derived mesenchyme populating the OFT ridges. Separating the endocardial and NCC functions would require considerable further analysis using transgenic mice.

The Sox4$^{ENU/ENU}$ Foxq1$^{sa/sa}$ cardiac phenotype partially overlaps with that of mouse models where the SHF is disrupted.

Defects to the anterior heart have not only been reported in the context of a disruption to NCC infiltration, but also the SHF population. Since these two cell populations occupy both adjacent and overlapping regions within the OFT, separation of gene function within either population is reliant upon specific inactivation. Using such methods, a study of the requirement for hedgehog signalling by the SHF has shown that Shh signalling from the pharyngeal endoderm is essential for OFT septation. In E12.5 embryos, the ability of anterior SHF cells to be responsive to Shh signalling had been selectively ablated *via.* conditional inactivation of *Smoothened* by use of the *Mef2C-AHF-Cre*. Hearts of mutant embryos demonstrated the presence of OFT cushions, yet there was a lack of septation between the pulmonary artery and the aorta (Goddeeris *et. al.* 2007). This phenotype overlaps with what has been observed in the OFT of the *Sox4^{ENU}* mutant, although comparison of stage and regionally-matched sections would be necessary to determine the extent of this phenotypic overlap in the anterior heart. Additionally, embryos in which the Shh-responsiveness of SHF had been disrupted survived until at least E18.5. If, in the *Sox4^{ENU}* mutant embryos, the anterior SHF is not able to function correctly, clearly additional roles for Sox4 exist in this cardiac domain to result in the E14.5 lethality.

Consequences of disruption to the SHF have also been shown at the venous pole of the heart, in developmental models altering the function of *Isl1*-expressing SHF cells. Migration of *Isl1* expressing cells was disrupted by conditional expression of a dominant-negative effector of RhoA signalling (Hildreth *et. al.* 2009). In this model, defects were observed at the venous pole at E10.5 and E14.5. Atrial septation was impaired as a proportion of embryos did not develop the vestibular spine (also, dorsal mesenchymal projection (DMP)) and thus the primary septum did not fuse with the atrioventricular cushion. Additionally, some mutant hearts demonstrated a common atrioventricular junction; ventricular septal defects; and exhibited abnormal OFT septation (Hildreth *et. al.* 2009). While the anterior defects of mutant hearts were not detailed in the above paper, a degree of overlap in the phenotype of hearts in which

SHF cell migration is impaired, and the phenotype described in this chapter for the *Sox4*^{ENU} allele is still evident. However, hearts in which *Isl1*-expressing cell migration was impaired further demonstrated a defect in the development of the venous valves – a phenotype not observed with the mutant *Sox4* allele. Thus it is possible that aspects of the *Sox4*^{ENU} phenotype are a consequence of disruption to SHF function.

This ENU-induced mutation in *Sox4* could not completely ablate the ability of SHF to contribute to cardiogenesis, since the defects are not as severe as loss of function of *Isl1* (Cai *et.al.* 2003). Nor does the *Sox4*^{ENU} mutant share enough phenotypic overlap with other homozygous mutants characterised with disruption to SHF genes where the predominant phenotype includes severe right ventricle and outflow tract abnormalities. Such mutants have predominantly been reported to be embryonic lethal about E10 including *Mef2c* (Lin *et. al.* 1997), a potential target gene of Isl1 (Dodou *et. al.* 2004); *Hand2* (Srivastava *et. al.* 1997) a marker of the SHF downstream of *Mef2c* (Lin, Q *et. al.* 1997); *Foxh1* (von Both *et. al.* 2004); or lethal about E11, such as *Tbx20* (Cai *et. al.* 2005; Singh *et. al.* 2005; Stennard *et. al.* 2005; Takeuchi *et. al.* 2005). An understanding of the expression pattern of *Sox4* is further required to investigate the possible connection between the SHF and Sox4 function. Clearly the phenotype of the *Sox4*^{ENU} allele requires considerable further analysis in order to determine which cell lineages in the heart are influenced by mutation of Sox4.

Distinguishing between a disruption to NCC and a disruption to the SHF.

In the initial studies of the *Sox4* null allele, the contribution of mesenchyme derived from NCC in *Sox4* null hearts was examined by the staining of sections for α-smooth muscle actin (α-SMA; also now known as Acta2), also a marker of vascular smooth muscle. α-SMA had been shown to differentiate between NCC-derived and endocardial-derived mesenchyme (Beall *et. al.* 1990; Ya *et. al.* 1997). Using this marker, Ya *et.al.* claimed that in *Sox4* null embryos, there was a variable ability of NCC to invade the outflow tract and contribute to arterial septation. Given this finding, it was suggested that the migration of NCC into the OFT is poorly guided in more severely affected *Sox4* null embryos (Ya *et. al.* 1998b). However, despite

being a marker of NCC-derived mesenchyme α-SMA is not specific for cells of NCC origin, since it marks cardiac smooth muscle cell differentiation and cells of the OFT myocardium. At E13.5, the *Cx43-lacZ* transgene, which marks NCC, is found in cells expressing *α-SMA*, while *α-SMA* is also expressed by cells of the OFT myocardium, not marked by the *Cx43-lacZ* reporter (Epstein *et. al.* 2000). In chick it has also been shown that *α-SMA* is expressed by a specific regional domain of cells of SHF origin as they commence differentiation into smooth muscle cells and then contribute to the vascular myocardium at the level of the semi-lunar valves (Waldo *et. al.* 2005a). OFT myocardium contributes to the process of myocardialisation of the OFT septum initially formed by NCC (van den Hoff *et. al.* 1999). Although myocardialisation has been best characterised in chick, the equivalent stage in mouse at which this process starts is E13.5, a stage examined in *Sox4* null embryos (Ya *et. al.* 1998b). Thus, a reduction in the cell population expressing α-SMA may reflect any of these possibilities, depending on the precise timing of expression and specific location within the arterial pole of the heart: reduced SHF-derived contribution to the OFT; reduced SHF-derived vascular myocardialisation; and the original possibility of an abnormality in the guidance of NCC into the endocardial tissue of the OFT. This, combined with the possibility that, like the $Sox4^{ENU}$ embryos shown in this study, there is a developmental delay, suggests that their work does not conclusively show that the defect lies in NCC (Schilham *et. al.* 1996; Ya *et. al.* 1998b).

Uncovering the molecular basis for the integration of NCC into the anterior heart, and the requirement of NCC by the SHF is still a complex challenge. Analysis of phenotypic mutants can contribute to this understanding. In order to investigate this issue - whether or not the defect resides with the NCC; the endocardial-derived cell interaction with NCC or SHF cells; or with the SHF cell infiltration into the heart - and thus explore the possibilities arising in this chapter (and those of Ya *et.al.*), specific markers need to be examined. *Wnt1-LacZ* labelled cells would reveal the extent of NCC infiltration and positioning in $Sox4^{ENU}$ embryos (as previously described), while the SHF derived cells could be examined by monitoring *Isl1* expressing cells (using an antibody to Isl1 or by use of *Isl1* reporter alleles (Pan *et. al.* 2008)) or by use of the *Mef2c-LacZ* allele (Dodou *et. al.* 2004), both of which

would reveal SHF-derived cells when combined with the *Sox4*^{ENU} allele. Initial examination of the contribution of Isl1 labelled cells, in sections through the relevant regions of E8.5-E10.5 embryos, could reveal a possible deficiency in SHF cells prior to and during the appearance of the phenotype in *Sox4* mutant hearts. Analysis of the contribution of SHF to cardiac development in *Sox4*$^{ENU/ENU}$ embryos would assist in establishing a possible SHF deficiency and thereby an SHF phenotype.

Thus it is possible to examine the separate contribution of NCC and SHF cells to the *Sox4* mutant heart. Whilst a number of crosses would need to be conducted in order to obtain sufficient embryos for this to be analysed in detail, such analysis would contribute to deciphering the involvement of these two cell populations in the *Sox4* mutant phenotype, as well as uncovering aspects of the role of Sox4 in cardiogenesis.

There is phenotypic overlap between the Sox4 mutant and the Nfatc mutant in which aspects of endocardial EMT are disrupted.

The phenotype observed is not restricted to the possibilities of a defect in neural crest or SHF infiltration to the heart, since other processes are integral to its development at this time. The process of EMT is essential for endocardial cushion and ridge formation. Thus it is possible that a defect in the development of the mesenchyme, and subsequent derived structures, is a consequence of abnormalities in the process of EMT within the heart.

Nfatc signalling is required for EMT within the developing heart (section 1.3.3). Aspects of the Sox4 cardiac phenotype described here at E12.5 and E13.5, and elsewhere at E14.5 (Bogani *et. al.* 2004) overlap with *Nfatc* mutant embryos, to the point that, in both the study of the *Nfatc* null allele (de la Pompa *et. al.* 1998) and the second study of the *Sox4* null allele (Ya *et. al.* 1998b), each group examined the expression of the other gene within the heart. Whilst neither group observed abnormal expression by *in situ* hybridisation, it was speculated that the pathways in which they act may converge on the same aspect of cardiac development. In the *Nfatc* null, although septation of the OFT is complete, the formation of the endocardial cushions into semi-lunar valves and the development of the mitral and tricuspid valves resembled that of earlier embryonic stages. Incomplete interventricular septation was also observed. Lethality at E14.5 in the case of *Nfatc*

mutant embryos was, like that of the *Sox4* null, attributed to valvular malfunction and thus severe defects in forward blood flow – which may also account for the peripheral oedema and haemorrhaging.

Thus, it is possible that aspects of the cardiac defects observed as part of the E12.5-E14.5 $Sox4^{ENU}$ phenotype, such as defects to the atrioventricular region, are a consequence of inappropriate or inadequate mesenchyme production or patterning from earlier stages. The section data presented in this chapter alone is not sufficient evidence to confirm an EMT defect. In the *Nfatc* mutant, regions of the heart which are dependent upon EMT still develop to an extent, as is observed in the *Sox4* mutant. The process of EMT is integral to the formation of the endocardial cushions and in order to uncover a defect in EMT, it is necessary to examine embryos at earlier stages. This will be discussed in the following section of this chapter.

Does a cardiac defect fully explain the embryonic lethality?

It has been discussed that the *Sox4* phenotype overlaps with the phenotype for mutants in which there is defective or inappropriately patterned NCC, SHF cells or endocardial EMT. While the overlap with the *Nfatc* mutant is intriguing and one of the more similar cardiac mutant phenotypes, the *Sox4* phenotype does not overlap with only one of these, nor can the phenotypes of the examples given completely explain the *Sox4* phenotype. This is particularly evident with respect to the embryonic lethality. It is possible that the cardiac defects alone are not sufficient to result in the lethal phenotype. However it is convincing that the valvular deficiency observed in the *Nfatc* mutant also results in lethality about E14.5, while mutants in which OFT and ventricular septation is incomplete, may survive until later stages of gestation. Although the valvular deficiency has already been proposed by others (Schilham *et. al.* 1996; Ya *et. al.* 1998b), another developmental factor should be examined in the *Sox4* mutant embryos. Data in this chapter has revealed placental abnormalities (section 3.2.6). While this may be a consequence of the cardiac defect, it may also be possible that Sox4 plays a role in extra-embryonic development. To determine this further would require further histology and subsequent analysis of molecular markers within the placenta, in the first instance, to examine whether the cell types of each of the layers are correctly patterned in the *Sox4* mutant.

Summary

There are similarities between the later *Sox4*^{ENU} phenotype described in this chapter and phenotypes in which NCC function is perturbed. It is likely that a role of Sox4 is within the field of NCC function, yet significant experiments need to be conducted to determine the precise nature of this possible role. As an alternative, some mouse models which have not been shown to have a defect within NCC have been discussed since there is overlap in aspects of their phenotype with that presented by the *Sox4*^{ENU} allele. In particular, a degree of overlap exists with mouse mutants in which the SHF contribution is diminished. Still, results in this chapter imply that the cardiac requirement for Sox4 begins at least as early as E9.5, and these earlier phenotypes remain a possible basis for the phenotype observed at the later stages. Given this, the possible dysregulation of NCC could not account for the earlier E9.5 phenotype. Our findings do not contradict those published, rather they further refine the regions and the temporal domains in which Sox4 may be required. An understanding of the expression domains of *Sox4* during cardiogenesis will assist in interpreting this further.

3.3.2 An early onset phenotype at E9.5 *may* contribute to the late stage heart defects in *Sox4* mutant embryos.

Analysis of the *Sox4* mutant allele demonstrates a number of morphological and histological abnormalities in homozygous class-I and class-II embryos at E9.5, which, if left to develop, may result in the cardiac defects observed later in gestation.

Aspects of the mutant phenotype suggest a possible role for Sox4 in regions of EMT during heart development

The process of EMT is essential for cardiac remodelling. It is not just essential for formation of the valves and intra-cardiac septation, but mesenchymal cells of the AVC cushions also give rise to the membranous component of the IVS, during interventricular septation (section 1.3.3). Coupled with the inadequate looping of the heart, a delay or a deficiency in mesenchyme production from the AVC could contribute to the defects observed in *Sox4* mutant hearts at E12.5 and E13.5.

At E9.5 *Sox4* mutants demonstrate cardiac defects in regions of the heart which normally involve the process of EMT. The AVC of mutant hearts exhibits variable

mesenchymal contribution to the endocardial cushions. It is possible that this is a consequence of delayed embryonic development as it appears that the AVC is able to recover to a certain degree, since the atrioventricular septum and primitive valves appear to develop about E12.5-E13.5. Given these results, it is possible that normal *Sox4* expression is required for appropriate timing of EMT within the developing heart. In order to discuss this further, the cardiac phenotype of mouse models which overlap with the phenotype observed here in $Sox4^{ENU/ENU}$ $Foxq1^{sa/sa}$ mutants will be discussed. This discussion will be followed by mention of key experiments in which a role for Sox4 in cardiac EMT could be determined, since section data alone, as presented in this chapter, is uninformative for determining involvement of Sox4 in this process.

Many signalling pathways have been identified in regulating aspects of EMT in valve morphogenesis. Characterisation of the phenotype in these mutant embryos contributes to our understanding of the genetic events that underlie EMT.

Among the mouse models with mutations in *Sox* genes, the cushion defect most closely resembles that of mutation in *Sox9* (Akiyama *et. al.* 2004). *Sox9* is expressed within the cells following initial delamination and migration into the ECM/cardiac jelly, but before definitive mesenchymal transformation. Sox9 resides upstream of ErbB3, Sox5 and Sox6, whose expression in the cushions is required for EMT. Given the phenotype of *Sox4* mutants, it is plausible that the function of Sox4 resides alongside that of Sox9. To determine whether this is the case, expression of Sox9 and its target genes would need to be examined in *Sox4* mutant heart. Interestingly, in the field of prostate cancer research, SOX4 has been proposed to function upstream of *SOX9* expression (Liu *et.al.* 2006). A mechanism for this remains to be described and, to date, this has not been explored in the heart.

Vegf plays a negative regulatory role in EMT within the heart (Dor, Y *et. al.* 2001; Dor, Y *et. al.* 2003), and its expression must be modulated both to initiate and cease mesenchyme production during valve formation. In order to initiate heart valve morphogenesis, *Vegf* expression in the myocardium must be repressed by calcineurin/NFATc1 signalling from the endocardium (Chang *et. al.* 2004). The activity of NFATc1 is then limited to the endocardial cells at the site of valve

formation, while adjacent myocardial cells continue to express *Vegf*. The levels of Vegf expression prior to EMT have been shown to be essential for cardiac EMT. Underdeveloped cushions are one aspect of the phenotype in embryos haploinsufficient for Vegf (Carmeliet *et. al.* 1996; Ferrara *et. al.* 1996). Given the effect of the ENU mutation on cushion development, it is possible that Vegf levels have been altered, which would be possible to determine by gene expression and protein analysis.

The early E9.5 phenotype observed in this study suggests that aspects of the OFT and AVC defects in *Sox4* mutants arise independently of neural crest infiltration. Whilst this does not eliminate the possibility that neural crest function in the heart is disrupted, it may be that these phenotypes arise secondary or parallel to a defect in either the endocardium or myocardium of the E9.5 heart, as a result of *Sox4* mutation. To investigate this issue, *in vitro* analysis of cell migration could be performed. Each of the OFT and AVC cushions could be microdissected from E9.5 class-I mutant and control heart tubes and grown in culture as explants. A protocol has been described that utilises collagen gels to examine the ability of cardiac cells to undergo EMT *in vitro* (Runyan *et. al.* 1983). Whole explants would enable distinction between a defect in the initial delamination of endocardial cells to migratory cells by the loss of cell-cell contacts, or an inability of endocardial cells to undergo the transformation from delaminated cells to mesenchyme. In both circumstances, comparative analysis may be achieved by counting cells which have moved into the matrix. By supplementing cultures with media conditioned with specific morphogens (such as BMP2, known to induce expression of the mesenchyme marker periostin (Inai *et. al.* 2008)), it would be possible to examine whether there is a recovery in the ability of mutant endocardial explants to generate mesenchyme. Further to this, analysis of the endocardial expression of VE-cadherin, and immunostaining to view localisation, would assist in concluding whether *Sox4* mutants retain inappropriate cell contacts, or whether the endocardium is unable to respond to inductive signals.

Sox4 mutant embryos demonstrate a swollen heart at E9.5 which may impair cardiac looping.

At E9.5, the most striking defect in wholemount *Sox4* homozygous mutant embryos is swelling of the heart at E9.5 (Figure 3.8), in 90% of homozygote embryos examined (n=50) (Table 3.2). It is possible that inappropriate placement of the primitive cardiac chambers, and of the regions that undergo septation, may account for aspects of the lethal E13.5 phenotype. In class-I mutant embryos, the heart tube had undergone looping; however the atria, ventricles and OFT appear distended relative to wild type. Some class-II mutants demonstrated more severe swelling such that boundaries of the primitive chambers were not identifiable. Consequently, in both classes of mutants, the atrioventricular groove and inner curvature are inadequately positioned. The E9.5 heart is enlarged in a way that may be disproportionate to cell proliferation and differentiation, which may exert consequences on cell-cell and cell-matrix interactions, and this may in turn affect cell fate. By E12.5 and E13.5, the cardiac structures which have formed appear smaller than the wild type control hearts. Whether *Sox4* is involved in the processes of proliferation or differentiation in the formation of the heart remains to be examined.

The most well described consequence of inadequate looping is DORV, one of the common malformations in human syndromes with congenital heart defects. At mid-gestation, the aorta and pulmonary trunk of the OFT undergo rotation such that they are appropriately positioned above the ventricles (Dor, X *et. al.* 1985; Lomonico *et. al.* 1986) (Section 1.3.3). Failure of this conotruncal rotation underlies aspects of congenital heart defects (Bajolle *et. al.* 2006; Bostrom *et. al.* 1988; Lomonico *et. al.* 1988). Thus inadequate spatial organisation at this stage in *Sox4* mutant embryos may contribute to the PTA and DORV septal defects observed.

Mutant *Sox4* E12.5 hearts demonstrated displaced ventricles within the cardiac cavity: the base of the muscular interventricular septum was angled to the left such that the right ventricle was in a more midline position, while the left ventricle occupied a more dorsal region of the cavity when compared with control embryos (Figures 3.4 and 3.5). The inadequate looping of the heart may also contribute to the

delay in ventricular septation and the VSD at E13.5. The muscular ventricular septum elongates anteriorly to fuse with the mesenchyme from the atrioventricular cushions and endocardial ridges. Fusion of the muscular portion to the mesenchyme creates the membranous septum continuous with the cushions of the OFT (section 1.3.3). These regions are displaced in *Sox4* mutant embryos. Although the muscular portion of the ventricular septum forms, it fails to make the appropriate connections. This is distinctly different from laterality defects in which rightward looping of the heart is reversed. *Sox4* mutant hearts did not demonstrate such directional looping defects.

In all embryos examined at dissection, the heart had looped in the normal direction. Furthermore, examination of serial sections through E12.5 and E13.5 hearts did not uncover evidence for laterality defects such as isomerism. In particular the atria appeared to have developed their appropriate left/right features, such as the systemic venous sinus connecting between the right atrium and the right superior caval vein. The primary atrial septum is a derivative of the left-programmed atrial myocardium. Although *Sox4* mutant mice do demonstrate an atrial septal defect, the defect appears to lie with either the development of this structure, possibly as a consequence of defective mesenchyme, and/or with the developmental delay. This is dissimilar to the severe ASD observed in mutants which exhibit right atrial isomerism such as *Pitx2* (Gage *et. al.* 1999; Kitamura *et. al.* 1999; Lin, C R *et. al.* 1999) and *Cited2* (Bamforth *et. al.* 2004; MacDonald *et. al.* 2008; Weninger *et. al.* 2005). In these mutants, the primary septum is either absent or does not develop correctly, with E15.5 embryos demonstrating a large primary atrial septal defect. Other aspects of correct patterning of the heart would be more prominent at later stages of heart development, for example, the right atrium develops significantly more pectinate muscle than the left atrium. Furthermore, extracardiac isomerism often occurs in parallel with cardiac isomerism since the entire embryo may be affected by bilateral right or left sidedness. Sidedness is reflected by the spleen, pancreas, stomach and other regions of the gut. Right atrial isomerism is usually accompanied by a loss of splenic tissue (asplenia); while embryos with left atrial isomerism also demonstrate polysplenia (additional splenic tissue). Pulmonary isomerism has been found to

accompany cardiac isomerism such that in cases of right isomerism, the lungs develop symmetrically, rather than four lobes on the right and one on the left. Thus, in addition to the heart, left-right positional information is reflected by other visceral organs. Although this was not examined in *Sox4* mutant embryos in this study, further examination of the data obtained by MRI of E14.5 embryos (obtained by Bogani *et.al.*) may assist in determining whether the $Sox4^{ENU}$ allele alters the positional information of other organs.

Mutations to the *Scrib* gene in the *Circletail* (*Crc*) mouse mutant , and the *Vangl2* gene in the *loop-tail* (*Lp*) mutant (Kibar *et. al.* 2001; Murdoch *et. al.* 2001) exert their biological effect by disruption to planar cell polarity (PCP) signalling. In control embryos, Scrib and Vangl2 both function at the cell membrane and are involved in cell-cell adhesion. At the cellular level mutation in *Scrib* relocates N-cadherin from the cell surface of cardiomyocytes to the cytoplasm, thereby disrupting cellular polarity and cell-cell adhesion (Phillips *et. al.* 2007). One aspect of the *Crc/Crc* and *Lp/Lp* mutant phenotypes is inadequate cardiac looping (Henderson *et. al.* 2001; Phillips *et. al.* 2007). While the initial rightward looping of the heart tube occurs, looping does not progress adequately beyond this conformation. Interestingly, mutation of *Scrib* does not inhibit regional specification of cardiomyocytes within the heart, since the expression of cardiac markers is normal. Yet by E13.5, some *Crc/Crc* hearts demonstrate a thin ventricular wall and minimal myocardial compaction compared with control embryos. DORV and OFT septation defects are also observed. Therefore, altering cell polarity and cell-cell contacts of cardiomyocytes can alter looping and result in defects that are similar to those found in *Sox4* mutants. Thus a disruption to looping may explain the *Sox4* mutant phenotype, although the specific cellular requirement for Sox4 is unclear.

Early trabeculation is abnormal in Sox4 mutant hearts.

Histological analysis of *Sox4* mutant hearts reveals that cardiac development in homozygotes is variable between embryos. As a component of this, a ventricular phenotype is evident in sections at E9.5 (Figure 3.9). At E9.5 myocardium at the outer curvature of the heart wall is programmed to develop into ventricular myocardium, which then diverges into two cell fates – compact or trabecular

myocardium. This process is highly dependent upon signalling, and establishing contact points with the endocardial cells lining the lumen of the heart (Icardo *et. al.* 1987). Even the least severe *Sox4* mutant E9.5 ventricles demonstrate a defect in the formation of trabeculae. In the least severe mutants, trabecular myocardium is constructed, but trabeculae appear to lack a cellular base where they join to the compact myocardium (Figure 3.9). In the more severe mutants the transformation of myocardium to trabeculae does not appear to take place, despite the endocardium having established contact points with the myocardium. This suggests that the defect resides in either: (1) the response of the myocardium to endocardial signals; or (2) the response of the endocardium to myocardial signals; or (3) proliferation of the cells that give rise to the trabeculae. Given the differing degree of developmental delay in mutant embryos, it is possible that the necessary signalling pathways for this early stage of ventricular development are not appropriately activated.

Several signalling pathways are known to be required for trabecular formation in ventricular maturation (section 1.3.2 and references therein). Neuregulin-1 (NRG1) signalling, through the ErbB2 and B4 receptors is critical for trabeculation of ventricles. NRG1 is expressed in the endocardium while components of its receptor are expressed on myocardial cells. Signalling through this pathway promotes proliferation of myocardial cells and their differentiation into trabecular myocardium. Abolishing NRG1, ErbB2 or ErbB4 ablates this process. Other signalling molecules are known to be involved in trabecular formation, including Bmp10 (Chen, H *et. al.* 2004) and Notch1/Delta1/Delta4 (Grego-Bessa *et. al.* 2007), and mutations in these pathways results in specific ventricular dysmorphology. To examine these processes in *Sox4* mutant embryos, analysis could be conducted by immunohistochemistry or by quantitative PCR to examine levels and distribution of these regulatory factors. These factors are expressed, as might be expected, in ventricular endocardium and myocardium, and therefore exert their function locally on cardiomyocyte proliferation or differentiation. Since some *Sox4* mutant embryos (from class-I) are able to form trabeculae at this stage, it may be that *Sox4* is important for creating a balance between the proliferation and differentiation of the myocardium in this process.

Interestingly, myocardial inactivation of *Hand1*, combined with and without heterozygous inactivation of *Hand2*, results in a phenotype at E9 whereby looping morphogenesis is abnormal and trabecular myocardium is poorly formed (McFadden *et. al.* 2005). This is similar to the delayed E9.5 phenotype observed in $Sox4^{ENU/ENU}$ $Foxq1^{sa/sa}$ mutants (Figure 3.8 and 3.9). While Hand1 is also a marker of the first heart field (FHF), it has been associated with proliferation of myocardium in the developing heart. The role of Hand1 in cell cycle progression has been described showing it to be a key regulator of the balance between proliferation and differentiation of cardiomyocytes (Martindill *et. al.* 2007; Risebro *et. al.* 2006). This role in the developing heart is cell-autonomous since overexpression of *Hand1* in *Hand1*-expressing cells results in enhanced proliferation both *in vivo* and *in vitro* (Risebro *et. al.* 2006). The phenotype of complete embryonic ablation of either *Hand1* (Riley *et. al.* 1998) or *Hand2* (Srivastava *et. al.* 1997) results in far more severe abnormalities and early embryonic lethality. Thus the overlap in phenotype of conditional removal of *Hand1* and haploinsufficient *Hand2* does not suggest that Sox4 function resides in the general regulation of either factor, rather it may be possible that the function of Sox4 in the heart acts in pathways that contribute to the regulation of proliferation in the early heart. However, the absence of *Sox4* expression in the ventricular chambers (ahead, in section 4.2.2) suggests that if it acts on proliferation, it acts indirectly. The precise mechanism by which this occurs would require knowledge of the localisation of the Sox4 protein, as well as its ability to interact with other proteins and downstream target genes.

IS THIS PHENOTYPE EVIDENCE FOR A GENETIC INTERACTION BETWEEN THE *SOX4* ALLELE AND *FOXQ1*?

Aside from the cardiac phenotype, results presented in this chapter reveal an interesting possibility – that there is a genetic interaction between *Sox4* and *Foxq1*. The *satin* homozygous phenotype has been well studied, and anterior dysmorphologies have not been reported, nor were any deviations from the expected Mendelian ratio stated for heterozygous crosses of the *satin* allele (Hong *et. al.* 2001). Likewise, the study of the *Sox4* null, did not detail a craniofacial phenotype (Schilham *et. al.* 1996; Ya *et. al.* 1998b), although it was implied to be present, yet mild, in a later study of the role of *Sox4* in development of the CNS (Cheung *et. al.* 2000). In contrast, more recently, the phenotype of a $Foxq1^{-/-}$ targeted null mutation has been reported (Goering *et. al.* 2008). Embryonic lethality was reported to be present only on a C57BL/6J x 129/Sv hybrid background. Lethality was not fully penetrant in heterozygous crosses, with 15% (rather than the expected 25%) of homozygotes present at birth, exhibiting the *Satin* phenotype upon hair shaft differentiation. Homozygous $Foxq1^{-/-}$ intercrosses to determine the timing of embryonic lethality revealed that only 44% of the expected number of embryos remained at E15.5. The loss of homozygotes was greatest between E10.5 and E12.5 (from 85% to 69%). At E10.5, a proportion of homozygotes were observed to have abnormal forebrain development. The research did not reveal the cause of lethality in these embryos (since forebrain deformities may still be observed in embryos that complete gestation). Importantly, the heart was morphologically normal and therefore cannot explain this lethality.

Further evidence for a genetic interaction between *satin* and another loci within the *Del(13)Svea36H* deleted region was obtained by Dr. Catherine Willoughby (Willoughby 2006), PhD thesis. It was found that some embryos (12/46) in a cross of *satin* homozygotes to mice heterozygous for the *Del(13)Svea36H* chromosome demonstrated a mild forebrain phenotype. Embryos were thus hemizygous for the *satin* allele and the region surrounding on chromosome 13, including the *Sox4* locus. These embyos are null for one *Foxq1* allele, while the second allele carries the *satin* mutation. Crossing to the deletion also causes haploinsufficiency of *Sox4*, although

the remaining allele is wild type. This experiment indicates that neighbouring loci (that is, those included in the *Del(13)Svea36H* deletion) may modify the *Foxq1* phenotype. Both the hemizygous *satin* phenotype and homozygous *Foxq1* null overlaps with the non-cardiac E9.5-E10.5 forebrain phenotype observed with the $Sox4^{ENU/ENU}$ $Foxq1^{sa/sa}$ mutant presented in this chapter, from the class-I and class-II phenotypes (Figure 3.8).

Since homozygous loss of function of *Foxq1* is common between the $Sox4^{ENU/ENU}$ $Foxq1^{sa/sa}$ and *satin/ Del(13)Svea36H* hemizygous mutants, it could be considered that *Sox4* is a candidate modifier of the *Foxq1* locus. The alternative explanation, that there exists an additional unidentified ENU-induced mutation, closely linked to both $Sox4^{ENU}$ and *satin,* has been ruled out, as discussed in chapter 1 (section 1.4.3).

3.4 SUMMARY: PHENOTYPE OF *Sox4*$^{ENU/ENU}$ *Foxq1*$^{sa/sa}$ EMBRYOS.

Examination of the phenotype of *Sox4*$^{ENU/ENU}$ *Foxq1*$^{sa/sa}$ embryos has enabled identification and characterisation of the early cardiac phenotype which gives rise to the ultimate lethal phenotype. By studying E9.5 embryos to determine the basis of the cardiac phenotype, we have also uncovered that the Sox4 defect is variable and can be grouped into three classes visible in wholemount. By conducting this analysis we have provided a possibility for the deficit in the Mendelian ratio observed in both the study of the null allele and this work at E11.5-E13.5. By analysis of the phenotype, we have provided new possibilities for the function of Sox4 although the precise nature of this remains to be elucidated by considerable further experimentation. This analysis of the phenotype enables us to determine at which stages of development Sox4 is required, and now provides a basis to explore the molecular mechanisms by which a Sox4 deficiency leads to cardiac malformations. Since it is apparent that there is a genetic interaction between *Sox4* and *Foxq1*, segregation of the two alleles will enable a study of the *Sox4* allele in isolation from *satin.*

CHAPTER 4: EXPRESSION OF *SOX4* AND *FOXQ1* DURING MOUSE EMBRYOGENESIS

4.1 INTRODUCTION

Little is known about the expression of *Sox4* and *Foxq1* during development. Determining the spatio-temporal expression pattern of *Sox4* and *Foxq1* is necessary for an understanding of the phenotype documented in Chapter 3. Limited documentation is available on the expression of *Sox4* during cardiogenesis. In chick, *Sox4* positive cells were found in the endocardial cushions of the atrioventricular canal and endocardial ridges of the outflow tract, at Hamburger and Hamilton (HH) stages 20-27 (approximately equivalent to E11.5-E13.5 in mouse) (Maschhoff *et. al.* 2003). In mouse, the E14.5 lethality observed in the *Sox4* null is attributed to a lack of *Sox4* expression at E13.5 in the endocardial ridges of the outflow tract and endocardial cushions of the atrioventricular septum (Schilham *et. al.* 1996). Since the process of valve formation begins several days prior to E13.5, and cellular patterning precedes the formation, it is difficult to reconcile the published phenotype with such a late underlying developmental cause; that is, a lack of *Sox4* expression at E13.5. In order to establish how disruption to *Sox4* causes the published phenotype (Schilham *et. al.* 1996) and the $Sox4^{ENU/ENU}$ $Foxq1^{sa/sa}$ phenotype (chapter 3), it is necessary to describe *Sox4* expression from a much earlier point in time, and in greater detail at the stages in which a phenotype develops.

Embryonic expression of *Foxq1* in *Xenopus* has been described (Choi *et. al.* 2006). During development, expression domains in *Xenopus* embryos include the pharyngeal pouches, gastrointestinal tract and tongue. Examination of adult human tissue revealed *FOXQ1* expression in the stomach, trachea, bladder and salivary gland, and cell line carcinomas of the colon and lung (Bieller *et. al.* 2001). Additionally, low expression of *FOXQ1* was detected in the adult lung and in both adult and embryonic kidney (Bieller *et. al.* 2001). Limited adult mouse expression

analysis has shown *Foxq1* to be expressed in the liver, kidney, lung, brain, testis, stomach and hair follicle (Frank *et. al.* 1998; Hong *et. al.* 2001). *Foxq1* transcripts were detected in whole embryo extracts from E10.5 to birth, yet the precise wholemount spatio-temporal domains have not been described for *Foxq1* in mouse embryogenesis.

The lack of detail of the published expression domains of *Sox4* and *Foxq1*, and the necessity for knowledge of the expression domains to describe the phenotype presented in this thesis thus forms the basis of this chapter, with the aim: *To characterise the expression of Sox4 and Foxq1 during mouse embryogenesis by in situ hybridisation.*

This chapter focuses primarily on documenting sites of *Sox4* expression from pre-gastrulation (E6.0) to E12.5. *Sox4* expression was examined by wholemount *in situ* hybridisation to embryos, followed by cryosection to examine expression domains in greater detail. To examine the expression in the developing heart from E10.5, where probe penetration was considered to be a problem, analysis was conducted by section *in situ* hybridisation. Knowledge of this expression will help to resolve how mutation in *Sox4* (and thus disruption to expression) could cause and perpetuate a visible phenotype from E9.5. It is pertinent to know where *Foxq1* is expressed, since the *satin* allele appears to influence aspects of the $Sox4^{ENU/ENU}$ $Foxq1^{sa/sa}$ phenotype. Thus some expression domains of *Foxq1* from E7 to E12.5 are also reported in this chapter.

4.2 RESULTS

4.2.1 Embryonic *Sox4* expression during early mouse development

Prior to gastrulation, expression of *Sox4* is observed throughout the epiblast (Figure 4.1a). Examination of the level of expression in an early-streak stage embryo revealed that the *Sox4* transcript is not uniform across the epiblast. Rather, embryos demonstrate a mosaic pattern of expression, which appears to be stronger in the ectoderm adjacent to the streak (Figure 4.1b). As gastrulation proceeds, the epiblast retains expression of *Sox4* and the definitive endoderm becomes a second embryonic expression domain (Figure 4.1c and d).

In headfold to early somitogenesis stage embryos, *Sox4* is detected in derivatives of all three germ layers. Expression is most striking in the involuting foregut endoderm (Figure 4.2 a, c and section b). This endoderm is adjacent to the cardiogenic mesoderm of the cardiac crescent, and the lateral mesoderm of the SHF. Sagittal sections demonstrate robust *Sox4* expression in the endoderm, predominantly at the foregut (Figure 4.2 b), but also posterior to the node in the prospective hindgut (data not shown, evident in wholemount Figure 4.2a). During early somitogenesis, *Sox4* expression continues in the epiblast adjacent to the primitive streak (Figure 4.2d). Anterior neural ectoderm and head mesenchyme also demonstrates low expression at this stage (Figure 4.2 b).

At E8.5 (approximately 10-somite stage) embryos reveal an increase in *Sox4* gene expression within neural ectoderm (Figure 4.3a and sections e to i). In a dorsal view of the whole embryo, particularly strong expression is observed in the hindbrain region (Figure 4.3a and b). This dorsal view also shows equally strong expression in posterior neural ectoderm adjacent to the primitive streak (Figure 4.3b and i). Sections through the neural folds of the anterior neural ectoderm reveal that *Sox4* expression appears mosaic in both the ectoderm and head mesenchyme, (Figure 4.3e, f, g and h). Expression is also apparent in cells immediately beneath the surface ectoderm, possibly corresponding to neural crest (Figure 4.3 e and f). Intense staining of a 6-somite stage embryo reveals that *Sox4* expression is undetectable by

these methods in the heart tube (Figure 4.3j) but present in the somitic mesoderm (Figure 4.3k).

To summarise, during development *Sox4* demonstrates a complex expression pattern from the earliest stages. Expression is evident in derivatives of all three germ layers although it is elevated in the endoderm, with notable expression also in the ectoderm of the neural plate. Sox4 may also function in the patterning of somites where it is expressed highly. Although it is expressed in endoderm adjacent to the heart, *Sox4* expression was not observed in the heart itself at these stages.

4.2.2 *Sox4* expression is highly restricted adjacent to and in cardiac tissues during development

The first observation of *Sox4* expression in mesoderm adjacent to cardiomyogenic tissue is during early somitogenesis (embryo shown has about 4 somites) (Figure 4.2d sections in e and f). In transverse sections through an embryo at this stage, *Sox4* transcripts appear in the mesoderm posterior to the cardiac crescent. This expression is at the junction where mesoderm divides into either splanchnic (ventral) or somatic (dorsal) mesoderm. The *Sox4* expression domain extends towards splanchnic mesoderm (Figure 4.2e and f). This region of cardiogenic mesoderm is adjacent to the region which contributes to the SHF - in contrast to anterior regions of the cardiac crescent, which contribute predominantly to the primary heart field (Chapter 1; section 1.3.1).

The mesodermal domain of expression is also present in an embryo with 10 somites. *Sox4* is expressed in mesoderm immediately posterior to the heart tube (Figure 4.3d, g and h). This expression appears to be continuous with the ventral pericardial mesenchyme, which is an additional site of *Sox4* expression at this stage (Figure 4.3f). Expression is not observed by *in situ* hybridisation in the heart tube at this stage, even when embryos are stained for long periods of time (Figure 4.3j).

By E9.5 cardiac expression appears in the endocardium of the outflow tract and atrioventricular canal, with expression apparent in embryos hybridised both in wholemount (Figure 4.4c and d) and in section (Figure 4.5a and d), to eliminate trapping as a possible source of false positive results and inadequate probe

penetration as a source of false negative results. Neither the control embryo for wholemount analysis, nor control slide for section analysis demonstrated sense probe binding (Figure 4.4a and Figure 4.5b). It appears that *Sox4* expression is certainly excluded from the myocardium and endocardium of the ventricles and atria. Clear expression of a marker of left ventricular myocardium, *eHand*, is detectable in an adjacent section (Figure 4.5c).

Expression domains in the AVC and OFT continue into the E10.5 stage (Figure 4.4e). Section *in situ* analysis from early E10.5 stage embryos reveals specific expression in the endocardium and nascent mesenchyme of the AVC (Figure 4.5e). These expression domains are continuous in sections from more developed E10.5, in which the inferior and superior atrioventricular cushions are more densely populated, than the earlier stage, with mesenchyme that expresses *Sox4* (Figure 4.5f and g). At the level of the OFT, expression is observed with the endocardium (Figue 4.5h and i). This localisation was confirmed by marker analysis of *Nfatc1* in an adjacent section (Figure 4.5i compared with *Nfatc1* in j). At this stage there is limited *Sox4*-expressing mesenchyme evident in these regions of the OFT and it is not possible here to distinguish between NCC-derived and endocardial-derived mesenchyme, without double *in situ* hybridisation analysis with *Sox4* and a marker for either NCC or endocardial-derived mesenchyme. At the level of the aortic sac, strong expression of *Sox4* is observed in the pharyngeal mesenchyme, foregut and endocardium, as well as the dorsal wall of the aortic sac (Figure 4.5k). Three-dimensional examination of the expression of *Sox4*, by optical projection tomography (OPT) of E10.5 embryos, further supported these results: That the only cardiac expression domains of *Sox4* are within the AVC and OFT endocardium and mesenchyme (data not shown). Expression is remains absent from the myocardium and endocardium of both atria and ventricles, as well as the non-chamber myocardium of the AVC and OFT.

At E11.5, expression of *Sox4* is retained in the endocardium and mesenchyme of the atrioventricular cushion, which is continuous *via* the vestibular spine with the expression in the mesenchymal cap on the developing atrial septum (Figure 4.6a and b). *Sox4* expression did not extend into the adjacent myocardium of the AVC, which

is marked by expression of *Bmp2* (Figure 4.6c). Expression of *Sox4* was further not detected in the atria or ventricles, including the ventricular trabeculae. At the level of the OFT, strong expression was evident in the endocardium and weak expression in the mesenchyme, yet no expression was observed in the adjacent myocardium (Figure 4.6d).

By E12.5, expression in the atrioventricular cushion mesenchyme is less prominent than in the outer regions from which the tricuspid and mitral valve leaflets develop (Figure 4.6e). The outer myocardial side of the primitive valve also showed expression (Figure 4.6f). Expression is absent from myocardial structures including the ventricles and trabeculae, as well as the atria and atrial septum. At the level of the OFT, strong expression is observed in the mesenchyme of the atrioventricular cushion at the anterior region of the ventricular septum (Figure 4.6g). Expression is further observed in both pulmonary and aortic endocardial ridges at E12.5 by section *in situ* analysis (Figure 4.6g and h for pulmonary endocardial ridges and data not shown for aortic endocardial ridges).

In summary, *Sox4* is initially expressed transiently in mesoderm adjacent to the splanchnic mesoderm of the SHF between the stages of cardiac crescent and linear heart-tube. In later stages of heart development expression is observed in the endocardium and endocardial-derived mesenchyme of the AVC and OFT from E9.5 to E11.5. By E11.5, this mesenchymal expression also includes the mesenchymal cap of the atrial septum. In the E12.5 heart, *Sox4* expression appears stronger in the presumptive leaflets of the developing mitral and tricuspid valves than in the atrioventricular cushion itself. In the OFT, expression is observed in the endocardium and mesenchyme of the endocardial ridges of both the pulmonary trunk and the aorta. Thus *Sox4* demonstrates an expression pattern which demonstrates continuity between developmental stages of the heart, implicating possible roles for the Sox4 protein in early cardiogenesis, and later in valve development and septation.

Figure 4.1: Sox4 expression is observed in early embryonic development from E6.5 to E7.5. Lateral view of Sox4 expression in embryos during early gastrulation stages. (A) Sox4 is expressed throughout the epiblast at the pre-streak (E6.0) stage; (B) By early-streak (E6.5) stages Sox4 is expression is revealed as mosaic across the epiblast, with stronger expression at the primitive streak (arrow); (C) By the late-bud stage, expression of Sox4 is retained through the epiblast but stronger expression appears at the anterior primitive-streak (arrow); (D) Sagittal section through a late-bud stage embryo demonstrates expression of Sox4 in the epiblast with stronger expression in the emerging definitive endoderm (arrow). At this stage of E7.5, clusters of cells in the ectoplacental cone demonstrate Sox4 expression (arrowhead, C and D). Brackets indicate the embryonic region distal to extraembryonic lineages.

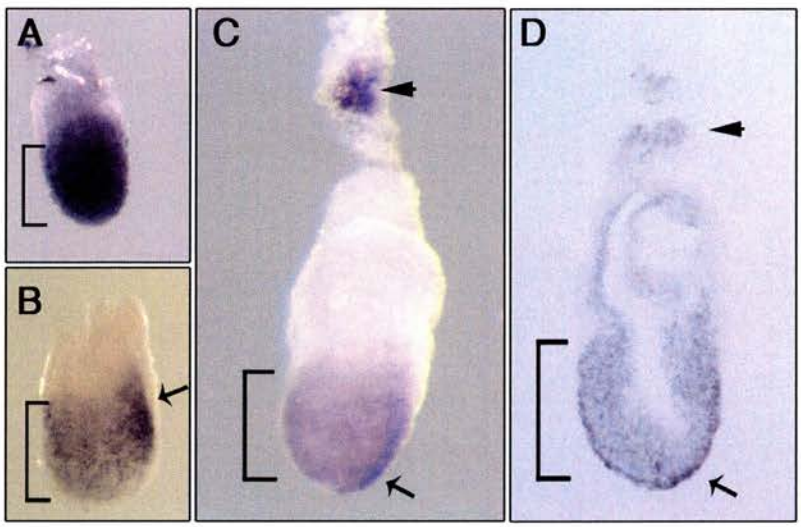
A
B
C
D

Figure 4.2: Sox4 is expressed during the late headfold stage and early somitogenesis. (A) Lateral view of an embryo with 2-3 somites. Robust expression is viewed in the endoderm of the foregut (arrow) and endoderm adjacent to the streak. Bracket indicates region of section enlarged in (B). (B) Sagittal section through the embryo in (A) revealing strong expression in the foregut endoderm and weak expression in the head mesenchyme and adjacent neurectoderm. (C) Frontal view of a late headfold stage embryo expressing Sox4 in the definitive endoderm and foregut (arrows). (D) An embryo with 4-5 somites reveals striking expression in both the foregut (arrow) and in posterior ectoderm adjacent to the streak (arrowhead). (E and F) Transverse section through the embryo shown in (D) as indicated, viewed by light microscopy with (E) and without (F) a white background to the section. Expression is revealed in the endoderm, with a low level of expression in the neurectoderm and head mesenchyme. Expression is also revealed, in this plane, in lateral mesoderm (white arrowhead). Abbreviations: hm, head mesenchyme; fge, foregut endoderm; ne, neurectoderm.

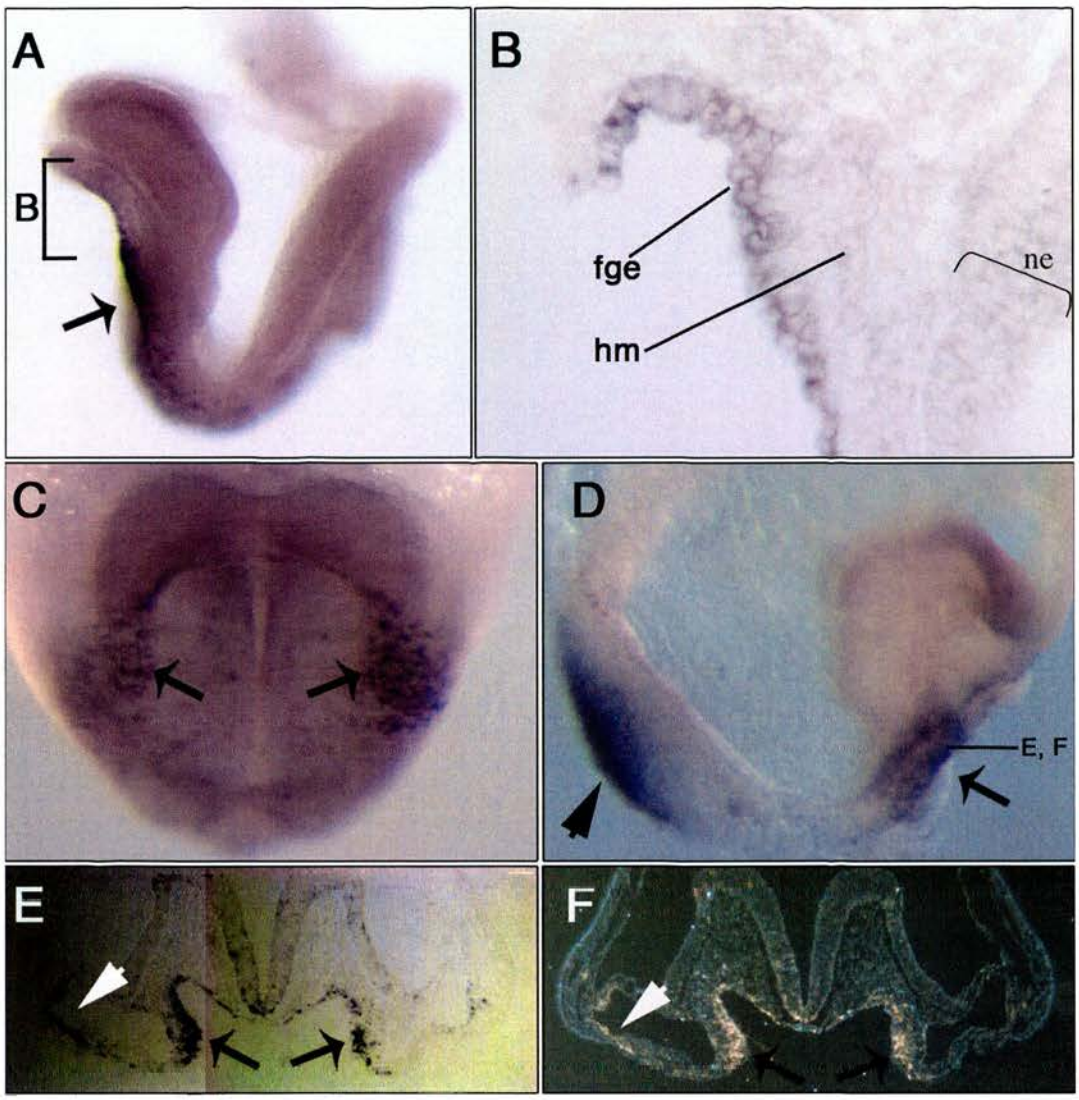
A
B
B
fge
hm
ne
C
D
E, F
E
F

Figure 4.3: Sox4 expression during early somitogenesis E8-8.5. An embryo with 10 somites demonstrates robust Sox4 expression in numerous domains (A-I). (A) Right lateral and (B) dorsal view reveals Sox4 expression in neural ectoderm (arrowhead). Expression in alternate rhombomeres of the hindbrain is marked with a bracket. Particularly strong expression is observed in the anterior neural folds. (C) Frontal view reveals expression in the anterior intestinal portal and a domain of mesoderm posterior to the heart. The heart does not demonstrate Sox4 expression at this stage. The region enlarged in (D) demonstrates these domains more clearly (endoderm, black arrowheads; mesoderm, white arrowhead). Additionally expression is revealed in nascent somties (black arrow). Sox4 expression is emphasised in cryo-sections of the same embryo (E-I) as indicated in (C). Expression is present in the neurectoderm (E-I) ventral foregut (E-G), anterior intestinal portal (black arrows, H) and below the surface ectoderm in some regions (black arrow E). Expression is not detected at any level in the dorsal mesocardium, or endocardium and myocardium of the developing heart at this stage. Mesodermal expression is shown at the base of the heart (white arrowhead H and G) and this appears to be continuous with the pericardial mesenchyme (F) but only at posterior regions (absent in E, white arrowhead). (J) An overstained embryo with 8 somites demonstrates strong expression of Sox4 in the neurectoderm and foregut. Expression appears absent from the heart tube (arrowhead) although expression is detected in the region of the septum transversum mesenchyme (black arrow). Expression in somites is emphasised in (K). Abbreviations: anf, anterior neural folds; hb, hindbrain; dm, dorsal mesocardium; ec, endocardium; mc, myocardium; ne, neurectoderm; nt, neural tube; fg, foregut.

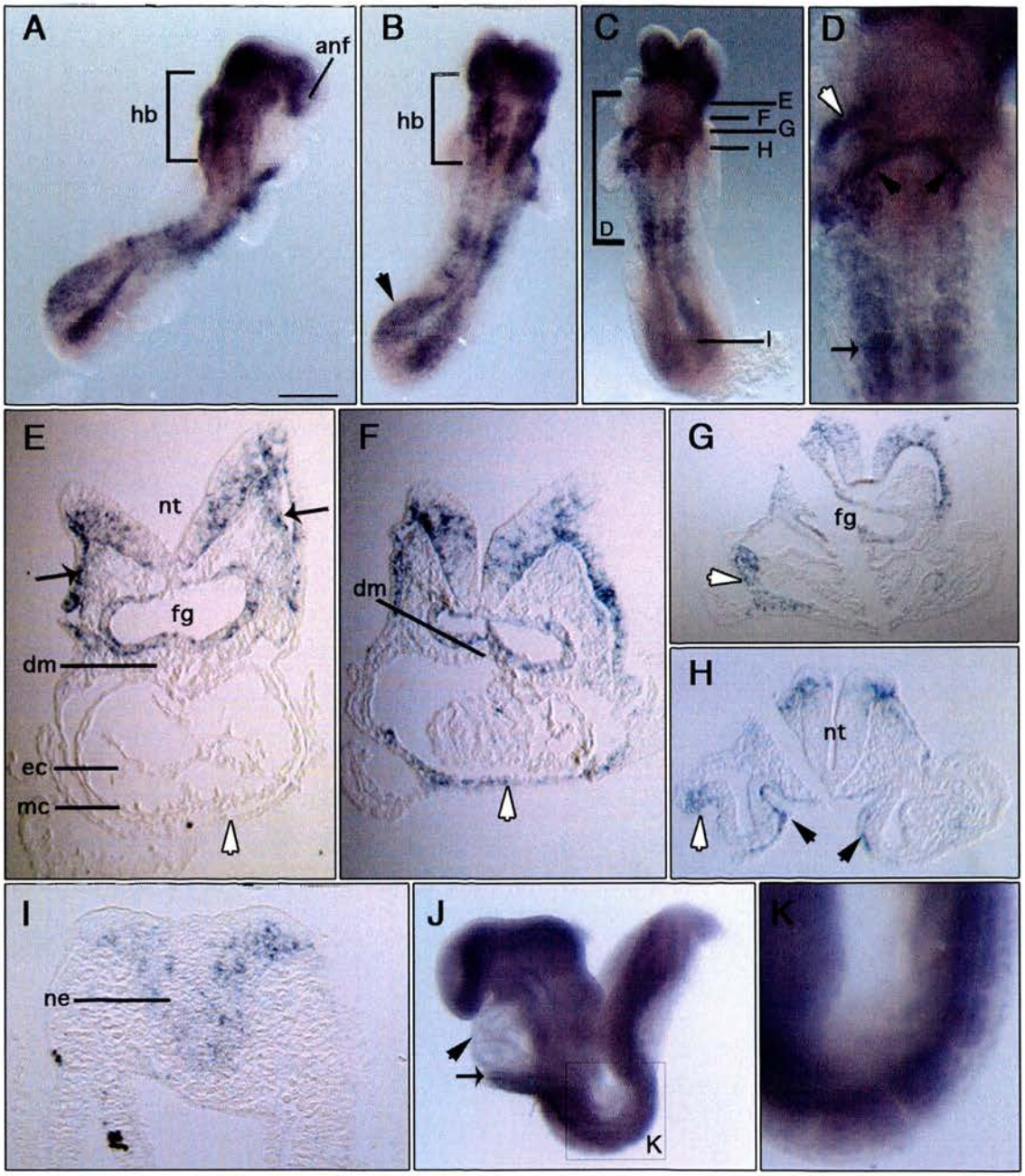
A
anf
hb
B
hb
C
E
F
G
H
D
I
D
E
nt
fg
dm
ec
mc
F
dm
G
fg
H
nt
I
ne
J
K
K

Figure 4.4: Expression domains of Sox4 in whole embryos staged E9.5 to E10.5. Sox4 transcripts are detected at multiple sites at E9.5 (B-D, sections J, K) and E10.5 (E-I, L-N), while no signal is detected with the sense probe for Sox4 (A). (B) Left lateral view of an E9.5 embryo reveals strong expression in the neural tube, particularly in the forebrain and midbrain. Expression is detected in the region of the olfactory placode (white bracket). Less expression is detected in the hindbrain (black arrow marks midbrain-hindbrain boundary). Expression appears intersomitic between the more rostral somites, while caudal somites appear to express Sox4 (black arrows). Within the E9.5 heart, Sox4 is detected in the atrioventricular canal (AVC, in C) and outflow tract (OFT, in D). (E) In the E10.5 heart Sox4 is expressed in the AVC and OFT, with strong expression also detected in the first and second pharyngeal arches (labelled I and II, in E, F, G, H). (F-G) Left lateral view of E10.5 embryos demonstrating expression of Sox4 in the neural tube, with strong expression detected in the forebrain telencephalon (Tel) and midbrain (MB); Expression is detected in the olfactory placode (marked with bracket in F) and the cleft between the mandibular and maxillary regions of the first pharyngeal arch of the craniofacial region (CF); The foregut endoderm (E) is another site of Sox4 expression; Sox4 is also expressed in the posterior region of the forelimb bud (arrow in F and G) and in the hindlimb bud. (H) Closer examination of the embryo in (G) reveals the extent of the wholemount craniofacial expression domains. (I) Along the axis, expression is observed in the dorsal- and ventral-most (dS and vS) regions of the interlimb somites, and also in the dorsal root ganglia (DRG). (J) Section through the neural tube of the embryo in (B) reveals expression in the dermomyotome. (K) Section through the neural tube at the level of the hindbrain reveals expression of Sox4 in cells of the dorsal neural tube and in cells beneath the surface ectoderm. (L) Dorsal view of an E10.5 embryo reveals expression along the length of the neural tube (arrow). (L)-(M) Sox4 is differentially expressed within recently formed somites (M) and between trunk somites (N), although expression is not detected in the tail bud (M). Abbreviations: I, first pharyngeal arch; II, second pharyngeal arch; avc, atrioventricular canal; CF, craniofacial region; DRG, dorsal root ganglia; E, endoderm; fg, foregut; lv, left ventricle; MB, midbrain; nt, neural tube; oft, outflow tract; som, somite; dS, dorsal somite; vS, ventral somite; Tel, telencephalon.

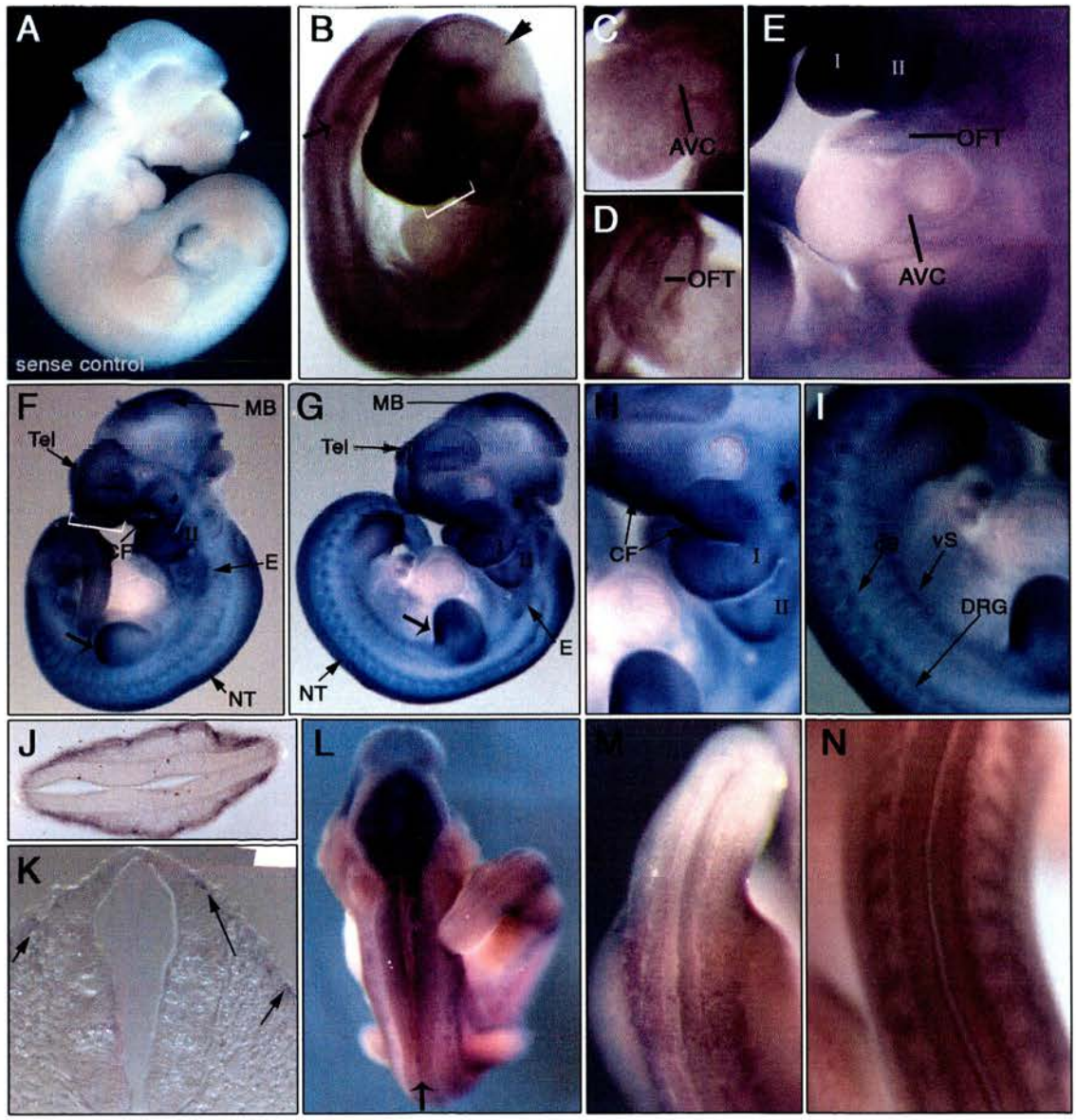
A
sense control
B
C
AVC
D
OFT
E
I
II
OFT
AVC
F
MB
Tel
CF
II
E
NT
G
MB
Tel
II
E
NT
H
CF
I
II
I
vS
DRG
J
K
L
M
N

Figure 4.5: Expression domains of Sox4 in the heart and adjacent regions, in sections of embryos staged E9.5 – E10.5. (A) At E9.5, section in situ hybridisation to Sox4 reveals that cardiac expression is observed in the endocardium of the atrioventricular canal (AVC); adjacent to the heart, the foregut endoderm (fg) is a site of strong Sox4 expression, and also the pharyngeal mesenchyme (arrows); at this level, expression is further detected in the neural tube (nt). (B) Transcript binding is not detected with the Sox4 sense probe by section in situ hybridisation. (C) In a section adjacent to that shown in (A), expression of a control transcript, eHand, is expressed in the outer curvature myocardium of the future left ventricle. (D) cryosection through the heart of an embryo stained for Sox4 expression in wholemount reveals expression in the endocardium of both the AVC and the outflow tract (OFT); expression is also shown in the endoderm of the foregut, pharyngeal mesenchyme beneath the surface ectoderm (arrows, in D); trunk somites (som) and the neural tube (nt) further demonstrate low detection of gene expression. (E) Early E10.5 stage embryos demonstrate cardiac expression of Sox4 in the endocardium and nascent mesenchyme of the atrioventricular canal (AVC, in E) but not in the adjacent non-chamber myocardium or in the cardiac chambers; expression continues from earlier stages in the foregut endoderm (fg), pharyngeal mesenchyme (arrows) and the neural tube (nt). (F-G) Expression of Sox4 in the E10.5 heart is detected in the endocardium and mesenchyme of the AVC but not elsewhere in the heart at this level of section. Adjacent to the heart, expression is detected in the foregut (fg, in F) and surrounding mesenchyme. (H-K) Gene expression at the level of the OFT shows Sox4 transcript present in the endocardium, but not adjacent myocardium (m, in H, I and K); this expression is consistent with expression of the endocardial marker Nfatc1 (shown in frame J); through the level of the aortic sac (AS), expression is strongly detected in the pharyngeal mesenchyme (arrows) and the foregut endoderm (fg), as well as the endocardium (labelled) but not myocardium (m) of the OFT. Abbreviations: as for previous figures, but also, a, atrium; as, aortic sac; m, myocardium; v, ventricle.

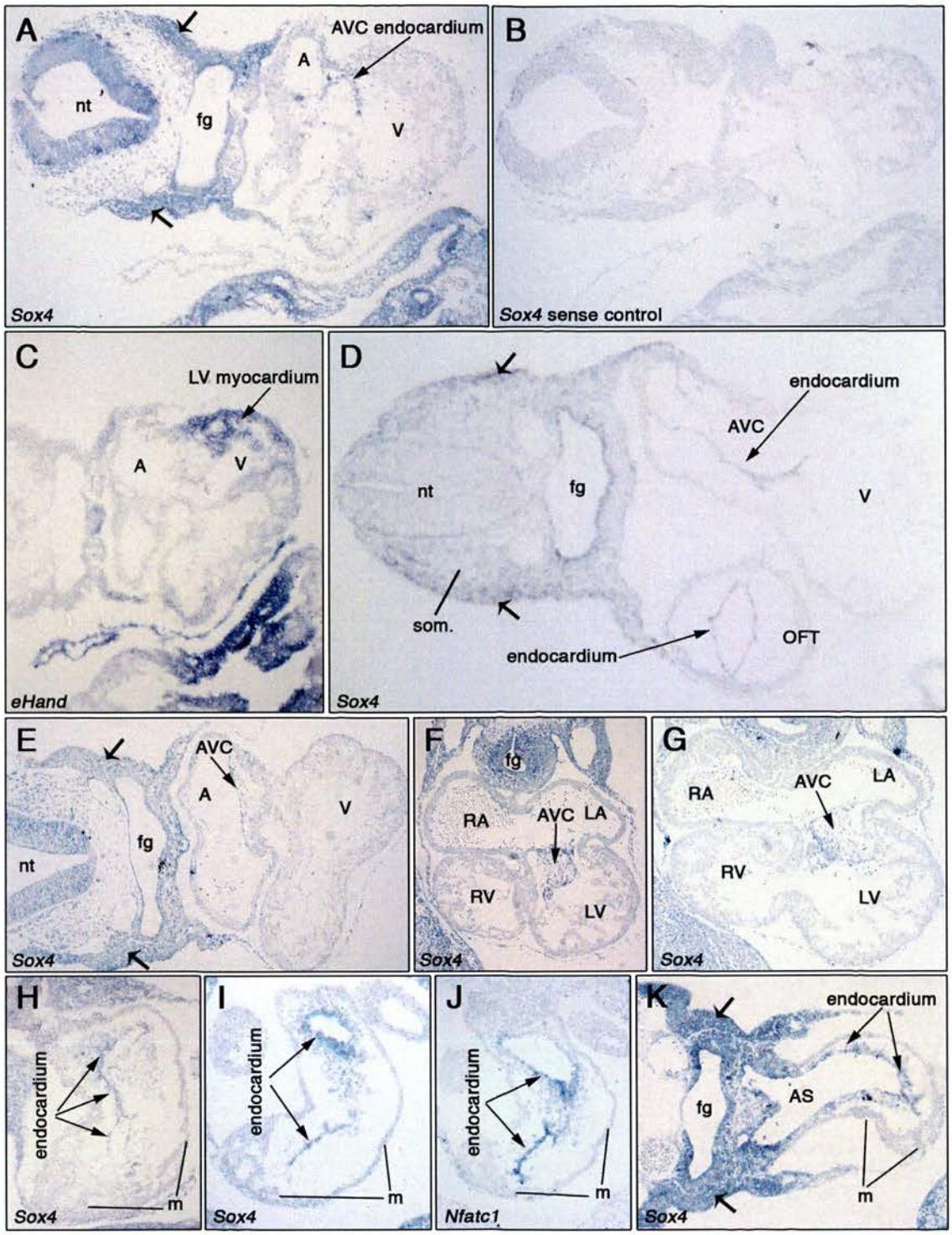
A
AVC endocardium
A
nt
fg
V
Sox4
B
Sox4 sense control
C
LV myocardium
A
V
eHand
D
endocardium
AVC
nt
fg
V
som.
endocardium
OFT
Sox4
E
AVC
A
V
fg
nt
Sox4
F
fg
RA
AVC
LA
RV
LV
Sox4
G
RA
AVC
LA
RV
LV
Sox4
H
endocardium
m
Sox4
I
endocardium
m
Sox4
J
endocardium
m
Nfatc1
K
endocardium
fg
AS
m
Sox4

Figure 4.6: Expression domains of Sox4 in sections through the heart of embryos staged E11.5-12.5. Transverse sections through an E11.5 embryo (A-D) stained to detect expression of Sox4 (A, B and D) and Bmp2 (C). (A, B) Expression of Sox4 is revealed in the mesenchyme of the atrioventricular cushion (AVC) and developing atrial septum (arrowhead). In an adjacent section, expression of Bmp2 was used to reveal the limits of the atrioventricular canal, since it labels non-chamber myocardium (arrowheads, C). (D) In the OFT of the E11.5 heart, expression is detected in the endocardium and mesenchyme of the developing OFT cushions, but not the adjacent myocardium; expression in the trachea (T) and esophagus (E) is also shown in this frame. (E-H) Frontal sections through an E12.5 heart shows low expression of Sox4 in the AVC, but strong expression in the regions of the developing tricuspid and mitral valves (TV and MV respectively, in F) between the atria and ventricles; at the level of the OFT, striking expression is revealed in the mesenchyme which contributes to both septation of the ventricles and the proximal OFT (arrowhead); expression is also detected in the endocardial ridges of the pulmonary trunk (ER in G, and H); outwith the heart, expression is detected in the trachea (T, in E and G). Abbreviations: as for previous figures, except for, A, aorta (in G); AS, atrial septum; AVC, atrioventricular cushion; E, esophagus; ER, endocardial ridges; MV, mitral valves; PT, pulmonary trunk; T, trachea; TV, tricuspid valves.

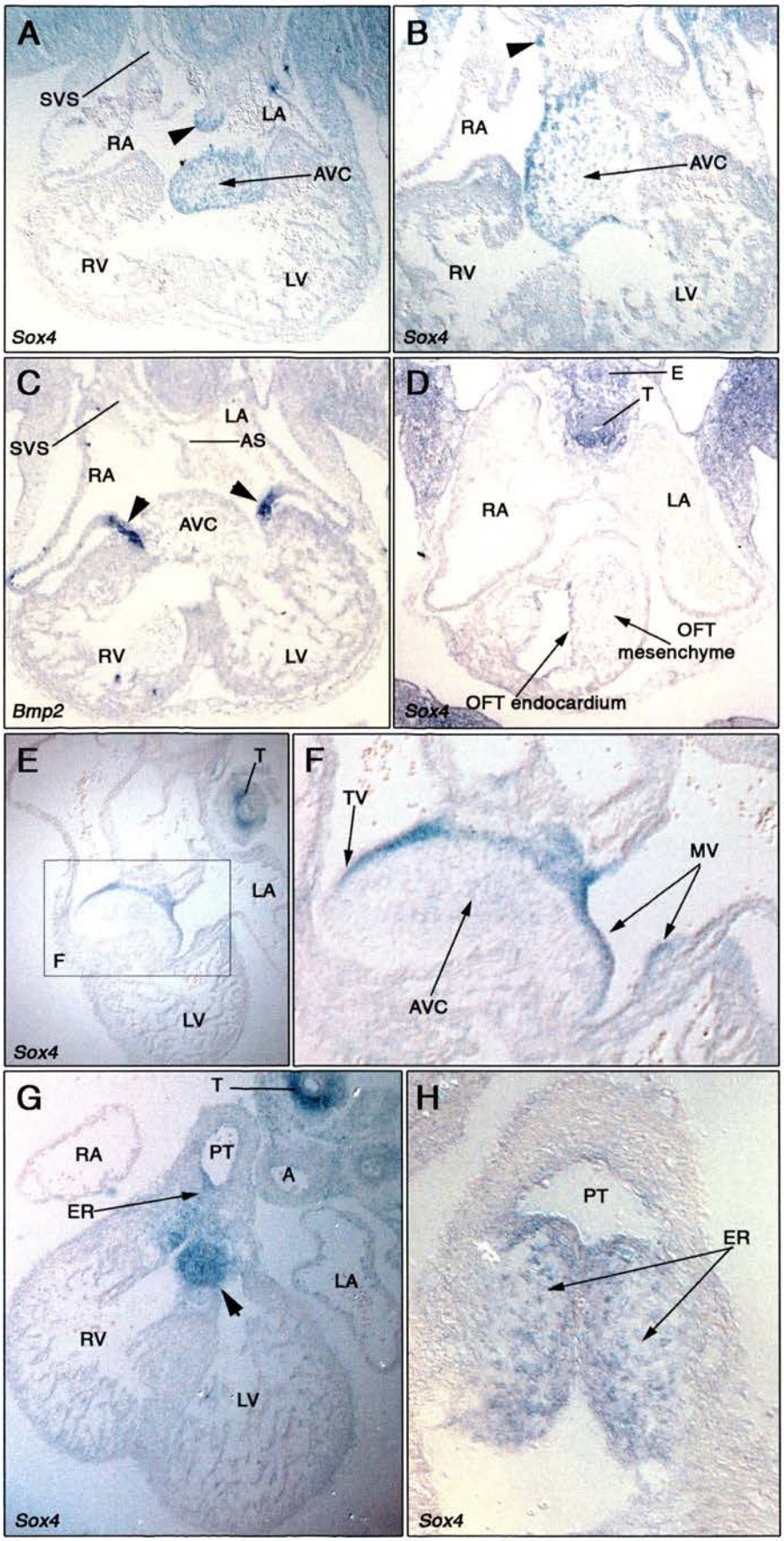
A
SVS
LA
RA
AVC
RV
LV
Sox4
B
RA
AVC
RV
LV
Sox4
C
SVS
LA
AS
RA
AVC
RV
LV
Bmp2
D
E
T
RA
LA
OFT
mesenchyme
OFT endocardium
Sox4
E
T
LA
F
LV
Sox4
F
TV
MV
AVC
G
T
RA
PT
A
ER
LA
RV
LV
Sox4
H
PT
ER
Sox4

4.2.3 There is widespread expression of *Sox4* in non-cardiac sites from mid gestation to late gestation

Sox4 expression is detected in many non-cardiac embryonic tissues from E9.5 to E12.5, although transcript levels vary.

From E9.5 to E12.5, *Sox4* is strongly expressed in the neural tube (E9.5, Figure 4.4b; E10.5, Figure 4.4f, g and j; E11.5, Figure 4.7a and d; E12.5, Figure 4.7e). In neural tissue, anterior regions of the forebrain and midbrain reveal elevated expression compared with more posterior neural tube. At E9.5, the transition from high to low expression at the midbrain-hindbrain junction is striking (Figure 4.4 b) while sections through the hindbrain reveal a domain of expression below the surface ectoderm at this level (Figure 4.4k). Strong expression continues in the forebrain and midbrain at E10.5 (Figure 4.4f and g), E11.5 (Figure 4.7a and d) and E12.5 (Figure 4.7e). Expression in the dorsal root ganglia (DRG) adjacent to the somites, is also evident from E10.5 (E10.5, Figure 4.4i; E11.5, Figure 4.7b; E12.5, Figure 4.7e). Closer examination of the dorsal neural tube reveals that *Sox4* is expressed in what may be delaminating neural crest (Figure 4.4k and m).

Expression of *Sox4* appears to be upregulated in more recently formed somites (E9.5, Figure 4.4b; E10.5, Figure 4.4l), where it may play a role in early somite patterning. Although elsewhere along the axis expression appears intersomitic (E9.5, Figure 4.4 b; E10.5, Figure 4.4m). *Sox4* expression is not observed in the tail bud (Figure 4.4l). At the level of the atrioventricular canal of the heart (Figure 4.5 d), expression of *Sox4* is apparent in the trunk somites with higher expression in lateral regions adjacent to the surface ectoderm. Sections through the thoracic region reveal expression just below the surface ectoderm, appearing to mark the dermomyotome (Figure 4.4j). Expression in the ventral-most and dorsal-most regions of trunk somites is evident between the fore- and hind- limb buds from E10.5 to E11.5 (E10.5, Figure 4.4i; E11.5 Figure 4.7 b and d).

Another site of *Sox4* expression is the foregut endoderm. In wholemount *in situ* hybridisation, expression is observed at E9.5 and E10.5, particularly in the ventral foregut adjacent to the developing heart (figure 4.4b, f and g). In sections,

expression is observed at E9.5 (Figure 4.5a and d) and E10.5 (Figure 4.5e, f and k). At E11.5, *in situ* to sections through whole embryos reveals strong expression of *Sox4* in the trachea, and also the esophagus, as well as the surrounding mesenchyme (Figure 4.6d). Expression in the trachea is also evident at E12.5 (Figure 4.6e and g).

Given the craniofacial phenotype of $Sox4^{ENU/ENU}$ $Foxq1^{sa/sa}$ embryos from E9.5 to E13.5, it is not surprising that *Sox4* is expressed in the developing craniofacial regions. At E9.5, transcript expression is observed in the olfactory placode and the branchial arches (Figure 4.4b). This is furthermore shown by section *in situ* hybridisation of regions adjacent to the heart where strong mesenchymal expression is detected (E9.5, Figure 4.5a; E10.5, Figure 4.5e and k). By E10.5, expression is still detected in the olfactory placode (Figure 4.4f). Strong expression is observed in the maxillary and mandibular regions of the first branchial arch (Figure 4.4f and h), while expression in the second arch is still evident (Figure 4.4e, f, g and h). Expression in the developing face is present at E11.5 (Figure 4.7a, c and d) and E12.5 (Figure 4.7e and f). Also from E12.5, expression is seen in or around the developing vibrissae follicles (Figure 4.7e and f) and the mammary glands (Figure 4.7e).

Expression of *Sox4* is detected in the developing limbs. At E9.5 expression is observed in the emerging forelimb bud (Figure 4.4b). E10.5 stage embryos demonstrate limb bud expression, with elevated expression in the superficial posterior region, possibly surface ectoderm (Figure 4.4 f and g). By E11.5 expression appears to be concentrated in the condensing mesenchyme of both limbs, as well as in a proximal domain in the region of the wrist (Figure 4.7a and d). The E12.5 limbs demonstrate strong expression of *Sox4* in the developing digits (Figure 4.7e).

To summarise, *Sox4* is expressed in numerous extra-cardiac sites during development. This includes sites which are known to regulate cardiac development. The hindbrain neural crest is a site from which cardiac neural crest originates. Additionally, it is known that the ventral foregut, a site of strong *Sox4* expression, provides inductive signals for heart development. However, not only is the foregut a source of signals for the heart, it also plays a key role in patterning other organs. A

number of sites which express *Sox4,* but are unlikely to impact on cardiogenesis include the craniofacial regions, somites, trunk neural crest and limb buds. These expression domains are novel findings and suggest novel roles of Sox4 in other organ systems.

4.2.4 *Sox4* demonstrates a novel expression pattern in the extraembryonic ectoderm that may correlate to trophoblast giant cells, not apoptotic cells.

Embryos staged E7-8.5 were dissected from the deciduas and examined for *Sox4* expression with extraembryonic membranes attached. *Sox4* is expressed in clusters of cells in the ectoplacental cone (Figure 4.1c and d; Figure 4.8a and b). This expression pattern resembles that of *placental-lactogen II* (*PL-II*), a marker of secondary trophoblast giant cells (TGC) (El-Hashash *et. al.* 2005).

Given the distinctive expression pattern of the *Sox4* transcript in what may be trophoblast-derived giant cells of the extraembryonic ectoderm, and the *in vitro* evidence that Sox4 attenuates the cytochrome c-dependent apoptotic pathway (Kim *et. al.* 2004), the question arose whether it is possible that *Sox4* marks distinct populations undergoing apoptosis. This was addressed using a wholemount protocol that reveals apoptotic cells. In E7-8.5 embryos cells of Reichert's membrane were marked - both trophoblast-derived giant cells and cells of the parietal yolk sac (Figure 4.9 a, b and c). Staining, representing apoptosis, was observed in individual cells in the extraembryonic ectoderm rather than as clusters of cells as *Sox4* expression demonstrates (Figure 4.8). This indicates that *Sox4* expression does not mark apoptotic cells in this tissue.

4.2.5 Attempted correlation with Sox4 protein localisation.

Three commercial antibodies (Sigma, Invitrogen and Santa Cruz) have been described as reacting to mouse Sox4. Immunohistochemistry of each of these was attempted on either wax sections with a chemical detection protocol or *in toto* using a fluorescent secondary antibody. Additionally, each was attempted on a western blot using a human colon cancer cell line (SW480) known to express high levels of *Sox4*. In all cases, a control antibody, α-tubulin, showed specific staining. However none of the commercial Sox4 antibodies yielded results (data not shown). Published

findings reporting successful immunohistochemistry of Sox4 utilise non-commercial antibodies (Liu *et. al.* 2006).

4.2.6 *Foxq1* demonstrates a widespread expression pattern in multiple lineages during mouse embryogenesis

During the early stages of mouse embryogenesis, *Foxq1* is expressed in cells of both embryonic and extraembryonic lineages. In a late-streak stage E7.5 embryo, *Foxq1* is observed strongly in the extraembryonic mesoderm proximal to the exocoelomic cavity (Figure 4.10a). Weak expression of *Foxq1* is observed at the distal tip in the anterior definitive endoderm (Figure 4.10a and b). In a 3-somite stage embryo *Foxq1* is highly expressed in the anterior neural ectoderm and adjacent head mesenchyme (Figure 4.10c, d and e). Lower expression is detected in the neural plate along the axis (Figure 4.10c and d). Ectoderm expression is weak along the primitive streak (Figure 4.10c and d). Low levels of expression are observed additionally in the allantois. Striking expression is identified in the amnion adjacent to the most anterior neurectoderm (Figure 4.10c and e).

By E8.5, the *Foxq1* transcript is evident in embryonic endodermal tissue of both the involuting fore- and hind-gut, although expression is highest in cells at the entrance to the foregut (Figure 4.11). Expression is weak in the forebrain, somites and postcranial neural ectoderm (Figure 4.11a and b).

In situ hybridisation analysis of embryonic tissue at E9.5-E12.5 reveals expression of *Foxq1* in a number of specific domains including neural tissue, endoderm, craniofacial domains and the developing limbs (Figure 4.12). The control (sense) probe does not demonstrate binding to endogenous transcripts (Figure 4.12c).

At E9.5, *Foxq1* is expressed in the anterior neural tissue and cranial-most extreme of the foregut, while expression is weak in the branchial arches and adjacent endoderm (Figure 4.12a). Expression late E9.5-E10 is evident in the forebrain, as well as the first branchial arch, while expression in the second branchial arch is considerably weaker (Figure 4.12b). Additionally weak expression is observed in the emerging limb (Figure 4.12b). By E11.5, expression is evident in the neural tissue of the forebrain, as well as the neural tube and dorsal root ganglia. In a more posterior

region of the axis, expression is evident in the somites (Figure 4.12d). Closer examination of the developing face reveals strong staining of *Foxq1* (Figure 4.12e). By E12.5, expression continues in the neural tissue, although successful section *in situ* analysis would be necessary to determine the precise tissue domains of *Foxq1* expression. Expression is still evident in the neural tube and in the posterior somites (Figure 4.12f). Craniofacial expression is retained (data not shown), and expression is now evident in the region of the developing ear (Figure 4.12g). Within the limb, expression is observed at the outermost anterior and posterior tissue (Figure 4.12f), as well as in the interdigital mesenchyme (Figure 4.12g). Further domains of expression of *Foxq1* at E12.5 include the tissue of or immediately surrounding the developing vibrissae and mammary glands (Figure 4.12g).

Figure 4.7: Expression domains of *Sox4* in whole embryos staged E11.5 – E12.5. *Sox4* is expressed in a number of specific domains at E11.5 (A-D) and E12.5 (E-F). (A-D) Left lateral views of E11.5 embryos reveals expression of *Sox4* in the neural tube (NT, in A and D), particularly strong in the telencephalon (Tel, in A and D) and the midbrain (MB, in A and D). Expression is identified in the dorsal root ganglia (DRG, B) and the ventral region of the somites (vS, B). Strong expression is detected in the craniofacial region (CF, in C and D). Expression in the limbs is detected strongly in the region of the wrist (white arrowhead, A and D), and also in condensing regions of limb mesenchyme (black arrow, A and D). (E) Right lateral view of and E12.5 embryo shows the domains of *Sox4* expression progressed from previous stages in: regions of the neural tube (NT, MB, and Tel); the dorsal root ganglion (DRG) of the developing spine; somites of the tail (S); the limb bud, where expression is both in the developing digits (black arrows) and the region of the wrist (white arrowhead); the mammary glands (black arrowhead); and the craniofacial (CF) expression domains around the nose and mouth. The face is shown from the front in (F), revealing expression in the face and developing vibrissae follicles. Abbreviations, as for previous figures.

A
MB
Tel
NT
B
vS
DRG
C
CF
D
MB
Tel
CF
NT
E
Tel
F
S
CF
MB
NT
DRG
F

Figure 4.8: Expression of Sox4 is detected in extraembryonic membranes at E7.5-E8.5. Embryos were dissected from deciduas and examined for expression of Sox4 in the extraembryonic tissue. (A) Lateral view of two E7.5 embryos demonstrating extraembryonic expression of Sox4 in Reichert's membrane. Arrowheads indicate the level of the embryonic/extraembryonic junction. (B) Proximal view of the extraembryonic tissue of an E8.5 embryo showing Sox4 transcript within clusters of cells at the location of early stage placenta formation.

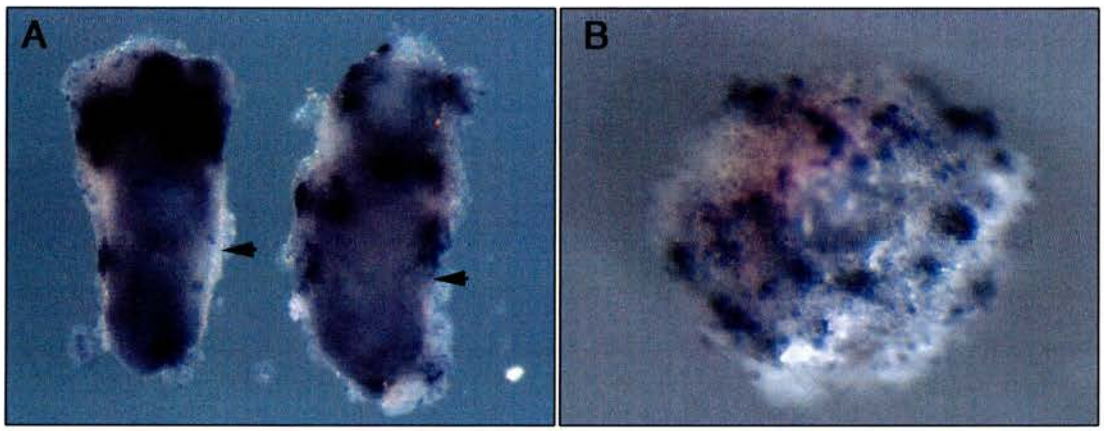
A
B

Figure 4.9: Apoptosis in the extraembryonic membranes during early development. Apoptosis was detected in extraembryonic membranes by in situ to TdT in (A) E7; (B) E7.5; and (C) E8.5 staged embryos. Brackets indicate the extraembryonic portion proximal to the embryo. In (C) Arrowhead indicates apoptosis in Reichert's membrane and the arrow, yolk sac. Scale bar: A and B, 140μm, C, 460 μm.

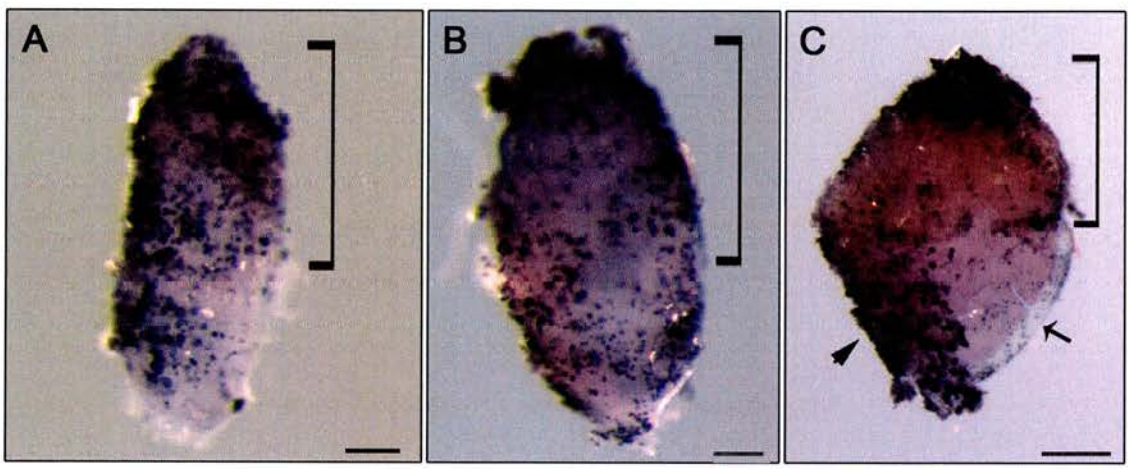
A
B
C

Figure 4.10: Foxq1 expression during early stages of development. (A) Lateral view (anterior to the left) of a late streak stage (E7.5) embryo, showing strongest Foxq1 expression in the extra-embryonic ectoderm of the proamniotic canal (black arrow), proximal to the exocoelomic cavity. Weak expression is seen at the distal tip in the emerging definitive endoderm (black arrowhead A, B). Bracket indicates the region of the embryo enlarged in (B). (B) Distal region of the embryo shown in (A) revealing expression in the definitive endoderm (black arrowhead). Early somite-stage embryos demonstrate expression throughout the anterior neural ectoderm (black arrowhead (C-E)). (C) Ventral view of a flat-mounted presomitic embryo (head fold stage) with neural ectoderm expression (black arrowhead) running adjacent to the midline. Weak expression is also observed in the allantois (white arrowhead). Strong amnion expression is observed adjacent to the head-folds (black arrow). Black lines indicate planes of sectioning for (D) - (E). (D) Sagittal section through the embryo in (C) shows the expression of Foxq1 in the head-fold neurectoderm, and weaker expression in the head-fold mesenchyme (black arrowhead). (E) Enlarged image of a sagittal section through the anterior region of the embryo in (C).

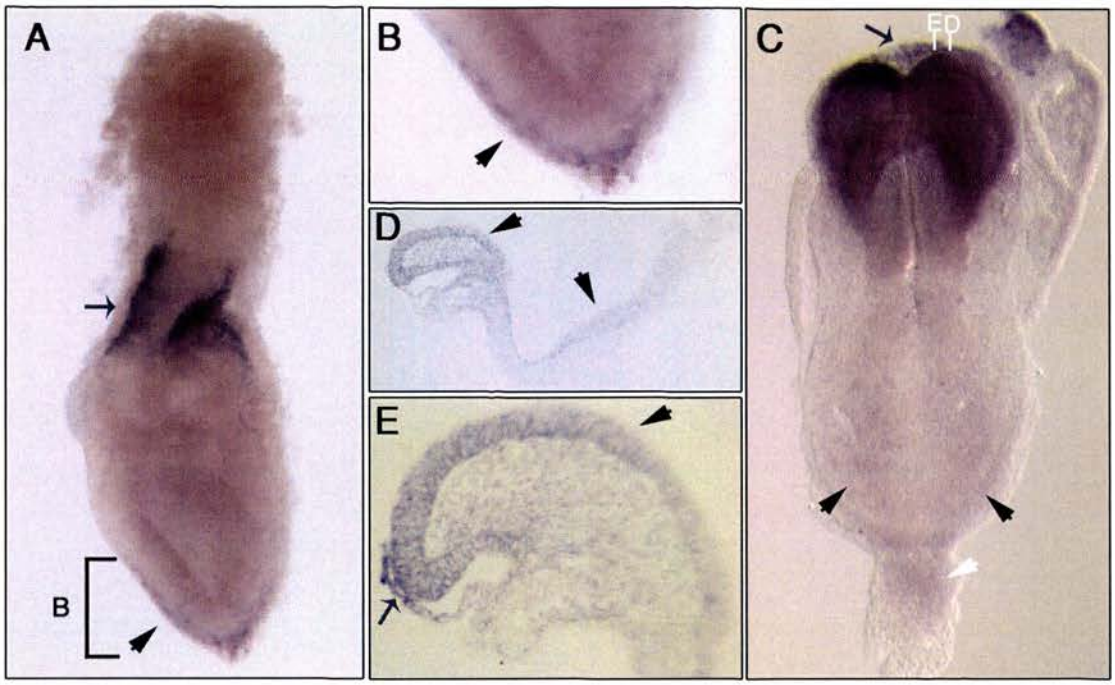
A
B
B
D
E
C
FD
IT

Figure 4.11: Foxq1 expression at E8.5. (A) Ventral view of a flatmounted 6-somite embryo, with strong expression in the anterior neural folds and endoderm. Expression is demonstrated in somitic mesoderm with expression higher in more recently formed somites towards the posterior (black arrowhead). Brackets indicate the regions of the embryo enlarged in (C and D). (B) Lateral view of the embryo in (A) showing Foxq1 transcripts are expressed prominently in the endoderm of the foregut (white arrow) and hindgut. (C) Enlarged frontal view of the embryo in (A and B), revealing expression in the involuting foregut (black arrow). (D) Frontal view of the involuting hindgut of the embryo shown in (A and B), demonstrating expression of Foxq1 in the endoderm (black arrow).

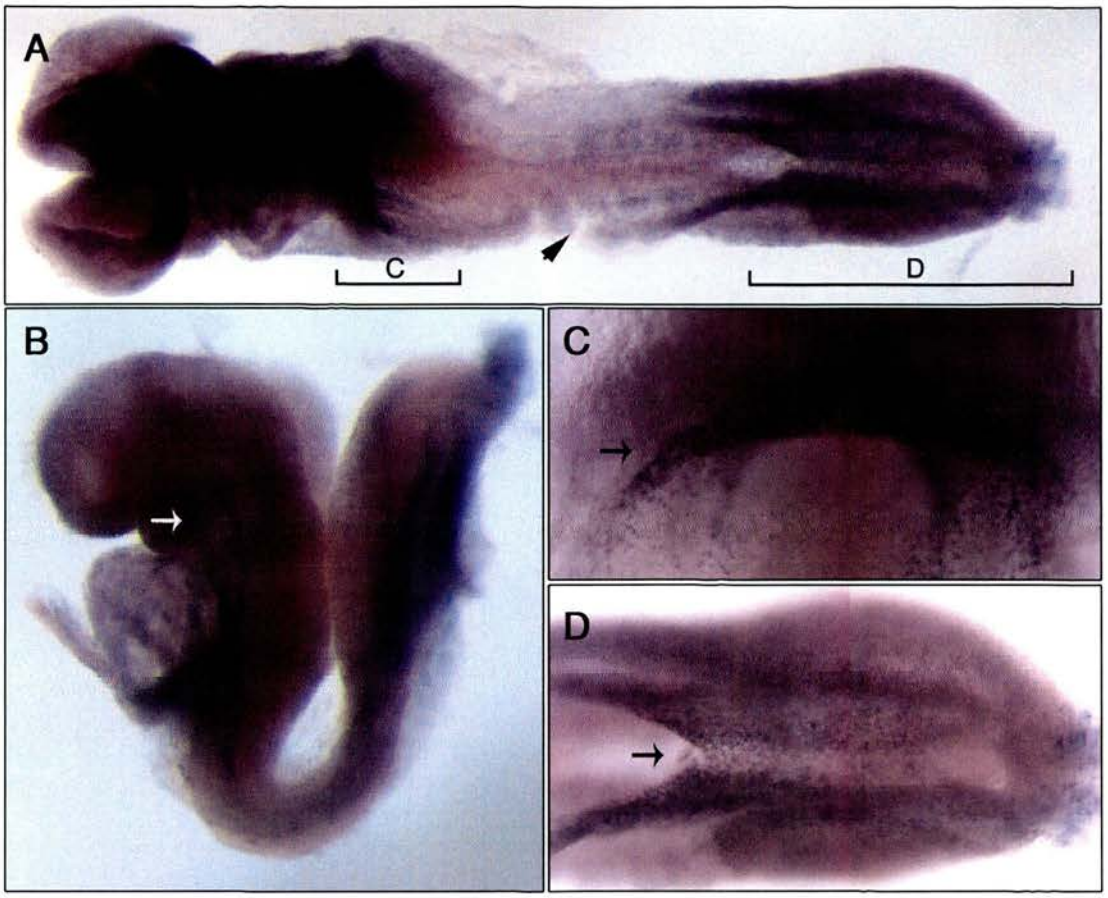
A
C
D
B
C
D

Figure 4.12: Foxq1 expression in embryos staged between E9-5-E12.5. (A) Right lateral view of an E9.5 embryo shows expression of Foxq1 prominently in the neural tissue of the head, from the caudal-most forebrain (FB) to the otic vesicle (OV). Expression is also detected in the branchial arches (white arrowhead), with weak expression in the gut endoderm (FG). (B) Left lateral view of an E10 stage embryo shows expression of Foxq1 in the pharyngeal arches (white arrowhead) and emerging limb buds (black arrow), while at the same developmental stage in (C), an embryo hybridised with the sense probe for Foxq1 does not demonstrate any transcript binding. At later developmental stages, embryos staged E11.5 (D, magnified in E) and E12.5 (F, magnified in G) continue to demonstrate weak expression throughout the neural tube (NT), while the expression is now also detected in the dorsal root ganglia (DRG) and the somites (S) at both stages. Furthermore, expression is detected in the limbs at E11.5 (arrow D) and E12.5 (F) by which stage expression appears at the wrist (arrows, F) and interdigital mesenchyme (arrows, G). (E) At E11.5 expression is detected in the craniofacial region (CF). Expression is also detected at E12.5 in the vibrissae follicles or adjacent tissue (Vib, in F), mammary glands (arrowheads, in G), and the tissue adjacent to the developing ear (E, in G). Abbreviations: As in previous figures, but additionally, E, ear; OV, otic vesicle.

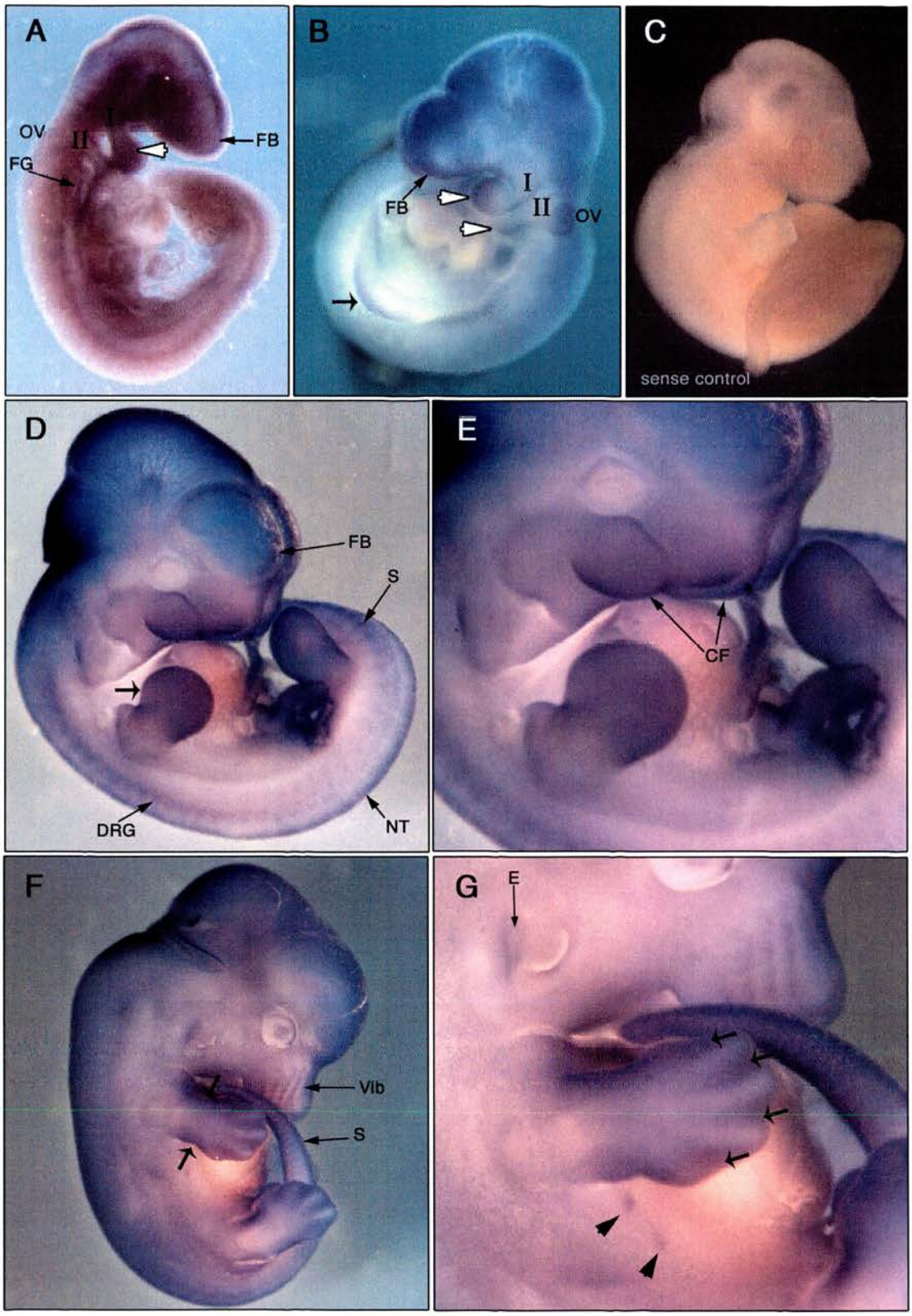
A
OV
I
II
FB
FG
B
FB
I
II
OV
C
sense control
D
FB
S
DRG
NT
E
CF
F
Vlb
S
G
E

4.3 DISCUSSION

To be able to understand the *Sox4*$^{ENU/ENU}$ *Foxq1*$^{sa/sa}$ phenotype, it is necessary to know where the genes are expressed during embryonic development, preceding the onset of the mutant phenotype (Chapter 3; (Bogani *et. al.* 2004; Schilham *et. al.* 1996)). Expression studies in this chapter focussed on comprehensively documenting *Sox4* expression in embryonic tissues from early to midgestation, suggesting a role in several developmental processes including, but not limited to, cardiogenesis.

Sox4 demonstrates dynamic expression patterns in many tissues, and does not seem limited to any one lineage. Expression of *Foxq1* overlaps with multiple embryonic *Sox4* expression domains at early stages. Consistent with a possible genetic interaction, both transcripts are expressed in the anterior neural ectoderm and first pharyngeal arch. These tissues give rise to the craniofacial structures with abnormal morphology in the *Sox4*$^{ENU/ENU}$ *Foxq1*$^{sa/sa}$ mutants presented in the previous chapter (Chapter 3).

Continuing with the primary focus of this thesis - to contribute to understanding the basis of the cardiac *Sox4* mutant phenotype - this section will focus on discussion of embryonic expression domains which might give insight into the embryonic requirement of *Sox4* in cardiogenesis. For this, expression of *Sox4* can be divided into two categories: 1) Expression domains in cardiogenic cells directly forming the heart; and 2) extra-cardiac embryonic expression domains which influence cardiac development.

In the first category, expression domains include the endocardium and mesenchyme from E9.5 in regions of the presumptive valves and septa, including regions of SHF and NCC infiltration (Figure 4.4 c, d and e; Figure 4.5a, d, e, f, g, h, i and k; Figure 4.6a, b, d, e, f, g and h).

In the second category, expression domains include the foregut endoderm, where expression was detected at the early headfold stage through to E9.5 (Figure 4.2, Figure 4.3 d, e to h and j, Figure 4.5a and d) and E10.5 (Figure 4.5e, f and k). Additionally, expression is observed in mesoderm adjacent to the posterior heart at

the 4-somite (Figure 4.2d) and 10-somite stage (Figure 4.3d, g, h and k), possibly continuous with posterior regions of pericardial mesenchyme (Figure 4.3f). *Sox4* is also expressed in the dorsal neural tube (Figure 4.4 k, l and n)

This suggests a role for *Sox4* at multiple stages of cardiogenesis through its embryonic expression within and outside the heart.

4.3.1 Possible roles of Sox4 based on expression domains in the heart

Sox4 is expressed in regions known to be infiltrated by NCC, supporting a possible requirement for Sox4 in NCC function.

Phenotypic analysis of E12.5- E13.5 $Sox4^{ENU/ENU}$ $Foxq1^{sa/sa}$ hearts revealed abnormalities in septation of the OFT. Defects including PTA, DORV and abnormal formation of the endocardial ridges, and their progression into semi-lunar valves, have been described in this and other *Sox4* mutants at E12.5-E13.5 (chapter 3). To a point, the $Sox4^{ENU}$ allele is consistent with the published null allele (Penzo-Mendez *et. al.* 2007; Ya *et. al.* 1998b). Analysis of the developmental progression of *Sox4* expression, in this chapter, has revealed that in the region of the OFT, *Sox4* is expressed in the endocardium at E9.5 to E11.5, with additional expression in OFT mesenchyme from E10.5 to E12.5. At E12.5, confirming previous expression data in the mouse heart at this stage (Hoser *et. al.* 2008), the OFT expression was restricted to the endocardial ridges of the pulmonary trunk and aorta, as well as the atrioventricular cushion mesenchyme which contributes to the proximal septation of the OFT and ventricles, positioning the exiting arterial vessels. This expression further supports the possibility that a requirement for *Sox4* may reside in NCC or in cells which interact with the infiltrating NCC at the level of the OFT.

The mesenchymal population expressing *Sox4* may be NCC or endocardial-derived mesenchyme. To distinguish these cell types, it would be necessary to examine expression of *Sox4* and a marker for NCC in parallel sections or, ideally by co-immunohistochemistry with antibodies to both Sox4 and, for example, Pax3 as a marker of NCC in the anterior heart. NCC *LacZ* reporter lines could, alternatively, be used, by examining *Sox4* mRNA expression by *in situ* hybridisation or protein by immunohistochemistry, in X-gal stained embryonic tissue (further to the genetic

crosses described in chapter 3, section 3.3.1). If it were found that *Sox4* were expressed in the NCC, then further genetic crosses involving the *Wnt1-cre* line (Jiang *et. al.* 2000) and the *Sox4*$^{flox/flox}$ line (Penzo-Mendez *et. al.* 2007) could be conducted to uncover this requirement, and thus a potential basis for aspects of the phenotype observed. If the NCC and *Sox4* expressing mesenchyme demonstrated adjacent, non-overlapping domains of expression, this would also help to clarify the potential function of *Sox4*, since the requirement would be in endocardial-derived mesenchyme, and could be verified by co-expression with *Tie2-cre/ R26R* lines (Kisanuki *et. al.* 2001; Soriano 1999). Further experiments have been detailed with respect to determining the potential dysregulation of endocardial function in the phenotype, presented in chapter 3 (section 3.3.1).

In addition to the intra-cardiac expression of *Sox4,* results in this chapter show strong expression of *Sox4* in the dorsal neural tube, from which neural crest delaminates, as well as expression below the surface ectoderm, which may pattern transitory cardiac neural crest (Figure 4.3a, b, e, f and h, Figure 4.4k). Furthermore, *Sox4* demonstrates strong expression in the pharyngeal mesenchyme adjacent to the developing heart, through which NCC migrate, leaving open the possibility that Sox4 may be required for appropriate patterning of NCC *en route* to the heart.

Sox4 demonstrates limited overlap with specific domains of Isl1 expression and thus may be required by the SHF.

Expression of *Sox4* within the OFT may also be required in cells of the SHF. While *Sox4* is not expressed in the SHF-derived myocardium, the expression domain of *Sox4* does encompass the pharyngeal mesenchyme at the level of the aortic sac and the dorsal wall of the aortic sac, between the arch arteries, which are fated to fuse with the distal OFT cushions. These domains are populated by cells of the SHF and cells which regulate SHF development, as shown by the markers Isl1 (Cai *et. al.* 2003; Yuan *et. al.* 2000) Mef2c (Dodou *et. al.* 2004) and Tbx1 (Xu *et. al.* 2004). As outlined in chapter 3, SHF markers applied to *Sox4* mutant hearts would clarify whether there is a requirement for Sox4 function in these cells. Co-expression of SHF markers and *Sox4* would further provide the indication that such a requirement is cell-autonomous. Now knowing that *Sox4* expression overlaps with this SHF

domain, there is a basis to examine inactivation of *Sox4* in the SHF. This would address the question: Does Sox4 function in cells of the SHF? To achieve this, ablation of *Sox4* through *Mef2c-AHF-cre* (Dodou *et. al.* 2004; Verzi *et. al.* 2008) would remove expression of *Sox4* specifically in the SHF. By analysis of the hearts of mutants derived from these crosses, with an antibody to Isl1, it would be possible to examine whether the population of the SHF in the heart is affected, thus determining whether the Sox4 defect resides in cells of the SHF. Nevertheless, it is not only the distal OFT of the aortic sac which demonstrates overlapping expression with the published SHF gene expression. At E11.5, expression of *Sox4* was identified in the mesenchymal cap of the atrial septum. This domain of mesenchyme is continuous with the mesenchyme of the AVC and the DMP. The DMP is of SHF origin and is initially identified about E10.5 by expression of SHF markers such as Isl1 and Mef2c, and additionally *Ptch*, since this structure is known to be responsive to Shh signalling from the pharyngeal endoderm. This expression domain of Sox4 provides a possible origin for the defects or delay in development of the atrial septum which may originate from a requirement by specific SHF domains for *Sox4* expression. Marker analysis with the DMP markers, or further by crossing the $Sox4^{ENU}$ allele to a *Ptch-LacZ* background to examine whether Shh patterning is abnormal in mutant embryos, may further elucidate a requirement for *Sox4* in this mesenchymal domain.

Sox4 is expressed in cardiac regions of the heart where the process of EMT occurs

In this analysis of the expression of *Sox4*, it has been shown that at E9.5 the non-chamber endocardium of the AVC and OFT express *Sox4*. The emerging mesenchyme in the cushions also clearly expresses *Sox4*. A possible disruption to cushion development in E9.5 mutant embryos has been described (section 3.2.4). $Sox4^{ENU/ENU}$ $Foxq1^{sa/sa}$ E9.5 mutants demonstrate either a delay or abnormalities in the production of mesenchyme and its population of the cushions. This implies a possible role for Sox4 in cushion morphogenesis. Cushion morphogenesis is initiated about E9.5 (Dor, Y *et. al.* 2003) (discussed in section 1.3.3). Cells in the endocardium respond to signals from the myocardium, both to commence and

terminate EMT. Cells of the endocardium delaminate from this epithelium, becoming mesenchyme within the extracellular matrix (ECM) separating the endocardium and myocardium in these non-chamber regions (presumptive valves). Correct formation of the cushions in these regions is necessary for later developmental processes of septation and valve formation (reviewed in (Armstrong *et. al.* 2004)).

Consistent with a possible requirement for Sox4 by the non-chamber endocardium and mesenchyme, the mid-gestation cardiac phenotype of $Sox4^{ENU/ENU}$ $Foxq1^{sa/sa}$, and of the *Sox4* null, includes septation defects (Chapter 3; (Bogani *et. al.* 2005) (Schilham *et. al.* 1996; Ya *et. al.* 1998b)). This may be a consequence of a requirement for Sox4 by the endocardium and mesenchyme from as early as E9.5. The expression in the cushion endocardium and mesenchyme continues at E10.5 and E11.5 in both the AVC and OFT. By E12.5, expression of *Sox4* is still restricted to these cardiac domains, although the structures have developed further. The AVC mesenchyme still retains low expression of *Sox4* with higher expression in the region of the developing valves – a domain of endothelial cell origin as shown by analysis of the *Tie2-cre/R26R* line (de Lange *et. al.* 2004).

In the OFT at E12.5, expression is observed in the endocardial ridges – consistent with the limited data published for expression of *Sox4* at this stage in mouse development (Hoser *et. al.* 2008). Proximal to the pulmonary trunk ridges, but in a continuous domain, strong expression is observed in the mesenchyme-derived tissue of the developing ventricular septum. These two domains have been discussed in the context of a possible role in NCC infiltration and function within the anterior heart. Further to this possibility, *Sox4* expression may be required solely by the mesenchyme in the OFT endocardial cushions to facilitate cushion maturation. The cardiac phenotype observed in mutant embryos may be a consequence of inadequate molecular programming for correct morphogenesis. Methods to examine the production of mesenchyme in these domains has been described (section 3.3.2), yet it remains possible that Sox4 function extends beyond the production of mesenchyme. To determine whether the function of Sox4 resides within the maintenance of

cushion mesenchyme, a starting point would be to examine the levels of proliferation and apoptosis in mutant embryos compared with control stage matched controls.

Whilst it is evident that Sox4 is expressed in mesenchyme throughout the body cavity, it has not yet been examined whether this expression is also evident at other sites of EMT. There are several means by which Sox4 may regulate appropriate EMT. Specifically, there are several processes in which Sox4 could act, from its expression in the endocardium and then mesenchyme from E9.5 in the heart:

- by the secretion of factors into the ECM to promote EMT;
- in the endocardial cells as they receive signals to prime endocardia to commence delamination into mesenchyme;
- in the endocardium as it proceeds with delamination, by a rearrangement of cellular proteins, such as surface cadherins;
- in the mesenchyme, to maintain or proliferate.

Certainly given the widespread expression of *Sox4* it is possible that it is involved in one of these cellular process associated with EMT. However the importance needs to be examined by assays and marker analysis of each of these possibilities (discussed further in a subsequent chapter, section 5.3.4).

4.3.2 Possible regulation of heart development by Sox4 function outwith the heart.

Expression of Sox4 in the foregut endoderm may play an indirect role in cardiogenesis

The foregut endoderm expresses *Sox4* from the pre-somitic stage of embryogenesis. The endoderm plays an important role in heart patterning from the early crescent-stage of development (section 1.3.4). At this early stage, these results of *Sox4* expression appear to overlap with that published for *Sox17* in the prospective foregut endoderm, although expression of *Sox17* is downregulated in the foregut as involution occurs, and is no longer expressed in the foregut during early somitogenesis (Kanai-Azuma *et. al.* 2002). *Sox17* null embryos demonstrate apoptosis in the prospective foregut endoderm. The foregut structure forms, but is

smaller than normal with fewer cells. The consequence of this, in terms of cardiogenesis, is mild cardiac swelling and aberrant looping from E8.75 (Sakamoto *et. al.* 2007). Since $Sox4^{ENU/ENU}$ $Foxq1^{sa/sa}$ embryos demonstrate a similar phenotype, although evident from E9.5, it is possible that the cardiac swelling is a consequence of inadequate cardiogenic cell patterning from adjacent endoderm at the headfold stage.

Gata4 is expressed in both the endoderm and mesoderm during the stage of early heart-tube formation (Watt *et. al.* 2007). Ablation of *Gata4* expression results in severe disruption to ventral morphogenesis, including an inability to form the heart tube (Molkentin *et. al.* 1997). Endodermal *Gata4* expression overlaps with that observed here for *Sox4*. It has been shown by studies of chimæric embryos (introducing *Gata4* null ES cells into wild type morulas) that embryonic endodermal expression of *Gata4* is essential for cardiogenesis, while expression from the embryonic mesoderm is not (Narita *et. al.* 1997). High contribution *Gata4* null chimæric embryos, with wild type cells only contributing to endoderm derivatives, were predominantly indistinguishable from wild type.

Although not as severe as either of the *Gata4* or *Sox17* null mutants, it is possible that components of the $Sox4^{ENU/ENU}$ $Foxq1^{sa/sa}$ cardiac phenotype may be a consequence of a requirement for endodermal expression of *Sox4*. This is especially the case since this *Sox4* expression domain precedes the onset of the visible cardiac phenotype. This suggests that Sox4 may be involved in early cardiac patterning from the endoderm.

The phenotype of the $Sox4^{ENU/ENU}$ $Foxq1^{sa/sa}$ embryos from E9.5 also supports a role for endodermal *Sox4* in cardiac structural morphogenesis. The pharyngeal endoderm is known to be an important source of signalling morphogens for both the SHF and NCC, as revealed by complex analysis of genetic crosses with conditional alleles. In an analysis of conditional mutants for *Fgf8* expression, Park *et.al.* identified that expression of *Fgf8* from the pharyngeal endoderm was necessary for OFT septation, with PTA only being evident in mutants in which *Fgf8* expression was also lacking from the endoderm compared with other genetic crosses examined in their study (Park, E J *et. al.* 2006). Furthermore, Shh responsiveness is crucial for both SHF and

NCC function in the development of the OFT (discussed in chapter 1; section 1.3.4). Specifically, it has been shown that Shh signalling is required for OFT septation (Goddeeris *et. al.* 2007). Embryos in which Shh-responsiveness was ablated in either lineage were capable of developing OFT cushions, but not undergo septation. Thus a lack of *Sox4* expression in the endoderm may disrupt signalling that contributes to septation. However since the development of the OFT cushions is additionally delayed or disrupted in *Sox4* mutants, other expression domains of *Sox4* clearly are required independently of the endodermal expression.

Of relevance to atrial septation, the DMP is of SHF origin, with its presence in the developing heart dependent upon expression of *Shh* from the endoderm, and the responsiveness of the SHF at this pole of the heart (Goddeeris *et. al.* 2008). While it has been shown that at E11.5, *Sox4* is expressed in the mesenchyme continuous with the DMP, it is possible that *Sox4* expression from the endoderm is also required for the appropriate molecular programming of this dynamic migratory structure.

Although the expression domain overlap of *Sox4* with *Shh* and *Fgf8* does not indicate functional overlap, it is possible that the role of Sox4 as a transcription factor may be to maintain appropriate levels of the expression of either of these factors. Whilst examining the regulatory regions of these genes for conserved Sox4 binding sites may suggest a mechanism, conclusive proof of an effect on downstream signalling by marker analysis or receptor activation would be required.

To conclude, the findings in this chapter, presenting the expression of *Sox4* in the pharyngeal endoderm at the stages examined, permit the proposal that this domain of expression is required for appropriate cardiogenesis. This is further supported by the overlap in aspects of the $Sox4^{ENU/ENU}$ $Foxq1^{sa/sa}$ cardiac phenotype with those described for mutants in which endodermal expression or target cell responsiveness to endodermally derived signalling factors is disrupted. Abolishing *Sox4* expression using *Shh-cre* (Harfe *et. al.* 2004) would allow a distinction to be made between the requirement for endodermal expression of *Sox4* and the cardiac expression within the endoderm and mesenchyme.

Does Sox4 mark the septum transversum mesenchyme?

Sox4 is expressed in the lateral mesoderm immediately caudal to the heart tube from the 4-somite stage. It is not clear from sections whether this domain is continuous with the base of the heart tube. At the 8-somite stage (Figure 4.3j) expression of *Sox4* appears to overlap with published domains of *Cited2* (Dunwoodie *et. al.* 1998). In an embryo with 10 somites, this *Sox4* domain appears to be continuous with pericardial mesenchyme of the posterior heart as shown by section analysis (Figure 4.3d and f). The fate of this group of *Sox4*-expressing cells is not clear, but given the timing and location of expression, they could be cells of the septum transversum mesenchyme (STM) which contributes to the early stages of pro-epicardial (PEO) development (section 1.3.5). *Cited2* and *Gata4* mark this mesodermal structure prior to formation of the PEO (Dunwoodie *et. al.* 1998; Watt *et. al.* 2007). Additionally, this domain of expression closely resembles that of *Tbx18*, a marker of the STM and PEO. In mouse, *Tbx18* expression in the lateral mesoderm appears bilateral (Kraus *et. al.* 2001a), however in chick, STM expression of both *Tbx18* and *Bmp4* are clearly unilateral and on the right side (Schlueter *et. al.* 2006). In chick, it has been shown that generation of the PEO is subject to left-right patterning, while in mouse this is yet to be reported. Expression of *Sox4* may correlate to a *Tbx18* or *Bmp4* right-sided expression domains in the mouse heart. However if this is so, then *Sox4* expression is downregulated prior to epicardial attachment to the heart - as the epicardium does not demonstrate *Sox4* expression.

4.4 SUMMARY

Identifying the expression pattern of *Sox4* was an essential first step to identifying which tissues require Sox4. *Sox4* is expressed across early developmental stages in most tissue, although some express *Sox4* more highly than others. The expression domains of *Sox4* which are most likely to be relevant for cardiogenesis are: (1) regions of the heart itself, including non-chamber endocardium and mesenchyme; and (2) domains of extra-cardiac origin, namely the foregut endoderm and possibly the STM. Expression of *Sox4* in regions unrelated to heart development includes the dermomyotome of the somites, limbs, trunk neural crest and anterior neural and craniofacial tissue. Some of these findings are novel and add to the existing knowledge of localisation of *Sox4*. The expression reported for *Foxq1* at this stage is also novel. Expression in the somitic mesoderm, limbs, neural tube, foregut and hindgut suggests potentially novel roles for Foxq1 as a factor in the development of these structures. The broad expression domains of *Sox4* and *Foxq1* suggest that these genes play more diverse roles than currently reported in the literature.

CHAPTER 5: EXAMINING ASPECTS OF THE MOLECULAR CONSEQUENCE OF THE *Sox4^{ENU} Foxq1^{SA}* MUTATION.

5.1 INTRODUCTION

The phenotype observed for *Sox4$^{ENU/ENU}$ Foxq1$^{sa/sa}$* (also, termed compound mutant) embryos is complex. By examining compound mutant embryos staged E7.5 to E13.5 we have determined that a cardiac abnormality is visible from E9.5. Among the embryos where a morphologically distinct heart had developed, a grading of deformity is evident with class-II embryos exhibiting a more severe phenotype than that of class-I. At E9.5, mutant hearts are distended to varying degrees. This impairs the ability of the heart tube to undergo adequate looping, although handedness appears normal. In order for a phenotype to present at E9.5, the first molecular requirement for Sox4 function must be prior to this stage. Given the expression domains of *Sox4* documented in the previous chapter, it is reasonable to suggest that *Sox4* expression in the endoderm is required for the patterning of adjacent cardiomyocytes in the SHF and/or NCC (section 4.3.2). Additionally expression of *Sox4* within the endocardium of the OFT may influence NCC infiltration and function in the OFT (Section 4.3.1). The E12.5 and E13.5 defects of proximal OFT septation and abnormalities in ventricular and atrial septation may be a consequence of inadequate *Sox4* expression from earlier developmental stages (section 3.3.2). Furthermore, cardiac expression of *Sox4* is observed from E9.5 in the endocardium and mesenchyme of the presumptive valve regions (Chapter 4; Figure 4.4 and 4.5), together with a consistent abnormal phenotype in the AVC at E9.5, this enables us to consider that Sox4 may be involved in endocardial cushion development, by way of the production and pattering or maintenance of the mesenchyme and thereby subsequent valve development in the AVC and proximal OFT.

Given these many potential functions of *Sox4*, it is of interest to examine markers at the earlier developmental stages - to uncover molecular dysregulation as it arises. Thus, the aim of this chapter is: *To examine aspects of the molecular consequence of the* $Sox4^{ENU}$ $Foxq1^{sa}$ *compound mutation.*

This study is the first in which the early *Sox4* cardiac phenotype is examined at the level of gene expression. Given the heterogeneity of the *Sox4* phenotype and the overlap of the resulting defects with those arising from other cardiac gene mutations, a selection of molecular markers were examined. Later in this chapter, a discussion of results from these markers will be further complemented by a discussion of more useful markers for the affected cardiac structures. An added complexity, in deciding which markers to use, comes from knowledge that, although there are a number of cardiac phenotypes that have been described which overlap with the $Sox4^{ENU/ENU}$ $Foxq1^{sa/sa}$ E9.5 phenotype, many of the genes dysregulated in these mutants do not overlap in their expression with domains of *Sox4*. This is particularly relevant for the cardiac phenotype which arises in the chambers of the heart – the looping defect in wholemount, cardiac swelling and abnormal trabeculation. *Sox4* is expression is not detected by *in situ* hybridisation in the myocardium of the heart. Indeed the only cardiac expression of *Sox4* is from E9.5 within cells of the endocardium and mesenchyme of non-chamber regions. If abnormal Sox4 exerts an effect on the SHF (as has been proposed in chapter 3) or if it is involved in regulation of proliferation or differentiation (also proposed in chapter 3, in the context of early defective trabeculation), then the role of Sox4 must be upstream of SHF colonisation of the heart, or Sox4 must act indirectly *via* signalling from the non-chamber expression domains or pharyngeal endoderm.

The cardiac defect appears to be largely restricted to derivatives of the secondary heart field. The proximity of the endodermal expression of *Sox4* to cells of the secondary heart field suggests an indirect patterning role. *Hand2* is a marker of the SHF, labelling the right ventricle and OFT within the anterior heart. Because of this *Hand2* was examined as a secondary heart field marker for the myocardium of the right ventricle and outflow tract. Given the degree to which *Sox4* mutant hearts are capable of developing (depending on the severity, *Sox4* mutants are capable of

forming the four-chambered heart), it is unlikely that the *Sox4* mutation alters expression of *Nkx2.5* or *Isl1*, since both of these genes are required at crucial early stages of cardiac patterning. Severe cardiac defects arise in the absence of either gene (Cai *et. al.* 2003; Lyons *et. al.* 1995). Thus expression of these genes was not examined in $Sox4^{ENU/ENU}$ $Foxq1^{sa/sa}$ mutant hearts. In hindsight, examination of Isl1 would have proved useful for determining the degree of SHF population in mutant hearts, as has been described (section 3.3.1 and 4.3.1).

The abnormal cardiac morphology of the $Sox4^{ENU/ENU}$ $Foxq1^{sa/sa}$ mutant at E9.5 resembles the phenotype of that described at E9 in the cardiac knockout of *Hand1*, both with and without heterozygous inactivation of *Hand2* (McFadden *et. al.* 2005) (Section 3.3.2). It is possible that this overlap in phenotype may be a consequence of *Sox4* and *Hand1* regulatory pathways converging at some level. To explore this further, expression domains of *Hand1* were examined. *Hand1* is expressed in the OFT and outer curvature of the left ventricular myocardium (Cserjesi *et. al.* 1995). Hand1 has been associated with proliferation in the developing heart, and therefore may give some indication whether proliferation is affected in $Sox4^{ENU/ENU}$ $Foxq1^{sa/sa}$ compound mutants (Risebro *et. al.* 2006). In addition to being a marker of the SHF, Hand2 is, in part, also responsible for stimulating the early proliferation and growth of regions of the heart tube, as indicated by the severely hypolastic right ventricular phenotype of *Hand2* null embryos (Yamagishi *et. al.* 2000). The *Hand2* transcript is controlled from E9.5 by the expression of the miRNA, *miR-1*. Transcription of *miR-1* is a target of cardiac muscle differentiation factors, including SRF, MyoD and Mef2. As the heart tube loops, expression of inhibitory micro RNA blocks *Hand2* translation and thus decreases the production of Hand2 protein and drives differentiation (Zhao *et. al.* 2005). Thus expression of *Hand2* was examined in mutant embryos, to label SHF cells and also to examine whether there is a disruption to proliferation and differentiation levels within the heart, although it is not a direct marker of either process.

To explore whether myocardial differentiation was affected as a consequence of the $Sox4^{ENU/ENU}$ $Foxq1^{sa/sa}$ phenotype, despite some mutant embryos appearing

developmentally delayed, *Nppa* expression was examined as a marker for chamber myocardium specification and differentiation.

Given the expression of *Sox4* (Chapter 4) and the phenotype described (Chapter 3) it has been proposed in previous chapters that a function of Sox4 may reside in the production of cushion mesenchyme in the AVC and OFT. In this chapter, gene expression was examined in the developing E9.5 OFT, since a dysregulation of gene expression would be detectable at this stage, resulting in the E9.5 phenotype, which further in development could lead to the septal defects observed from E12.5. *Wnt11* is expressed by the myocardium and endocardium of the OFT (Christiansen *et. al.* 1995). Fibroblasts expressing *Wnt11* have been shown to transform epithelial cells to mesenchyme in co-culture experiments (Christiansen *et. al.* 1996). Embryos null for *Wnt11* demonstrate OFT defects similar to those observed with *Sox4* mutant homozygotes (Zhou, W *et. al.* 2007). To date, a direct role of Wnt11 in the EMT of the OFT endocardium has not been described. It has been shown that Wnt11 induces expression of *Tgfβ2* in the myocardium of the OFT (Zhou, W *et. al.* 2007). Downregulation of *Tgfβ2* expression in *Wnt11* null mutant hearts results in double outlet right ventricle (DORV) and ventricular septal defects (Zhou, W *et. al.* 2007) as a consequence of inadequate OFT development. In mouse, Tgfβ2 has been shown to be required for EMT in cardiogenesis. Blocking the function of Tgfβ2 prevents the initial transformation of epithelial cell into mesenchyme during EMT of the AVC in explant cultures (Camenisch *et. al.* 2002). Little is known about the downstream targets of Sox4 (section 1.1.3). If Sox4 plays a role in development of the OFT, then it may be involved in Wnt11 signalling. To explore this, *Wnt11*, its receptor *Fzd7*, and the Wnt11 target *Tgfβ2* mRNA levels were examined in micro-dissected outflow tracts, comparing a mutant OFT with pooled control outflow tracts.

The appearance of three classes of phenotype, and at least two periods of embryonic lethality, highlights that Sox4 and Foxq1 proteins have roles at multiple stages during development. In addition to the cardiac defects, which are attributed solely to the *Sox4* mutation, some class-I and all class-II mutants examined demonstrate variable anterior defects (Figure 3.8). This implies that either, or both, Sox4 and Foxq1 are involved in forebrain patterning.

The development of the forebrain requires signalling from two domains: (1) the anterior-most region of neurectoderm (anterior neural ridge, ANR); and (2) the prechordal plate, which is the anterior-most axial mesoderm continuous with the notochord. (Figure 5.1). Expression of *Fgf8* from the ANR and of *Shh* from the prechordal plate is essential for regionalisation of the forebrain at E9.5 ((Shimamura *et. al.* 1997); reviewed in (Rubenstein *et. al.* 1998)). Since $Sox4^{ENU/ENU}$ $Foxq1^{sa/sa}$ embryos demonstrate variable forebrain abnormalities, it is possible that signalling through these two domains, the ANR and prechordal plate, is disturbed. Furthermore both *Sox4* and *Foxq1* are expressed in the anterior neural folds (Chapter 4). It has been shown that, at E8.5, prior to a morphological defect arising, expression of *Sox4* and *Foxq1* is detected in the neurectoderm of the prospective forebrain. This expression further supports a genetic interaction in anterior development at this embryonic stage, namely in patterning the presumptive telencephalon. Co-expression of *Sox4* and *Foxq1* at E9.5 in the forebrain and first pharyngeal arch suggests that both proteins are required for aspects of craniofacial morphology, since facial development, including formation of the nasal structures and jaw, also appears impaired in compound mutants at E12.5 (Section 3.2.5; Figure 3.17). An examination of the molecular changes accompanying this phenotype may provide information useful to understand the basis of the interaction. In addition to the primary investigation into the cardiac abnormalities, this chapter shows an *in situ* analysis of some forebrain markers in $Sox4^{ENU/ENU}$ $Foxq1^{sa/sa}$ embryos.

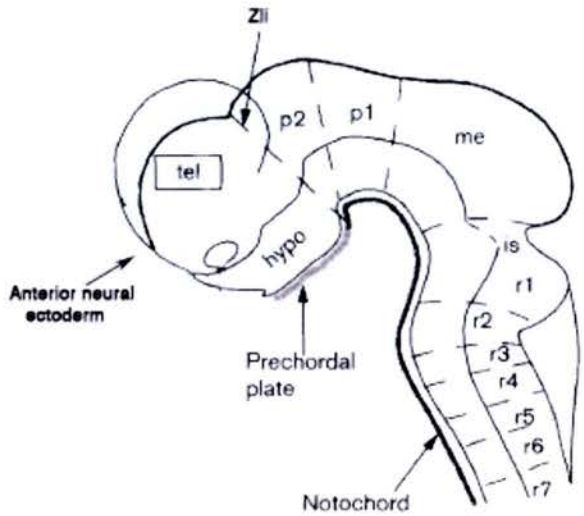

Figure 5.1: Schematic diagram showing the locations of the signalling centres of the developing forebrain at E9.5.

Within the developing forebrain, the anterior neural ectoderm is the anterior-most region of the developing telencephalon. A second signalling centre is the prechordal plate, which is continuous with the notochord, adjacent to the hypothalamus (hypo). The zona limitans intrathalamica (zli) marks the boundary between the forebrain and midbrain. Abbreviations: hypo, hypothalamus, tel, telencephalic vesicles; p, prosomere; me, mesencephalon; is, isthmus; r, rhombomere; zli, zona limitans intrathalamica. Adapted from: Rubenstein and Beachy, 1998.

5.2 RESULTS

5.2.1 Homozygosity of *Sox4*^{ENU} causes an alteration to the expression of *Hand2* and *Hand1* and an increase in the expression of *Nppa* at E9.5-E10.

To explore the molecular basis of the *Sox4* mutant cardiac phenotype, we examined the expression of genes whose products are associated with myocardial cell proliferation in the heart (*Hand2* and *Hand1*) or myocardial cell differentiation (*Nppa)* within the heart. Given that *Sox4* mutant embryos demonstrate a predominantly right-sided, and possibly a secondary heart field defect, it was also predicted that changes in gene expression would be observed in SHF-derived cardiac regions.

At E9.5 *Hand2* expression is observed in the OFT extending into the adjacent region of the RV (Figure 5.2a and c, (Srivastava *et. al.* 1997)). At this stage, weak expression is also observed through the posterior heart. Adjacent to the heart, expression of *Hand2* is detected in the dorsal mesocardium and the pharyngeal arches. In *Sox4* mutant hearts (n=2), the *Hand2* expression is not lost but rather appears reduced, with weak staining throughout the expression domains observed in the control (Figure 5.2b and d). The control embryo shown (Figure 5.2a and c) was a littermate to the mutant embryos. All embryos were subjected to the same *in situ* hybridisation conditions, including the *in situ* development time. It is possible that the developmental delay in the mutants has contributed to the different level of expression in mutant hearts. However the extent of this delay, combined with the cardiac defect, renders the results from this probe inconclusive, since the mutant embryos could neither be compared with the control littermates nor subsequently with younger E9 developmental controls, since the normal cardiac development of earlier stages did not resemble the phenotype of the mutant embryos in which *Hand2* was examined. In order to concluded from analysis of the expression of *Hand2*, or any other SHF marker, it is necessary to examine mutant embryos at earlier stages, before the phenotype progresses, or examine embryos at this stage with a less severe phenotype, such that control embryos are developmentally matched to the mutant embryos.

Late-stage E9.5 control hearts demonstrate *Hand1* expression in the OFT and outer curvature of the left ventricle (Figure 5.3a, (Cserjesi *et. al.* 1995)). In stage matched littermate embryos subjected to the same *in situ* hybridisation conditions, $Sox4^{ENU/ENU}$ $Foxq1^{sa/sa}$ mutants exhibit reduced cardiac *Hand1* expression (n=2/2). In the less severe class-I mutant there is a decrease in the *Hand1* transcript in both cardiac domains of expression (Figure 5.3b). *Hand1* expression is barely detectable in the more severe class-I mutant, where the heart is more swollen and has failed to undergo adequate looping (Figure 5.3c). The *in situ* detection was deliberately understained to observe this difference between control and mutant embryos. In contrast, extraembryonic expression of *Hand1* appeared to develop to the same intensity in all three embryos examined. Despite the looping defects, and although *Hand1* expression in the OFT is diminished, the length of the OFT does not appear to have been reduced – although this was not subjected to quantitative measurement. OFT length should be examined given the possible involvement of SHF and/or NCC in the Sox4 phenotype (as discussed in chapter 3). Extraembryonic expression of *Hand1* in the yolk-sac membranes appears unaffected by the $Sox4^{ENU/ENU}$ $Foxq1^{sa/sa}$ mutation (data not shown).

Nppa expression marks the differentiation of embryonic myocardium into chamber myocardium of the atria and ventricles ((Zeller *et. al.* 1987); reviewed in (Houweling *et. al.* 2005)). To examine whether the cardiac phenotype of *Sox4* mutant embryos was accompanied by increased differentiation, *in situ* to *Nppa* transcripts was conducted on a control and homozygous mutant heart (n=1 at E9.5). At this stage, as shown by the control littermate, normal expression of *Nppa* is strong in both atria and in the left ventricle (Figure 5.4a and b, (Zeller *et. al.* 1987)). The right ventricle reveals a gradient of *Nppa* transcript – extending from the weakest point of expression at the outer curvature of the myocardium which is continuous with the OFT, to stronger expression adjoining the left ventricle. The $Sox4^{ENU/ENU}$ $Foxq1^{sa/sa}$ heart did not demonstrate this gradient. The right ventricle of the mutant heart demonstrated uniform elevated expression (Figure 5.4c, d), suggestive of either abnormal right ventricular patterning or increased differentiation. Nevertheless, at E9.5, expression is distinctly absent from the AVC in both control and mutant, and

expression levels in the adjacent atrium and left ventricle appear unaffected at this stage, suggesting that the *Sox4* mutation does not alter the patterning and regulation of *Nppa* expression in the AVC or to the left side of the heart. Interestingly, the elevated ventricular expression of *Nppa* is reminiscent of that in later stage (E11) embryos which contain just the *Sox4* mutation (chapter 6). However whether it is reproducible at E9.5 in compound mutants remains to be determined. This *in situ* is not quantitative and to determine levels of *Nppa* it would be necessary to examine a greater number of hearts both by quantitative-PCR of specific cardiac regions and also *in situ* of additional mutant embryos with alternative markers of myocardial differentiation.

5.2.2 Micro-dissection of E9.5 cardiac regions enabled examination of gene expression in the OFT.

Often in the literature, comparative results of quantitative cardiac gene expression are presented from procedures carried out on total heart extracts. To determine more precisely the genetic alterations within discrete cardiac regions, E9.5 control (Figure 5.5a) and class-I mutant (Figure 5.5b) hearts were micro-dissected into OFT, RV, LV, AVC and IFT, using glass needles (Figure 5.5c, d and e). Only the mild class-I mutant embryos could be micro-dissected in this procedure as severe swelling of the heart tube did not permit visual distinction of the regions in class-II mutants. Given that even within the class-I mutants the phenotype may be varied, for the purpose of examining an alteration to gene expression it was decided that samples from mutant embryos be kept separate for expression analysis. Using this technique, gene expression in the OFT was assessed for the expression of genes with a known association to EMT either in the heart (*Tgfβ2*) or elsewhere in the embryo (*Wnt11*).

The levels of *Wnt11*, its receptor *Fzd7* and the *Wnt11* transcriptional target *Tgfβ2* were compared between pooled control OFT and a class-I mutant OFT (Figure 5.5f). The one class-I mutant OFT examined demonstrated elevated levels of all three transcripts.

Figure 5.2: Difference in the expression domain of *Hand2* in *Sox4*$^{ENU/ENU}$ *Foxq1*$^{sa/sa}$ E9.5 embryos. (A) Wild type and (B) mutant expression of *Hand2* is detected throughout the looping heart tube, with higher expression in the outflow tract (red arrowhead) and right ventricle. Expression is weak in the left ventricle, atrioventricular canal and inflow tract of the developing atria. Adjacent to the heart, expression is observed in pharyngeal arches (yellow arrow). (C) Wild type cardiac expression viewed from a right-lateral orientation. Strong expression in the outflow tract is indicated (red arrow) and the domain of right ventricular staining is marked with lines. (D) Mutant embryos demonstrate lower expression of *Hand2* (outflow tract and right ventricle marked as for wild type). Abbreviations: AVC, atrioventricular canal; LV, left ventricle; OFT, outflow tract; RV right ventricle. Scale bar: A,B 233μm; C,D enhanced region of A,B.

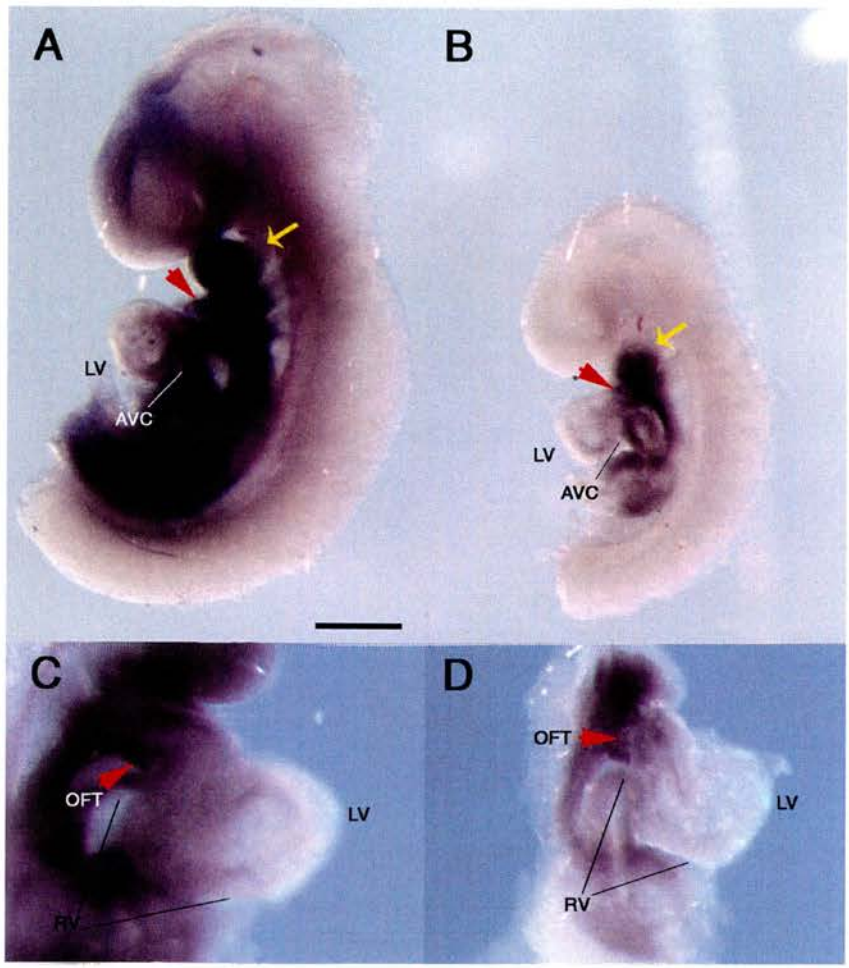
A
LV
AVC
B
LV
AVC
C
OFT
LV
RV
D
OFT
LV
RV

Figure 5.3: Disruption to expression of *Hand1* in *Sox4*$^{ENU/ENU}$ *Foxq1*$^{sa/sa}$ embryos at 9.5dpc. (A) Expression of *Hand1* is detected in wild type embryos the outflow tract (arrow) and in the outer curvature of the left ventricle (arrowhead). Mutant embryos (B,C) demonstrate lower expression of *Hand1* in these regions. Scale bar: A, B, C, 1mm.

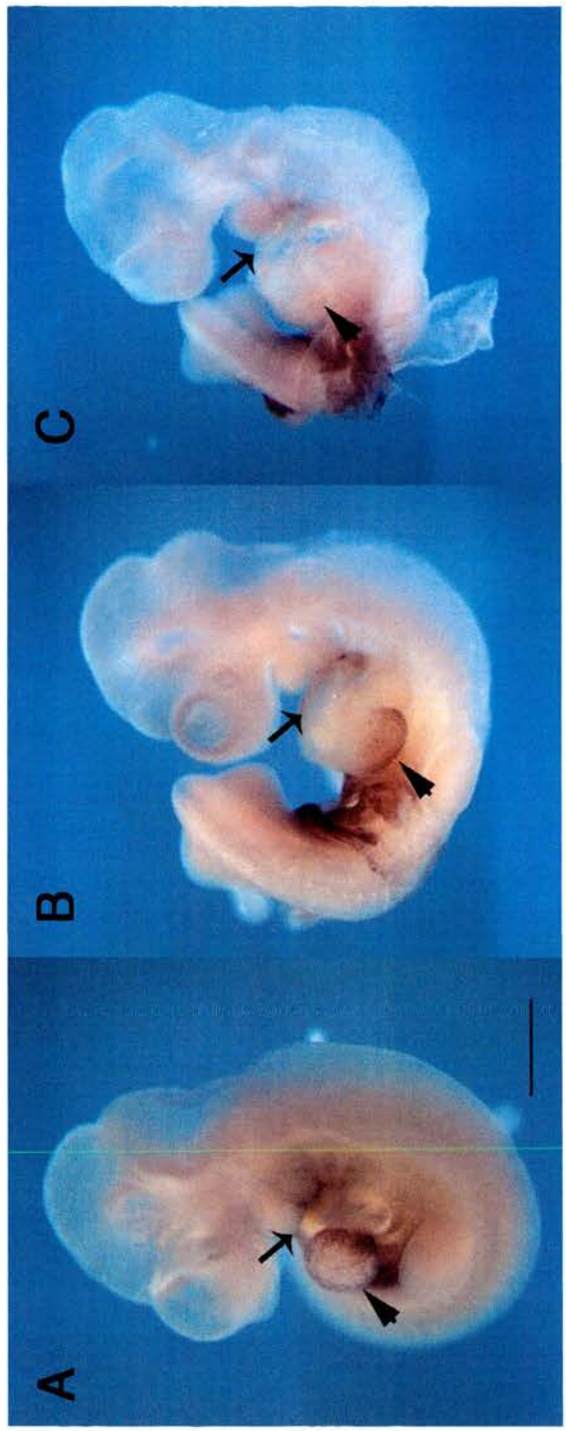
A
B
C

Figure 5.4: Elevated expression of Nppa in Sox4$^{ENU/ENU}$ Foxq1$^{sa/sa}$ embryos at E9.5. Wild type (A,B) and mutant (C,D) hearts were examined for Nppa expression. Hearts are viewed from the posterior side (A,C) and the left side (B,D). At this stage, expression is strong in the atria and left ventricle of both wild type and mutant hearts and absent from the atrioventricular canal (bracket, A, C). A notable difference is observed in the right ventricle (arrow C compared with A) and outer curvature of the right ventricle leading into the outflow tract (arrowhead B compared with D). Abbreviations: LA, left atrium; LV, left ventricle; OFT, outflow tract; RA, right atrium; RV, right ventricle. Scale bar: A – D 143.5μm

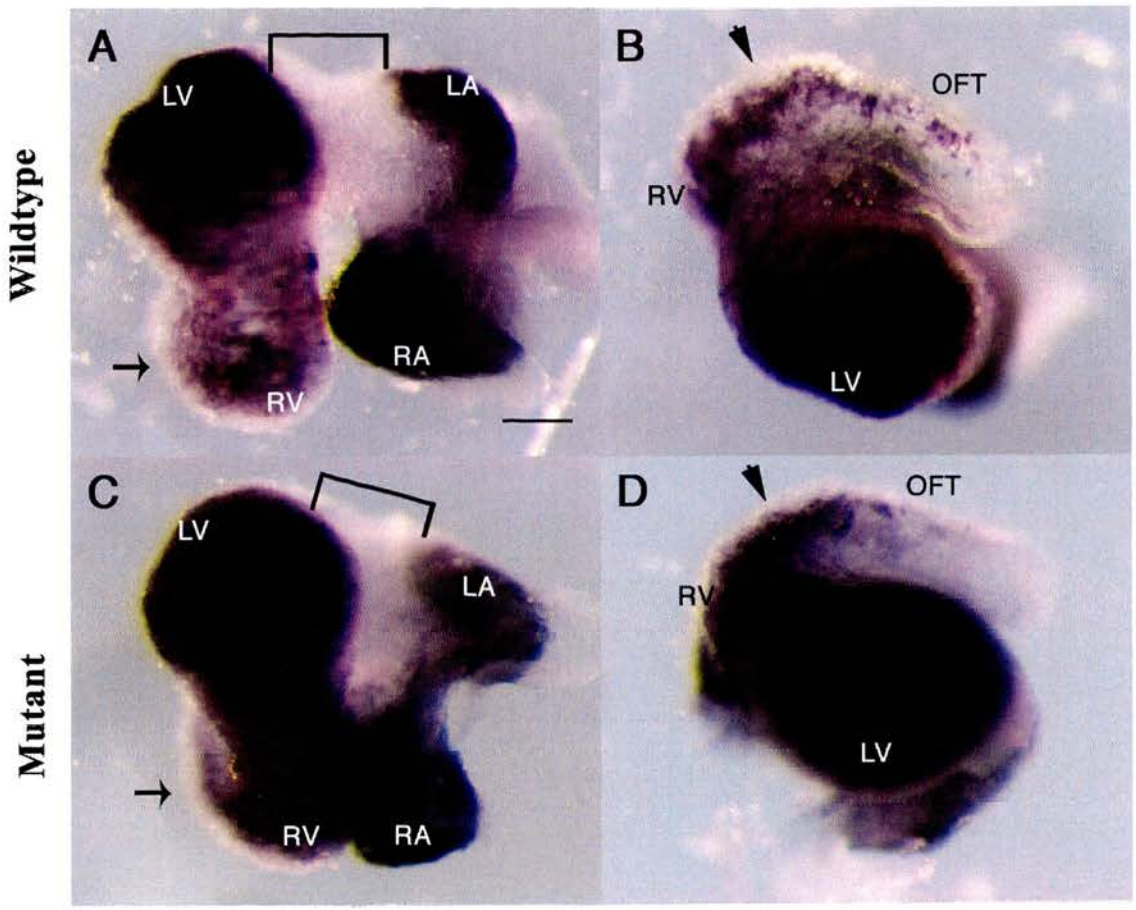
Wildtype
Mutant
A
LV
LA
RA
RV
B
OFT
RV
LV
C
LV
LA
RV
RA
D
OFT
RV
LV

Figure 5.5: Microdissection of E9.5 hearts for expression analysis of developmental genes. Analysis of cardiac gene expression by PCR to microdissected regions of wild type and mutant hearts. Hearts from a wild type embryos (A) and mutant embryos (B) were microdissected for quantitative PCR analysis. (C) A whole heart dissected from a wild type embryo body. A glass needle was used to cut between the left ventricle and the presumptive right ventricle (bulbus cordis, BC), in the region indicated (black arrowhead). (D) The outflow tract and bulbus cordis were then separated as indicated (black arrowhead) as were the (E) left ventricle from the atrioventricular canal and part of the inflow tract (presumptive atria). (F) Quantitative expression analysis was performed on cDNA reverse-transcribed from RNA extracts from the outflow tract, normalised to *Tbp* as an internal control. One mutant outflow tract was compared with pooled wild type samples for gene expression with UPL probes to *Wnt11, Fzd7* and *Tgfb2*. Error bars represent experimental replicates from the pooled control RNA and one mutant RNA extracted from a single OFT. Abbreviations: AVC, atrioventricular canal; BC, bulbus cordis; IFT, inflow tract; LV, left ventricle; Mu, mutant; Wt, wild type.

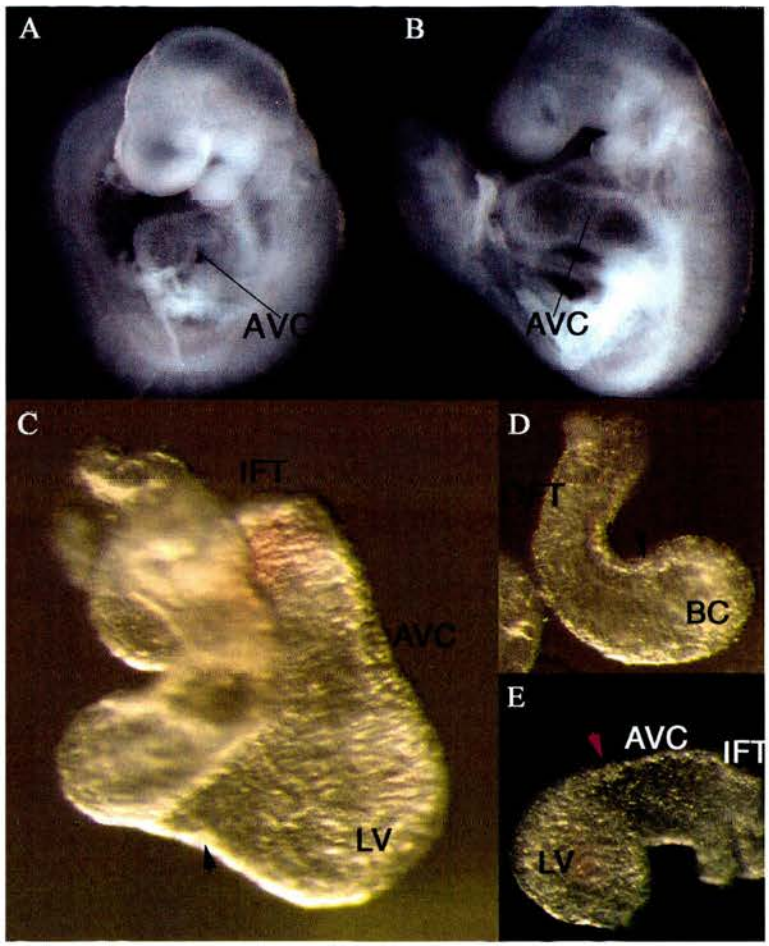
A
AVC
B
AVC
C
IFT
AVC
LV
D
T
BC
E
AVC
IFT
LV

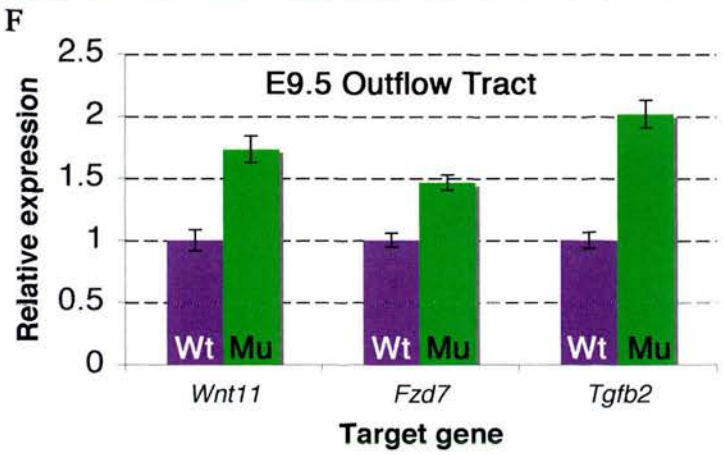
F
E9.5 Outflow Tract
Relative expression
2.5
2
1.5
1
0.5
0
Wt
Mu
Wnt11
Fzd7
Tgfb2
Target gene

5.2.3 Aspects of the anterior phenotype are revealed by a reduction in Fgf8 expression in class-I and class-II mutant embryos.

To begin to analyse the forebrain defect in *Sox4*$^{ENU/ENU}$ *Foxq1*$^{sa/sa}$ embryos, *Fgf8* expression was examined. Alteration to *Fgf8* expression has demonstrated it to be essential for anterior patterning and forebrain development (Meyers *et. al.* 1998). At E9.5, a lateral view of an *Fgf8* stained embryo reveals expression in the first pharyngeal arch in both mandibular and maxillary regions (Figure 5.6a, (Crossley *et. al.* 1995)). Analysis of the staining pattern from the frontal orientation exposes anterior *Fgf8* expression in the telencephalic commissural plate, marking the midline of the anterior neural endoderm (Figure 5.6c). Adjacent to this domain, expression is observed in the surface ectoderm of the olfactory placode. These expression domains are observed in the *Sox4*$^{ENU/ENU}$ *Foxq1*$^{sa/sa}$ class-I embryos (n=2). However, the regions are diminished, with reduced staining at the midline and weaker staining in the olfactory placode (Figure 5.6d). It is from this region that the midline structures of the face are generated and *Fgf8* expression in this region is critical for appropriate patterning of the facial primordium. Additionally, the first pharyngeal arch is poorly formed such that both the maxillar and mandibular domains are markedly smaller (Figure 5.6b). Interestingly, class-I mutant embryos revealed a normal level of *Fgf8* expression in the isthmus – a signalling centre responsible for patterning the adjacent midbrain and anterior hindbrain. This suggests that caudal brain structures may be unaffected by the compound mutation.

Comparison of wild type expression (Figure 5.6e and f), with that of a class-II mutant embryo (Figure 5.6g and h), revealed an almost complete absence of *Fgf8* expression at the midline, exposing the severity of the forebrain defect in this class of phenotype. Fgf8 expression is observed in the isthmus. However, this expression domain is reduced, seemingly proportional to the deformed appearance of the embryo. The expression domain in pharyngeal arches also appears slightly diminished in the mutant embryo (Figure 5.6g and h).

5.2.4 Expression of *Shh* in a class-II mutant embryo marks the presence of the forebrain-midbrain boundary, but reveals an absence of regions further anterior.

Shh is a useful marker at E9.5 for regions of the developing brain, the axis and, of significance for heart development, foregut and pharyngeal endoderm (Echelard *et. al.* 1993). Since class-II mutant embryos demonstrate the most severe forebrain defect (while still retaining evidence of rostro-caudal neural differentiation), the expression of *Shh* was used to detect the presence or absence of specific regions. Control (Figure 5.7a) and class-II *Sox4* mutant (Figure 5.7b) embryos each demonstrated *Shh* transcript labelling in the rostral foregut and the *zona limitans intrathalamica* (ZLI). The ZLI marks the boundary between the forebrain and midbrain and signals to pattern the adjacent forebrain and midbrain. *Shh* expression is undetected regions anterior to the ZLI in class-II embryos, while expression in the control is identified in the prechordal plate (Figure 5.7b). It is notable from this expression analysis that the ventral foregut, and the pharyngeal endoderm of class-II embryos appear to retain normal expression of *Shh* (Echelard *et. al.* 1993), suggesting that the *Sox4* mutation acts either downstream of Shh function, or in a separate pathway.

Figure 5.6: Expression of *Fgf8* in *Sox4*$^{ENU/ENU}$ *Foxq1*$^{sa/sa}$ embryos at E9.5. Heads of a wild type and class-I mutant were examined for *Fgf8* expression (A-D). In wild type embryos, expression is observed in the mandibular (Md) and maxillary (Mx) regions of the 1st pharyngeal arch (labelled in A,C). In the lateral view (A) expression is detected in the isthmus (Isth), while the frontal view (C) reveals normal expression in the anterior neural ectoderm at the commissural plate (black arrowhead) and the olfactory placode (black arrows). Mutant embryos demonstrate expression in the 1st pharyngeal arch, however this domain is reduced (labelled in B,D). The lateral view (B) reveals that expression in the isthmus appears similar to wild type. In contrast the frontal view of a mutant embryo (D) demonstrates a considerable reduction in the expression of *Fgf8* in the commissural plate (black arrowhead) and olfactory placode (black arrows). Comparison of a class-II mutant embryo (G,H) with litter-matched wild type (E,F) reveals considerable developmental delay, accompanied by diminished expression of *Fgf8* in the mutant forebrain (frontal view, H). In the mutant, expression is detected in the isthmus (arrowhead) tailbud (arrow) and pharyngeal arches adjacent to the heart (bracket G compared with E, F). These domains appear slightly reduced in the class-II embryo. Abbreviations: Isth., Isthmus; Md, mandibular first pharyngeal arch; Mx, Maxillary first pharyngeal arch. Images A-D same magnification; Images E-H same magnification.

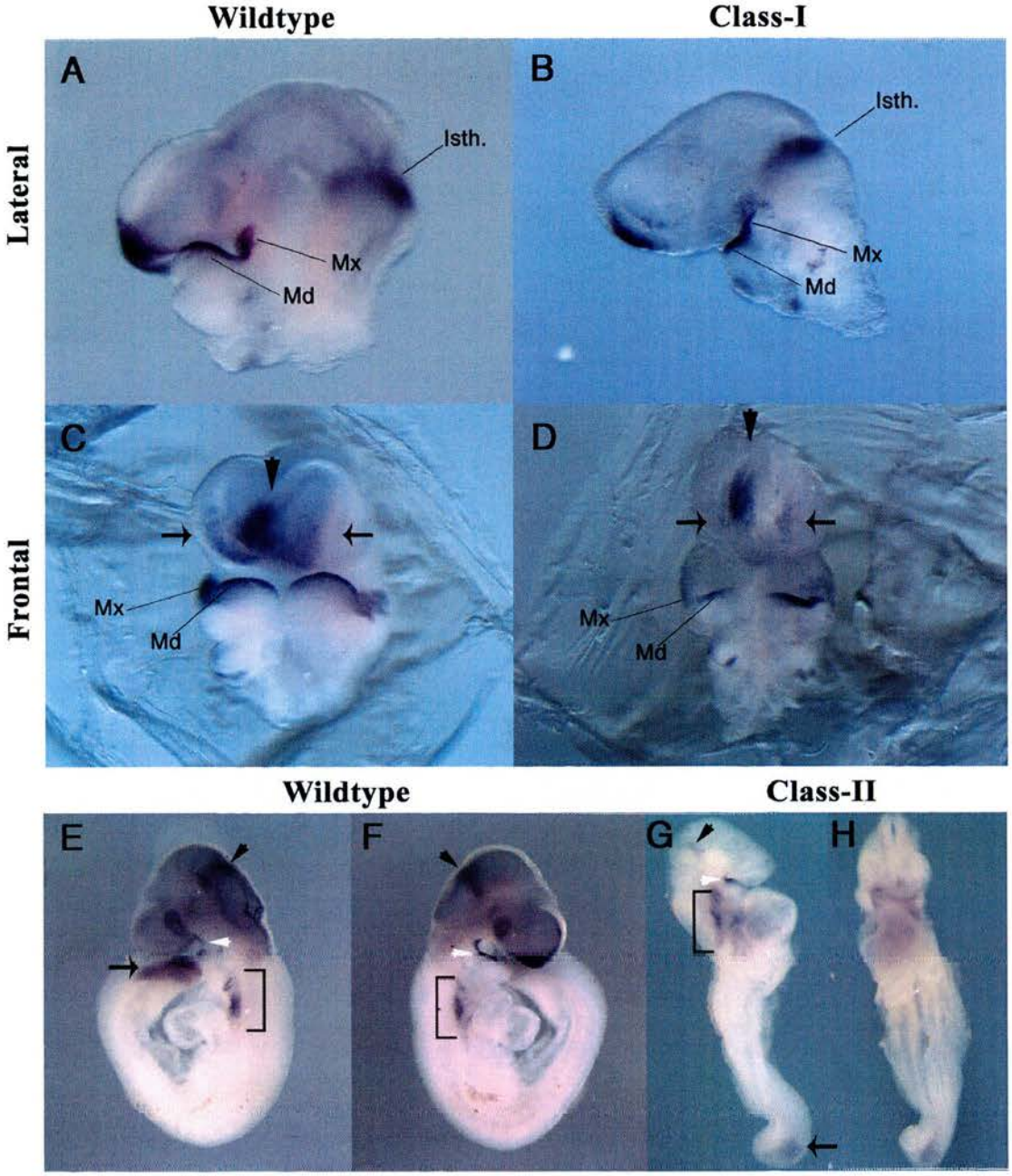
Wildtype
Class-I
Lateral
Frontal
A
B
C
D
Isth.
Mx
Md
Wildtype
Class-II
E
F
G
H

Figure 5.7: Expression of *Shh* in *Sox4*$^{ENU/ENU}$ *Foxq1*$^{sa/sa}$ embryos at E9.5. Wild type (A) and Class II mutant (B) embryos examined together for *Shh* expression by *in situ* hybridisation. Expression is detected in both the mutant and wild type embryo within the rostral foregut (FG), the zona limitans intrathalamica (ZLI), ventral foregut (bracket) and forelimb bud (FL), as well as the notochord and floorplate along the anterior-posterior axis of the embryo. Expression in the mutant embryo was detected in the same expression domains as in the wild type. Notably in the mutant embryo expression of *Shh* ceased at the ZLI and expression was not observed adjacent to the telencephalon in the prechordal plate as indicated in the wild type embryo (A, absent domains in B) Abbreviations: FG, foregut; FL, forelimb bud; Tele., Telencephalon; ZLI, zona limitans intrathalamica. Scale bar: A,380μm; B, 458μm.

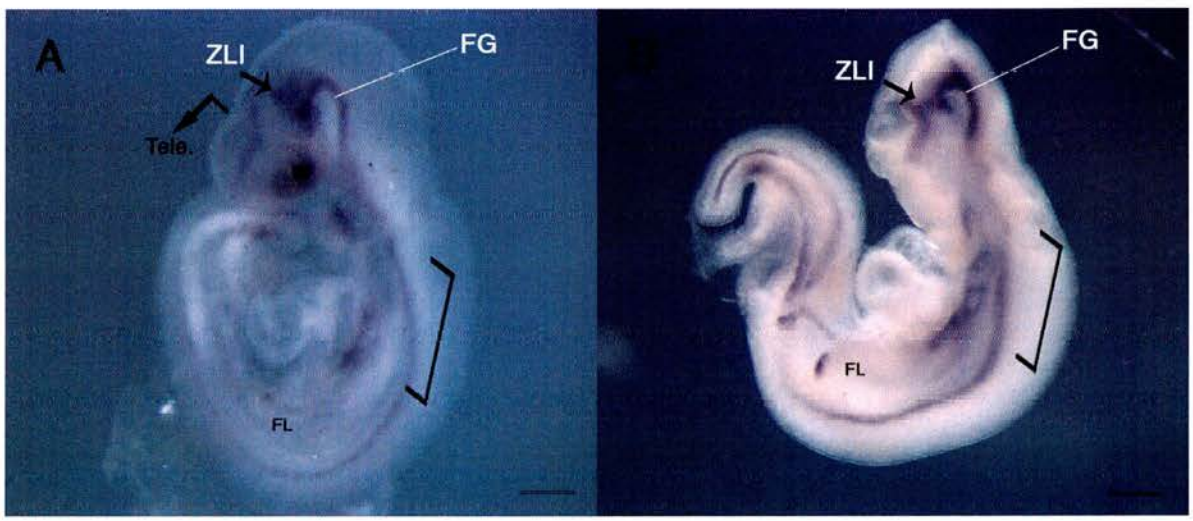
A
ZLI
FG
Tele.
FL
B
ZLI
FG
FL

5.3 DISCUSSION

Development of the heart relies on strict control over the regional differences of gene expression. There is a delicate balance between proliferation, growth, expansion of chambers and differentiation, in addition to appropriate molecular programming. Alterations to the normal progression of signalling may result in a primary phenotype. However the reaction of the heart to a primary phenotype may result in subsequent abnormalities, not directly related to the initial aberration. By examining dysregulation to gene expression in class-I and class-II embryos at E9.5, we are able to expand on our understanding of the possible causative embryonic origin of the cardiac deficiency observed by dysregulation of *Sox4*. Additionally, these results enable a degree of dissection of the forebrain abnormalities observed due to a possible genetic interaction between the mutant allele of *Sox4* and *satin*.

5.3.1 Mutation in *Sox4* alters the expression level of *Hand1*.

The dose-sensitivity of the heart to Hand1 and Hand2 proteins has been well characterised (McFadden *et. al.* 2005). It is possible that at least part of the *Sox4* phenotype is caused by a mild *Hand1/Hand2* deficit. Whilst there is evidence of right ventricle specification in *Sox4* mutant hearts, as shown by the presence of *Hand2* expression (Figure 5.2), there is also abnormal looping and poorly trabeculated myocardium at this stage (Results, Chapter 3). This degree of overlap with the phenotype resulting from conditional ablation of *Hand1* in myocardium combined with heterozygosity of *Hand2,* suggests that Sox4 may be involved in similar cellular processes as the Hand proteins. It is interesting that expression domains of *Hand2* are not abolished. Although examined in only two embryos at this stage, the cardiac expression domains appear to correspond with those of the control littermate embryo (developed under the same conditions), suggesting that ectopic expression is not observed. Due to the control not being appropriately staged, it is not possible to draw conclusions about whether *Hand2* expression is reduced. *Sox4* mutant embryos demonstrated a reduction in the embryonic expression domain of *Hand1*. However, expression of *Hand1* was not reduced in all expression domains, since expression in extraembryonic lineages was still retained at

equally strong levels across control and mutant. Whilst it may be the case that the lineage differences are due to the action of different promoters, the lack of overlap in expression of *Sox4* with *Hand1* (in the left ventricular myocardium) could only be explained if there was an indirect regulation of the embryonic promoter *via* additional intermediate secreted factors. A second explanation is also possible – mutation in *Sox4* has resulted in a reduction of the number of *Hand1* expressing cells by this stage of development. If aspects of the E9.5 phenotype of *Sox4* mutants are a consequence of reduced *Hand1*, the disruption to *Hand1* and expressing cells may occur prior to the phenotype arising. To clarify whether a role of *Sox4* exists in the regulation of *Hand1* requires substantial further investigation of their expression from an earlier stage of cardiogenesis.

5.3.2 Is Sox4 involved in processes leading to cardiac cellular proliferation or differentiation?

Outwith the heart, studies on Sox4 supports the possibility that Sox4 is involved in cellular processes leading to proliferation and/ or differentiation during development. BMP signalling is implicated in hair follicle differentiation from hair follicle stem cells, which are normally retained as slow-cycling cells in a small niche (termed the bulge). In this system, the hair germ at the base of the follicle, below the bulge, normally expresses a low level of *Sox4* transcript. Removal of Bmpr1a leads to proliferation of cells and ectopic expression of *Sox4* within the bulge and elevated expression in the adjacent hair germ (Kobielak *et. al.* 2007). In this system it appears that the hair follicle stem cell population undergoes excessive proliferation. Furthermore the population affected by the elevated expression of *Sox4* is that of the hair-follicle stem cells, which retain a more undifferentiated state. Further support for a possible role of Sox4 in the regulation of proliferation has come from analysis SOX4 in a cancer cell line. Expression of *cyclin D1* is regulated by SOX4 in the human colon cancer cell line, SW480 (Sinner *et. al.* 2007). It was observed that knockdown of *SOX4* by siRNA resulted in a decrease in proliferation (detected by phospho-histone H3 staining) and a decrease in *cyclin D1* expression. This was suggested to be due to knockdown of the interaction of SOX4 with β-catenin, which is also known to regulate expression of *cyclin D1*.

Results presented in this chapter suggest that expression of a cardiac marker associated with proliferation is reduced while at the same time, a marker of chamber myocardial differentiation is enhanced in a *Sox4*$^{ENU/ENU}$ *Foxq1*$^{sa/sa}$ E9.5 embryo. This is a starting point to exploring whether Sox4 plays an indirect role in regulating proliferation or differentiation of cells which form the heart. There are two ways in which Sox4 could act in this manner: The first possibility is that wild type Sox4 is involved in cellular proliferation and thus converges on a function of Hand1 or *Hand1*-expressing cells. The second possibility is a role of Sox4 in repressing differentiation and thus differentiation markers, such as *Nppa.* Analysis of these markers alone is insufficient to conclude whether the phenotype in mutant embryos is a consequence of either a reduction in proliferation or enhanced differentiation, although their association supports these possibilities. Analysis of the number of proliferative cells in mutant hearts would be the first step in examining this further. Detection of phospho-histone H3 levels in sections of mutant hearts prior to and during development of the abnormal phenotype would be useful to examine this possibility. Given that *Hand1* expression commences at earlier stages of development than that shown as results for class-I mutant embryos, this proposed analysis would be conducted from earlier stages, to examine whether proliferation is reduced from the heart tube stage prior to and during looping.

5.3.3 What is the cause of increased *Nppa* expression in the right ventricle in *Sox4*$^{ENU/ENU}$ *Foxq1*$^{sa/sa}$ mutant hearts?

In a normal E9.5 heart, *Nppa* transcripts appear lower in the right ventricle, compared with the left ventricle, during the transition from embryonic myocardium to functional myocardium. Results in this chapter reveal elevated expression of *Nppa* in the right ventricle. Ectopic expression of *Nppa* may suggest that a lack of *Sox4* results in enhanced differentiation. The only possibility for this change in expression at the molecular level would be an indirect role of Sox4 from the OFT, being to direct expression of a signalling factor, which in-turn regulated *Nppa* expression in a gradient across the developing RV myocardium. As *Sox4* is expressed in the endocardium of the OFT, adjacent to the SHF myocardial cells which contribute to RV development, it may also be possible that expression of *Sox4* is required for contribution of progenitor cells to the RV. In the absence of this, the

RV may be more populated with normally left ventricular, or FHF, myocardium. However *in situ* analysis of *Nppa* alone is not sufficient to reveal if this is the case. Rather, it would be necessary to examine mutant embryos for expression of LV or FHF myocardial markers, such as Tbx5 (Bruneau *et. al.* 1999).

An alternative possibility, for the increase in expression of *Nppa,* is that the expression could be induced as a consequence of the malformed heart attempting to compensate for the early cardiac defects by enhancing myocardial differentiation and thus is an indirect consequence of the phenotype. It is known that *Nppa* expression is dynamic during the life of the adult heart (reviewed in (Houweling *et. al.* 2005)). In cases of heart failure, expression of *Nppa* is reactivated. During embryogenesis the heart undergoes a response to cardiac stress if demands on early cardiac function outweigh the ability of the heart to pump. In the developing mouse heart at E11.5, the expression of *Nppa* has been shown to be associated with populations of more differentiated cardiomyocytes (Zhang *et. al.* 2007). However, *Nppa* expression and thus differentiation occurs much earlier than this. The cardiac knockout of *Hand1* demonstrates a substantial increase in the expression of *Nppa* in the right ventricular chamber at E9.5 (McFadden *et. al.* 2005). This is not an expression domain of *Hand1* and thus expression of *Nppa* at this stage was attributed to be a secondary response to cardiac stress. Neither is the RV an expression domain of *Sox4.* Furthermore, *Sox4* mutants demonstrate inadequate looping and cardiac swelling at the stage of *Nppa* upregulation. Thus it is possible that expression of *Nppa* is an effect of the phenotype, rather than a contributing cause. Although to verify this hypothesis, it is necessary to examine cardiomyocyte differentiation by other markers of differentiation such as by immunohistochemistry on sarcomeric proteins.

There still remains the appearance that the ectopic expression occurs only within the myocardium of the RV. This may be a consequence of the quality of the *Nppa* probe and strong expression already existing within the other three cardiac chambers, leaving little ability for the *in situ* hybridisation to be semi-quantitative. To examine whether the phenotype is RV specific, it would be necessary to examine gene expression quantitatively in micro-dissected hearts (as detailed in this chapter) to determine whether the elevation only occurs in the RV.

5.3.4 Determining whether Sox4 plays a role in the process of EMT in the developing OFT

To date, the association of Sox4 with the morphological process of an epithelial to mesenchymal transition comes from examination of cancer cell lines in culture. Expression of inhibitory micro-RNAs, which block *Sox4* translation, is specifically lost when breast cancer cells develop metastatic potential (Tavazoie *et. al.* 2008). Indeed in tumorigenesis, *Sox4* expression is predominantly enhanced (section 1.1.3). It has been proposed, from results in previous chapters, that there is an association of *Sox4* expression with regions in which EMT is required for cardiac development. The phenotype of the $Sox4^{ENU/ENU}$ mutant may include abnormal production of mesenchyme. This study has also raised the possibility that the severest class-III embryos are deformed as a consequence of abnormal gastrulation – a process that also requires EMT. Additionally, it is evident from histology shown in chapter 3 that a disruption to the body mesenchyme is also a component of the phenotype (chapter 3, not discussed, also evident from sections Figures 3.1, 3.3 and 3.5). *Sox4* expression is consistently observed in mesenchyme in all regions examined (chapter 4, not discussed, also evident from section *in situ* figures 4.5 and 4.6). Thus there may be a role for Sox4 in the development of mesenchyme. A developmental role for Sox4 in EMT has not been characterised, nor have other extracardiac domains in which EMT is required for development, such as the kidney, been examined for a phenotype in this mutant. The marker analysis conducted by quantitative PCR on extracts from the OFT was intended to uncover a possible mechanism through which Sox4 may act.

Embryos null for *Wnt11* demonstrate some overlap in OFT defects with those observed in *Sox4* mutant homozygotes (Zhou, W *et. al.* 2007). It is for this reason, and that Wnt11 was identified as a regulator of *Tgfβ2,* that *Wnt11* expression was examined. By microdissection and quantitative PCR, one class-I OFT revealed an increase in the transcript levels of *Wnt11*, its receptor *Fzd7* and immediate downstream target gene *Tgfβ2.* Whilst this may seem initially to be a contradiction, since it is embryos which lack *Wnt11* that resemble the *Sox4* mutant OFT phenotype, it is plausible that Wnt11 levels are dependent upon expression of *Sox4* from the endocardium or from within the mesenchyme once it is produced. Evidently this

potential function of Sox4 requires further investigation with increased sample size, since this analysis was performed on only a single mutant sample compared with pooled control tissue from multiple hearts. Nevertheless, a few possibilities arise that require further investigation, with a greater number of mutant embryo OFT samples:

(1) It may be possible that Tgfβ2 acts through Sox4 to regulate an aspect of the cardiac EMT, and the mutant Sox4 is incapable of transducing the Tgfβ2 message.

(2) Given the elevated levels of *Wnt11, Fzd7* and *Tgfβ2* expression, it may be possible that *Sox4* expression from the endocardium and subsequent myocardium serves to feed back on *Wnt11/Fzd7* expressing cells to regulate gene transcription both of *Wnt11* and *Fzd7* and thereby expression of *Tgfβ2.*

(3) The normal transcriptional level of gene expression may be initially higher than subsequent developmental stages. Although the mutant embryo was stage matched to the pooled control embryo tissue, it is possible that not all were developmentally matched. The elevated gene expression in the mutant may simply be another consequence of the of a developmental delay.

Whilst these are interesting possibilities, clearly they require further investigation with an increased number of samples, not only examining expression by quantitative PCR, but also expression by *in situ.* Furthermore, although *Tgfβ2* is known to be involved in cardiac EMT, and Wnt11 is known to function upstream of *Tgfβ2* expression in the heart, Wnt11 signalling has not yet been shown directly to induce EMT in the heart, despite evidence from other systems (as outlined in the introduction to this chapter). Explant cultures (Runyan *et. al.* 1983), of the OFT from hearts of *Wnt11* null embryos, would enable determination of whether the morphogen is essential for normal endocardial EMT. If abnormal migration is observed in this assay, subsequent addition of Wnt11 (as conditioned media) and a recovery of the ability of endocardial cells to undergo EMT would support this function of Wnt11 in the heart. Blocking signalling through Fzd7 would further enable it to be shown conclusively that Wnt11 signals through this receptor in the

heart. Additionally, it would be possible to determine whether *Sox4* mutant OFT are able to respond to Wnt11 signalling by conducting an explant assay. If an EMT defect was observed in *Sox4* mutant tissue, and if this was not recovered by Wnt11 stimulus, Sox4 would be known to function downstream or independently of Wnt11.

Whilst the markers examined in this study were initially considered to be most useful, for the reasons outlined in the introduction to this chapter, in hindsight there are additional markers which would be useful for uncovering the role of Sox4 in cardiogenesis. A number of these have been described in detail within earlier chapters. For the purpose of discerning whether a role for Sox4 exists in cardiac EMT, an explant assay of mutant cardiac tissue would be informative (as detailed, chapter 3, section 3.3.2). In the context of marker analysis, E9.5 –E10.5 hearts could be examined for the localisation of markers, the presence of which is known to be altered at the cellular level during EMT. Examination of the endocardial cells and subsequent mesenchyme by immunohistochemistry could show whether the endocardium inappropriately retains cell-cell contacts and whether the mesenchyme expresses an appropriate repertoire of markers (for example, Sox9 (Akiyama *et. al.* 2004), ErbB3 (Lakkis *et. al.* 1998)). Certainly, examination of these aspects of EMT biology will contribute substantially to the understanding of the role of Sox4 in cardiogenesis.

It has been proposed that Sox4 may play a role in the cellular processes regulating proliferation. Combining this with a possible role for Sox4 in EMT, it may be that reduced cell number of *Sox4* expressing cells may contribute to the phenotype of the OFT. Whilst the examination of cell number in the developing OFT cushions has not been quantitative, the E12.5 OFT endocardial cushions demonstrate less population by cushion mesenchyme (smaller cushions, observed in E12.5 embryos, Figure 3.2 g, k and h, l, compared with control c, d). Dysmorphology of the OFT at E9.5, in addition to the abnormal swelling, may be a consequence of reduced cell number. It has been shown and discussed in this thesis that the level of Vegf signalling is critical for EMT and that both elevated levels and haploinsufficiency are capable of disrupting cardiac EMT (Carmeliet *et. al.* 1996). A reduced cell number in the OFT may be causative of a delay or defect in the process of EMT. It has been

shown that both *Sox4* and *Nfatc* are expressed in the OFT endocardium. Although the *Nfatc* expression domain has not been altered in *Sox4* null hearts at E12.5 (Ya *et. al.* 1998b), expression levels of *Nfatc* have not been examined at earlier stages in $Sox4^{ENU/ENU}$ mutants at the stage in which Nfatc protein is known to act to induce cardiac EMT (Chang *et. al.* 2004). A reduced cell number in the endocardium, which initially is the only site of *Sox4* expression in the heart, may alter Vegf levels. Thus two markers of the process of endocardial cushion formation, which should also be examined in $Sox4^{ENU/ENU}$ mutant hearts, are *Nfatc* and Vegf.

5.3.5 Reduced expression of *Fgf8* and *Shh* in anterior domains exposes the degree of forebrain abnormality in Class-I and Class-II mutants.

Class-I and class-II mutant embryos were examined to determine the extent of the forebrain abnormality. *Fgf8* expression marks the anterior-most neurectoderm, the anterior structures of the commissural plate and olfactory placodes (section 5.1). *Shh* marks the prechordal plate and is also useful for analysing the caudal extremity of the telencephalon, since it marks the ZLI (section 5.1).

It has been shown that even class-II mutants express *Shh* in the expected pattern at the telencephalic boundary, whilst development is abnormal anterior to the ZLI. *Shh* expression does not appear to be detected in the prechordal plate. Thus, anterior regions are either incorrectly patterned or are absent. Furthermore, expression of *Fgf8* is barely detectable in the anterior region of class-II embryos, while a reduction is observed in the anterior expression domains of class-I embryos. Given that $Sox4^{ENU/ENU}$ $Foxq1^{sa/sa}$ phenotype is observed at E9.5, and that at E8.5 homozygotes are largely indistinguishable from heterozygotes or control embryos, it is likely that Sox4 and Foxq1 are required around E8.5. Since *Sox4* and *Foxq1* demonstrate strong expression in the endoderm from early head-fold stage, it is possible that the requirement for these genes resides in their endodermal and neurectodermal expression from the head-fold stages (Chapter 4; figures 4.2 and 4.11).

The anterior phenotype revealed in this study is similar to that reported for other mutants isolated from the ENU mutagenesis screen, using *satin* as a selective recessive marker (Bogani *et. al.* 2005; Willoughby 2006). Interestingly, $Sox4^{ENU/ENU}$ $Foxq1^{sa/sa}$ class-I mutants demonstrate a similar reduction or loss of *Fgf8* and *Shh*

expression as that reported for other isolated ENU mutant lines which do not demonstrate the cardiac phenotype observed in *Sox4* mutant embryos. Other ENU mutant phenotypes were analysed in hemizygous mutant embryos (crossing to the *Del(13)Svea36H* mouse), which lacked one allele of both *Sox4* and *Foxq1*, while the remaining *Foxq1* allele contained the *satin* deletion. Given this, and the overlap of phenotype (Chapter 3 discussion, section 3.3 part 2), it is increasingly likely that Sox4 and Foxq1 co-function during early anterior patterning, prior to a visible defect arising at E9.5. Clearly, the requirement for *Sox4* and *Foxq1* in anterior structures requires further investigation.

5.4 SUMMARY OF THE IDENTIFIED MOLECULAR CHANGES IN *Sox4*$^{ENU/ENU}$ *Foxq1*$^{SA/SA}$ EMBRYOS, COMPARED WITH CONTROL EMBRYOS

We have been able to study the effect of the dual *satin* and *Sox4* mutations. While *Sox4* null embryos were suggested to have a mild anterior phenotype, the presence of the *satin* allele modulates this. This chapter has shown that the development of anterior structures is severely compromised in a class-II mutant which lacks *Shh* expression in anterior domains. Although still defective, class-I mutants demonstrate some anterior patterning, as indicated by the presence of *Fgf8* expression, although this is reduced relative to wild type.

During cardiogenesis, it appears that homozygosity for the mutant *Sox4* allele causes expression domains *Hand1* to be reduced, but not ablated – perhaps due to an underlying defect in proliferation, which needs to be examined. An upregulation of the cardiac marker *Nppa* in the right ventricle is suggestive of enhanced differentiation in mutant embryos; although this could be a consequence of cardiac stress. In order to be conclusive about the embryonic function of Sox4, further marker analysis is required. In addition it is necessary to explore the phenotype and molecular consequences of *Sox4*$^{ENU/ENU}$ with normal expression from the *Foxq1* allele.

CHAPTER 6: ANALYSIS OF *Sox4*$^{ENU/ENU}$ EMBRYOS, WILD TYPE FOR *Foxq1*.

6.1 INTRODUCTION

Previous chapters have documented aspects of the embryonic phenotype arising from the *Sox4*$^{ENU/ENU}$ *Foxq1*$^{sa/sa}$ genotype in compound mutant embryos (chapter 3). Results indicate that components of this phenotype are a consequence of a genetic interaction between the *Foxq1*^{sa} allele and the *Sox4*^{ENU} allele, while others are a consequence of mutation in *Sox4* alone. Expression analysis of *Sox4* and *Foxq1* reveals co-expression of these two transcripts in the developing endoderm and anterior neural ectoderm from the early somitogenesis stage (chapter 4). Together with evidence of a reduction or absence of anterior structures in some mutant embryos, as shown by *Shh* and *Fgf8* expression at E9.5 (chapter 5), it is clear that for normal development, there is a requirement for Sox4 and Foxq1 in patterning of the telencephalon and adjacent anterior tissues (eye, olfactory placode, mandibular and maxillary arches that contribute to the structures of the face) from the early stages of anterior morphogenesis. Whilst such defects have not been reported for *Foxq1*$^{sa/sa}$ embryos (Hong *et. al.* 2001), anterior defects have been observed in some *Foxq1*$^{-/-}$ embryos (Goering *et. al.* 2008). It is possible that aspects of this phenotype may still be observed in some *Sox4* single mutant embryos. However, if the phenotype is exacerbated because of the compound mutation then it would be expected that *Sox4* mutants demonstrate a less severe phenotype. Whether there is a direct interaction between both proteins; whether they act independently on the same signalling pathway; or whether they exert their function on pathways which simultaneously or sequentially act in the same tissue, remains unknown. It has been shown that the phenotype of the compound mutant, *Sox4*$^{ENU/ENU}$ and *Foxq1*$^{sa/sa}$, differs from the phenotype published for *Foxq1*^{sa}, *Foxq1*$^{-}$ and *Sox4*$^{-}$ alleles. Such an interaction is

novel and requires further investigation to determine the embryonic origin of the defect, and protein analysis to examine functional overlap.

The findings presented in previous chapters have also suggested that mutant *Sox4* in the endoderm from the head-fold stage, combined with expression in OFT and AVC endocardium and mesenchyme from E9.5, accounts for the cardiac abnormalities observed in the compound mutant. Although the precise requirement, whether it be by the NCC, the SHF cells or by endocardium undergoing EMT, remains to be determined. In order to state conclusively which aspects of the compound mutant phenotype are attributable to $Sox4^{ENU}$, this allele needs to be examined in the genomic context of wild type *Foxq1*. Thus, the aim of this chapter is to: *Commence analysis of the phenotype of* $Sox4^{ENU/ENU}$ *embryos wild type for Foxq1 combining methods of analysis used in chapters (3) and (5).*

Segregation of the two alleles through breeding was one method through which this could be accomplished. After six generations of backcrossing from the M91 line onto C57Bl/6J, two mice (from different litters) were observed to have segregated the mutant alleles and thus harboured only the ENU-induced *Sox4* mutation. These mice were backcrossed to C57Bl/6J mice to expand the line and generate sufficient mice for intercrossing and thus examination of the homozygous phenotype. Marker analysis in this chapter largely overlaps with that performed on compound mutant embryos in the previous chapter with the intent to enable comparison of expression. In addition, given that looping defects appear consistent between the $Sox4^{ENU/ENU}$ single mutant hearts (results in this chapter) and the $Sox4^{ENU/ENU}$ $Foxq1^{sa/sa}$ compound mutant hearts (results, chapter 3), the expression of *Pitx2* was examined. Pitx2 marks the inner curvature of the looping heart tube (Campione *et. al.* 2001). It was intended to establish whether abnormal looping correlated to perturbed expression of *Pitx2* in this domain in both single and compound mutants. However time constraints and lack of availability of compound mutants, at the stage at which *Pitx2* was examined in single mutants, prevented this comparison. Continuing with the analysis of compound mutants in chapter 5, the expression of *Fgf8*, *Hand1* and *Nppa* are examined here with single mutant $Sox4^{ENU/ENU}$ embryos. The preliminary

results in this chapter thus contribute to determining the origin of the cardiac phenotype induced by mutation in *Sox4*.

6.2 RESULTS

6.2.1 Phenotypic analysis of homozygosity of the Sox4^{ENU} allele

To determine which regions require *Sox4* in development, embryos from heterozygous intercrosses were examined from E9.5-E13.5. For the analysis of phenotype, the limited number of embryos examined reflects that this data was obtained at the end of the breeding programme.

In a manner similar to *Sox4*$^{-/-}$ and *Sox4*$^{ENU/ENU}$ *Foxq1*$^{sa/sa}$ E12.5-E14.5 embryos, one E13 *Sox4*^{ENU} homozygote (n=1/1) revealed a visible embryonic phenotype when compared with a control littermate. Pericardial swelling and severe oedema in the body cavity was observed, accompanied by trapped blood, both in the heart and body cavity (Figure 6.1a (control), b and c (frontal and dorsal view of the one mutant E13 embryo)). Clearly cardiac insufficiency is retained as part of the *Sox4*$^{ENU/ENU}$ mutant phenotype. At E13 anterior defects were not observed. Craniofacial development appears normal, as does eye pigmentation. The difference in eye pigmentation was a key differential between all observed compound mutants at this stage (Chapter3; n=5 E12.5; n=6 E13.5; Table 3.3) and control embryos (chapter 3; Figure 3.1 and 3.17). An embryo examined at E11 demonstrated normal anterior development but slight swelling of the pericardial cavity and, upon dissection, swelling of the heart was evident (Section 6.2.2 *Nppa* expression; Figure 6.5). Although neither the E13 nor E11 embryo demonstrated a craniofacial phenotype, the low number examined in this study (n=2/2) does not eliminate the possibility that mutation in *Sox4* alone is capable of causing a craniofacial phenotype of variable penetrance and/or expressivity.

In *Sox4* heterozygote crosses, the phenotype was also examined from E9.5-E10.5. The phenotype of *Sox4*$^{ENU/ENU}$ embryos is similar to that described for the compound mutation (Figure 3.8). The phenotype appears to follow a similar pattern of severity as that of the cardiac aspect of the *Sox4*$^{ENU/ENU}$ *Foxq1*$^{sa/sa}$ mutants. In comparison to control littermates (Figure 6.2a, b), of five homozygotes examined, three class-I

mutants demonstrated a mild defect in cardiac looping (Figure 6.2c, d), while one class-II mutant demonstrates a "class-II" swollen heart (as classified in chapter 3) but only a slightly deficient forebrain (Figure 6.2e). This is in contrast to class-II compound mutants in which the forebrain defect was significantly more pronounced (compare figure 6.2 with figure 3.4). Examination of *Fgf8* expression revealed that, even in the one $Sox4^{ENU/ENU}$ class-II embryo (n=1/1), *Fgf8* domains at the anterior midline and olfactory placode are present (Figure 6.3). One embryo examined at this stage could be classified as demonstrating a severe class-II phenotype (Figure 6.2f). This particular embryo lacked appropriate anterior development and demonstrated exposed cranial neural folds, although neural tube closure has occurred below the hindbrain. Axis extension had progressed to 30 somites (compared with 35 in a control littermate) and limb development had commenced. Despite the low number (n=1/5 of all E9.5-10.5), this suggests that a small proportion of embryos homozygous for *Sox4* still undergo a severe disruption at an early stage of development, prior to the requirement of *Sox4* in formation of the heart. This is also shown by the ratio of genotypes from heterozygous crosses. (Table 6.1). As the numbers of embryos was small, it is not possible to state whether there is a statistically significant change to the expected Mendelian ratio. However, the presence of one reabsorption site at E11.5-13.5 suggests that embryonic death before this stage occurs in $Sox4^{ENU/ENU}$ mutants.

From these results it seems that the craniofacial phenotype observed in the $Sox4^{ENU/ENU}$ $Foxq1^{sa/sa}$ compound mutant is possibly derived from a genetic interaction between these two factors. Additionally, these preliminary results further suggest the requirement of *Sox4* at early stages of development, causing embryonic death prior to that which is a consequence of cardiac insufficiency at E14.5.

Figure 6.1: One embryo at E13, homozygous for *Sox4*^{ENU}, shows pericardial swelling, haemorrhaging and generalised oedema. The whole-embryo phenotype of *Sox4*$^{ENU/ENU}$ is pronounced at E13. When compared with a wild-type littermate (A), the homozygote embryo (B, frontal; C, dorsal) exhibits trapped blood in the heart (white arrow, B compared with wild-type A) and haemorrhaging within the body cavity (black arrowhead, C), as well as oedema, revealed by swelling and folds of skin (white arrowhead, C). Scale bar: A – C, 361μm

A
B
C

Figure 6.2: Embryos at E9.5 homozygous for *Sox4*^{ENU} demonstrate a complex phenotype. Wild-type embryos (A,B) demonstrate normal cardiac development . In contrast, mutant embryos (C-F) demonstrate defective looping. The mild class-I mutant embryos (C,D) demonstrate inadequate looping. (E) A severe class-I mutant embryo demonstrated significant cardiac swelling. (F) One severe class-II mutant embryo was examined at this stage and demonstrates hypoplasia of the heart tube and inadequate folding of the neural tube. Mutant embryos (C-D) do not demonstrate a significant reduction in anterior structures (arrow indicates rostral telencephalon). Abbreviations: LV, left ventricle; OFT, outflow tract. Scale bar: A – F, 570μm.

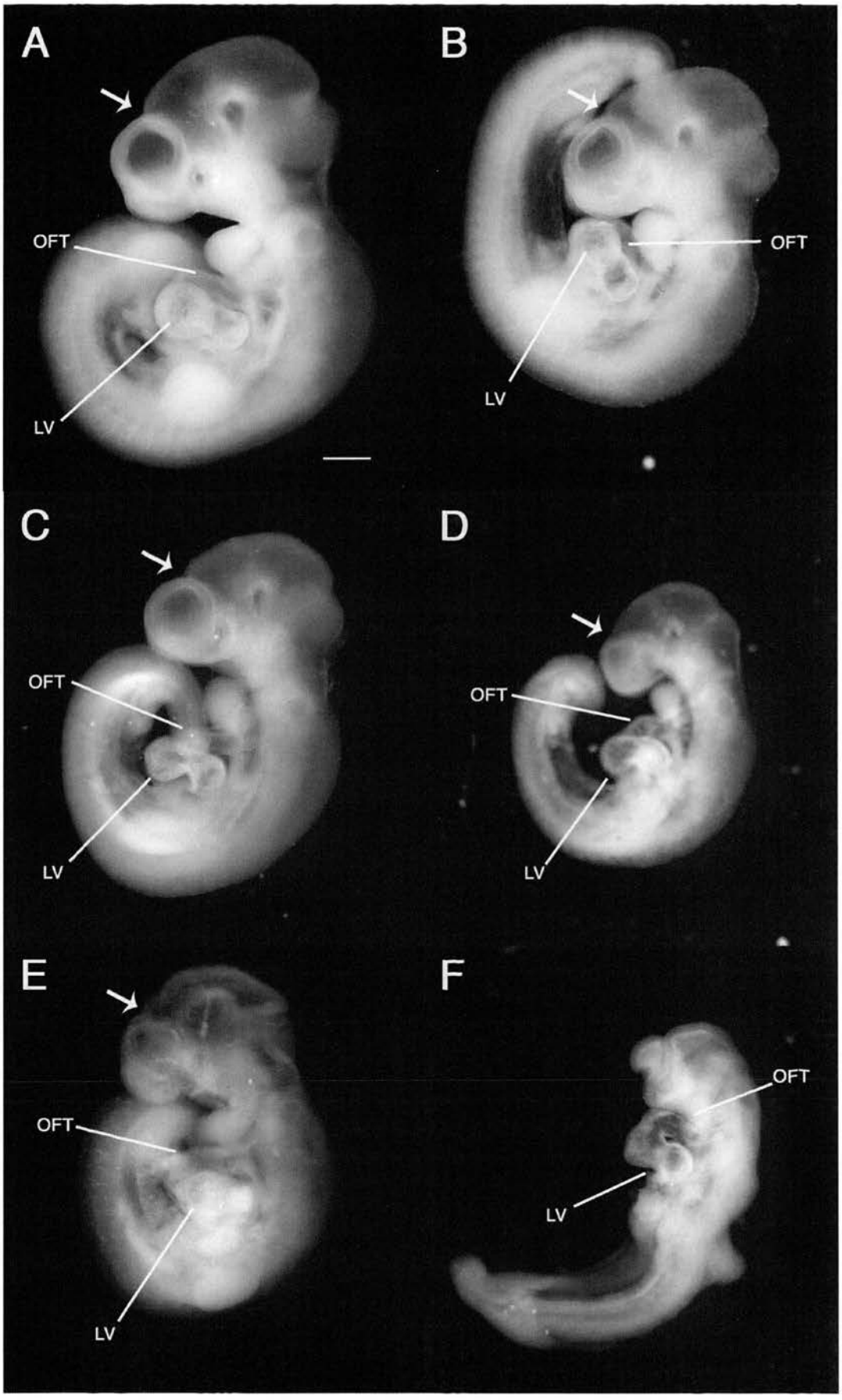
A
OFT
LV
B
OFT
LV
C
OFT
LV
D
OFT
LV
E
OFT
LV
F
OFT
LV

Figure 6.3: Expression of *Fgf8* in *Sox4*$^{ENU/ENU}$ mutant embryos E9.5. (A) Wild-type embryos demonstrate normal expression of *Fgf8*. (B) A class-II mutant embryo do not demonstrate a lack of any expression domains observed in the wild-type (pharyngeal arches indicated by bracket). However, expression in the pharyngeal arches appeared reduced (white arrowhead, B compared with A). *Fgf8* expression in the anterior neurectoderm persists in the mutant embryo (olfactory placode, white arrow; midline, black arrow). Abbreviations: FL, forelimb bud; HL, hindlimb bud; Isth., Isthmus; Tele., telencephalon. Images A and B are the same magnification.

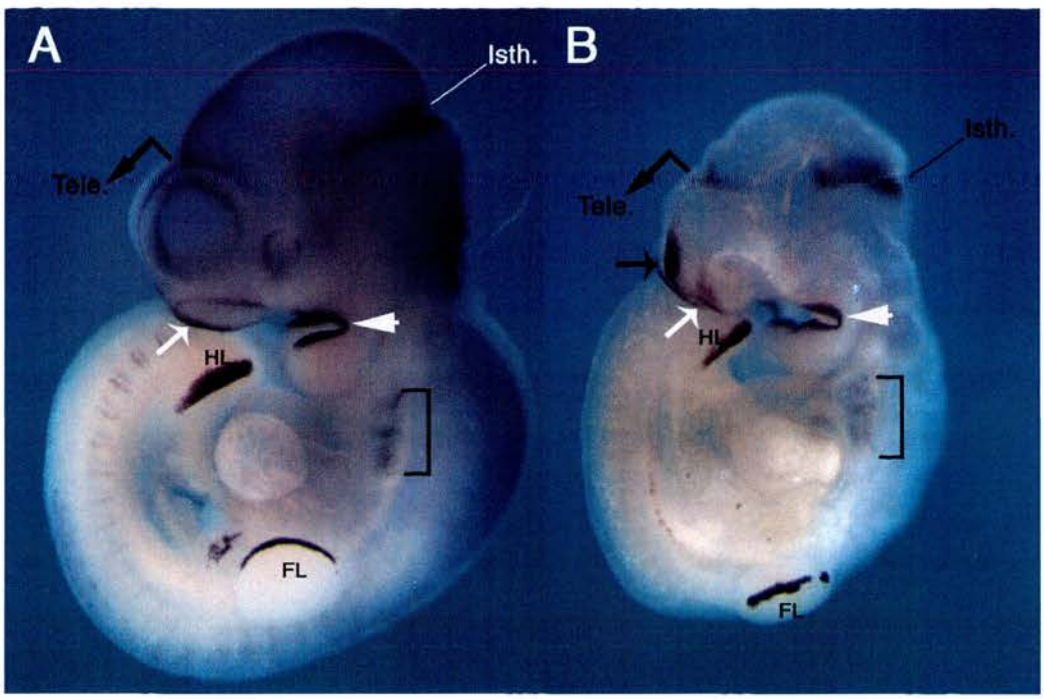
A
Isth.
Tele.
HL
FL
B
Isth.
Tele.
HL
FL

Table 6.1: Ratio of genotypes in *Sox4*$^{+/ENU}$ intercrosses at selected stages during development.

Stage	Number	Homozygous		Heterozygous		Wild type	
9.5-10.5	19	5	26%	9	47%	5	26%
11.5-13.5	17	3 (1)	18%	10	59%	4	24%

Stage, embryonic stage of development; *Number*, observed number of embryos genotyped at the *Sox4* locus, subsequently grouped according to genotype. Findings are depicted as both the number of embryos for each stage and genotype, and the percentage for each genotype. Value in brackets shows the number of reabsorption sites for that genotype at that stage. Reabsorption sites were excluded from calculation of the percentage of genotype.

6.2.2 Embryos homozygous for *Sox4*$^{ENU/ENU}$ demonstrate an alteration to cardiac gene expression.

To examine whether the alterations to cardiac gene expression observed in the compound mutant also occur in single mutant embryos with the *Sox4* mutation, we examined *Hand1* and *Nppa* expression.

Expression of *Hand1* is associated with proliferative cells in the OFT and in the outer curvature of the left ventricle (as discussed section 3.3.2). Cardiac *Hand1* transcript is detected in both regions in the E9.5 single mutant and control embryos. Lower magnification reveals expression to be relatively similar in both the wild type control (Figure 6.4a) and class-I mutant (Figure 6.4c). Higher magnification of the cardiac expression reveals the control heart to have undergone correct looping, and normal *Hand1* expression is reflected as a gradient of staining along the length of the OFT, with higher intensity at the dorsal aspect (Figure 6.4b). In the *Sox4* mutant this domain of expression appears reduced in length, although the OFT itself does not appear to have shortened, as examined here (Figure 6.4d). A degree of defective looping is prominent in this class-I embryo as the heart is not as tightly looped as in the control, causing the OFT to still extend anteriorly rather than posteriorly towards the atria. Expression appears unchanged in the left ventricle, although this was not confirmed by quantitative analysis.

The domains of cardiac expression are consistent between this experiment and the *Hand1* analysis in chapter 5. It is striking though, that the intensity of staining differs. This is due to different *in situ* conditions in the process of staining. The gradient of reduced *Hand1* expression, shown in chapter 5, was revealed by understaining the signal (section 5.2.1). In hindsight consistent timing for exposure would have enabled a better comparison in this study between the two mutant lines. Longer staining times may reveal the extent of disruption to the *Hand1* expression domain more fully. Nevertheless, the cardiac expression domains of *Hand1* differ consistently in expression levels between the mutant embryo and control embryo. Since the pattern is similar between both mutant *Sox4* lines, the possibilities discussed in Chapter 5, whereby it was suggested that Sox4 function may converge on that of Hand1, and play a role in proliferation, are further supported here. This

provides a further reason to explore proliferation in the developing heart, and examine whether this correlates with a developmental point at which a loss of *Sox4* may cause the initial step to result in the appearance of a phenotype.

At E9.5, a $Sox4^{ENU/ENU}$ $Foxq1^{sa/sa}$ mutant demonstrated elevated expression of *Nppa* in the right ventricle (Chapter 5; figure 5.4). Since the affected domain of *Nppa* expression does not express *Sox4*, it was proposed that this expression can be attributed to altered maturation and differentiation of the myocardium. With a lack of any evidence for downstream signalling by Sox4 target genes at this stage, which could result in dysregulation of *Nppa* expression, the enhanced differentiation could equally be attributed to the abnormal cardiac morphology resulting in stresses on the early cardiac chambers and thus premature differentiation in RV myocardium.

To explore whether this was consistent in $Sox4^{ENU/ENU}$ embryos, and whether the elevated expression levels persisted in the subsequent days of development, *Nppa* expression was characterised in E11 embryos (Figure 6.5a, b). Control hearts demonstrated strong expression of *Nppa* in the left ventricular chamber and in both atria. Expression in the right ventricle is weak and *Nppa* transcript is not detected in the AVC or OFT (Figure 6.5c). Aberrant Sox4 function does not appear to alter expression of *Nppa* significantly in the left ventricle or left atrium, nor does it induce *Nppa* expression within the OFT or AVC. However, consistent with findings for the younger compound mutant embryo, the single mutant $Sox4^{ENU/ENU}$ embryo demonstrates striking right ventricular expression (Figure 6.5d). Furthermore, the single mutant heart demonstrates substantially stronger staining in the right atrium.

The heart appears larger in the mutant embryo at this stage, with the OFT exhibiting swelling (Figure 6.5d, compared with control c, further emphasised in (d) by the red line indicating the extension, on the length of the line shown in (c)). It is possible that the right atrium is also larger, although the postero-dorsal side of these hearts were not imaged and this can not be said with certainty.

In the normal heart, the stresses caused by peristaltoid contraction along the heart tube are thought to regulate the initial formation of trabeculae (Thompson *et. al.* Chapter in (Clark *et. al.* 2000)). With looping and the commencement of ventricular

septation, the pressure on the myocardium becomes uneven across the heart, and trabeculations in the left ventricle appear thicker than those in the right ((Sedmera *et. al.* 1997; 1998; Wenink 1992; Wenink *et. al.* 1982) and reviewed in (Sedmera *et. al.* 2000)). The enhanced level of *Nppa* expression shown here, combined with the appearance of a swollen heart in the $Sox4^{ENU/ENU}$ mutant embryo, further supports the possibility that enhanced differentiation is occurring as a consequence of the abnormal cardiac morphology and thus elevated stress on the cardiac tissue. Examination of the histology of the cardiac tissue may reveal this further. Abnormal maturation of right ventricular myocardium may exert an effect on the development of anterior cardiac structures, including formation of the OFT endocardial cushions if the myocardium extends into this region. This, in turn, may contribute to the septation defects, including DORV and PTA below the developing semi-lunar valves, as observed with mutation to *Sox4* described in chapter 3.

In the normal developing heart, the atria also respond to increases in myocardial stresses by changes the myocardial architechure (Anderson *et. al.* 1996; Hu *et. al.* 1995). The right atrium develops significantly more pectinate muscle than the left. Elevated staining of *Nppa* expression in the right atrium is suggestive of altered differentiation within this chamber, which is not an expression domain of *Sox4*. Elevated right atrial contractility may contribute to the defects at the venous pole of the heart. Although the atrial myocardium was not examined in detail for the stages shown, the delay in formation of the atrial septum and the appearance of a common atrioventricular valve through some sections of each mutant heart may be a consequence of an increase in the stresses on right atrial development from this earlier E11 stage.

Figure 6.4: A *Sox4*$^{ENU/ENU}$ embryo shows abnormal expression of *Hand1* at E9.5. In both wildtype (A) and mutant (C) *Hand1* is expressed in the outflow tract (OFT) and adjacent continuous region of the pharyngeal arches (I and II). Expression is also detected in the outer curvature of the left ventricle (LV) and the lateral plate mesoderm (LPM). The cardiac region is enlarged in (B) wild-type and (D) mutant, as indicated by the bracket in (A) and (C). (D) The mutant embryo demonstrates a reduced expression domain of *Hand1* in the outflow tract. Additionally cardiac looping is impaired, compared with wild-type (B). The magnified region does not reveal alteration to gene expression in the left ventricle of the mutant compared with wild-type. Abbreviations: I, first pharyngeal arch; II, second pharyngeal arch; LV, left ventricle; LPM, lateral plate mesoderm; OFT, outflow tract. Scalebar: A,C 500μm; B,D enlarged from A,C by same magnification.

Wildtype

Mutant

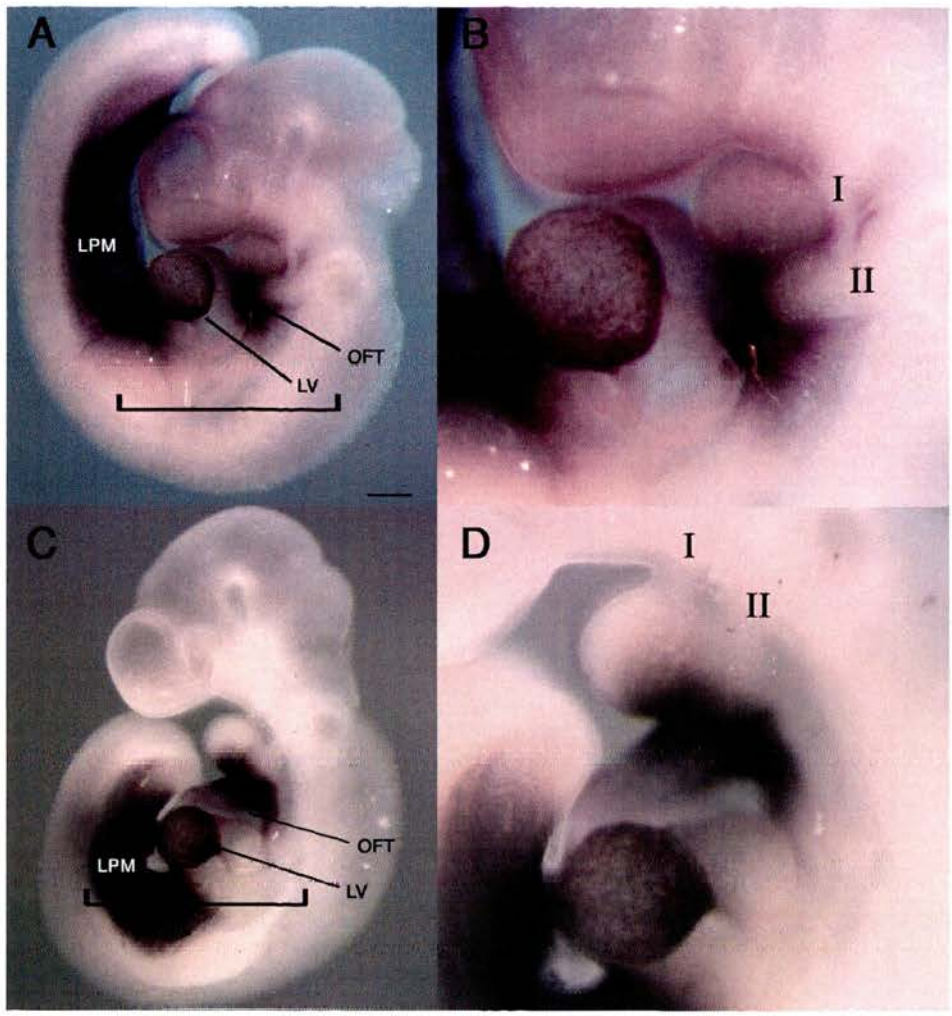

Figure 6.5: A *Sox4*$^{ENU/ENU}$ embryo demonstrates elevated right ventricular expression of *Nppa* at E11. Wild-type (A,C) and mutant (B,D) embryos were examined for expression of *Nppa*. Expression of *Nppa* is observed in the maturing myocardium of all four cardiac chambers – atria and ventricles. In the wildtype (A,C) expression is reduced in the right ventricle, at this stage. In contrast, the mutant heart (B,D) demonstrates elevated level of expression in the right ventricle. Additionally it is evident that the heart is distended. The outflow tract is swollen in the mutant heart as indicated (bracket D, with extension in red, compared with bracket C). Abbreviations: LA, left atrium; LV, left ventricle; RA, right atrium; RV, right ventricle. Images A, B are of the same magnification; Images C, D are of the same magnification.

Wildtype **Mutant**

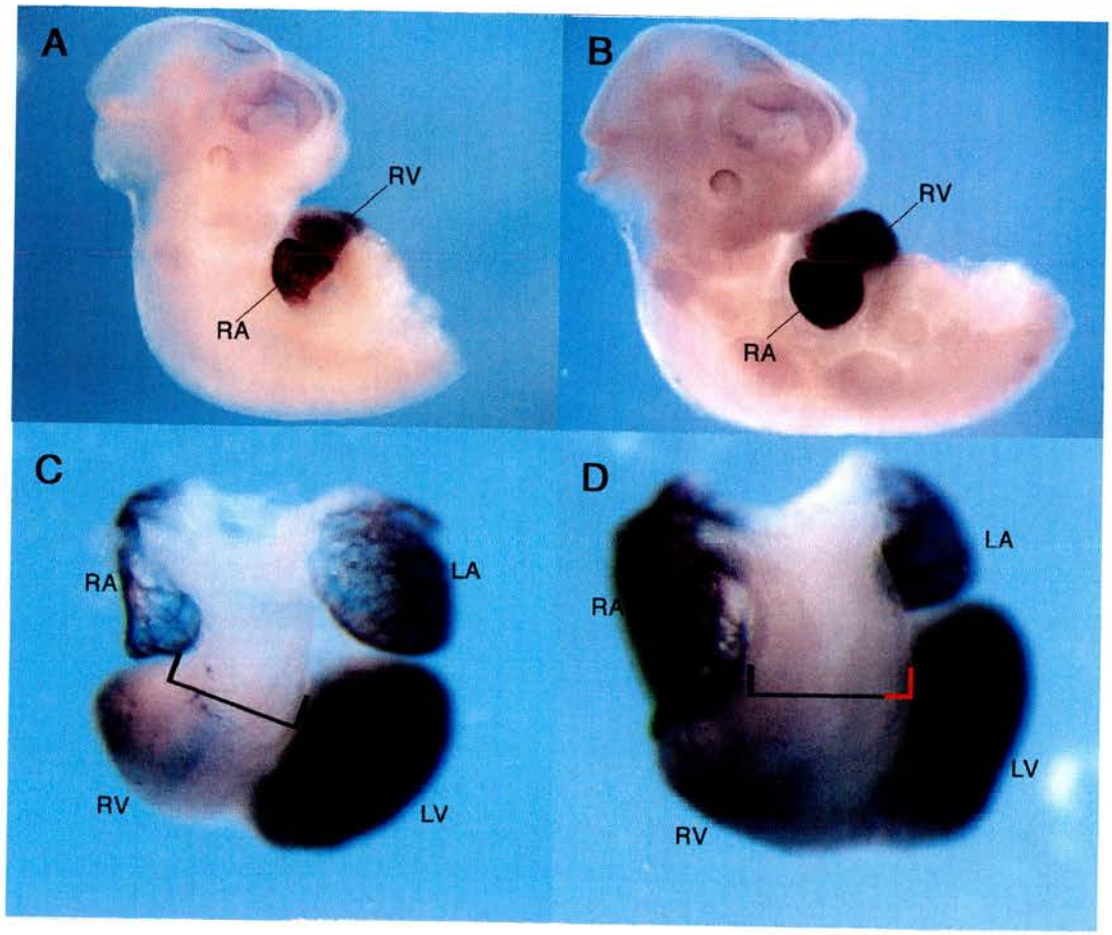

Figure 6.6: A *Sox4*$^{ENU/ENU}$ embryo exhibits a reduction in the expression of *Pitx2* at E9.5. In both a wild-type embryo (staged 33 somite pairs) (A,B,C) and mutant embryo (staged 31 somite pairs) (D,E,F), expression of *Pitx2* is revealed in the mandibular (Md) and maxillary (Mx) regions of the pharyngeal arch (labelled in A,B,D,E) and in the lateral plate mesoderm (left in B,E). Enlargement of the cardiac region, reveals expression of *Pitx2* in the inner curvature of the atrioventricular canal and atrium is undetectable in the mutant embryo (arrows F compared with C). Abbreviations: I, first pharyngeal arch; L-LM, left lateral plate mesoderm; Md, Mandibular region of the first pharyngeal arch; Mx, Maxillary region of the first pharyngeal arch. Scale bar: A, B, D, E, 500μm; C, F, 233μm.

A
Mx
Md
B
Mx
Md
L-LM
C
I
D
Mx
Md
E
Mx
Md
L-LM
F
I
Wildtype
Mutant

Pitx2 isoforms are largely responsible for patterning left-side identity of the heart and indeed left patterning of the embryo (Ryan *et. al.* 1998). Although *Sox4* mutant hearts do not demonstrate an abnormal direction of looping or cardiac isomerism, they do demonstrate abnormal looping and inadequate positioning of the future chambers. Expression of *Pitx2* marks the inner curvature (Campione *et. al.* 2001) and this domain contributes to appropriate cardiac looping. To examine whether *Sox4* mutation alters *Pitx2* expression, a class-I mutant was compared with a stage-matched control embryo (Figure 6.6a to f). These embryos were matched within two somite pairs (mutant 31 somite pairs; control 33 somite pairs). At E9.5, *Sox4* mutant hearts lack detectable cardiac expression of *Pitx2* in the inner curvature of the AVC and left atrium (Figure 6.6f compared with c). This domain of expression was the only significant decrease in *Pitx2* expression. Other regions of expression displayed the expected pattern, although expression appeared slightly reduced consistent with the smaller embryo size.

The expression of *Pitx2* has been shown to be strong in the inner curvature of the AVC and left atrium at E10.0 (Campione *et. al.* 2001). The embryos examined in this study are staged late on the 10^{th} day of gestation (E9.5- E10). To examine whether a developmental delay may contribute to the differences in expression, embryos with 7-8 fewer somite pairs, earlier 10^{th} day of gestation, were examined for expression of *Pitx2* in this domain. The younger control embryos did not demonstrate visible expression of *Pitx2* in the inner curvature and left atrium (data not shown). Thus it is possible that the lack of expression in this domain in the mutant embryo is a consequence of a cardiac developmental delay.

6.3 DISCUSSION.

This chapter has presented novel findings from studying embryos homozygous for the ENU-induced mutation in *Sox4*. Segregation of the *satin* allele removes the potential for a genetic interaction to modulate the phenotype, leaving it possible to uncover a phenotype that is solely the consequence of mutation in *Sox4*. The results presented in this chapter have enabled several points suggested in previous chapters to be analysed further:

(1) In terms of the craniofacial abnormalities observed in the compound mutant phenotype, results from this chapter suggest that abnormal *Sox4* is capable of causing a mild anterior phenotype. It is possible that this mild anterior abnormality is an indirect consequence of the developmental delay in mutant embryos of the genotype examined in this chapter. If this were the case, expanding on the number of embryos and developmental stages examined to explore specific markers for anterior patterning will enable further dissection of this role. It is interesting that the phenotype observed in this limited number embryos was not as severe as that observed in embryos harbouring the compound mutation (Figure 6.2, compare with figure 3.8). This suggests that the severe anterior defects observed with the compound mutation are a consequence of a genetic interaction between *Sox4* and *Foxq1*, although the nature of this is yet to be determined.

(2) The point mutation in *Sox4* results in more severe abnormalities than those described in published work on Sox4 mutations (Penzo-Mendez *et. al.* 2007; Schilham *et. al.* 1996; Ya *et. al.* 1998b). Still, embryos with a class-III phenotype were not observed in the $Sox4^{ENU/ENU}$ study. This is not surprising since class-III comprises 5% of $Sox4^{ENU/ENU}$ $Foxq1^{sa/sa}$ embryos and in this study only five E9.5-10.5 $Sox4^{ENU/ENU}$ embryos were examined.

(3) $Sox4^{ENU/ENU}$ mutant embryos demonstrate a reduction to the OFT domain expression of *Hand1* at E9.5 and elevated expression in the *Nppa* right ventricular domain and also in the right atrium at E11. In chapter 5, it was shown that in $Sox4^{ENU/ENU}$ $Foxq1^{sa/sa}$ hearts the level of *Hand1* expression appeared proportional to the severity of the compound mutant phenotype. The lower the level of *Hand1*

expression, the more severe the phenotype appeared to be (Chapter 5; figure 5.3). Additionally, the level of *Nppa* expression was shown to be elevated in the right ventricle (Chapter 5; figure 5.4). Whilst the combined results from this and previous chapters does not pinpoint further the level at which mutation in *Sox4* causes an alteration to gene expression, these results do verify that mutation in *Sox4* and the phenotype that arises is capable of contributing to a reduction in *Hand1* and an increase in *Nppa.* Since the *Hand1* expression domain is reduced, there still remains the possibility that components of the *Sox4* phenotype are a consequence of reduced levels of proliferation and elevated levels of differentiation. As described in chapter 5 (section 5.3.2), markers of proliferation, as well as cardiac differentiation would be useful to investigate this further.

A reduction in expression of Pitx2 in the inner curvature correlates to the phenotype of inadequate looping.

The first visible E9.5 cardiac phenotype observed in both $Sox4^{ENU/ENU}$ and $Sox4^{ENU/ENU}$ $Foxq1^{sa/sa}$ embryos was that of inadequate looping. Hearts appeared distended to varying degrees and curvature was abnormal (this chapter, Figure 6.2; Chapter 3, Figure 3.8). To examine this and whether the inadequate cardiac looping could be a consequence of mis-expression of genes known to play a role in looping, the expression of *Pitx2* was examined in a class-I $Sox4^{ENU/ENU}$ mutant embryo. Expression of *Pitx2c* within the inner curvature of the heart marks a specific domain important for cardiac remodelling (Kitamura *et. al.* 1999).

This domain appeared substantially reduced in the $Sox4^{ENU/ENU}$ mutant, relative to *Pitx2* expression in other areas. Whilst it may be a novel aspect of the role of *Sox4* in cardiogenesis, analysis of expression by *in situ* hybridisation is not necessarily conclusive. To state with certainty that *Sox4* mutation reduces *Pitx2* expression in the inner curvature, it would be necessary to examine expression by more quantitative methods in this tissue from a larger number of embryos across this developmental stage, as it is possible that the result is a consequence of a developmental delay.

If the reduction in *Pitx2* expression in this domain is not a consequence of a possible cardiac developmental delay two possibilities remain: The first possibility in

embryos at this stage, is that Sox4 functions in the endocardium of the AVC, or *via* induction of indirect signalling from the ventral foregut, to act on *Pitx2* expressing cells to repress this specific domain of expression. The second possibility is that the number of *Pitx2* expressing cells in the inner curvature is dependent upon *Sox4* expression at an earlier stage of development.

The first possibility could be examined by *in situ* of *Pitx2* at E8, when expression in the heart is first observed (Campione *et. al.* 2001) until E10.5, beyond the embryonic stage when $Sox4^{ENU/ENU}$ mutants demonstrate lower expression than control embryos. The second possibility could be explored by histological analysis of a number of mutant embryos at this stage and cell counting in this region. This early loss of *Pitx2* may contribute to the phenotype observed in *Sox4* mutants, since both gain and loss of *Pitx2* is associated with DORV. It is possible that the loss of *Pitx2* levels in *Sox4* mutant hearts is causative of the inadequate looping and later E12.5 phenotypes (as observed in sections of $Sox4^{ENU/ENU}$ $Foxq1^{sa/sa}$ embryos – chapter 4).

A further possibility, as an explanation for the loss of *Pitx2* expression in the left atrium is that this embryo demonstrates early evidence for right atrial isomerism (RAI). *Pitx2* expression is restricted to the left atrium as it develops a molecular left-identity (Campione *et. al.* 2001; Ryan *et. al.* 1998). The cardiac phenotype of $Sox4^{ENU/ENU}$ $Foxq1^{sa/sa}$ embryos does not appear to include RAI in the hearts examined (Chapter 3; section 3.3.2). Since the hearts of compound mutant embryos do not appear to demonstrate RAI, it is unlikely that single mutant embryos would.

6.4 SUMMARY OF THE *Sox4*$^{ENU/ENU}$ PHENOTYPE AND RESULTING MOLECULAR ABERRATION.

This final chapter has documented the embryonic phenotype of a point mutation in *Sox4*. Interpreting from whole single mutant embryos at E9.5, the cardiac morphology appears to be consistent with that described for the compound mutant embryos presented in previous chapters. A reduction in *Pitx2* expression for this stage of development in the inner curvature of the heart may contribute to the inability of *Sox4* mutant hearts to loop adequately. Given the expression domains of *Sox4*, and the continuity of results from those shown in chapter 5, it can be proposed that Sox4 may play a role converging on a pathway which regulate *Hand1*-expressing cells. The observed increase in *Nppa* expression, reflecting myocardial differentiation, is a likely consequence of cardiac stress. This chapter provides the first molecular analysis of mutation in *Sox4* within the heart at these embryonic stages. This study has enabled determination of the onset of the cardiac phenotype with this allele and supported the concept that Sox4 acts prior to a visible phenotype from E9.5. The molecular analysis has allowed the formulation of novel hypotheses about the action of Sox4 in cardiogenesis. Additionally, since *Sox4*$^{ENU/ENU}$ embryos do not yet appear to demonstrate a severe defect in anterior development, we can conclude that a genetic interaction with *Foxq1* modulated the severity of the anterior phenotype presented in previous chapters.

CHAPTER 7: GENERAL DISCUSSION AND CONCLUDING REMARKS

The principal objective of my project is to gain novel insights into the embryonic requirement for Sox4. My reasoning for this is threefold:

1. The *Sox4* null phenotype has been reported (Schilham *et. al.* 1996; Ya *et. al.* 1998b), but the underlying embryonic defect which caused the cardiac phenotype has not been examined.

2. A novel *Sox4* ENU-induced mutant allele was identified that phenocopies the *Sox4* null (Bogani *et. al.* 2005). This provided a system in which to explore the primary embryonic requirement for Sox4.

3. Studies in cancer genetics show that a wide range of tumours result from aberrant activity of developmental pathways. Thus, characterising the multiple roles of Sox4 in mouse embryonic development may contribute to understanding the molecular basis for dysregulation of SOX4 in tumorigenesis.

This study contributes to this research by adopting three approaches:

I. Evidence has been presented in this thesis to show that a mutation in *Sox4* results in a heterogeneous cardiac phenotype from an early developmental stage. This extends well beyond the published description of the null allele cardiac deficiency reported in the literature. These results overlap with published findings, and furthermore expand upon the current understanding of the role of Sox4 during cardiogenesis. Firstly, mutant embryos demonstrate a visible cardiac phenotype from E9.5 (Chapters 3 and 6). This phenotype varies in severity between embryos, resulting in at least two time points of embryonic

lethality. Many aspects of the E12.5-E14.5 published phenotype could result from the early dysmorphology (Chapter 3).

II. Secondly, a comprehensive analysis of the expression of *Sox4* revealed previously uncharacterised cardiac and extra-cardiac expression domains during early embryogenesis (Chapter 4). Mis-expression from some of these domains may account for the cardiac phenotype observed, since these domains coincide with regions of cardiac abnormality in mutants. Thus, it is possible that Sox4 acts in a multifaceted manner, at a number of different sites and stages to enable appropriate heart development.

III. Finally, molecular analysis of the cardiac phenotype has given insight into the possible molecular requirement for Sox4 function during heart development (Chapter 5 and 6).

Determining the origin of the cardiac defect in Sox4 mutant embryos.

The early cardiac phenotype is grouped into two categories: class-I and class-II (class-III mutants do not demonstrate a functional heart, nor survive past E10.5) (Chapter 3). Both classes demonstrate a degree of distension of the looping heart tube at about E9.5 and a variable developmental delay. Also at this stage these results have shown that early ventricular trabeculation and cushion formation are disrupted.

Since the visible cardiac phenotype arises about E9.5, the earliest requirement for appropriate expression of *Sox4* must be prior to this developmental stage. Additionally, results show that expression of *Sox4* occurs within the foregut endoderm adjacent to the cardiac crescent (Chapter 4). Given the importance of the endoderm for cardiac development (section 1.3.4), dysregulated expression in this domain, at this stage, may be responsible for the onset of the cardiac phenotype.

Sox4 is also expressed in the endocardial cushions from E9.5 (Chapter 4). Whilst it may be thought to be too late for the onset of a phenotype at E9.5, it is possible that *Sox4* is expressed earlier at low levels beyond the detection by *in situ* hybridisation. Without verification by quantitative analysis of expression in specific regions, from

the crescent stage, it is not possible to say for certain that *Sox4* is not expressed in endocardium prior to E9.5. Hence, dysregulated expression of *Sox4* in the endocardium may in addition be responsible for the onset of the cardiac phenotype.

Thus two possibilities exist: First, that the early defects are a consequence of aberrant *Sox4* expression within endoderm and/or second, that the early defects are a consequence of aberrant *Sox4* expression within mesoderm. This presents a distinctly different question from that asked in previous discussions, which relates to later expression of *Sox4*.

Further investigations on the conditional *Sox4* allele (Penzo-Mendez *et. al.* 2007) would be useful to examine this quandary. To distinguish between the two lineage requirements would require conditional deletion of either endodermal or mesodermal *Sox4* expression at the crescent stage. Although *Isl1* expression is not specific to the endoderm at the crescent and headfold stages of development, its expression in the definitive endoderm appears to be the only domain of overlap with the *Sox4* expression shown in this thesis. Thus, the *Isl1-cre* may be useful for ablation of *Sox4* specifically in the definitive endoderm (Srinivas *et. al.* 2001). Before proceeding with genetic crosses, co-localisation of Sox4 with Isl1 should be examined to validate the overlapping domains. The cardiac mesoderm cre-recombinase, *Mesp-1-cre,* is well characterised (Saga *et. al.* 1999). By removing expression of *Sox4* in cells derived from *Mesp-1*-expressing mesoderm, it would be possible to examine which components of the phenotype are caused by mis-expression of *Sox4* in mesoderm-derived cells.

As an alternative approach to this method, it has been shown that ES cells can be derived from $Sox4^{ENU/ENU}$ $Foxq1^{sa/sa}$ embryos (Appendix 1). Thus it is equally possible for ES cells to be derived from $Sox4^{ENU/ENU}$ embryos. By introducing a *GFP* or *lacZ* expression cassette into these derived cell lines, the potential of the *Sox4* mutant ES cells to contribute to chimæric embryos could then be examined. Preferential inclusion of wild type cells in a specific lineage implies that mutant cells are unable to contribute due to dysfunction. This method was used to demonstrate the essential requirement for *Gata4* expression by the endoderm, but not the mesoderm during early heart development (Narita *et. al.* 1997). It would be equally

effective in determining whether *Sox4* expression is required by either or both the endoderm and mesoderm.

Thus, this thesis shows that *Sox4* is expressed in regions highly relevant for cardiogenesis. Further work to find the precise requirement of *Sox4* expression in these lineages is discussed.

Determining the possible functions of Sox4 in embryogenesis.

These results also progress our understanding of the role of Sox4 outwith heart development. Findings in this project have exposed a novel early embryonic phenotype (class-III mutants) linked to the $Sox4^{ENU}$ $Foxq1^{sa}$ mutation. It is not clear yet whether this is entirely a consequence of $Sox4^{ENU/ENU}$, since the $Sox4^{ENU/ENU}$ phenotype has not been examined in detail (Chapter 6). However, class-III mutant embryos demonstrate a severe phenotype which may have its origins during gastrulation. In addition to the usefulness of $Sox4^{ENU/ENU}$ ES cells for observing the ability of these cells to contribute to cardiac development, such ES cells will also be useful to examine whether mutant cells are able to gastrulate correctly and whether they are able to contribute equally to all three germ layers in the early class-III mutants. A major limitation to this is the substantial number of chimæric embryos which would need to be created and examined considering this phenotype comprises about 5% of any litter. Nevertheless, such a study would demonstrate the requirement for normal Sox4 function during early developmental stages.

As this work has successfully characterised the embryonic expression domains of *Sox4*, it is relevant now to explore the requirement for *Sox4* expression by other tissue. Examining the action of Sox4 in multiple tissues will help to uncover the function of Sox4 as a protein, not just in the process of cardiogenesis, but also for embryonic development.

Functional analysis of the ENU mutation

Work presented in this thesis provides a fundamental basis for use of the $Sox4^{ENU}$ allele in characterising the embryonic function of Sox4. The phenotype has been presented and discussed, and molecular aberrations resulting from mutation in *Sox4*

have been shown. In addition to this, it is also necessary to determine how Sox4 acts at the molecular level.

It is not expected that the point mutation would alter the expression of *Sox4*, unless expression in a specific domain is autoregulatory. Indeed, it has been shown that embryonic stem cells derived from $Sox4^{ENU/ENU}$ $Foxq1^{sa/sa}$ embryos, as well as heterozygous and control embryos express the *Sox4* transcript (Appendix 1). In order to proceed further with use of the $Sox4^{ENU}$ allele, it will be first necessary to conduct experiments to answer the following questions:

- Does translation occur from the mutant *Sox4* transcript and is mutant Sox4 protein present in $Sox4^{ENU/ENU}$ embryos?
- Does the mutant protein demonstrate differences in activity compared with wild type Sox4?

Progress into the functional aspects of Sox4 during development has been hampered by the lack of a reliable Sox4 antibody. Although some publications have reported protein localisation studies using commercial Sox4 antibodies (Park, Y K *et. al.* 2005; Sinner *et. al.* 2007), further information about the localisation of Sox4 appears to be from use of non-commercial antibodies (Kim *et. al.* 2004; Liu *et. al.* 2006). Immunohistochemistry to mutant embryos *in toto* or sections of embryonic tissue will assist in determining whether cells of the $Sox4^{ENU/ENU}$ genotype generate mutant Sox4 protein. Undoubtedly, this would assist in answering the first question, as to whether the mutant protein is generated in $Sox4^{ENU/ENU}$ embryos.

Cloning of the $Sox4^{ENU}$ coding sequence into an expression vector would enable a number of molecular assays to be carried out, with the intention of characterising how the mutant protein functions differently from normal Sox4. There are two aspects of the binding potential of Sox4, as a transcription factor, which must be examined: 1) Does mutant Sox4 still interact with other proteins?; and 2) Does mutant Sox4 still bind DNA?

1. To examine the first, requires knowledge of Sox4 binding partners which, to date, is under-examined. SOX4 has been shown, *in vitro*, to bind β-catenin or Tcf4 (both, but not together) (Sinner *et. al.* 2007). Additionally,

overexpression of *Sox4* in culture enhanced Wnt-reporter gene expression. Thus, expression of mutant *Sox4* in HEK293 cells could be used to examine protein interactions. Moreover, co-transfection of HEK293 cells with constructs designed to demonstrate functional levels of canonical Wnt signalling (Vleminckx *et. al.* 1999; Zamparini *et. al.* 2006) could aid in assaying transcriptional function, thereby determining whether the mutation in *Sox4* alters canonical Wnt signalling.

2. Examination of the DNA-binding potential of the Sox4 HMG box has been conducted by other research groups (van Beest *et. al.* 2000; van de Wetering *et. al.* 1993; van Houte *et. al.* 1995). By the proposed cloning and expression steps, the mutant protein may be created *in vitro* and extracted for use in a DNA binding assay. This would enable us to answer the important question –does mutant Sox4 still bind DNA?

Both of these assays would give clues as to the mechanism by which the ENU induced mutation results in aberrant function of Sox4, thereby answering the second question posed – How does the mutant protein function differently from the wild type?

Could there be a genetic interaction between Sox4^{ENU} and satin?

Throughout this thesis, results have implied a possible genetic interaction between the two mutant alleles *Sox4^{ENU}* and *satin.*

- Chapter 3 demonstrated the variability of the wholemount craniofacial phenotype in embryos staged E9.5 and E12.5. This aspect of the phenotype was abrogated in E9.5 and E12.5 embryos which harboured only the *Sox4^{ENU}* mutation, as shown in Chapter 6.

- Results in Chapter 3 reveal an anterior deficiency, consistent in embryos homozygous for *Sox4^{ENU}* and *satin*, after two to five generations of backcrossing to C57Bl/6J mice. This is supported by previous work (Willoughby 2006) which suggested that a genetic cause of the anterior phenotype resided on the *satin* chromosome and this could be observed in

some embryos where this region was hemizygous, from a cross of the *satin* chromosome with an intra-chromosomal deletion (*Del(13)Svea36H*) (section 1.4 and 3.3 part 2).

- Chapter 4 reported the expression domains of *Sox4* and *Foxq1* transcripts and, although co-expression studies have not been conducted, *in situ* analysis of each gene suggests that both are expressed in the developing anterior neurectoderm during early somitogenesis (E8-8.5). Additionally, both are expressed at E9.5 in the pharyngeal arches, which later contribute to the affected craniofacial structures.

A recent paper examining gene expression in hepatocellular carcinoma observed *FOXQ1* expression elevated in cells in which *SOX4* was also highly expressed (Liao *et. al.* 2008). Expression levels of *FOXQ1* could be reduced upon knockdown of endogenous *SOX4* transcript by RNA interference. The authors subsequently identified that the *FOXQ1* promoter could be bound by SOX4 in chromatin immunoprecipitation experiments. Although this study focussed on cancer cells and not embryonic development, these findings further support a possible interaction between the two genes which may also relate to other systems.

During development, further work is needed to determine the underlying cause of the embryological defect. In the first instance, evidence in support of a functional interaction could come from co-localisation of *Sox4* and *Foxq1* expression domains within the anterior neurectoderm. Also examination of whether the Sox4 and Foxq1 proteins co-localise could assist in examining functional overlap.

Although the phenotype of the *Foxq1* null includes malformation of the forebrain (Goering *et. al.* 2008) and *Sox4* has been implicated in neural development (Cheung *et. al.* 2000), it is possible that the final phenotypic outcome of the $Sox4^{ENU}$ *satin* compound mutation is influenced by other segregating loci from the original *satin* chromosome. It has been argued that it is unlikely that another *ENU* mutation resides in this region and segregates with $Sox4^{ENU}$ and *satin* alleles (section 1.4.3). However, this does not exclude the possibility that the genetic construct of this region contains modifier loci existing prior to mutagenesis by ENU.

To determine conclusively whether aspects of the compound phenotype are a consequence of a genetic interaction between *Sox4* and *Foxq1*, the phenotype observed here would need to be recapitulated using *Sox4* null and *Foxq1* null alleles. A detailed breeding programme between mutant *Sox4* heterozygotes and mutant *Foxq1* null mice (as homozygous *Foxq1* null are viable) would need to be conducted to ensure generation of heterozygotes with both null alleles on the same chromosome. It is possible that a shorter route towards generating such mutants would be to us ES cell recombineering to generate targeted mutations in both genes on the same chromosome. Generation of homozygous *Sox4* null: *Foxq1* null embryos could then be achieved and the phenotype examined for anterior malformation and aberrant gene expression.

In addition to uncovering a novel possibility – that *Sox4* and *Foxq1* interact genetically – this finding also highlights the importance of considering gene function in the context of the genetic neighbourhood.

Summary

The search for a clear function of Sox4 remains in its infancy. This study has contributed to this search in many respects. Mutation in *Sox4* results in a lethal cardiac deformity which has its origins at early stages of heart development. This phenotype is highly variable. It appears that certain aspects of the phenotype can be attributed to dysregulation of *Sox4* gene expression in specific cardiac and extra-cardiac domains. The mouse model characterised in this project will prove relevant for increasing on the current understanding of heart development. Extended breeding programmes involving other transgenic mouse lines, together with chimæra analysis from derived ES cells, will enable further dissection of specific requirements for *Sox4* in embryogenesis. Moreover, cloning of the *ENU* mutant allele will enable cell culture and protein experiments to determine the functional properties of the mutant protein. Combining results from proposed analyses with the findings presented within this thesis will give insight into determining the molecular and functional action of Sox4.

APPENDIX 1: Derivation of *Sox4*$^{ENU/ENU}$ *Foxq1*$^{sa/sa}$ ES cells; and the contribution of ES cells in chimæric mice

It is well established that chimæric mice and chimæric embryos are useful tools to study the ability of embryonic stem (ES) cells to contribute to the development and function of a specific tissue. When subjected to morula aggregation with a control embryo or micro-injected into the ICM of a wild type blastocyst, ES cells are equally capable of contributing to all embryonic tissue and, in the case of morula aggregation, extraembryonic derivatives too (Beddington *et. al.* 1989). If ES cells are tagged, by expression of *lacZ* or GFP, then it is possible to examine contribution of introduced ES cells within the embryo or mouse. Any unequal distribution between ES cells and cells from the host blastocyst indicates a problem with the potential of the ES cells. If the ES cells are of a mutant mouse line, analysis of the chimæras can assist in describing the requirement of the mutated gene in embryonic development.

The following two figures and one table show:

1. *Sox4*$^{ENU/ENU}$ *Foxq1*$^{sa/sa}$ ES cells express *Sox4* (Figure 1);
2. ES cells, derived from *Sox4*$^{ENU/ENU}$ *Foxq1*$^{sa/sa}$ delayed-implantation blastocysts can be grown in culture (Figure 2);
3. *Sox4*$^{ENU/ENU}$ *Foxq1*$^{sa/sa}$ ES cells are able to contribute to chimæric mice (Figure 2);
4. *Sox4*$^{ENU/ENU}$*Foxq1*$^{sa/sa}$ ES cells demonstrate variable contribution to organs of chimæric mice (Table 1).

Cell line reference	*Sox4* genotype	*Foxq1* genotype
B4	homozygote	homozygote
A1	heterozygous	heterozygous
B3	wild-type	heterozygous
C2	heterozygous	heterozygous

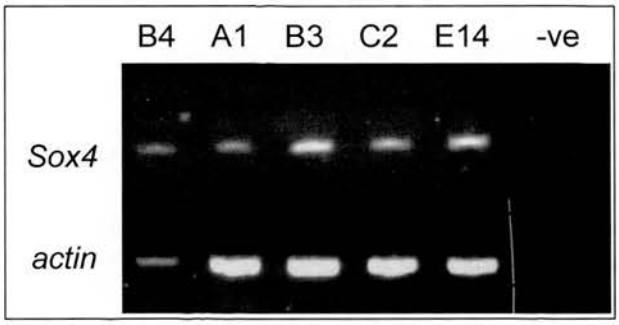

Appendix Figure 1: Sox4 is expressed in ES cells.

ES cells heterozygous or homozygous for Sox4ENU were derived from Sox4+/ENU Foxq1+/sa intercross embryos (table, upper). Sox4 transcript (top row of bands) is expressed in all ES cell lines examined. E14 is a control wild type ES cell line. Expression of actin control for amplification is shown. Final lane reveals no amplification from genomic DNA (minus reverse transcriptase control). Labels correspond to table as shown.

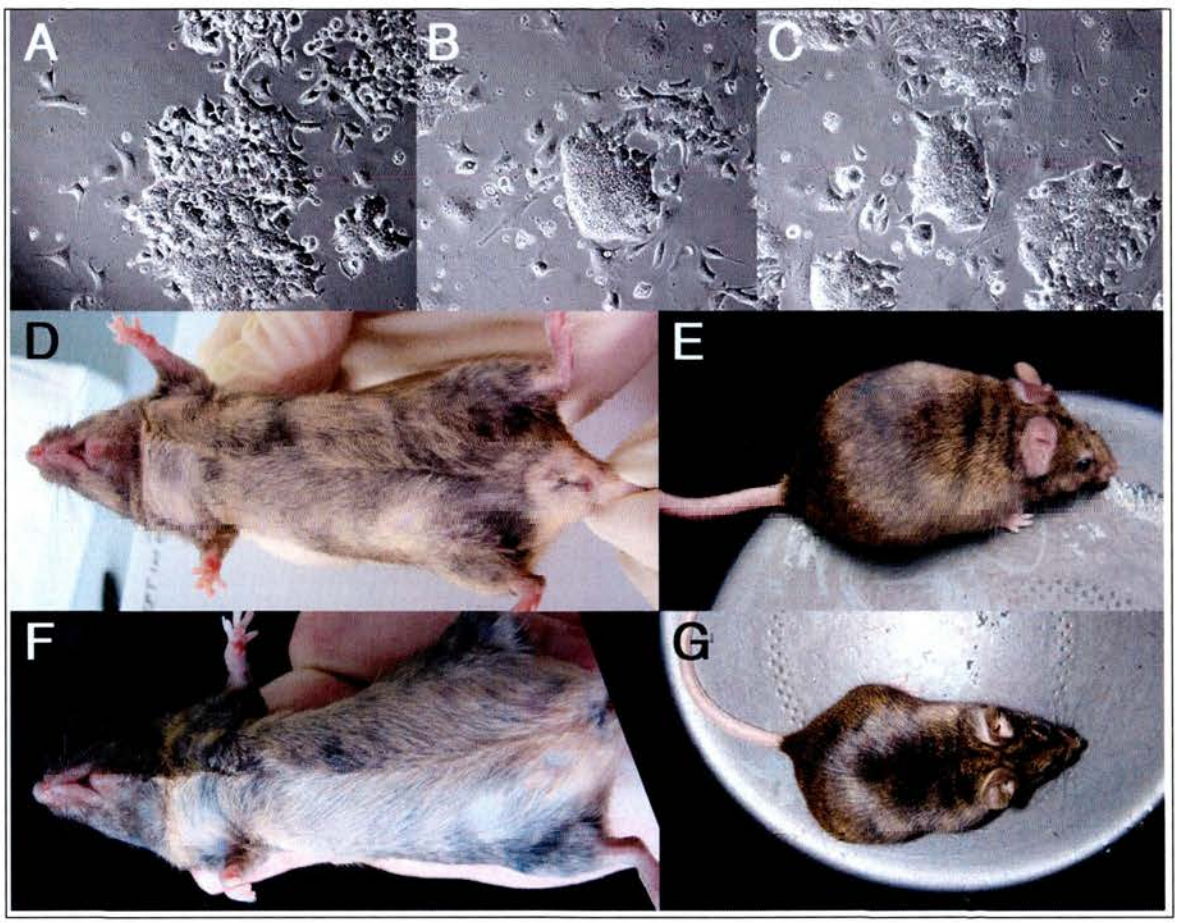

Appendix Figure 2: Derived ES cells may be grown in culture, and are able to contribute to chimæric mice.

Heterozygous (A,B) and homozygous Sox4ENU/ENU Foxq1sa/sa (C) ES cells grown in culture. Sox4ENU/ENU Foxq1sa/sa ES cells can contribute to chimæric mice (D,E,F,G).

Appendix Table 1: Contribution of ES cells to organs in chimæric mice.

Tissue	Chimaera 1	Chimaera 2	Chimaera 3
gut	equal	mostly wildtype	equal
eye	equal	wildtype	wildtype
tongue	mostly wildtype	equal	
brain	mostly wildtype	equal	mostly wildtype
ovary	equal	wildtype	
anterior brain	mostly wildtype	equal	mostly wildtype
thymus	wildtype	mostly wildtype	
lung	wildtype	wildtype	wildtype
thyroid	equal	mostly wildtype	wildtype
diaphragm	mostly wildtype	mostly wildtype	equal
tail	mostly wildtype	mostly wildtype	mostly wildtype
skin	mostly wildtype	mostly wildtype	
skull	equal	wildtype	mostly wildtype
spleen	mostly wildtype	wildtype	mostly wildtype
pancreas	mostly wildtype	equal	
kidney	wildtype	mostly wildtype	mostly wildtype
liver	equal	wildtype	wildtype
muscle	wildtype	equal	equal
femur	wildtype	wildtype	mostly wildtype
bone marrow	mostly wildtype	wildtype	wildtype
atria	wildtype	mostly wildtype	equal
IVS	mostly wildtype	wildtype	
ventricle	mostly wildtype	mostly wildtype	mostly wildtype
heart	mostly wildtype	mostly wildtype	

Semi-quantitative analysis of adult mouse tissue for contribution of the *satin* allele as a marker of $Sox4^{ENU/ENU}$ $Foxq1^{sa/sa}$ ES cell contribution to adult chimæric mice. White space in chimaera 3 indicates that a particular tissue was not examined.

Summary

Tissue analysis of chimæric mice revealed highly variable contribution of homozygous mutant ES cells to the construction of adult organs (Appendix Table 1). Although some tissues demonstrate predominantly wild type contribution (particularly lung), these results are inconclusive because of the significant variability between other samples. Whilst this was conducted as a general observation of contribution, cells in adult tissue arise from different origins. Since the *Sox4*$^{ENU/ENU}$ *Foxq1*$^{sa/sa}$ phenotype is considerably variable (Chapter 3) by labelling ES cells prior to introduction into host blastocysts, these cell lines may prove useful for determining the function of Sox4 and Foxq1 by further analysis with chimæric embryos.

REFERENCES:

Abu-Issa, R., Smyth, G., Smoak, I., Yamamura, K. and Meyers, E. N. (2002). Fgf8 is required for pharyngeal arch and cardiovascular development in the mouse. *Development* **129**(19): 4613-25.

Ahn, S. G., Cho, G. H., Jeong, S. Y., Rhim, H., Choi, J. Y. and Kim, I. K. (1999). Identification of cDNAs for Sox-4, an HMG-Box protein, and a novel human homolog of yeast splicing factor SSF-1 differentially regulated during apoptosis induced by prostaglandin A2/delta12-PGJ2 in Hep3B cells. *Biochem Biophys Res Commun* **260**(1): 216-21.

Ahn, S. G., Kim, H. S., Jeong, S. W., Kim, B. E., Rhim, H., Shim, J. Y., Kim, J. W., Lee, J. H. and Kim, I. K. (2002). Sox-4 is a positive regulator of Hep3B and HepG2 cells' apoptosis induced by prostaglandin (PG)A(2) and delta(12)-PGJ(2). *Exp Mol Med* **34**(3): 243-9.

Akiyama, H., Chaboissier, M. C., Behringer, R. R., Rowitch, D. H., Schedl, A., Epstein, J. A. and de Crombrugghe, B. (2004). Essential role of Sox9 in the pathway that controls formation of cardiac valves and septa. *Proc Natl Acad Sci U S A* **101**(17): 6502-7.

Anderson, R. H. and Brown, N. A. (1996). The anatomy of the heart revisited. *Anat Rec* **246**(1): 1-7.

Anderson, R. H., Brown, N. A. and Moorman, A. F. (2006). Development and structures of the venous pole of the heart. *Dev Dyn* **235**(1): 2-9.

Anderson, R. H., Webb, S. and Brown, N. A. (1999). Clinical anatomy of the atrial septum with reference to its developmental components. *Clin Anat* **12**(5): 362-74.

Anderson, R. H., Webb, S., Brown, N. A., Lamers, W. and Moorman, A. (2003). Development of the heart: (3) formation of the ventricular outflow tracts, arterial valves, and intrapericardial arterial trunks. *Heart* **89**(9): 1110-8.

Arkell, R. M., Cadman, M., Marsland, T., Southwell, A., Thaung, C., Davies, J. R., Clay, T., Beechey, C. V., Evans, E. P., Strivens, M. A., Brown, S. D. and Denny, P. (2001). Genetic, physical, and phenotypic characterization of the Del(13)Svea36H mouse. *Mamm Genome* **12**(9): 687-94.

Armstrong, E. J. and Bischoff, J. (2004). Heart valve development: endothelial cell signaling and differentiation. *Circ Res* **95**(5): 459-70.

Bajolle, F., Zaffran, S., Kelly, R. G., Hadchouel, J., Bonnet, D., Brown, N. A. and Buckingham, M. E. (2006). Rotation of the myocardial wall of the outflow tract is implicated in the normal positioning of the great arteries. *Circ Res* **98**(3): 421-8.

Bamforth, S. D., Braganca, J., Farthing, C. R., Schneider, J. E., Broadbent, C., Michell, A. C., Clarke, K., Neubauer, S., Norris, D., Brown, N. A., Anderson, R. H. and Bhattacharya, S.

(2004). Cited2 controls left-right patterning and heart development through a Nodal-Pitx2c pathway. *Nat Genet* **36**(11): 1189-96.

Baraban, S. C., Dinday, M. T., Castro, P. A., Chege, S., Guyenet, S. and Taylor, M. R. (2007). A large-scale mutagenesis screen to identify seizure-resistant zebrafish. *Epilepsia* **48**(6): 1151-7.

Barbaric, I., Wells, S., Russ, A. and Dear, T. N. (2007). Spectrum of ENU-induced mutations in phenotype-driven and gene-driven screens in the mouse. *Environ Mol Mutagen* **48**(2): 124-42.

Beall, A. C. and Rosenquist, T. H. (1990). Smooth muscle cells of neural crest origin form the aorticopulmonary septum in the avian embryo. *Anat Rec* **226**(3): 360-6.

Beddington, R. S. and Robertson, E. J. (1989). An assessment of the developmental potential of embryonic stem cells in the midgestation mouse embryo. *Development* **105**(4): 733-7.

Bernard, P., Tang, P., Liu, S., Dewing, P., Harley, V. R. and Vilain, E. (2003). Dimerization of SOX9 is required for chondrogenesis, but not for sex determination. *Hum Mol Genet* **12**(14): 1755-65.

Bewley, C. A., Gronenborn, A. M. and Clore, G. M. (1998). Minor groove-binding architectural proteins: structure, function, and DNA recognition. *Annu Rev Biophys Biomol Struct* **27**: 105-31.

Biben, C. and Harvey, R. P. (1997). Homeodomain factor Nkx2-5 controls left/right asymmetric expression of bHLH gene eHand during murine heart development. *Genes Dev* **11**(11): 1357-69.

Bieller, A., Pasche, B., Frank, S., Glaser, B., Kunz, J., Witt, K. and Zoll, B. (2001). Isolation and characterization of the human forkhead gene FOXQ1. *DNA Cell Biol* **20**(9): 555-61.

Bogani, D., Warr, N., Elms, P., Davies, J., Tymowska-Lalanne, Z., Goldsworthy, M., Cox, R. D., Keays, D. A., Flint, J., Wilson, V., Nolan, P. and Arkell, R. (2004). New semidominant mutations that affect mouse development. *Genesis* **40**(2): 109-17.

Bogani, D., Willoughby, C., Davies, J., Kaur, K., Mirza, G., Paudyal, A., Haines, H., McKeone, R., Cadman, M., Pieles, G., Schneider, J. E., Bhattacharya, S., Hardy, A., Nolan, P. M., Tripodis, N., Depew, M. J., Chandrasekara, R., Duncan, G., Sharpe, P. T., Greenfield, A., Denny, P., Brown, S. D., Ragoussis, J. and Arkell, R. M. (2005). Dissecting the genetic complexity of human 6p deletion syndromes by using a region-specific, phenotype-driven mouse screen. *Proc Natl Acad Sci U S A* **102**(35): 12477-82.

Bostrom, M. P. and Hutchins, G. M. (1988). Arrested rotation of the outflow tract may explain double-outlet right ventricle. *Circulation* **77**(6): 1258-65.

Bowles, J., Schepers, G. and Koopman, P. (2000). Phylogeny of the SOX family of developmental transcription factors based on sequence and structural indicators. *Dev Biol* **227**(2): 239-55.

Boyd, K. E., Xiao, Y. Y., Fan, K., Poholek, A., Copeland, N. G., Jenkins, N. A. and Perkins, A. S. (2006). Sox4 cooperates with Evi1 in AKXD-23 myeloid tumors via transactivation of proviral LTR. *Blood* **107**(2): 733-41.

Boyer, A. S., Ayerinskas, II, Vincent, E. B., McKinney, L. A., Weeks, D. L. and Runyan, R. B. (1999). TGFbeta2 and TGFbeta3 have separate and sequential activities during epithelial-mesenchymal cell transformation in the embryonic heart. *Dev Biol* **208**(2): 530-45.

Bradshaw, L., Chaudhry, B., Hildreth, V., Webb, S. and Henderson, D. J. (2009). Dual role for neural crest cells during outflow tract septation in the neural crest-deficient mutant Splotch(2H). *J Anat* **214**(2): 245-57.

Brown, S. D. and Peters, J. (1996). Combining mutagenesis and genomics in the mouse--closing the phenotype gap. *Trends Genet* **12**(11): 433-5.

Bruneau, B. G., Logan, M., Davis, N., Levi, T., Tabin, C. J., Seidman, J. G. and Seidman, C. E. (1999). Chamber-specific cardiac expression of Tbx5 and heart defects in Holt-Oram syndrome. *Dev Biol* **211**(1): 100-8.

Bruneau, B. G., Nemer, G., Schmitt, J. P., Charron, F., Robitaille, L., Caron, S., Conner, D. A., Gessler, M., Nemer, M., Seidman, C. E. and Seidman, J. G. (2001). A murine model of Holt-Oram syndrome defines roles of the T-box transcription factor Tbx5 in cardiogenesis and disease. *Cell* **106**(6): 709-21.

Buckingham, M., Meilhac, S. and Zaffran, S. (2005). Building the mammalian heart from two sources of myocardial cells. *Nat Rev Genet* **6**(11): 826-35.

Cai, C. L., Liang, X., Shi, Y., Chu, P. H., Pfaff, S. L., Chen, J. and Evans, S. (2003). Isl1 identifies a cardiac progenitor population that proliferates prior to differentiation and contributes a majority of cells to the heart. *Dev Cell* **5**(6): 877-89.

Cai, C. L., Martin, J. C., Sun, Y., Cui, L., Wang, L., Ouyang, K., Yang, L., Bu, L., Liang, X., Zhang, X., Stallcup, W. B., Denton, C. P., McCulloch, A., Chen, J. and Evans, S. M. (2008). A myocardial lineage derives from Tbx18 epicardial cells. *Nature* **454**(7200): 104-8.

Cai, C. L., Zhou, W., Yang, L., Bu, L., Qyang, Y., Zhang, X., Li, X., Rosenfeld, M. G., Chen, J. and Evans, S. (2005). T-box genes coordinate regional rates of proliferation and regional specification during cardiogenesis. *Development* **132**(10): 2475-87.

Camenisch, T. D., Molin, D. G., Person, A., Runyan, R. B., Gittenberger-de Groot, A. C., McDonald, J. A. and Klewer, S. E. (2002). Temporal and distinct TGFbeta ligand requirements during mouse and avian endocardial cushion morphogenesis. *Dev Biol* **248**(1): 170-81.

Campione, M., Ros, M. A., Icardo, J. M., Piedra, E., Christoffels, V. M., Schweickert, A., Blum, M., Franco, D. and Moorman, A. F. (2001). Pitx2 expression defines a left cardiac lineage of cells: evidence for atrial and ventricular molecular isomerism in the iv/iv mice. *Dev Biol* **231**(1): 252-64.

Carmeliet, P., Ferreira, V., Breier, G., Pollefeyt, S., Kieckens, L., Gertsenstein, M., Fahrig, M., Vandenhoeck, A., Harpal, K., Eberhardt, C., Declercq, C., Pawling, J., Moons, L., Collen, D., Risau, W. and Nagy, A. (1996). Abnormal blood vessel development and lethality in embryos lacking a single VEGF allele. *Nature* **380**(6573): 435-9.

Chalepakis, G., Stoykova, A., Wijnholds, J., Tremblay, P. and Gruss, P. (1993). Pax: gene regulators in the developing nervous system. *J Neurobiol* **24**(10): 1367-84.

Chang, C. P., Neilson, J. R., Bayle, J. H., Gestwicki, J. E., Kuo, A., Stankunas, K., Graef, I. A. and Crabtree, G. R. (2004). A field of myocardial-endocardial NFAT signaling underlies heart valve morphogenesis. *Cell* **118**(5): 649-63.

Chen, C. Y. and Schwartz, R. J. (1996). Recruitment of the tinman homolog Nkx-2.5 by serum response factor activates cardiac alpha-actin gene transcription. *Mol Cell Biol* **16**(11): 6372-84.

Chen, H., Shi, S., Acosta, L., Li, W., Lu, J., Bao, S., Chen, Z., Yang, Z., Schneider, M. D., Chien, K. R., Conway, S. J., Yoder, M. C., Haneline, L. S., Franco, D. and Shou, W. (2004). BMP10 is essential for maintaining cardiac growth during murine cardiogenesis. *Development* **131**(9): 2219-31.

Cheung, M., Abu-Elmagd, M., Clevers, H. and Scotting, P. J. (2000). Roles of Sox4 in central nervous system development. *Brain Res Mol Brain Res* **79**(1-2): 180-91.

Chiang, C., Litingtung, Y., Lee, E., Young, K. E., Corden, J. L., Westphal, H. and Beachy, P. A. (1996). Cyclopia and defective axial patterning in mice lacking Sonic hedgehog gene function. *Nature* **383**(6599): 407-13.

Choi, V. M., Harland, R. M. and Khokha, M. K. (2006). Developmental expression of FoxJ1.2, FoxJ2, and FoxQ1 in Xenopus tropicalis. *Gene Expr Patterns* **6**(5): 443-7.

Christiansen, J. H., Dennis, C. L., Wicking, C. A., Monkley, S. J., Wilkinson, D. G. and Wainwright, B. J. (1995). Murine Wnt-11 and Wnt-12 have temporally and spatially restricted expression patterns during embryonic development. *Mech Dev* **51**(2-3): 341-50.

Christiansen, J. H., Monkley, S. J. and Wainwright, B. J. (1996). Murine WNT11 is a secreted glycoprotein that morphologically transforms mammary epithelial cells. *Oncogene* **12**(12): 2705-11.

Christoffels, V. M., Burch, J. B. and Moorman, A. F. (2004a). Architectural plan for the heart: early patterning and delineation of the chambers and the nodes. *Trends Cardiovasc Med* **14**(8): 301-7.

Christoffels, V. M., Hoogaars, W. M., Tessari, A., Clout, D. E., Moorman, A. F. and Campione, M. (2004b). T-box transcription factor Tbx2 represses differentiation and formation of the cardiac chambers. *Dev Dyn* **229**(4): 763-70.

Christoffels, V. M., Keijser, A. G., Houweling, A. C., Clout, D. E. and Moorman, A. F. (2000). Patterning the embryonic heart: identification of five mouse Iroquois homeobox genes in the developing heart. *Dev Biol* **224**(2): 263-74.

Clark, E. B., Nakazawa, M. and Takao, A. (2000). Etiology and morphogenesis of congenital heart disease : twenty years of progress in genetics and developmental biology. Armonk, Futura.

Clevidence, D. E., Overdier, D. G., Peterson, R. S., Porcella, A., Ye, H., Paulson, K. E. and Costa, R. H. (1994). Members of the HNF-3/forkhead family of transcription factors exhibit distinct cellular expression patterns in lung and regulate the surfactant protein B promoter. *Dev Biol* **166**(1): 195-209.

Clevidence, D. E., Overdier, D. G., Tao, W., Qian, X., Pani, L., Lai, E. and Costa, R. H. (1993). Identification of nine tissue-specific transcription factors of the hepatocyte nuclear factor 3/forkhead DNA-binding-domain family. *Proc Natl Acad Sci U S A* **90**(9): 3948-52.

Conway, S. J., Henderson, D. J. and Copp, A. J. (1997). Pax3 is required for cardiac neural crest migration in the mouse: evidence from the splotch (Sp2H) mutant. *Development* **124**(2): 505-14.

Cordes, S. P. (2005). N-ethyl-N-nitrosourea mutagenesis: boarding the mouse mutant express. *Microbiol Mol Biol Rev* **69**(3): 426-39.

Critcher, R., Stitson, R. N., Wade-Martins, R., Easty, D. J. and Farr, C. J. (1998). Assignment of Sox4 to mouse chromosome 13 bands A3-A5 by fluorescence in situ hybridization; refinement of the human SOX4 location to 6p22.3 and of SOX20 to chromosome 17p12.3. *Cytogenet Cell Genet* **81**(3-4): 294-5.

Crossley, P. H. and Martin, G. R. (1995). The mouse Fgf8 gene encodes a family of polypeptides and is expressed in regions that direct outgrowth and patterning in the developing embryo. *Development* **121**(2): 439-51.

Cserjesi, P., Brown, D., Lyons, G. E. and Olson, E. N. (1995). Expression of the novel basic helix-loop-helix gene eHAND in neural crest derivatives and extraembryonic membranes during mouse development. *Dev Biol* **170**(2): 664-78.

Davies, A. F., Olavesen, M. G., Stephens, R. J., Davidson, R., Delneste, D., Van Regemorter, N., Vamos, E., Flinter, F., Abusaad, I. and Ragoussis, J. (1996). A detailed investigation of two cases exhibiting characteristics of the 6p deletion syndrome. *Hum Genet* **98**(4): 454-9.

Davis, A. and Bradley, A. (1993). Mutation of N-myc in mice: what does the phenotype tell us? *Bioessays* **15**(4): 273-5.

Davis, A. C., Wims, M., Spotts, G. D., Hann, S. R. and Bradley, A. (1993). A null c-myc mutation causes lethality before 10.5 days of gestation in homozygotes and reduced fertility in heterozygous female mice. *Genes Dev* **7**(4): 671-82.

Davis, D. L., Edwards, A. V., Juraszek, A. L., Phelps, A., Wessels, A. and Burch, J. B. (2001). A GATA-6 gene heart-region-specific enhancer provides a novel means to mark and probe a discrete component of the mouse cardiac conduction system. *Mech Dev* **108**(1-2): 105-19.

de la Pompa, J. L., Timmerman, L. A., Takimoto, H., Yoshida, H., Elia, A. J., Samper, E., Potter, J., Wakeham, A., Marengere, L., Langille, B. L., Crabtree, G. R. and Mak, T. W. (1998). Role of the NF-ATc transcription factor in morphogenesis of cardiac valves and septum. *Nature* **392**(6672): 182-6.

de Lange, F. J., Moorman, A. F., Anderson, R. H., Manner, J., Soufan, A. T., de Gier-de Vries, C., Schneider, M. D., Webb, S., van den Hoff, M. J. and Christoffels, V. M. (2004). Lineage and morphogenetic analysis of the cardiac valves. *Circ Res* **95**(6): 645-54.

Delorme, B., Dahl, E., Jarry-Guichard, T., Briand, J. P., Willecke, K., Gros, D. and Theveniau-Ruissy, M. (1997). Expression pattern of connexin gene products at the early developmental stages of the mouse cardiovascular system. *Circ Res* **81**(3): 423-37.

DeRuiter, M. C., Poelmann, R. E., VanderPlas-de Vries, I., Mentink, M. M. and Gittenberger-de Groot, A. C. (1992). The development of the myocardium and endocardium in mouse embryos. Fusion of two heart tubes? *Anat Embryol (Berl)* **185**(5): 461-73.

DeScipio, C. (2007). The 6p subtelomere deletion syndrome. *Am J Med Genet C Semin Med Genet* **145**(4): 377-82.

Dodou, E., Verzi, M. P., Anderson, J. P., Xu, S. M. and Black, B. L. (2004). Mef2c is a direct transcriptional target of ISL1 and GATA factors in the anterior heart field during mouse embryonic development. *Development* **131**(16): 3931-42.

Dong, C., Wilhelm, D. and Koopman, P. (2004). Sox genes and cancer. *Cytogenet Genome Res* **105**(2-4): 442-7.

Dor, X. and Corone, P. (1985). Migration and torsions of the conotruncus in the chick embryo heart: observational evidence and conclusions drawn from experimental intervention. *Heart Vessels* **1**(4): 195-211.

Dor, Y., Camenisch, T. D., Itin, A., Fishman, G. I., McDonald, J. A., Carmeliet, P. and Keshet, E. (2001). A novel role for VEGF in endocardial cushion formation and its potential contribution to congenital heart defects. *Development* **128**(9): 1531-8.

Dor, Y., Klewer, S. E., McDonald, J. A., Keshet, E. and Camenisch, T. D. (2003). VEGF modulates early heart valve formation. *Anat Rec A Discov Mol Cell Evol Biol* **271**(1): 202-8.

Downs, K. M. and Davies, T. (1993). Staging of gastrulating mouse embryos by morphological landmarks in the dissecting microscope. *Development* **118**(4): 1255-66.

Dunwoodie, S. L. (2007). Combinatorial signaling in the heart orchestrates cardiac induction, lineage specification and chamber formation. *Semin Cell Dev Biol* **18**(1): 54-66.

Dunwoodie, S. L., Rodriguez, T. A. and Beddington, R. S. (1998). Msg1 and Mrg1, founding members of a gene family, show distinct patterns of gene expression during mouse embryogenesis. *Mech Dev* **72**(1-2): 27-40.

Dyer, L. A. and Kirby, M. L. (2009). Sonic hedgehog maintains proliferation in secondary heart field progenitors and is required for normal arterial pole formation. *Dev Biol* **330**(2): 305-17.

Echelard, Y., Epstein, D. J., St-Jacques, B., Shen, L., Mohler, J., McMahon, J. A. and McMahon, A. P. (1993). Sonic hedgehog, a member of a family of putative signaling molecules, is implicated in the regulation of CNS polarity. *Cell* **75**(7): 1417-30.

Echelard, Y., Vassileva, G. and McMahon, A. P. (1994). Cis-acting regulatory sequences governing Wnt-1 expression in the developing mouse CNS. *Development* **120**(8): 2213-24.

El-Hashash, A. H., Esbrit, P. and Kimber, S. J. (2005). PTHrP promotes murine secondary trophoblast giant cell differentiation through induction of endocycle, upregulation of giant-cell-promoting transcription factors and suppression of other trophoblast cell types. *Differentiation* **73**(4): 154-74.

Epstein, J. A., Li, J., Lang, D., Chen, F., Brown, C. B., Jin, F., Lu, M. M., Thomas, M., Liu, E., Wessels, A. and Lo, C. W. (2000). Migration of cardiac neural crest cells in Splotch embryos. *Development* **127**(9): 1869-78.

Ferrara, N., Carver-Moore, K., Chen, H., Dowd, M., Lu, L., O'Shea, K. S., Powell-Braxton, L., Hillan, K. J. and Moore, M. W. (1996). Heterozygous embryonic lethality induced by targeted inactivation of the VEGF gene. *Nature* **380**(6573): 439-42.

Ferrari, S., Harley, V. R., Pontiggia, A., Goodfellow, P. N., Lovell-Badge, R. and Bianchi, M. E. (1992). SRY, like HMG1, recognizes sharp angles in DNA. *Embo J* **11**(12): 4497-506.

Fischer, A., Steidl, C., Wagner, T. U., Lang, E., Jakob, P. M., Friedl, P., Knobeloch, K. P. and Gessler, M. (2007). Combined loss of Hey1 and HeyL causes congenital heart defects because of impaired epithelial to mesenchymal transition. *Circ Res* **100**(6): 856-63.

Franco, D., Campione, M., Kelly, R., Zammit, P. S., Buckingham, M., Lamers, W. H. and Moorman, A. F. (2000). Multiple transcriptional domains, with distinct left and right components, in the atrial chambers of the developing heart. *Circ Res* **87**(11): 984-91.

Frank, S. and Zoll, B. (1998). Mouse HNF-3/fork head homolog-1-like gene: structure, chromosomal location, and expression in adult and embryonic kidney. *DNA Cell Biol* **17**(8): 679-88.

Friedman, R. S., Bangur, C. S., Zasloff, E. J., Fan, L., Wang, T., Watanabe, Y. and Kalos, M. (2004). Molecular and immunological evaluation of the transcription factor SOX-4 as a lung tumor vaccine antigen. *J Immunol* **172**(5): 3319-27.

Frierson, H. F., Jr., El-Naggar, A. K., Welsh, J. B., Sapinoso, L. M., Su, A. I., Cheng, J., Saku, T., Moskaluk, C. A. and Hampton, G. M. (2002). Large scale molecular analysis identifies genes with altered expression in salivary adenoid cystic carcinoma. *Am J Pathol* **161**(4): 1315-23.

Fukiishi, Y. and Morriss-Kay, G. M. (1992). Migration of cranial neural crest cells to the pharyngeal arches and heart in rat embryos. *Cell Tissue Res* **268**(1): 1-8.

Gage, P. J., Suh, H. and Camper, S. A. (1999). Dosage requirement of Pitx2 for development of multiple organs. *Development* **126**(20): 4643-51.

Gannon, M. and Bader, D. (1995). Initiation of cardiac differentiation occurs in the absence of anterior endoderm. *Development* **121**(8): 2439-50.

Garratt, A. N., Ozcelik, C. and Birchmeier, C. (2003). ErbB2 pathways in heart and neural diseases. *Trends Cardiovasc Med* **13**(2): 80-6.

Geijsen, N., Uings, I. J., Pals, C., Armstrong, J., McKinnon, M., Raaijmakers, J. A., Lammers, J. W., Koenderman, L. and Coffer, P. J. (2001). Cytokine-specific transcriptional regulation through an IL-5Ralpha interacting protein. *Science* **293**(5532): 1136-8.

Gittenberger-de Groot, A. C., Vrancken Peeters, M. P., Bergwerff, M., Mentink, M. M. and Poelmann, R. E. (2000). Epicardial outgrowth inhibition leads to compensatory mesothelial outflow tract collar and abnormal cardiac septation and coronary formation. *Circ Res* **87**(11): 969-71.

Goddeeris, M. M., Rho, S., Petiet, A., Davenport, C. L., Johnson, G. A., Meyers, E. N. and Klingensmith, J. (2008). Intracardiac septation requires hedgehog-dependent cellular contributions from outside the heart. *Development* **135**(10): 1887-95.

Goddeeris, M. M., Schwartz, R., Klingensmith, J. and Meyers, E. N. (2007). Independent requirements for Hedgehog signaling by both the anterior heart field and neural crest cells for outflow tract development. *Development* **134**(8): 1593-604.

Goering, W., Adham, I. M., Pasche, B., Manner, J., Ochs, M., Engel, W. and Zoll, B. (2008). Impairment of gastric acid secretion and increase of embryonic lethality in Foxq1-deficient mice. *Cytogenet Genome Res* **121**(2): 88-95.

Goldsworthy, M., Hugill, A., Freeman, H., Horner, E., Shimomura, K., Bogani, D., Pieles, G., Mijat, V., Arkell, R., Bhattacharya, S., Ashcroft, F. M. and Cox, R. D. (2008). Role of the transcription factor sox4 in insulin secretion and impaired glucose tolerance. *Diabetes* **57**(8): 2234-44.

Graham, J. D., Hunt, S. M., Tran, N. and Clarke, C. L. (1999). Regulation of the expression and activity by progestins of a member of the SOX gene family of transcriptional modulators. *J Mol Endocrinol* **22**(3): 295-304.

Grego-Bessa, J., Luna-Zurita, L., del Monte, G., Bolos, V., Melgar, P., Arandilla, A., Garratt, A. N., Zang, H., Mukouyama, Y. S., Chen, H., Shou, W., Ballestar, E., Esteller, M., Rojas, A., Perez-Pomares, J. M. and de la Pompa, J. L. (2007). Notch signaling is essential for ventricular chamber development. *Dev Cell* **12**(3): 415-29.

Gubbay, J., Collignon, J., Koopman, P., Capel, B., Economou, A., Munsterberg, A., Vivian, N., Goodfellow, P. and Lovell-Badge, R. (1990). A gene mapping to the sex-determining region of the mouse Y chromosome is a member of a novel family of embryonically expressed genes. *Nature* **346**(6281): 245-50.

Habets, P. E., Moorman, A. F., Clout, D. E., van Roon, M. A., Lingbeek, M., van Lohuizen, M., Campione, M. and Christoffels, V. M. (2002). Cooperative action of Tbx2 and Nkx2.5 inhibits ANF expression in the atrioventricular canal: implications for cardiac chamber formation. *Genes Dev* **16**(10): 1234-46.

Harfe, B. D., Scherz, P. J., Nissim, S., Tian, H., McMahon, A. P. and Tabin, C. J. (2004). Evidence for an expansion-based temporal Shh gradient in specifying vertebrate digit identities. *Cell* **118**(4): 517-28.

Hargrave, M., Bowles, J. and Koopman, P. (2006). In situ hybridization of whole-mount embryos. *Methods Mol Biol* **326**: 103-13.

Hargrave, M., Wright, E., Kun, J., Emery, J., Cooper, L. and Koopman, P. (1997). Expression of the Sox11 gene in mouse embryos suggests roles in neuronal maturation and epithelio-mesenchymal induction. *Dev Dyn* **210**(2): 79-86.

Henderson, D. J. and Anderson, R. H. (2009). The development and structure of the ventricles in the human heart. *Pediatr Cardiol* **30**(5): 588-96.

Henderson, D. J., Conway, S. J., Greene, N. D., Gerrelli, D., Murdoch, J. N., Anderson, R. H. and Copp, A. J. (2001). Cardiovascular defects associated with abnormalities in midline development in the Loop-tail mouse mutant. *Circ Res* **89**(1): 6-12.

Hildreth, V., Webb, S., Bradshaw, L., Brown, N. A., Anderson, R. H. and Henderson, D. J. (2008). Cells migrating from the neural crest contribute to the innervation of the venous pole of the heart. *J Anat* **212**(1): 1-11.

Hildreth, V., Webb, S., Chaudhry, B., Peat, J. D., Phillips, H. M., Brown, N., Anderson, R. H. and Henderson, D. J. (2009). Left cardiac isomerism in the Sonic hedgehog null mouse. *J Anat* **214**(6): 894-904.

Hiroi, Y., Kudoh, S., Monzen, K., Ikeda, Y., Yazaki, Y., Nagai, R. and Komuro, I. (2001). Tbx5 associates with Nkx2-5 and synergistically promotes cardiomyocyte differentiation. *Nat Genet* **28**(3): 276-80.

Hitotsumachi, S., Carpenter, D. A. and Russell, W. L. (1985). Dose-repetition increases the mutagenic effectiveness of N-ethyl-N-nitrosourea in mouse spermatogonia. *Proc Natl Acad Sci U S A* **82**(19): 6619-21.

Hong, H. K., Noveroske, J. K., Headon, D. J., Liu, T., Sy, M. S., Justice, M. J. and Chakravarti, A. (2001). The winged helix/forkhead transcription factor Foxq1 regulates differentiation of hair in satin mice. *Genesis* **29**(4): 163-71.

Hoser, M., Baader, S. L., Bosl, M. R., Ihmer, A., Wegner, M. and Sock, E. (2007). Prolonged glial expression of Sox4 in the CNS leads to architectural cerebellar defects and ataxia. *J Neurosci* **27**(20): 5495-505.

Hoser, M., Potzner, M. R., Koch, J. M., Bosl, M. R., Wegner, M. and Sock, E. (2008). Sox12 deletion in the mouse reveals nonreciprocal redundancy with the related Sox4 and Sox11 transcription factors. *Mol Cell Biol* **28**(15): 4675-87.

Houweling, A. C., van Borren, M. M., Moorman, A. F. and Christoffels, V. M. (2005). Expression and regulation of the atrial natriuretic factor encoding gene Nppa during development and disease. *Cardiovasc Res* **67**(4): 583-93.

Hrabe de Angelis, M. H., Flaswinkel, H., Fuchs, H., Rathkolb, B., Soewarto, D., Marschall, S., Heffner, S., Pargent, W., Wuensch, K., Jung, M., Reis, A., Richter, T., Alessandrini, F., Jakob, T., Fuchs, E., Kolb, H., Kremmer, E., Schaeble, K., Rollinski, B., Roscher, A., Peters, C., Meitinger, T., Strom, T., Steckler, T., Holsboer, F., Klopstock, T., Gekeler, F., Schindewolf, C., Jung, T., Avraham, K., Behrendt, H., Ring, J., Zimmer, A., Schughart, K., Pfeffer, K., Wolf, E. and Balling, R. (2000). Genome-wide, large-scale production of mutant mice by ENU mutagenesis. *Nat Genet* **25**(4): 444-7.

Hu, N. and Keller, B. B. (1995). Relationship of simultaneous atrial and ventricular pressures in stage 16-27 chick embryos. *Am J Physiol* **269**(4 Pt 2): H1359-62.

Hunt, S. M. and Clarke, C. L. (1999). Expression and hormonal regulation of the Sox4 gene in mouse female reproductive tissues. *Biol Reprod* **61**(2): 476-81.

Icardo, J. M. and Fernandez-Teran, A. (1987). Morphologic study of ventricular trabeculation in the embryonic chick heart. *Acta Anat (Basel)* **130**(3): 264-74.

Inai, K., Norris, R. A., Hoffman, S., Markwald, R. R. and Sugi, Y. (2008). BMP-2 induces cell migration and periostin expression during atrioventricular valvulogenesis. *Dev Biol* **315**(2): 383-96.

Jacobson, A. G. and Sater, A. K. (1988). Features of embryonic induction. *Development* **104**(3): 341-59.

Jalife, J., Morley, G. E. and Vaidya, D. (1999). Connexins and impulse propagation in the mouse heart. *J Cardiovasc Electrophysiol* **10**(12): 1649-63.

Jiang, X., Rowitch, D. H., Soriano, P., McMahon, A. P. and Sucov, H. M. (2000). Fate of the mammalian cardiac neural crest. *Development* **127**(8): 1607-16.

Juriloff, D. M. and Harris, M. J. (2008). Mouse genetic models of cleft lip with or without cleft palate. *Birth Defects Res A Clin Mol Teratol* **82**(2): 63-77.

Justice, M. J., Noveroske, J. K., Weber, J. S., Zheng, B. and Bradley, A. (1999). Mouse ENU mutagenesis. *Hum Mol Genet* **8**(10): 1955-63.

Kanai-Azuma, M., Kanai, Y., Gad, J. M., Tajima, Y., Taya, C., Kurohmaru, M., Sanai, Y., Yonekawa, H., Yazaki, K., Tam, P. P. and Hayashi, Y. (2002). Depletion of definitive gut endoderm in Sox17-null mutant mice. *Development* **129**(10): 2367-79.

Kaufman, M. H. (1992). The atlas of mouse development. London, Academic Press.

Keays, D. A., Clark, T. G. and Flint, J. (2006). Estimating the number of coding mutations in genotypic- and phenotypic-driven N-ethyl-N-nitrosourea (ENU) screens. *Mamm Genome* **17**(3): 230-8.

Kelly, R. G., Brown, N. A. and Buckingham, M. E. (2001). The arterial pole of the mouse heart forms from Fgf10-expressing cells in pharyngeal mesoderm. *Dev Cell* **1**(3): 435-40.

Kibar, Z., Vogan, K. J., Groulx, N., Justice, M. J., Underhill, D. A. and Gros, P. (2001). Ltap, a mammalian homolog of Drosophila Strabismus/Van Gogh, is altered in the mouse neural tube mutant Loop-tail. *Nat Genet* **28**(3): 251-5.

Kim, B. E., Lee, J. H., Kim, H. S., Kwon, O. J., Jeong, S. W. and Kim, I. K. (2004). Involvement of Sox-4 in the cytochrome c-dependent AIF-independent apoptotic pathway in HeLa cells induced by Delta12-prostaglandin J2. *Exp Mol Med* **36**(5): 444-53.

Kirby, M. L. (1990). Alteration of cardiogenesis after neural crest ablation. *Ann N Y Acad Sci* **588**: 289-95.

Kirby, M. L. (2007). Cardiac development. New York ; Oxford, Oxford University Press.

Kirby, M. L. and Waldo, K. L. (1995). Neural crest and cardiovascular patterning. *Circ Res* **77**(2): 211-5.

Kisanuki, Y. Y., Hammer, R. E., Miyazaki, J., Williams, S. C., Richardson, J. A. and Yanagisawa, M. (2001). Tie2-Cre transgenic mice: a new model for endothelial cell-lineage analysis in vivo. *Dev Biol* **230**(2): 230-42.

Kitamura, K., Miura, H., Miyagawa-Tomita, S., Yanazawa, M., Katoh-Fukui, Y., Suzuki, R., Ohuchi, H., Suehiro, A., Motegi, Y., Nakahara, Y., Kondo, S. and Yokoyama, M. (1999). Mouse Pitx2 deficiency leads to anomalies of the ventral body wall, heart, extra- and periocular mesoderm and right pulmonary isomerism. *Development* **126**(24): 5749-58.

Kobielak, K., Stokes, N., de la Cruz, J., Polak, L. and Fuchs, E. (2007). Loss of a quiescent niche but not follicle stem cells in the absence of bone morphogenetic protein signaling. *Proc Natl Acad Sci U S A* **104**(24): 10063-8.

Komiyama, M., Ito, K. and Shimada, Y. (1987). Origin and development of the epicardium in the mouse embryo. *Anat Embryol (Berl)* **176**(2): 183-9.

Kramer, R., Bucay, N., Kane, D. J., Martin, L. E., Tarpley, J. E. and Theill, L. E. (1996). Neuregulins with an Ig-like domain are essential for mouse myocardial and neuronal development. *Proc Natl Acad Sci U S A* **93**(10): 4833-8.

Kraus, F., Haenig, B. and Kispert, A. (2001a). Cloning and expression analysis of the mouse T-box gene Tbx18. *Mech Dev* **100**(1): 83-6.

Kraus, F., Haenig, B. and Kispert, A. (2001b). Cloning and expression analysis of the mouse T-box gene tbx20. *Mech Dev* **100**(1): 87-91.

Kuhlbrodt, K., Herbarth, B., Sock, E., Enderich, J., Hermans-Borgmeyer, I. and Wegner, M. (1998). Cooperative function of POU proteins and SOX proteins in glial cells. *J Biol Chem* **273**(26): 16050-7.

Kuo, C. T., Morrisey, E. E., Anandappa, R., Sigrist, K., Lu, M. M., Parmacek, M. S., Soudais, C. and Leiden, J. M. (1997). GATA4 transcription factor is required for ventral morphogenesis and heart tube formation. *Genes Dev* **11**(8): 1048-60.

Kwee, L., Baldwin, H. S., Shen, H. M., Stewart, C. L., Buck, C., Buck, C. A. and Labow, M. A. (1995). Defective development of the embryonic and extraembryonic circulatory systems in vascular cell adhesion molecule (VCAM-1) deficient mice. *Development* **121**(2): 489-503.

Lakkis, M. M. and Epstein, J. A. (1998). Neurofibromin modulation of ras activity is required for normal endocardial-mesenchymal transformation in the developing heart. *Development* **125**(22): 4359-67.

Lamers, W. H., Viragh, S., Wessels, A., Moorman, A. F. and Anderson, R. H. (1995). Formation of the tricuspid valve in the human heart. *Circulation* **91**(1): 111-21.

Lamers, W. H., Wessels, A., Verbeek, F. J., Moorman, A. F., Viragh, S., Wenink, A. C., Gittenberger-de Groot, A. C. and Anderson, R. H. (1992). New findings concerning ventricular septation in the human heart. Implications for maldevelopment. *Circulation* **86**(4): 1194-205.

Larsen, W. J., Sherman, L. S., Potter, S. S. and Scott, W. J. (2001). Human embryology. New York ; Edinburgh, Churchill Livingstone.

Lavine, K. J., Yu, K., White, A. C., Zhang, X., Smith, C., Partanen, J. and Ornitz, D. M. (2005). Endocardial and epicardial derived FGF signals regulate myocardial proliferation and differentiation in vivo. *Dev Cell* **8**(1): 85-95.

Lawson, K. A. and Pedersen, R. A. (1987). Cell fate, morphogenetic movement and population kinetics of embryonic endoderm at the time of germ layer formation in the mouse. *Development* **101**(3): 627-52.

Le Douarin, N. (1982). The neural crest. Cambridge, Cambridge University Press.

Lee, C. J., Appleby, V. J., Orme, A. T., Chan, W. I. and Scotting, P. J. (2002). Differential expression of SOX4 and SOX11 in medulloblastoma. *J Neurooncol* **57**(3): 201-14.

Lefebvre, V., Li, P. and de Crombrugghe, B. (1998). A new long form of Sox5 (L-Sox5), Sox6 and Sox9 are coexpressed in chondrogenesis and cooperatively activate the type II collagen gene. *Embo J* **17**(19): 5718-33.

Lemmens, K., Segers, V. F., Demolder, M. and De Keulenaer, G. W. (2006). Role of neuregulin-1/ErbB2 signaling in endothelium-cardiomyocyte cross-talk. *J Biol Chem* **281**(28): 19469-77.

Liao, Y. L., Sun, Y. M., Chau, G. Y., Chau, Y. P., Lai, T. C., Wang, J. L., Horng, J. T., Hsiao, M. and Tsou, A. P. (2008). Identification of SOX4 target genes using phylogenetic footprinting-based prediction from expression microarrays suggests that overexpression of SOX4 potentiates metastasis in hepatocellular carcinoma. *Oncogene*.

Lie-Venema, H., Eralp, I., Maas, S., Gittenberger-De Groot, A. C., Poelmann, R. E. and DeRuiter, M. C. (2005). Myocardial heterogeneity in permissiveness for epicardium-derived cells and endothelial precursor cells along the developing heart tube at the onset of coronary vascularization. *Anat Rec A Discov Mol Cell Evol Biol* **282**(2): 120-9.

Lin, C. R., Kioussi, C., O'Connell, S., Briata, P., Szeto, D., Liu, F., Izpisua-Belmonte, J. C. and Rosenfeld, M. G. (1999). Pitx2 regulates lung asymmetry, cardiac positioning and pituitary and tooth morphogenesis. *Nature* **401**(6750): 279-82.

Lin, Q., Schwarz, J., Bucana, C. and Olson, E. N. (1997). Control of mouse cardiac morphogenesis and myogenesis by transcription factor MEF2C. *Science* **276**(5317): 1404-7.

Linask, K. K. (1992). N-cadherin localization in early heart development and polar expression of Na+,K(+)-ATPase, and integrin during pericardial coelom formation and epithelialization of the differentiating myocardium. *Dev Biol* **151**(1): 213-24.

Lincoln, J., Alfieri, C. M. and Yutzey, K. E. (2004). Development of heart valve leaflets and supporting apparatus in chicken and mouse embryos. *Dev Dyn* **230**(2): 239-50.

Lints, T. J., Parsons, L. M., Hartley, L., Lyons, I. and Harvey, R. P. (1993). Nkx-2.5: a novel murine homeobox gene expressed in early heart progenitor cells and their myogenic descendants. *Development* **119**(2): 419-31.

Lioubinski, O., Muller, M., Wegner, M. and Sander, M. (2003). Expression of Sox transcription factors in the developing mouse pancreas. *Dev Dyn* **227**(3): 402-8.

Liu, P., Ramachandran, S., Ali Seyed, M., Scharer, C. D., Laycock, N., Dalton, W. B., Williams, H., Karanam, S., Datta, M. W., Jaye, D. L. and Moreno, C. S. (2006). Sex-determining region Y box 4 is a transforming oncogene in human prostate cancer cells. *Cancer Res* **66**(8): 4011-9.

Lo, C. W., Cohen, M. F., Huang, G. Y., Lazatin, B. O., Patel, N., Sullivan, R., Pauken, C. and Park, S. M. (1997). Cx43 gap junction gene expression and gap junctional communication in mouse neural crest cells. *Dev Genet* **20**(2): 119-32.

Lomonico, M. P., Bostrom, M. P., Moore, G. W. and Hutchins, G. M. (1988). Arrested rotation of the outflow tract may explain tetralogy of Fallot and transposition of the great arteries. *Pediatr Pathol* **8**(3): 267-81.

Lomonico, M. P., Moore, G. W. and Hutchins, G. M. (1986). Rotation of the junction of the outflow tract and great arteries in the embryonic human heart. *Anat Rec* **216**(4): 544-9.

Lough, J. and Sugi, Y. (2000). Endoderm and heart development. *Dev Dyn* **217**(4): 327-42.

Lu, C. C., Brennan, J. and Robertson, E. J. (2001). From fertilization to gastrulation: axis formation in the mouse embryo. *Curr Opin Genet Dev* **11**(4): 384-92.

Lyons, I., Parsons, L. M., Hartley, L., Li, R., Andrews, J. E., Robb, L. and Harvey, R. P. (1995). Myogenic and morphogenetic defects in the heart tubes of murine embryos lacking the homeo box gene Nkx2-5. *Genes Dev* **9**(13): 1654-66.

MacDonald, S. T., Bamforth, S. D., Chen, C. M., Farthing, C. R., Franklyn, A., Broadbent, C., Schneider, J. E., Saga, Y., Lewandoski, M. and Bhattacharya, S. (2008). Epiblastic Cited2 deficiency results in cardiac phenotypic heterogeneity and provides a mechanism for haploinsufficiency. *Cardiovasc Res* **79**(3): 448-57.

Major, M. H. (1955). Satin, *sa. Mouse News Letter* **12**: 47.

Mallon, A. M., Wilming, L., Weekes, J., Gilbert, J. G., Ashurst, J., Peyrefitte, S., Matthews, L., Cadman, M., McKeone, R., Sellick, C. A., Arkell, R., Botcherby, M. R., Strivens, M. A., Campbell, R. D., Gregory, S., Denny, P., Hancock, J. M., Rogers, J. and Brown, S. D. (2004). Organization and evolution of a gene-rich region of the mouse genome: a 12.7-Mb region deleted in the Del(13)Svea36H mouse. *Genome Res* **14**(10A): 1888-901.

Manasek, F. J. (1968). Embryonic development of the heart. I. A light and electron microscopic study of myocardial development in the early chick embryo. *J Morphol* **125**(3): 329-65.

Manasek, F. J. (1975). The extracellular matrix: a dynamic component of the developing embryo. *Curr Top Dev Biol* **10**: 35-102.

Manner, J., Perez-Pomares, J. M., Macias, D. and Munoz-Chapuli, R. (2001). The origin, formation and developmental significance of the epicardium: a review. *Cells Tissues Organs* **169**(2): 89-103.

Markwald, R. R., Fitzharris, T. P. and Manasek, F. J. (1977). Structural development of endocardial cushions. *Am J Anat* **148**(1): 85-119.

Martindill, D. M., Risebro, C. A., Smart, N., Franco-Viseras Mdel, M., Rosario, C. O., Swallow, C. J., Dennis, J. W. and Riley, P. R. (2007). Nucleolar release of Hand1 acts as a molecular switch to determine cell fate. *Nat Cell Biol* **9**(10): 1131-41.

Maschhoff, K. L., Anziano, P. Q., Ward, P. and Baldwin, H. S. (2003). Conservation of Sox4 gene structure and expression during chicken embryogenesis. *Gene* **320**: 23-30.

McBride, R. E., Moore, G. W. and Hutchins, G. M. (1981). Development of the outflow tract and closure of the interventricular septum in the normal human heart. *Am J Anat* **160**(3): 309-31.

McCracken, S., Kim, C. S., Xu, Y., Minden, M. and Miyamoto, N. G. (1997). An alternative pathway for expression of p56lck from type I promoter transcripts in colon carcinoma. *Oncogene* **15**(24): 2929-37.

McFadden, D. G., Barbosa, A. C., Richardson, J. A., Schneider, M. D., Srivastava, D. and Olson, E. N. (2005). The Hand1 and Hand2 transcription factors regulate expansion of the embryonic cardiac ventricles in a gene dosage-dependent manner. *Development* **132**(1): 189-201.

Meilhac, S. M., Esner, M., Kelly, R. G., Nicolas, J. F. and Buckingham, M. E. (2004). The clonal origin of myocardial cells in different regions of the embryonic mouse heart. *Dev Cell* **6**(5): 685-98.

Meilhac, S. M., Kelly, R. G., Rocancourt, D., Eloy-Trinquet, S., Nicolas, J. F. and Buckingham, M. E. (2003). A retrospective clonal analysis of the myocardium reveals two phases of clonal growth in the developing mouse heart. *Development* **130**(16): 3877-89.

Mercado-Pimentel, M. E. and Runyan, R. B. (2007). Multiple transforming growth factor-beta isoforms and receptors function during epithelial-mesenchymal cell transformation in the embryonic heart. *Cells Tissues Organs* **185**(1-3): 146-56.

Meyers, E. N., Lewandoski, M. and Martin, G. R. (1998). An Fgf8 mutant allelic series generated by Cre- and Flp-mediated recombination. *Nat Genet* **18**(2): 136-41.

Molkentin, J. D., Lin, Q., Duncan, S. A. and Olson, E. N. (1997). Requirement of the transcription factor GATA4 for heart tube formation and ventral morphogenesis. *Genes Dev* **11**(8): 1061-72.

Mommersteeg, M. T., Soufan, A. T., de Lange, F. J., van den Hoff, M. J., Anderson, R. H., Christoffels, V. M. and Moorman, A. F. (2006). Two distinct pools of mesenchyme contribute to the development of the atrial septum. *Circ Res* **99**(4): 351-3.

Moon, B. G., Yoshida, T., Shiiba, M., Nakao, K., Katsuki, M., Takaki, S. and Takatsu, K. (2001). Functional dissection of the cytoplasmic subregions of the interleukin-5 receptor

alpha chain in growth and immunoglobulin G1 switch recombination of B cells. *Immunology* **102**(3): 289-300.

Moore, A. W., McInnes, L., Kreidberg, J., Hastie, N. D. and Schedl, A. (1999). YAC complementation shows a requirement for Wt1 in the development of epicardium, adrenal gland and throughout nephrogenesis. *Development* **126**(9): 1845-57.

Murdoch, J. N., Doudney, K., Paternotte, C., Copp, A. J. and Stanier, P. (2001). Severe neural tube defects in the loop-tail mouse result from mutation of Lpp1, a novel gene involved in floor plate specification. *Hum Mol Genet* **10**(22): 2593-601.

Nakajima, Y., Yamagishi, T., Hokari, S. and Nakamura, H. (2000). Mechanisms involved in valvuloseptal endocardial cushion formation in early cardiogenesis: roles of transforming growth factor (TGF)-beta and bone morphogenetic protein (BMP). *Anat Rec* **258**(2): 119-27.

Nakamura, T., Colbert, M. C. and Robbins, J. (2006). Neural crest cells retain multipotential characteristics in the developing valves and label the cardiac conduction system. *Circ Res* **98**(12): 1547-54.

Narita, N., Bielinska, M. and Wilson, D. B. (1997). Wild-type endoderm abrogates the ventral developmental defects associated with GATA-4 deficiency in the mouse. *Dev Biol* **189**(2): 270-4.

Nichols, J. and Ying, Q. L. (2006). Derivation and propagation of embryonic stem cells in serum- and feeder-free culture. *Methods Mol Biol* **329**: 91-8.

Nishibatake, M., Kirby, M. L. and Van Mierop, L. H. (1987). Pathogenesis of persistent truncus arteriosus and dextroposed aorta in the chick embryo after neural crest ablation. *Circulation* **75**(1): 255-64.

Palmer, S., Groves, N., Schindeler, A., Yeoh, T., Biben, C., Wang, C. C., Sparrow, D. B., Barnett, L., Jenkins, N. A., Copeland, N. G., Koentgen, F., Mohun, T. and Harvey, R. P. (2001). The small muscle-specific protein Csl modifies cell shape and promotes myocyte fusion in an insulin-like growth factor 1-dependent manner. *J Cell Biol* **153**(5): 985-98.

Pan, L., Deng, M., Xie, X. and Gan, L. (2008). ISL1 and BRN3B co-regulate the differentiation of murine retinal ganglion cells. *Development* **135**(11): 1981-90.

Parameswaran, M. and Tam, P. P. (1995). Regionalisation of cell fate and morphogenetic movement of the mesoderm during mouse gastrulation. *Dev Genet* **17**(1): 16-28.

Park, E. J., Ogden, L. A., Talbot, A., Evans, S., Cai, C. L., Black, B. L., Frank, D. U. and Moon, A. M. (2006). Required, tissue-specific roles for Fgf8 in outflow tract formation and remodeling. *Development* **133**(12): 2419-33.

Park, Y. K., Franklin, J. L., Settle, S. H., Levy, S. E., Chung, E., Jeyakumar, L. H., Shyr, Y., Washington, M. K., Whitehead, R. H., Aronow, B. J. and Coffey, R. J. (2005). Gene expression profile analysis of mouse colon embryonic development. *Genesis* **41**(1): 1-12.

Peirano, R. I. and Wegner, M. (2000). The glial transcription factor Sox10 binds to DNA both as monomer and dimer with different functional consequences. *Nucleic Acids Res* **28**(16): 3047-55.

Pennisi, D. J., Ballard, V. L. and Mikawa, T. (2003). Epicardium is required for the full rate of myocyte proliferation and levels of expression of myocyte mitogenic factors FGF2 and its receptor, FGFR-1, but not for transmural myocardial patterning in the embryonic chick heart. *Dev Dyn* **228**(2): 161-72.

Penzo-Mendez, A., Dy, P., Pallavi, B. and Lefebvre, V. (2007). Generation of mice harboring a Sox4 conditional null allele. *Genesis* **45**(12): 776-80.

Phillips, H. M., Rhee, H. J., Murdoch, J. N., Hildreth, V., Peat, J. D., Anderson, R. H., Copp, A. J., Chaudhry, B. and Henderson, D. J. (2007). Disruption of planar cell polarity signaling results in congenital heart defects and cardiomyopathy attributable to early cardiomyocyte disorganization. *Circ Res* **101**(2): 137-45.

Potzner, M. R., Griffel, C., Lutjen-Drecoll, E., Bosl, M. R., Wegner, M. and Sock, E. (2007). Prolonged Sox4 expression in oligodendrocytes interferes with normal myelination in the central nervous system. *Mol Cell Biol* **27**(15): 5316-26.

Prall, O. W., Menon, M. K., Solloway, M. J., Watanabe, Y., Zaffran, S., Bajolle, F., Biben, C., McBride, J. J., Robertson, B. R., Chaulet, H., Stennard, F. A., Wise, N., Schaft, D., Wolstein, O., Furtado, M. B., Shiratori, H., Chien, K. R., Hamada, H., Black, B. L., Saga, Y., Robertson, E. J., Buckingham, M. E. and Harvey, R. P. (2007). An Nkx2-5/Bmp2/Smad1 negative feedback loop controls heart progenitor specification and proliferation. *Cell* **128**(5): 947-59.

Rathkolb, B., Fuchs, E., Kolb, H. J., Renner-Muller, I., Krebs, O., Balling, R., Hrabe de Angelis, M. and Wolf, E. (2000). Large-scale N-ethyl-N-nitrosourea mutagenesis of mice--from phenotypes to genes. *Exp Physiol* **85**(6): 635-44.

Rehberg, S., Lischka, P., Glaser, G., Stamminger, T., Wegner, M. and Rosorius, O. (2002). Sox10 is an active nucleocytoplasmic shuttle protein, and shuttling is crucial for Sox10-mediated transactivation. *Mol Cell Biol* **22**(16): 5826-34.

Riley, P., Anson-Cartwright, L. and Cross, J. C. (1998). The Hand1 bHLH transcription factor is essential for placentation and cardiac morphogenesis. *Nat Genet* **18**(3): 271-5.

Rimini, R., Beltrame, M., Argenton, F., Szymczak, D., Cotelli, F. and Bianchi, M. E. (1999). Expression patterns of zebrafish sox11A, sox11B and sox21. *Mech Dev* **89**(1-2): 167-71.

Risebro, C. A., Smart, N., Dupays, L., Breckenridge, R., Mohun, T. J. and Riley, P. R. (2006). Hand1 regulates cardiomyocyte proliferation versus differentiation in the developing heart. *Development* **133**(22): 4595-606.

Romano, L. A. and Runyan, R. B. (2000). Slug is an essential target of TGFbeta2 signaling in the developing chicken heart. *Dev Biol* **223**(1): 91-102.

Rubenstein, J. L. and Beachy, P. A. (1998). Patterning of the embryonic forebrain. *Curr Opin Neurobiol* **8**(1): 18-26.

Runyan, R. B. and Markwald, R. R. (1983). Invasion of mesenchyme into three-dimensional collagen gels: a regional and temporal analysis of interaction in embryonic heart tissue. *Dev Biol* **95**(1): 108-14.

Russell, W. L., Hunsicker, P. R., Raymer, G. D., Steele, M. H., Stelzner, K. F. and Thompson, H. M. (1982). Dose--response curve for ethylnitrosourea-induced specific-locus mutations in mouse spermatogonia. *Proc Natl Acad Sci U S A* **79**(11): 3589-91.

Russell, W. L., Kelly, E. M., Hunsicker, P. R., Bangham, J. W., Maddux, S. C. and Phipps, E. L. (1979). Specific-locus test shows ethylnitrosourea to be the most potent mutagen in the mouse. *Proc Natl Acad Sci U S A* **76**(11): 5818-9.

Ryan, A. K., Blumberg, B., Rodriguez-Esteban, C., Yonei-Tamura, S., Tamura, K., Tsukui, T., de la Pena, J., Sabbagh, W., Greenwald, J., Choe, S., Norris, D. P., Robertson, E. J., Evans, R. M., Rosenfeld, M. G. and Izpisua Belmonte, J. C. (1998). Pitx2 determines left-right asymmetry of internal organs in vertebrates. *Nature* **394**(6693): 545-51.

Saga, Y., Miyagawa-Tomita, S., Takagi, A., Kitajima, S., Miyazaki, J. and Inoue, T. (1999). MesP1 is expressed in the heart precursor cells and required for the formation of a single heart tube. *Development* **126**(15): 3437-47.

Sakamoto, Y., Hara, K., Kanai-Azuma, M., Matsui, T., Miura, Y., Tsunekawa, N., Kurohmaru, M., Saijoh, Y., Koopman, P. and Kanai, Y. (2007). Redundant roles of Sox17 and Sox18 in early cardiovascular development of mouse embryos. *Biochem Biophys Res Commun* **360**(3): 539-44.

Sambrook, J., Fritsch, E. F. and Maniatis, T. (1989). Molecular cloning : a laboratory manual. Cold Spring Harbor, Cold Sprng Harbor Laboratory Press.

Schilham, M. W., Moerer, P., Cumano, A. and Clevers, H. C. (1997). Sox-4 facilitates thymocyte differentiation. *Eur J Immunol* **27**(5): 1292-5.

Schilham, M. W., Oosterwegel, M. A., Moerer, P., Ya, J., de Boer, P. A., van de Wetering, M., Verbeek, S., Lamers, W. H., Kruisbeek, A. M., Cumano, A. and Clevers, H. (1996). Defects in cardiac outflow tract formation and pro-B-lymphocyte expansion in mice lacking Sox-4. *Nature* **380**(6576): 711-4.

Schlueter, J., Manner, J. and Brand, T. (2006). BMP is an important regulator of proepicardial identity in the chick embryo. *Dev Biol* **295**(2): 546-58.

Schroeder, J. A., Jackson, L. F., Lee, D. C. and Camenisch, T. D. (2003). Form and function of developing heart valves: coordination by extracellular matrix and growth factor signaling. *J Mol Med* **81**(7): 392-403.

Sedmera, D., Pexieder, T., Hu, N. and Clark, E. B. (1997). Developmental changes in the myocardial architecture of the chick. *Anat Rec* **248**(3): 421-32.

Sedmera, D., Pexieder, T., Hu, N. and Clark, E. B. (1998). A quantitative study of the ventricular myoarchitecture in the stage 21-29 chick embryo following decreased loading. *Eur J Morphol* **36**(2): 105-19.

Sedmera, D., Pexieder, T., Vuillemin, M., Thompson, R. P. and Anderson, R. H. (2000). Developmental patterning of the myocardium. *Anat Rec* **258**(4): 319-37.

Sengbusch, J. K., He, W., Pinco, K. A. and Yang, J. T. (2002). Dual functions of [alpha]4[beta]1 integrin in epicardial development: initial migration and long-term attachment. *J Cell Biol* **157**(5): 873-82.

Shimamura, K. and Rubenstein, J. L. (1997). Inductive interactions direct early regionalization of the mouse forebrain. *Development* **124**(14): 2709-18.

Singh, M. K., Christoffels, V. M., Dias, J. M., Trowe, M. O., Petry, M., Schuster-Gossler, K., Burger, A., Ericson, J. and Kispert, A. (2005). Tbx20 is essential for cardiac chamber differentiation and repression of Tbx2. *Development* **132**(12): 2697-707.

Sinner, D., Kordich, J. J., Spence, J. R., Opoka, R., Rankin, S., Lin, S. C., Jonatan, D., Zorn, A. M. and Wells, J. M. (2007). Sox17 and Sox4 differentially regulate beta-catenin/T-cell factor activity and proliferation of colon carcinoma cells. *Mol Cell Biol* **27**(22): 7802-15.

Snarr, B. S., O'Neal, J. L., Chintalapudi, M. R., Wirrig, E. E., Phelps, A. L., Kubalak, S. W. and Wessels, A. (2007). Isl1 expression at the venous pole identifies a novel role for the second heart field in cardiac development. *Circ Res* **101**(10): 971-4.

Sock, E., Rettig, S. D., Enderich, J., Bosl, M. R., Tamm, E. R. and Wegner, M. (2004). Gene targeting reveals a widespread role for the high-mobility-group transcription factor Sox11 in tissue remodeling. *Mol Cell Biol* **24**(15): 6635-44.

Song, W., Jackson, K. and McGuire, P. G. (2000). Degradation of type IV collagen by matrix metalloproteinases is an important step in the epithelial-mesenchymal transformation of the endocardial cushions. *Dev Biol* **227**(2): 606-17.

Soriano, P. (1999). Generalized lacZ expression with the ROSA26 Cre reporter strain. *Nat Genet* **21**(1): 70-1.

Srinivas, S., Watanabe, T., Lin, C. S., William, C. M., Tanabe, Y., Jessell, T. M. and Costantini, F. (2001). Cre reporter strains produced by targeted insertion of EYFP and ECFP into the ROSA26 locus. *BMC Dev Biol* **1**: 4.

Srivastava, D. and Olson, E. N. (2000). A genetic blueprint for cardiac development. *Nature* **407**(6801): 221-6.

Srivastava, D., Thomas, T., Lin, Q., Kirby, M. L., Brown, D. and Olson, E. N. (1997). Regulation of cardiac mesodermal and neural crest development by the bHLH transcription factor, dHAND. *Nat Genet* **16**(2): 154-60.

Stalsberg, H. and DeHaan, R. L. (1969). The precardiac areas and formation of the tubular heart in the chick embryo. *Dev Biol* **19**(2): 128-59.

Stennard, F. A., Costa, M. W., Lai, D., Biben, C., Furtado, M. B., Solloway, M. J., McCulley, D. J., Leimena, C., Preis, J. I., Dunwoodie, S. L., Elliott, D. E., Prall, O. W., Black, B. L., Fatkin, D. and Harvey, R. P. (2005). Murine T-box transcription factor Tbx20 acts as a repressor during heart development, and is essential for adult heart integrity, function and adaptation. *Development* **132**(10): 2451-62.

Strauss, M., Arrechedera, H., Arguello, C., Ayesta, C., Alvarez, M. and Anselmi, G. (1987). Mesenchymal tissue of the interventricular septum. Structural and ultrastructural study. *Anat Embryol (Berl)* **176**(2): 231-7.

Stuckmann, I., Evans, S. and Lassar, A. B. (2003). Erythropoietin and retinoic acid, secreted from the epicardium, are required for cardiac myocyte proliferation. *Dev Biol* **255**(2): 334-49.

Sun, X., Meyers, E. N., Lewandoski, M. and Martin, G. R. (1999). Targeted disruption of Fgf8 causes failure of cell migration in the gastrulating mouse embryo. *Genes Dev* **13**(14): 1834-46.

Suzuki, K., Nakamura, M., Amano, E., Mokuno, K., Shirai, S. and Terasaki, H. (2006). Case of chromosome 6p25 terminal deletion associated with Axenfeld-Rieger syndrome and persistent hyperplastic primary vitreous. *Am J Med Genet A* **140**(5): 503-8.

Takeuchi, J. K., Mileikovskaia, M., Koshiba-Takeuchi, K., Heidt, A. B., Mori, A. D., Arruda, E. P., Gertsenstein, M., Georges, R., Davidson, L., Mo, R., Hui, C. C., Henkelman, R. M., Nemer, M., Black, B. L., Nagy, A. and Bruneau, B. G. (2005). Tbx20 dose-dependently regulates transcription factor networks required for mouse heart and motoneuron development. *Development* **132**(10): 2463-74.

Tam, P. P. and Beddington, R. S. (1992). Establishment and organization of germ layers in the gastrulating mouse embryo. *Ciba Found Symp* **165**: 27-41; discussion 2-9.

Tavazoie, S. F., Alarcon, C., Oskarsson, T., Padua, D., Wang, Q., Bos, P. D., Gerald, W. L. and Massague, J. (2008). Endogenous human microRNAs that suppress breast cancer metastasis. *Nature* **451**(7175): 147-52.

Thomas, T., Yamagishi, H., Overbeek, P. A., Olson, E. N. and Srivastava, D. (1998). The bHLH factors, dHAND and eHAND, specify pulmonary and systemic cardiac ventricles independent of left-right sidedness. *Dev Biol* **196**(2): 228-36.

Timmerman, L. A., Grego-Bessa, J., Raya, A., Bertran, E., Perez-Pomares, J. M., Diez, J., Aranda, S., Palomo, S., McCormick, F., Izpisua-Belmonte, J. C. and de la Pompa, J. L.

(2004). Notch promotes epithelial-mesenchymal transition during cardiac development and oncogenic transformation. *Genes Dev* **18**(1): 99-115.

Tonks, A., Pearn, L., Musson, M., Gilkes, A., Mills, K. I., Burnett, A. K. and Darley, R. L. (2007). Transcriptional dysregulation mediated by RUNX1-RUNX1T1 in normal human progenitor cells and in acute myeloid leukaemia. *Leukemia* **21**(12): 2495-505.

van Beest, M., Dooijes, D., van De Wetering, M., Kjaerulff, S., Bonvin, A., Nielsen, O. and Clevers, H. (2000). Sequence-specific high mobility group box factors recognize 10-12-base pair minor groove motifs. *J Biol Chem* **275**(35): 27266-73.

van de Wetering, M., Oosterwegel, M., van Norren, K. and Clevers, H. (1993). Sox-4, an Sry-like HMG box protein, is a transcriptional activator in lymphocytes. *Embo J* **12**(10): 3847-54.

van den Hoff, M. J., Moorman, A. F., Ruijter, J. M., Lamers, W. H., Bennington, R. W., Markwald, R. R. and Wessels, A. (1999). Myocardialization of the cardiac outflow tract. *Dev Biol* **212**(2): 477-90.

van Houte, L. P., Chuprina, V. P., van der Wetering, M., Boelens, R., Kaptein, R. and Clevers, H. (1995). Solution structure of the sequence-specific HMG box of the lymphocyte transcriptional activator Sox-4. *J Biol Chem* **270**(51): 30516-24.

Verzi, M. P., Khan, A. H., Ito, S. and Shivdasani, R. A. (2008). Transcription factor foxq1 controls mucin gene expression and granule content in mouse stomach surface mucous cells. *Gastroenterology* **135**(2): 591-600.

Verzi, M. P., McCulley, D. J., De Val, S., Dodou, E. and Black, B. L. (2005). The right ventricle, outflow tract, and ventricular septum comprise a restricted expression domain within the secondary/anterior heart field. *Dev Biol* **287**(1): 134-45.

Viragh, S., Szabo, E. and Challice, C. E. (1989). Formation of the primitive myo- and endocardial tubes in the chicken embryo. *J Mol Cell Cardiol* **21**(2): 123-37.

Vleminckx, K., Kemler, R. and Hecht, A. (1999). The C-terminal transactivation domain of beta-catenin is necessary and sufficient for signaling by the LEF-1/beta-catenin complex in Xenopus laevis. *Mech Dev* **81**(1-2): 65-74.

von Both, I., Silvestri, C., Erdemir, T., Lickert, H., Walls, J. R., Henkelman, R. M., Rossant, J., Harvey, R. P., Attisano, L. and Wrana, J. L. (2004). Foxh1 is essential for development of the anterior heart field. *Dev Cell* **7**(3): 331-45.

Vong, L., Bi, W., O'Connor-Halligan, K. E., Li, C., Cserjesi, P. and Schwarz, J. J. (2006). MEF2C is required for the normal allocation of cells between the ventricular and sinoatrial precursors of the primary heart field. *Dev Dyn* **235**(7): 1809-21.

Wagner, M. and Siddiqui, M. A. (2007). Signal transduction in early heart development (II): ventricular chamber specification, trabeculation, and heart valve formation. *Exp Biol Med (Maywood)* **232**(7): 866-80.

Waldo, K. L., Hutson, M. R., Stadt, H. A., Zdanowicz, M., Zdanowicz, J. and Kirby, M. L. (2005a). Cardiac neural crest is necessary for normal addition of the myocardium to the arterial pole from the secondary heart field. *Dev Biol* **281**(1): 66-77.

Waldo, K. L., Hutson, M. R., Ward, C. C., Zdanowicz, M., Stadt, H. A., Kumiski, D., Abu-Issa, R. and Kirby, M. L. (2005b). Secondary heart field contributes myocardium and smooth muscle to the arterial pole of the developing heart. *Dev Biol* **281**(1): 78-90.

Wang, D. Z., Li, S., Hockemeyer, D., Sutherland, L., Wang, Z., Schratt, G., Richardson, J. A., Nordheim, A. and Olson, E. N. (2002). Potentiation of serum response factor activity by a family of myocardin-related transcription factors. *Proc Natl Acad Sci U S A* **99**(23): 14855-60.

Warkman, A. S., Yatskievych, T. A., Hardy, K. M., Krieg, P. A. and Antin, P. B. (2008). Myocardin expression during avian embryonic heart development requires the endoderm but is independent of BMP signaling. *Dev Dyn* **237**(1): 216-21.

Washington Smoak, I., Byrd, N. A., Abu-Issa, R., Goddeeris, M. M., Anderson, R., Morris, J., Yamamura, K., Klingensmith, J. and Meyers, E. N. (2005). Sonic hedgehog is required for cardiac outflow tract and neural crest cell development. *Dev Biol* **283**(2): 357-72.

Watt, A. J., Battle, M. A., Li, J. and Duncan, S. A. (2004). GATA4 is essential for formation of the proepicardium and regulates cardiogenesis. *Proc Natl Acad Sci U S A* **101**(34): 12573-8.

Watt, A. J., Zhao, R., Li, J. and Duncan, S. A. (2007). Development of the mammalian liver and ventral pancreas is dependent on GATA4. *BMC Dev Biol* **7**: 37.

Webb, S., Brown, N. A. and Anderson, R. H. (1998a). Formation of the atrioventricular septal structures in the normal mouse. *Circ Res* **82**(6): 645-56.

Webb, S., Brown, N. A., Wessels, A. and Anderson, R. H. (1998b). Development of the murine pulmonary vein and its relationship to the embryonic venous sinus. *Anat Rec* **250**(3): 325-34.

Webb, S., Qayyum, S. R., Anderson, R. H., Lamers, W. H. and Richardson, M. K. (2003). Septation and separation within the outflow tract of the developing heart. *J Anat* **202**(4): 327-42.

Weber, J. S., Salinger, A. and Justice, M. J. (2000). Optimal N-ethyl-N-nitrosourea (ENU) doses for inbred mouse strains. *Genesis* **26**(4): 230-3.

Wegner, M. (1999). From head to toes: the multiple facets of Sox proteins. *Nucleic Acids Res* **27**(6): 1409-20.

Weninger, W. J., Lopes Floro, K., Bennett, M. B., Withington, S. L., Preis, J. I., Barbera, J. P., Mohun, T. J. and Dunwoodie, S. L. (2005). Cited2 is required both for heart morphogenesis and establishment of the left-right axis in mouse development. *Development* **132**(6): 1337-48.

Wenink, A. C. (1992). Quantitative morphology of the embryonic heart: an approach to development of the atrioventricular valves. *Anat Rec* **234**(1): 129-35.

Wenink, A. C. and Gittenberger-de Groot, A. C. (1982). Left and right ventricular trabecular patterns. Consequence of ventricular septation and valve development. *Br Heart J* **48**(5): 462-8.

Willoughby, C. (2006). Functional annotation of the 'Del(13)Svea36H' region of mouse chromosome 13. Oxford, University of Oxford

University of Oxford**:** xvii, 273 leaves.

Wilson, M. E., Yang, K. Y., Kalousova, A., Lau, J., Kosaka, Y., Lynn, F. C., Wang, J., Mrejen, C., Episkopou, V., Clevers, H. C. and German, M. S. (2005). The HMG box transcription factor Sox4 contributes to the development of the endocrine pancreas. *Diabetes* **54**(12): 3402-9.

Xu, H., Morishima, M., Wylie, J. N., Schwartz, R. J., Bruneau, B. G., Lindsay, E. A. and Baldini, A. (2004). Tbx1 has a dual role in the morphogenesis of the cardiac outflow tract. *Development* **131**(13): 3217-27.

Ya, J., Erdtsieck-Ernste, E. B., de Boer, P. A., van Kempen, M. J., Jongsma, H., Gros, D., Moorman, A. F. and Lamers, W. H. (1998a). Heart defects in connexin43-deficient mice. *Circ Res* **82**(3): 360-6.

Ya, J., Schilham, M. W., Clevers, H., Moorman, A. F. and Lamers, W. H. (1997). Animal models of congenital defects in the ventriculoarterial connection of the heart. *J Mol Med* **75**(8): 551-66.

Ya, J., Schilham, M. W., de Boer, P. A., Moorman, A. F., Clevers, H. and Lamers, W. H. (1998b). Sox4-deficiency syndrome in mice is an animal model for common trunk. *Circ Res* **83**(10): 986-94.

Yamagishi, H., Olson, E. N. and Srivastava, D. (2000). The basic helix-loop-helix transcription factor, dHAND, is required for vascular development. *J Clin Invest* **105**(3): 261-70.

Yelbuz, T. M., Waldo, K. L., Kumiski, D. H., Stadt, H. A., Wolfe, R. R., Leatherbury, L. and Kirby, M. L. (2002). Shortened outflow tract leads to altered cardiac looping after neural crest ablation. *Circulation* **106**(4): 504-10.

Yuan, S. and Schoenwolf, G. C. (2000). Islet-1 marks the early heart rudiments and is asymmetrically expressed during early rotation of the foregut in the chick embryo. *Anat Rec* **260**(2): 204-7.

Zamparini, A. L., Watts, T., Gardner, C. E., Tomlinson, S. R., Johnston, G. I. and Brickman, J. M. (2006). Hex acts with beta-catenin to regulate anteroposterior patterning via a Groucho-related co-repressor and Nodal. *Development* **133**(18): 3709-22.

Zeller, R., Bloch, K. D., Williams, B. S., Arceci, R. J. and Seidman, C. E. (1987). Localized expression of the atrial natriuretic factor gene during cardiac embryogenesis. *Genes Dev* **1**(7): 693-8.

Zhang, F. and Pasumarthi, K. B. (2007). Ultrastructural and immunocharacterization of undifferentiated myocardial cells in the developing mouse heart. *J Cell Mol Med* **11**(3): 552-60.

Zhao, Y., Samal, E. and Srivastava, D. (2005). Serum response factor regulates a muscle-specific microRNA that targets Hand2 during cardiogenesis. *Nature* **436**(7048): 214-20.

Zhou, B., Ma, Q., Rajagopal, S., Wu, S. M., Domian, I., Rivera-Feliciano, J., Jiang, D., von Gise, A., Ikeda, S., Chien, K. R. and Pu, W. T. (2008). Epicardial progenitors contribute to the cardiomyocyte lineage in the developing heart. *Nature* **454**(7200): 109-13.

Zhou, W., Lin, L., Majumdar, A., Li, X., Zhang, X., Liu, W., Etheridge, L., Shi, Y., Martin, J., Van de Ven, W., Kaartinen, V., Wynshaw-Boris, A., McMahon, A. P., Rosenfeld, M. G. and Evans, S. M. (2007). Modulation of morphogenesis by noncanonical Wnt signaling requires ATF/CREB family-mediated transcriptional activation of TGFbeta2. *Nat Genet* **39**(10): 1225-34.